The Role of the Vitamin D Receptor in Skeletal Muscle Protein Metabolism

Joseph Bass

Thesis submitted to the University of Nottingham for the degree of Doctor of Philosophy

September 2016

Authors Declaration

I declare that the work in this thesis was carried out in accordance with the regulations of the University of Nottingham. The following collaborations were undertaken for this thesis:

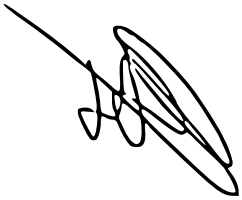
In vitro – VDR-KD and scramble control cells were produced by Abid Kazi, Cancer institute, College of Medicine, Penn State University. All remaining *in vitro* work was undertaken by the author.

In vivo – All animal procedures were undertaken at the Royal Veterinary College by the author, supervised by Mark Cleasby, Dept of Comparative Biomedical Sciences.

Co-localization immunofluorescence was undertaken by Andy Philp, School of Sport, Exercise and Rehabilitation Sciences, University of Birmingham. Fibre diameter immunofluorescence and analysis was carried out by the author.

Satellite cell immunohistochemistry was undertaken by Fawzi Kadi, School of Health Sciences, Örebro University. Data analysis was undertaken by the author.

Human – The Derby resistance exercise training study was originally undertaken by Bethan Philips, University of Nottingham. All subsequent analysis was undertaken by the author.

Signed: 

Date: 30/09/2016

Acknowledgements

I would like to thank my supervisors Prof Philip Atherton and Dr Nathaniel Szewczyk for their guidance and patience, keeping me on the right track while I undertook this research.

I would also like to thank Dr Ken Smith and Dr Daniel Wilkinson who gave a considerable amount of time and trust in teaching me new skills that will serve me well in the future.

I wish to acknowledge Dr Mark Cleasby, Dr Andy Philp and Prof Fawzi Kadi and the tremendous help and expertise they have given me through our collaborations.

I would also like to thank all the members of the laboratory group for their assistance, guidance and many cups of coffee.

Finally, I want to thank Aminta for her continual encouragement and support throughout this entire time.

The Role of the Vitamin D Receptor in Skeletal Muscle Protein Metabolism

I. Table of Contents

I. TABLE OF CONTENTS I

II. LIST OF TABLES V

III. LIST OF FIGURES VI

IV. ABBREVIATIONS IX

CHAPTER 1 – GENERAL INTRODUCTION 1

1.1 Setting the scene 2

1.2 Skeletal Muscle 3
1.2.1 Background 3
1.2.2 Skeletal Muscle Structure 3

1.3 Skeletal Muscle Health and Metabolism 6
1.3.1 Satellite cells and myogenesis 6
1.3.2 Muscle protein metabolism 8
1.3.3 Muscle protein synthesis 9
1.3.4 Muscle protein breakdown 13
1.3.4.1 Ubiquitin-proteasomal degradation 14
1.3.4.2 Caspase and calpain degradation 15
1.3.4.3 Autophagy mediated degradation 16
1.3.5 Glucose metabolism 18
1.3.6 Regulation of muscle protein metabolism 19
1.3.6.1 Regulation of muscle metabolism by environmental stimuli 19
1.3.6.2 Regulation by catabolic conditions 21
1.3.6.3 Sarcopenia 22

1.4 Vitamin D and the vitamin D receptor 24
1.4.1 Potential importance in muscle 24
1.4.2 Background 24
1.4.3 Vitamin D synthesis and metabolism 25
1.4.4 The Vitamin D Receptor (VDR) 28
1.4.5 Vitamin D status 32
1.4.6 Skeletal Muscle and vitamin D: Observational Studies 36
1.4.7 Skeletal Muscle and vitamin D: Supplementation Studies 39
1.4.8 Skeletal Muscle and the vitamin D Receptor: Human Studies 43
1.4.9 Skeletal Muscle and vitamin D: Animal Models 44

1.4.10 Skeletal Muscle and the vitamin D Receptor: Animal Models . 45
1.4.11 Skeletal Muscle and the vitamin D Receptor: Cell Culture Models 47

1.5 Summary 50

CHAPTER 2 – GENERAL METHODS 51

2.1 Immunoblotting 52

2.2 Total Protein, RNA and DNA 52

2.3 Muscle protein synthesis 53

2.4 Statistical analysis 55

CHAPTER 3 – THE ROLE OF THE VITAMIN D RECEPTOR DURING MYOGENESIS 56

3.1 Introduction 57

3.2 Aims and Hypothesis 59

3.3 Methodology 59
3.3.1 Cell culture 59
3.3.2 shRNA interference 60
3.3.3 Myoblast population counts and BrdU assay 61
3.3.4 Cell cycle analysis 61
3.3.5 Myotube morphology 62
3.3.6 Muscle protein synthesis (MPS) measures 62
3.3.7 Quantitative RT-PCR 63
3.3.8 Immunoblotting 64

3.4 Results 66
3.4.1 Efficiency of lentiviral-mediated VDR knockdown 66
3.4.2 Influence of VDR-KD upon myoblast proliferation 67
3.4.2.1 Myoblast population measures 67
3.4.2.2 Proliferating myoblast DNA synthesis 68
3.4.2.3 Cell cycle analysis of proliferating myoblasts 69
3.4.3 Morphology of VDR-KD myotubes 70
3.4.4 Differentiation characteristics 72
3.4.4.1 Myosin expression 72
3.4.4.2 Total protein, DNA and RNA 73
3.4.5 Differentiated myotubes 75
3.4.5.1 Myogenic regulatory factors and markers of differentiation 75
3.4.5.2 Myofibrillar fractional synthetic rates (FSR) 76
3.4.5.3 Anabolic signalling 77

3.5 Discussion 78

3.6 Conclusion 84

CHAPTER 4 – THE INFLUENCE OF VITAMIN D RECEPTOR EXPRESSION ON SKELETAL MUSCLE METABOLISM *IN VIVO* 85

4.1 Introduction 86

4.2 Aims and hypothesis 88

4.3 Methodology 88
4.3.1 Animal handling and study design 88
4.3.2 *In vivo* electrotransfer 90
4.3.2.1 VDR-KD vector information 90
4.3.2.2 VDR-OE vector information 92
4.3.2.3 In vivo electrotransfer (IVE) 94
4.3.3 Muscle protein synthesis measures 95
4.3.4 Intraperitoneal glucose tolerance test (IPGTT) 96
4.3.5 Quantitative RT-PCR 97
4.3.6 Immunoblotting 99
4.3.7 Immunofluorescence, co-localization and satellite cell content 101

4.4 Results – Vitamin D receptor knockdown 103
4.4.1 Efficacy of VDR-KD 103
4.4.2 Muscle fibre cross sectional area 104
4.4.3 Total protein, DNA and RNA 105
4.4.4 Protein fractional synthetic rates 106
4.4.5 Anabolic signalling 106
4.4.6 Ribosomal mRNA expression 109
4.4.7 Catabolic signalling 109
4.4.7.1 mRNA expression 109
4.4.7.2 Protein expression 111
4.4.8 Muscle glucose and glycogen 112

4.5 Results – Vitamin D receptor over-expression 113
4.5.1 Efficacy of VDR-OE 113
4.5.2 Muscle fibre cross sectional area 114
4.5.3 Total protein, DNA and RNA 115
4.5.4 Protein fractional synthetic rates 116
4.5.5 Anabolic signalling 117
4.5.5.1 mRNA expression 117
4.5.5.2 Protein expression 118
4.5.6 mTOR co-localization 121
4.5.7 Ribosomal mRNA expression 122
4.5.8 ATP synthase mRNA expression 123
4.5.9 Catabolic signalling 124
4.5.10 Satellite cell content 125
4.5.11 Proliferative and myogenic mRNA expression 126
4.5.12 Muscle glucose and glycogen 127

4.6 Discussion 128

4.7 Conclusion 139

CHAPTER 5 – THE ROLE OF VITAMIN D AND THE VITAMIN D RECEPTOR IN RESPONSE TO RESISTANCE EXERCISE TRAINING IN HUMANS 140

5.1 Introduction 141

5.2 Aims and hypothesis 142

5.3 Methodology 142
5.3.1 Study information and resistance exercise training 142
5.3.2 Microarray analysis 145
5.3.3 HOMA-IR 145
5.3.4 Plasma 25[OH]D analysis 145

5.4 Results 149
5.4.1 Participant quartile grouping 149
5.4.2 Whole-body lean mass changes 150
5.4.3 VDR mRNA expression 151
5.4.3.1 Pre and post training 151
5.4.3.2 VDR mRNA Expression change 152
5.4.3.3 VDR mRNA and lean mass changes 153
5.4.4 Plasma Vitamin D status 154
5.4.4.1 Pre and post training 154
5.4.4.2 Vitamin D status change 155
5.4.4.3 Vitamin D and lean mass changes 156
5.4.4.4 Vitamin D and VDR mRNA pre and post training 157
5.4.4.5 Vitamin D and VDR mRNA changes 158
5.4.5 CYP27B1 mRNA expression 159
5.4.5.1 Pre and post training 159
5.4.5.2 CYP27B1 mRNA expression change 160
5.4.5.3 CYP27B1, lean mass and VDR changes 161
5.4.6 CYP24A1 mRNA expression 162
5.4.6.1 Pre and post training 162
5.4.6.2 CYP24A1 mRNA expression change 163
5.4.6.3 CYP24A1, lean mass and VDR changes 164
5.4.7 HOMA-IR analysis 165

5.5 Discussion 166

5.6 Conclusion 171

CHAPTER 6 – DISCUSSION AND OVERVIEW 172

REFERENCES 179

II. List of Tables

Table 1.1 Skeletal muscle fibre characteristics

Table 1.2 Vitamin D status classification

Table 1.3 Observational studies between vitamin D status and skeletal muscle function

Table 1.4 Influence of vitamin D supplementation on skeletal muscle – Randomized control trials

Table 3.1 Primer sequences for cell culture qRT-PCR

Table 4.1 Animal groups

Table 4.2 VDR-KD shRNA sequences

Table 4.3 Primer sequences for *in vivo* qRT-PCR

Table 4.4 Primary and secondary antibody information

Table 5.1 Resistance exercise training program

Table 5.2 Participant quartile grouping characteristics

III. List of Figures

Figure 1.1 Skeletal muscle structure

Figure 1.2 Skeletal muscle fibre structure

Figure 1.3 Sarcomere structure

Figure 1.4 Cell cycle

Figure 1.5 Ribosomal biogenesis and translation initiation

Figure 1.6 AKT/mTOR anabolic signalling

Figure 1.7 Vitamin D metabolism

Figure 1.8 Worldwide prevalence of vitamin D deficiency in adults

Figure 3.1 Efficacy of VDR-KD *in vitro*

Figure 3.2 Proliferating myoblast populations

Figure 3.3 BrdU incorpetation

Figure 3.4 Cell cycle analysis

Figure 3.5 Myotube morphology characteristics

Figure 3.6 Distribution of myonuclei per myotube

Figure 3.7 Myosin IIx protein expression throughout differentiation

Figure 3.8 Total protein, DNA and RNA measures throughout differentiation

Figure 3.9 mRNA expression of myogenic regulatory factors

Figure 3.10 Myofibrillar fractional synthetic rates

Figure 3.11 Anabolic signalling

Figure 4.1 Schematic representation of study protocol

Figure 4.2 VDR-KD shRNA alignment

Figure 4.3 Mouse VDR cDNA homology

Figure 4.4 Principle of IVE

Figure 4.5 Body water enrichment

Figure 4.6 Efficacy of VDR-KD *in vivo*

Figure 4.7 VDR-KD muscle fibre CSA measures

Figure 4.8 VDR-KD total protein, RNA and DNA

Figure 4.9 VDR-KD fractional synthetic rates

Figure 4.10 VDR-KD total and phosphorylated anabolic signalling

Figure 4.11 VDR-KD anabolic signalling activation

Figure 4.12 VDR-KD ribosomal RNA expression

Figure 4.13 VDR-KD catabolic markers mRNA expression

Figure 4.14 VDR-KD autophagy protein markers

Figure 4.15 VDR-KD glucose metabolism

Figure 4.16 Efficacy of VDR-OE

Figure 4.17 VDR-OE muscle fibre CSA measures

Figure 4.18 VDR-OE total protein, RNA and DNA

Figure 4.19 VDR-OE fractional synthetic rates

Figure 4.20 VDR-OE anabolic signalling mRNA expression

Figure 4.21 VDR-OE total and phosphorylated anabolic signalling

Figure 4.22 VDR-OE anabolic signalling activation

Figure 4.23 VDR-OE mTOR/LAMP2 co-localization

Figure 4.24 VDR-OE ribosomal mRNA expression

Figure 4.25 VDR-OE ATP synthase mRNA expression

Figure 4.26 VDR-OE catabolic markers mRNA expression

Figure 4.27 VDR-OE fibre type distribution and satellite cell content

Figure 4.28 VDR-OE proliferative marker mRNA expression

Figure 4.29 VDR-OE glucose metabolism

Figure 4.30 Summary of anabolic and catabolic markers

Figure 4.31 Potential mechanisms of VDR

Figure 5.1 Chromatogram of 25[OH]D_2 and $^2H_3$-25[OH]D_2

Figure 5.2 Chromatogram of 25[OH]D_3 and $^2H_3$-25[OH]D_3

Figure 5.3 25[OH]D_2 range of detection

Figure 5.4 25[OH]D_3 range of detection

Figure 5.5 Quartiles of lean mass changes

Figure 5.6 VDR expression pre and post training

Figure 5.7 VDR expression change

Figure 5.8 VDR mRNA and lean mass change correlations

Figure 5.9 Vitamin D status pre and post training

Figure 5.10 Vitamin D status change

Figure 5.11 Vitamin D and lean mass change correlation

Figure 5.12 Vitamin D levels and VDR mRNA expression pre and post correlations

Figure 5.13 Vitamin D and VDR mRNA change correlation

Figure 5.14 CYP27B1 mRNA expression pre and post training
Figure 5.15 CYP27B1 mRNA expression change
Figure 5.16 CYP27B1, lean mass and VDR correlations
Figure 5.17 CYP24A1 expression pre and post training
Figure 5.18 CYP24A1 expression change
Figure 5.19 CYP24A1, lean mass and VDR correlations
Figure 5.20 HOMA-IR, VDR expression and 25[OH]D correlations

IV. Abbreviations

1α,25[OH]2D	1α,25-dihydroxyvitamin D
25[OH]D	25-hydroxyvitamin D
3-MH	3-methylhistidine
AA	Amino acid
ACN	Acetonitrile
ASP	Alkaline soluble protein
BMI	Body mass index
Ca2+	Calcium
CSA	Cross sectional area
DBP	Vitamin D binding protein
DRIP	Vitamin D receptor interacting protein
EAA	Essential amino acid
ECM	Extra-cellular matrix
eIF4E	Eukaryotic translation initiation factor 4E
ERK 1/2	Extracellular signal-regulated kinase 1/2
FGF 23	Fibroblast growth factor 23
G-6-P	Glucose 6 phosphate
GC-MS/MS	Gas chromatograph-mass spectrophotometry
GLUT-4	Glucose transporter 4
HDAC	Histone deacetylator complex
HOMA-IR	Homeostatic model assessment of insulin resistance
HV	High voltage
IGF	Insulin like growth factor
IPGTT	Intraperitoneal glucose tolerance test
IVE	*In vivo* electroporation
LBD	Ligand-binding domain
LC-MS/MS	Liquid chromatography–mass spectrometry
LC3-I	Light chain 3
LV	Low voltage
MAPKs	Mitogen-activated protein kinases
MCF	Methylchloroformate
MHC	Myosin heavy chain
MRF4	Muscle-specific regulatory factor 4

MRFs	Myogenic regulatory factors
MPB	Muscle protein breakdown
MPS	Muscle protein synthesis
mTOR	Mammalian target of rapamycin
MYF5	Myogenic factor 5
MYOD	Myoblast determination protein
P4Hβ	Prolyl-4-hydroxylase-β
PBS	Phosphate buffered saline
Pi	Phosphate
PTH	Parathyroid hormone
RCTs	Randomized control trials
RET	Resistance exercise training
RPL	Ribosomal long protein
RPS	Ribosomal short protein
rRNA	Ribosomal RNA
RXR	9-cis-retinoic acid receptor
SC	Satellite cells
Serca	Sarco-endoplasmic reticulum calcium transport ATPase
SIM	Selected ion monitoring
SR	Sarcoplasmic reticulum
SRC-1	Steroid receptor coactivator-1
TAM	Tibialis anterior muscle
TF2B	Transcription factor 2B
TIF-I	Transcription initiation factor I
TSC	Tuberous sclerosis
UBF	Upstream binding factor
UV	Ultra violet
UPP	Ubiquitin-proteasome pathway
VDIR	VDR-interacting repressors
VDR	Vitamin D receptor
VDR-KD	Vitamin D receptor knockdown
VDREs	Vitamin D receptor response elements
VitD	Vitamin D

Chapter 1 – General introduction

1.1 Setting the scene

Vitamin D (VitD) deficiency (25[OH]D <50 nmol/L) affects 40% of adults in the US (Forrest & Stuhldreher 2011). The classical action of VitD is in the regulation of calcium (Ca^{2+}) and phosphate (P_i) homeostasis to maintain bone health, e.g. prevent rickets (Arthur W. Ham 1934), osteomalacia (Bhan et al. 2010) and osteoporosis (Rizzoli et al. 2008). However, VitD deficiency affects tissues other than bone. For example, epidemiological studies have linked VitD deficiency with a reduction in skeletal muscle mass and function (Dhanwal et al. 2013), increased risk of falls in elderly individuals (Bischoff-Ferrari, Dietrich, et al. 2004) and development of type 2 diabetes (T2D) (Pittas et al. 2007). VitD supplementation has been shown to enhance muscle function and myofibre cross sectional area (CSA) in the elderly (Ceglia et al. 2013; Sato et al. 2005) and increase muscle function in athletes (Close, Russell, et al. 2013; Trial et al. 2015). While not entirely consistent (Halfon et al. 2015), these data suggest that VitD deficiency may have a deleterious impact on skeletal muscle. VitD acts through its ubiquitously expressed cognate vitamin D receptor (VDR) (Norman 2008), with recent studies confirming expression of the VDR in skeletal muscle (Pike 2014). Rodent VDR-KO models had suggested an autonomous role of the VDR within skeletal muscle, however these have been confounded by disruption to mineral ion homeostasis and developmental dysregulation.

This work aims to investigate the autonomous role the VDR has within skeletal muscle myogenesis (Chapter 3), protein metabolism (Chapter 4) and the translational relevance it has within muscle hypertrophy (Chapter 5).

1.2 Skeletal Muscle

1.2.1 Background

Skeletal muscle is a multifunctional tissue, well appreciated for its role in locomotion, postural support and whole-body protein metabolism, comprising ~35-40% of total body mass (Cohn et al. 1980; Janssen et al. 2000). Furthermore, skeletal muscle contains the bulk of protein stores (50-75%), and is the prevalent tissue for insulin mediated glucose uptake. Exercise training and nutrition, stimulate hypertrophic growth in skeletal muscle, while inactivity, starvation and some disease states result in the loss of muscle mass. Indeed, altered protein metabolism is a major contributor and propagator of multiple chronic diseases and pathological conditions, including type II diabetes mellitus, obesity, response to critical illness and age related loss of muscle mass (sarcopenia) (Wolfe 2006).

1.2.2 Skeletal Muscle Structure

Skeletal muscle structure is highly organised, based upon the organisation of muscle fibres, the basic contractile unit. Each muscle fibre is surrounded by endomysium connective tissue, with multiple fibres clustered together into fascicles by additional connective tissue called the perimysium. Numerous fascicles are further grouped together by epimysium tissue, surrounding the entire muscle (Figure 1.1).

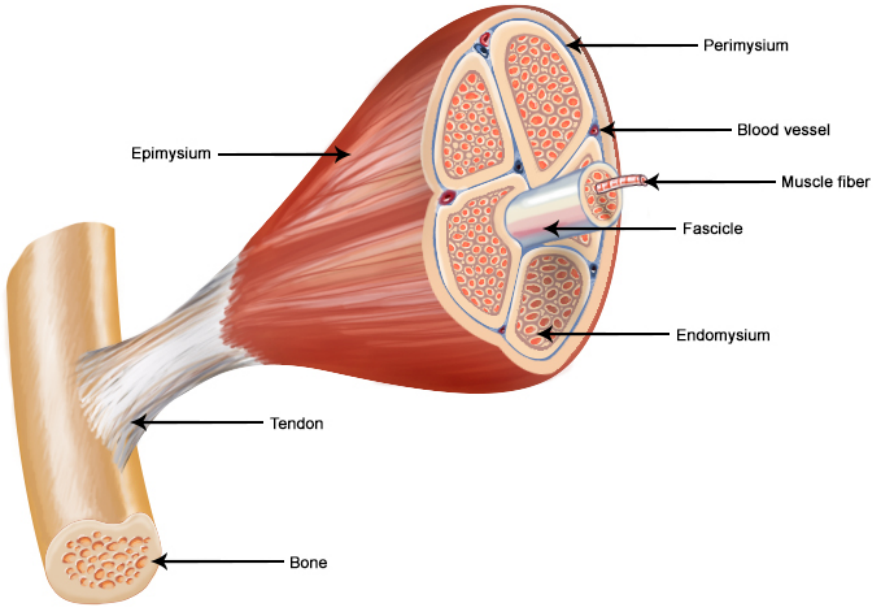


Figure 1.1 Skeletal muscle structure

Adapted from: brachialartery.com

Individual muscle fibres are further organized, being surrounded by a plasma membrane called the sarcolemma. Within the sarcolemma, multiple contractile subunits called myofibrils are grouped, surrounded by the sarcoplasm. Extensions from the sarcolemma extend into the muscle fibre, called transverse tubules (T tubules), passing within and around each myofibril. T tubules allow rapid transport of substances and action potentials to the sarcoplasmic reticulum (SR), a longitudinal network of tubules within each muscle fibre, acting as calcium storage (Figure 1.2).

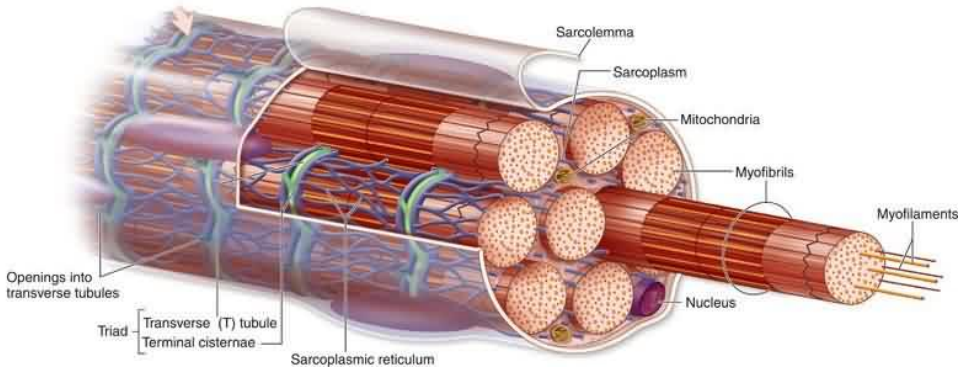


Figure 1.2 Skeletal muscle fibre structure

Adapted from: http://fau.pearlashes.com/anatomy

Transversely, myofibrils may be designated into continuously joined sarcomeres. Sarcomeres contain two types of organised proteins, muscle specific myosin (thick filaments) and actin (thin filaments). At the boundary to each sarcomere, termed Z-disks; actin is anchored, extending towards the centre. The Z-disks contain α-actin arranged in a stabilising framework, supporting contraction (Sjöblom et al. 2008). Within the central region of a sarcomere, myosin proteins overlap the extended actin fibres (Figure 1.3). Contraction of muscle occurs, not through the shortening of these proteins, but rather by actin moving along myosin filaments. This happens simultaneously within each sarcomere, shortening the distance between Z-disks. This occurrence is an ATP driven series of reactions, which are repeated to allow full movement of actin along myosin filaments.

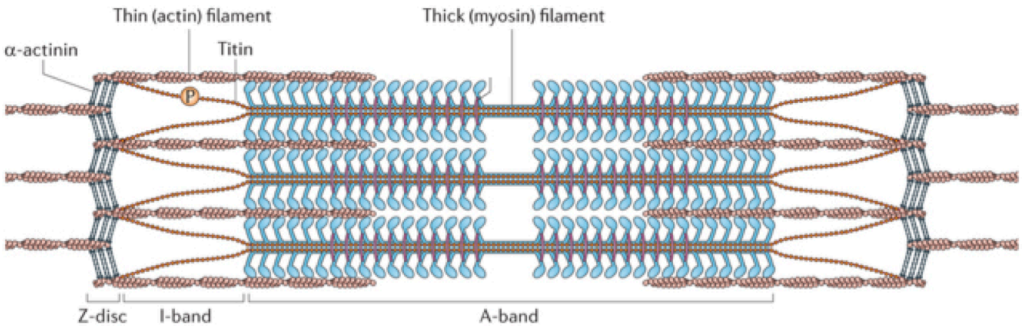


Figure 1.3 Sarcomere structure

Adapted from: (Hwang & Sykes 2015)

Within mammalian skeletal muscle there are several fibre types, dependant on the expression of specific myosin isoforms and energetic properties (Schiaffino & Reggiani 2011). Fibre types were initially classified based upon their appearance and contractile aspects: red slow contractile and white fast contractile (Brooke & Kaiser 1970). Further investigations clarified specific myosin isoform expression and oxidative characteristics within these fibres, leading to their reclassification as: slow red type I, fast

red type IIa and fast red type IIx (Table 1.1) (Harridge et al. 1996; Smerdu et al. 1994; Peter et al. 1972). Hybrid fibres co-expressing multiple myosin isoforms have also been observed (Kohn et al. 2007; Sant'ana Pereira et al. 1995). Rodents and other mammals additionally express type IIb fibres, similar to type IIx ones (Tasi et al. 2011). The functional aspects of individual muscles are determined by the proportion and distribution of fibre types it contains, differing based upon the location and function of the muscle.

Table 1.1 Skeletal muscle fibre characteristics

Classification scheme	**Fibre type**			
Contractile speed	Slow-twitch	Fast-twitch	Fast-twitch	Fast-twitch
Myosin heavy chain	Type I	Type IIa	Type IIX	Type IIb
Metabolic function	Oxidative	Oxidative	Glycolytic	Glycolytic
Fibre CSA	Small	Medium	Large	Large

Table adapted from: (Spangenburg & Booth 2003)

1.3 Skeletal Muscle Health and Metabolism

1.3.1 Satellite cells and myogenesis

Skeletal muscle precursors arise from mesodermal progenitor cells, with development occurring through the fusion of elongated myoblasts to form myotubes. Developed myotubes are mitotically inactive, multinucleated cells, containing large volumes of contractile proteins. Myotubes increase in size through the synthesis of additional contractile proteins and the acquisition of new nuclei through myoblast fusion, resulting in the development of large multinucleated myotubes. Fully developed muscle has the distinguished ability for regeneration through the fusion of

mononucleated quiescent satellite cells. Satellite cells are thought to occupy approximately 4% of muscle nuclei within healthy adults (Hawke & Garry 2001) and are situated underneath the basal lamina abutting adjacent myofibrils.

Once activated, satellite cells undergo proliferation producing myoblast cells as well as another quiescent satellite cell, potentially replenishing the population (Tedesco & Dellavalle 2010). During proliferation, quiescent satellite cells enter the cell cycle from either G0 or G1, progressing into S phase, before G2 and M phase (Figure 1.4).

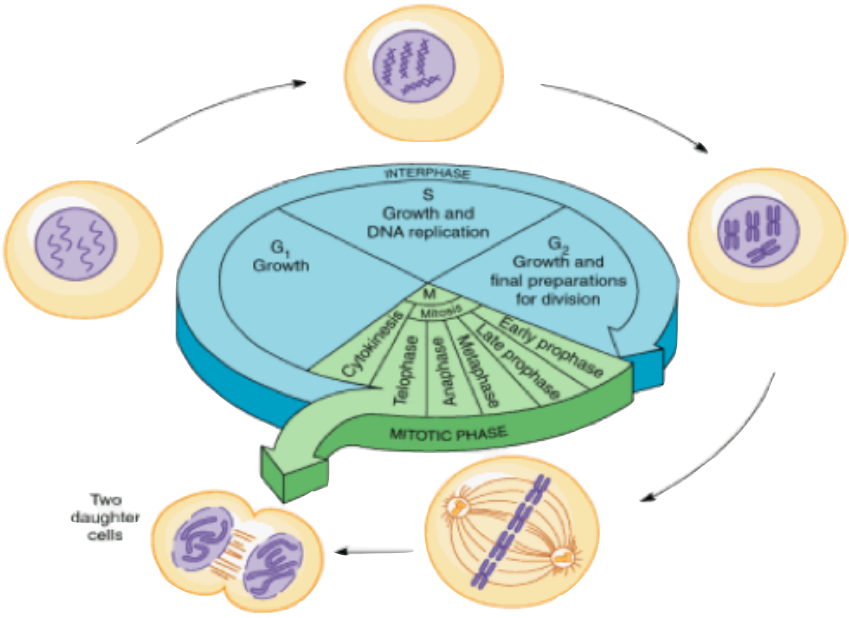


Figure 1.4 Cell cycle

Illustration of the mitotic cell cycle progression from G1, S, G2 and M phase. Adapted from: studyblue.com

The regulation of satellite cell regenerative abilities are not fully understood, however hierarchical expression of myogenic factor 5 (*MYF5*) and myoblast determination protein (*MyoD*) induces activation of satellite cells into myoblasts (Rudnicki & Jaenisch 1995). These satellite cell derived myoblasts are capable fusing with myofibrils, increasing the total number

of myonuclei as well as cytosolic volume. Further sequential expression of myogenin and muscle-specific regulatory factor 4 (*MRF4*) induce cell cycle withdrawal, and the fusion of myoblasts into terminally differentiated multinucleated myotubes (Andrés & Walsh 1996). Transcription factors such as the continually expressed *Pax7* by quiescent satellite cells, are known to be of key importance for regulation of the previously mentioned myogenic regulatory factors (MRFs) *MyoD* and *MYF5* (Program 2008; Sambasivan et al. 2011). Overall, satellite cells are believed to be required for muscle repair. Their loss is known to lead to skeletal muscle degeneration in diseases such as muscular dystrophies. Satellite cell proliferation may be induced through skeletal muscle damage and their subsequent regeneration (Hardy et al. 2016; Lepper et al. 2011). However, the role of satellite cells within skeletal muscle hypertrophy is unclear (Wang & Rudnicki 2011). Within one study, mechanical overload upon satellite cell deplete plantaris muscles, demonstrated fibre hypertrophy similar to control animals. However, increased Pax7 positive and BrdU labelled nuclei were observed, indicating a role of satellite cells in hypertrophy but not a requirement (McCarthy et al. 2011).

1.3.2 Muscle protein metabolism

The maintenance of skeletal muscle mass is regulated by the dynamic equilibrium of protein turnover, namely the balance between muscle protein synthesis (MPS) and muscle protein breakdown (MPB) (Volpi et al. 2001). For protein anabolism to occur, net MPS needs to exceed net MPB, whereas catabolism is the reverse. Exercise and nutrition are robust stimulators of MPS, promoting protein anabolism and increasing muscle mass, whilst reducing MPB (Tipton & Ferrando 2008). Starvation or immobilisation result in a loss of muscle mass. However this may not occur

necessarily through increases in MPB, but rather through a suppression of MPS and anabolic stimulation (Marimuthu et al. 2011). Ultimately, the regulation and balance of MPS and MPB over an extended period will determine changes in muscle mass.

1.3.3 Muscle protein synthesis

The synthesis of proteins requires the genetic information from DNA transcribed to mRNA, allowing the correct sequential assembly of amino acids (AA). Initially transcription factors bind to DNA response elements found within premotor regions, ahead of the desired coding sequence. Various additional transcriptional proteins including RNA polymerase further bind to the response elements to produce the mRNA transcripts. Termination is induced by specific nucleotide sequences that when transcribed, form complementary 'hairpin' sequences. Post-transcriptional mRNA modification may also be required before translation can occur; for instance, addition of poly (A) tails or the removal of intron regions.

Once synthesised, mRNA strands provide the correct AA sequence for the transcription of the desired protein. Single AA residues do not bind directly to mRNA, but are instead bound to tRNA with a specific corresponding codon. The sequence of the codon will determine which of the 20 amino acid residues or a 'stop' signal will be designated. Translation occurs within a ribosomal unit, and happens in stages of initiation, elongation and termination. Translation begins with the formation of the preinitiation complex, through eIF4E (eukaryotic translation initiation factor 4E) incorporating into the eIF4F complex (Hershey & Merrick 2000). The complex binds to mRNA, before further interactions with eIF4A, eiF4B and eIF4G, and subsequent binding of the 40S ribosomal subunit along with eIF2 and eIF3. Methionyl-tRNA supplies the primary amino acid,

whereupon the initiation factors disassociate from 40S subunit allowing the attachment of the 60S subunit (Figure 1.5) (Gingras et al. 2001). The resultant 80S ribosome consequently instigates elongation, as tRNA complementary to the mRNA transcript becomes bound to the ribosomal unit. The process of elongation will continue until a stop codon within the transcript initiates termination, through the addition of a polypeptide release factor. Once the polypeptide has begun to emerge from a ribosome it will undergo post-translational modification, such as folding into its tertiary structure with the aid of chaperone proteins. Further modification may still occur such as glycosylation or methylation. Interestingly an increase in mRNA abundance may not necessarily be the determining factor of the rate of synthesis; instead it may be due to an increase of translational efficiency throughout translation (Laurent et al. 1978).

The formation of the 40S and 60S subunits occurs through ribosomal biogenesis. This process is highly coordinated, synthesising ribosomal RNA (rRNA), ribosomal proteins and their ensuing assembly (Chaillou et al. 2014). Ribosomal biogenesis is directed by three nuclear RNA polymerases, Pol I, II and III. Structural rRNA components are transcribed by Pol I, producing a single 47S precursor rRNA (Roeder & Rutter 1970). This subsequently undergoes exonucleolytic and endonucleolytic cleavage to produce 18S, 5.8S and 28S rRNA components (Bowman et al. 1981). An additional 5S rRNA is transcribed by Pol III, along with tRNA (Weinmann & Roeder 1974). Pol II transcribes many ribosomal proteins for assembly into 40S and 60S subunits. 40S subunits are produced by the formation of 18S rRNA and approximately 32 ribosomal short proteins (RPS), whereas 60S subunits are formed from 5S, 5.8S and 28S rRNA with roughly 47 ribosomal long proteins (RPL) (van Riggelen et al. 2010). Assembled

subunits are exported to the cytoplasm, whereby they are utilised for translation (Figure 1.5). It is generally considered that 85% of total cellular RNA is comprised of rRNA, allowing assessment of ribosomal biogenesis through changes in tissue RNA content (Nader et al. 2002).

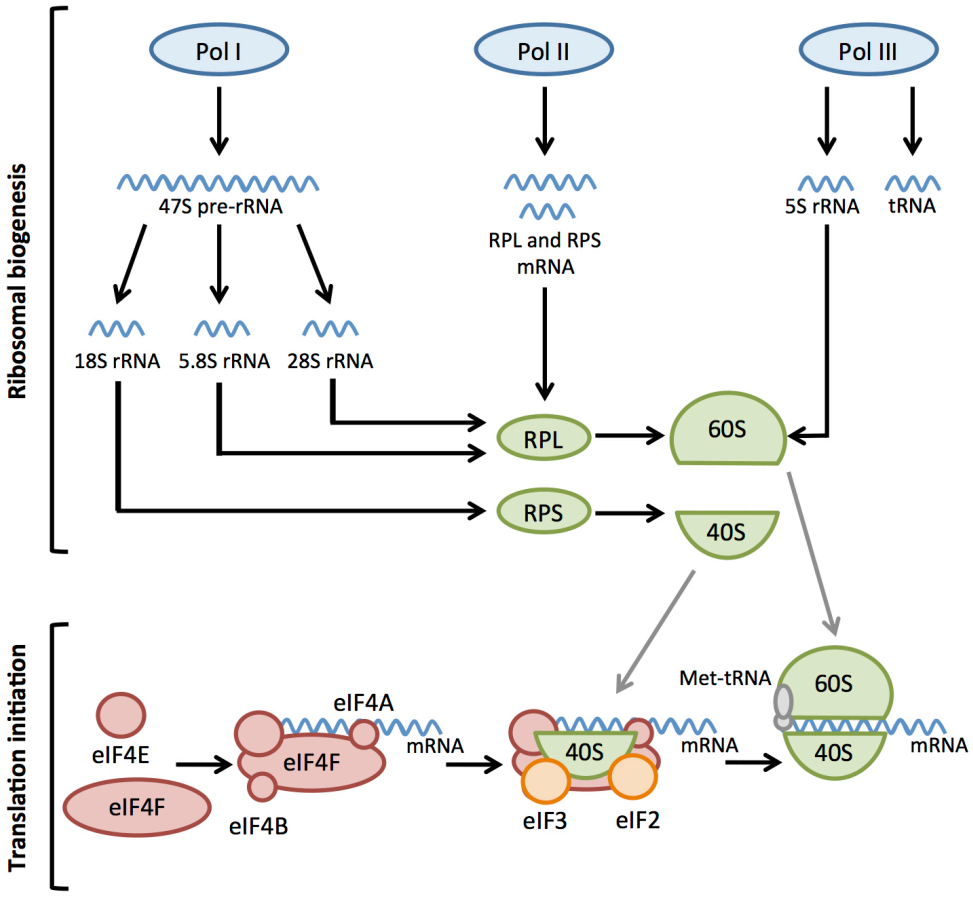


Figure 1.5 Ribosomal biogenesis and translation initiation

Ilistration of the multiple pathways required for ribosomal biogenesis by POL I, II and III. Ribosomal long and short proteins produce the 60s and 40s ribosomal subunits respectively, allowing the formation of the initiation complex. Adapted from: (van Riggelen et al. 2010)

The mammalian target of rapamycin (mTOR) is a central regulator of protein synthesis, responding to nutrient availability, growth factors, energy status and stress (Proud 2013). Activated mTOR is known to phosphorylate S6K1 (additionally known as P70S6K1) and 4E-BP1, key regulators of protein synthesis (Baar & Esser 1999). S6K1 regulates

translation initiation through the subsequent phosphorylation of multiple proteins, namely eIF4B, which allows an elevation in eIF4A helicase activity (Dennis et al. 2012). Furthermore, S6K1 phosphorylates and activates ribosomal protein S6 (RPS6), a component of the 40S ribosomal complex (Magnuson et al. 2012). Additionally, S6K1 phosphorylates and prevents the inhibitory action of eukaryotic elongation factor 2 kinase (eEF2K) involved within translation elongation. 4E-BP1 is an inhibitory protein bound to eIF4E, whereby phosphorylation by mTOR triggers dissociated from eIF4E, allowing assembly of the initiation complex (Figure 1.6) (Rong et al. 2008).

Additional to the control of translation, mTOR regulates ribosomal biogenesis, enhancing protein synthetic capacity (Proud 2013). Pol I transcriptional activity requires the basal factors transcription initiation factor I (TIF-1) A, SL1 and upstream binding factor (UBF), with mTOR regulating their activity (Mayer et al. 2004). Furthermore, UBF have been demonstrated to be regulated by mTOR in an S6K1 dependant manner (Hannan et al. 2003). Additionally, mTOR acts to regulate Pol III transcription of 5S rRNA and tRNA through arrest of MafI inhibition of Pol III (Figure 1.6) (Shor et al. 2010).

Signalling proximal to mTOR allows its regulation in response from internal or external stimuli. Phosphorylation of the insulin-like growth factor (IGF) receptor by a substrate subsequently recruits insulin receptor substrate (IRS1), activating PI3K. PI3K activation subsequently results in AKT phosphorylation, which in turn phosphorylates tuberous sclerosis (TSC) 1/2 complex (Weigl 2012). It has been demonstrated that TSC1/2 inhibits mTORc1 activity until phosphorylated by Akt (Inoki et al. 2002). To

prevent over-activation of mTOR, a feedback loop exists utilising S6K1 to directly phosphorylate IRS1; inhibiting further IRS induced signalling (Figure 1.6) (Tremblay et al. 2007).

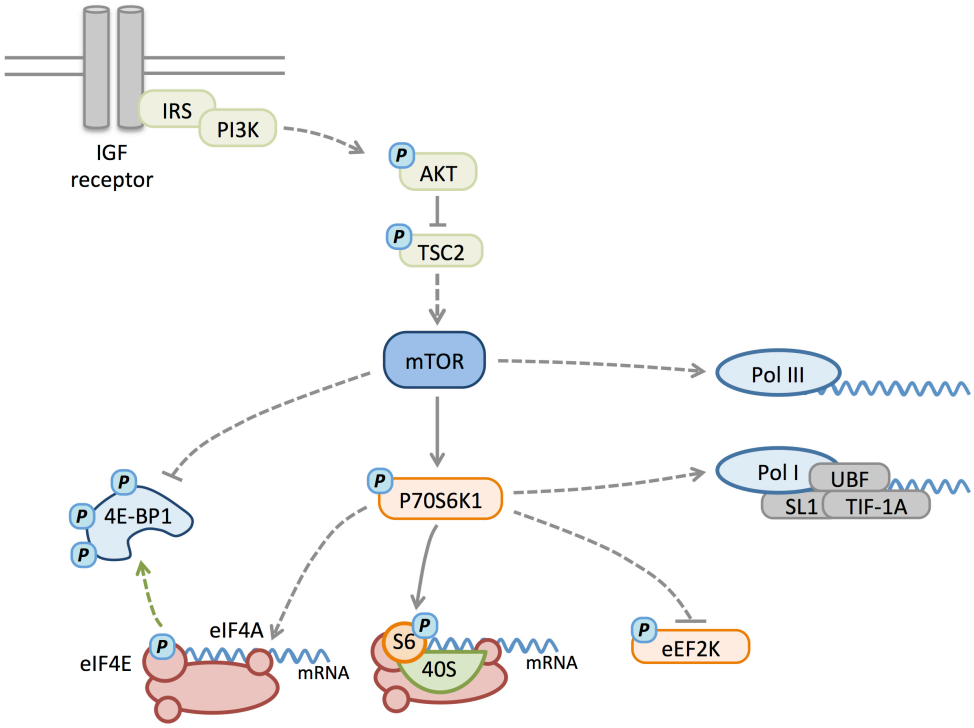


Figure 1.6 AKT/mTOR anabolic signalling

Illustration of the AKT/mTOR anabolic pathway, initiated by IGF-R. Phosphorylation of AKT results in subsequent phosphorylation of TSC2, mTOR, 4E-BP1 and P70S6K1. Phosphorylation of 4E-BP1 and P70S6K1 allows the formation of the initiation complex and translation initiation respectively.

1.3.4 Muscle protein breakdown

Various mechanisms for the degradation of proteins within muscle have been identified, and have been shown be initiated by various stimuli are occur to remove specific proteins that are either incorrect or no longer required. Through the removal or alteration of some inhibitory proteins, various signalling cascades may become initiated. However degradation is regulated at various steps to allow target specificity and modulation to occur.

1.3.4.1 Ubiquitin-proteasomal degradation

The ubiquitin-proteasome pathway (UPP) relies up the trafficking of targeted proteins from other regions of the cell *via* ATP dependant ubiquitation (Glickman & Ciechanover 2002; Mitch & Goldberg 1996). An E1 enzyme through an ATP dependant reaction initially activates Ubiquitin (Ub), which is subsequently transferred by an E2 carrier protein to a lysine (Lys) residue on the target protein. The reaction is catalysed by an E3 ligase specific to a target protein. The initial Ub will then be further ubiquitated, generating a chain of Ub molecules. This process allows recognition by a 26s proteasome and will undergo degradation, generating cleavage products of approximately 7-9 residues (Baumeister et al. 1998). However these short peptide chains can readily undergo further degradation by endopeptidases such as thimet oligopeptidase (TOP) or by aminopeptidases, producing free amino acids for further protein synthesis or metabolism (Saric et al. 2004).

Within muscle, two particular ubiquitinating enzymes, $E2_{14K}$ and E3α have been shown to be involved in UPP degradation (Jagoe & Goldberg 2001). Inhibitors targeted to E3α have shown decreased ubiquitation of muscle proteins as well as proteasomal degradation (Solomon et al. 1998). However the major components of myofibrils, actin and myosin cannot initially be degraded through the UPP and require disassociation from one another to reveal the destabilising amino acid. This may be achieved through various mechanisms, such as caspase or (Du et al. 2004) calpain (Williams et al. 1999) activation and may be a rate limiting step in myofibril degradation. This disassociation may expose the destabilising amino acid terminal required for ubiquitation allowing degradation to follow (Solomon & Goldberg 1996). Fundamentally, the majority of muscle

protein degradation may occur through ubiquitation, but protein complexes such as actin and myosin may require initial degradation through alternate methods.

1.3.4.2 Caspase and calpain degradation

As previously discussed, actin-myosin complexes require initial cleavage to allow degradation through the UPP. Caspase-3 has been demonstrated to degrade these complexes, producing an actin fragment capable of ubiquitation (Du et al. 2004). Increased levels of caspase-3 have been observed in diabetic rat muscle with rates of degradation reduced in the presence of a caspase-3 inhibitor (Du et al. 2004). Another study using cachexic mice (Belizário et al. 2001), showed various increases in the expression of multiple caspases within muscle. Thus, caspases provide a rate-limiting step within protein degradation, by the creation of substrate capable of ubiquitation.

Calpains are a family of cytosolic proteases that rely upon Ca^{2+} activation to cleave various proteins. It is thought the human genome contains genes for multiple calpain variants, including calpain-1 (μ-calpain) and calpain-2 (m-calpain) which require micromolar and millimolar concentrations of Ca^{2+} respectively (Goll et al. 2003). Their involvement in cellular processes is widespread, ranging from apoptosis, cell migration, differentiation and cytoskeletal reorganisation (Khorchid & Ikura 2002). As they are involved in various processes, it is no surprise altered expression or activity have been linked to several diseases including; type 2 diabetes, Alzheimer's, muscular dystrophies and multiple sclerosis (MS) (Goll et al. 2003). Moreover, calpains have increasingly been linked with muscle protein degradation. Evidence showing the disruption of Z-disks during starvation, causes disassociation between actin-myosin complexes (Dahlmann et al.

1986). Z-disk disruption may also be a result of intense exercise (Belcastro et al. 1998). It has been speculated, Z-disk disruption is influenced through Ca^{2+} dependant calpain cleavage within rat skeletal muscle (Williams et al. 1999). Additionally, calpain inhibition has been shown to reduce MPB within MS rat models (Park et al. 2012). Z-disk disruption may also be prevented through the addition of inhibitors targeted towards the release of cytosol Ca^{2+} stores (Williams et al. 1999). Similar to the role caspases play in the initiation of the UPP; calpains may also provide a similar role (Jackman & Kandarian 2004). Although caspases and calpains may not perform the majority of muscle protein degradation, they may provide regulation, through the production of substrate for other degradation processes such as UPP.

1.3.4.3 Autophagy mediated degradation

The final major proteolytic mechanism is autophagy mediated degradation, primarily utilised in the degradation and recycling of various proteins, protein aggregates, as well as dysfunctional organelles such as mitochondria (mitophagy) (Ashrafi & Schwarz 2013). Degradation occurs within vesicles and happens in four stages: induction, autophagosome formation, fusion and vesicle breakdown. Various regulatory mechanisms can induce autophagy, causing proteins intended for degradation to be become contained and transported within membrane bound autophagosomes. Microtubule-associated protein light chain 3 (LC3-I) is essential during autophagosome membrane formation, whereby it is conjugated to phosphatidylethanolamine, producing LC3-II (Kabeya et al. 2000). Once produced, autophagosomes fuse with lysosomal vacuoles, releasing the contents into the highly acidic environment of the lysosome.

This low pH allows denaturing of proteins to occur as well as activating various proteolytic enzymes such as cathepsin proteases and hydrolases.

Much speculation has occurred into the role of lysosomal mechanisms in MPB. Originally, lysosomes were not thought to play a major role in degradation. Studies demonstrated the addition of lysosomal inhibitors leupeptin and Ep-475 did not reduce protein degradation in damaged rat muscle (Furuno & Goldberg 1986). However, these inhibitors are specific towards cathepsin B among others, but not towards additional ones involved in autophagy such as cathepsin A and D. There now appears to be growing evidence suggesting lysosomal degradation does in fact play a role in muscle atrophy in conditions such as fasting (Mammucari et al. 2007), denervation (O'Leary et al. 2012) and cancer cachexia (Penna et al. 2013). Furthermore, autophagy mediated degradation has been demonstrated to contribute to denervation induced proteolysis (Furuno et al. 1990), with cathepsin L being upregulated in muscle atrophy (Deval et al. 2001).

Moreover, lysosomal degradation seems to play an important function in the maintenance of overall muscle health. Mitochondrial dysfunction is speculated to be involved within various diseased states having been thoroughly reviewed for associations in neurodegeneration (Lin & Beal 2006), Parkinson's disease (Abou-Sleiman et al. 2006), Alzheimer's disease (Castellani et al. 2002), type II diabetes (Lowell & Shulman 2005) as well as sarcopenia (Marzetti et al. 2013). Along with various disease states, mitochondrial dysfunction will also alter muscle metabolism, greatly influencing overall muscle homeostasis. Mitophagy has been implicated in the regulation of dysfunctional mitochondria *via* lysosomal degradation,

allowing the accumulation of dysfunctional organelles to be limited, preventing cellular damage.

1.3.5 Glucose metabolism

Glucose is an essential fuel for skeletal muscle contraction and normal metabolic processes. Skeletal muscle is heavily involved in the overall glucose metabolism, functioning as the largest insulin sensitive tissue within the body. As such regulation of insulin mediated uptake and metabolism is vital to respond effectively to changes in nutrition and expenditure. Exercise has long been recognised to induce skeletal muscle uptake of glucose (Goldstein et al. 1953), principally determined by exercise duration and intensity (Wahren et al. 1971). Glucose transporter 4 (GLUT-4) is responsible for exercise and insulin mediated glucose uptake into skeletal muscle; furthermore being shown to be upregulated in trained individuals (Hickner et al. 1997).

Plasma glucose concentrations are regulated by the rate of glucose entering the circulation, balanced by the rate of removal. Insulin mediated glucose uptake is the predominant means of glucose disposal, with skeletal muscle the key tissue. Principally, removal by muscle occurs through glucose transported through the muscular capillary network, before binding to GLUT-4 at the plasma membrane and internalised. Once internalized, glucose is phosphorylated to glucose 6-phosphate (G-6-P), whereby it subsequently undergoes glycolysis or glycogenesis. Approximately 70% of ingested glucose is utilised immediately through catabolism, while the remaining 30% may be stored as glycogen (Shulman et al. 1990). These stores may be consumed during exercise to provide the required energy for contraction. Greater glycogen stores are typically found within trained muscles, along with a more acute sensitivity to insulin.

Expression and localization of GLUT-4 to the plasma membrane is a rate-limiting step within glucose uptake (Bryant et al. 2002). Insulin stimulates the release of GLUT-4 from intracellular storage sites, whereby it translocates to the plasma membrane, facilitating glucose transport (Suzuki & Kono 1980). Dysregulation in either the production or sensitivity to insulin, disrupting the body's regulation of blood glucose may result in the development of type II diabetes (T2D).

1.3.6 Regulation of muscle protein metabolism

1.3.6.1 Regulation of muscle metabolism by environmental stimuli

It has long been known that feeding causes changes in our overall health including increases in muscle mass. Initial studies identified macronutrient containing mixed meals, stimulated greater rates of muscle protein synthesis. Further studies recognised AAs as the stimulating factor, with essential amino acids (EAAs) being further identified to be the origin of this occurrence, particularly leucine. Branched chain AAs have been suggested to act as an assessor of AA availability due to their inability to be synthesised within humans (Bohé et al. 2003; Kimball et al. 1999). One method of effect EAAs is the through the formation of Rag A/B and Rag C/D heterodimer complexes (Sancak et al. 2008). This complex further binds GTP and GDP, causing an association with mTOR, leading to the initiation of protein synthesis (Sancak & Sabatini 2009). It also has been demonstrated that amino acids are capable of activating hVps34, a class III PI3K, further activating mTOR, resulting in S6K1 phosphorylation (Nobukuni et al. 2005). Interestingly, administration of L-leucine has been shown to greatly increase insulin secretion from rat pancreatic cells. This

suggests availability of AAs not only initiates MPS through anabolic stimulation, but also inhibits degradation *via* insulin signalling (Sener & Malaisse 1981).

Continual muscle use in various forms such as exercise and manual labour causes a hypertrophic response. Numerous factors will influence the rate of this increase, for example the duration of exercise, nutritional status, intensity and arguably the most important, the type of exercise. Resistance exercise training (RET) has been demonstrated in many studies to be an effective stimulant of MPS, with continual training over time resulting in muscle hypertrophy (Phillips et al. 1997; West et al. 2015; Brook et al. 2015; Phillips et al. 2013). This increase is MPS interestingly does not occur during the resistance exercise bout, and has in fact been shown to be suppressed within humans (Fujita et al. 2009; Kumar et al. 2009b). This reduction of synthesis may in part occur as a result of a reduction in 4EBP1 phosphorylation essential for translation initiation (Dreyer et al. 2006). AMPK activation, an important mTOR inhibitor was also observed have increased activity during resistance exercise. Ultimately this reduction in protein synthesis during exercise initially seems counter intuitive but may in fact have arisen to reorganise ATP utilisation.

Once exercise has concluded, MPS increases during a recovery period that is initially small before greatly increasing. Various investigations using different stable isotope tracers have reported increases in fractional synthesis rates (FSR) 1 hour post exercise to increase between 0.06%.h^{-1} (Kumar et al. 2009a) and 0.08%.h^{-1} (Dreyer et al. 2006), increasing approximately 0.02%.h^{-1} from basal measurements. Within these studies the greatest FSR increase was observed 2-4 hours post exercise and can

persist for up to 48 hours (Phillips et al. 1997). Increases in protein synthesis post exercise may be a result of increased phosphorylation of mTOR and S6K1 leading to more efficient translational initiation and elongation (Dreyer et al. 2006). Ingestion of EAAs immediately prior to exercise has been shown increases in the duration as well as potency of the enhanced protein synthesis (Kumar et al. 2009b). These increases in protein synthesis however do not seem to be as effective when only one stimulus is available indicating it may result from the combined influence (Bohé et al. 2001).

1.3.6.2 Regulation by catabolic conditions

Increases in the expression of mRNAs crucial for UPP have been observed within various atrophy models such as cancer cachexia (Baracos et al. 1995), diabetes (Price et al. 1996; Lecker et al. 1999), renal failure (Debigaré & Price 2003) and starvation (Medina et al. 1995). Expression of mRNAs for Ub fusion proteins, Ub ligases as well as multiple components of the 26s proteasome have also been observed to increase within these disease states in rats (Lecker et al. 2004).

Changes in muscle usage are well known to influence muscle mass and mechanisms that allow its regulation. Muscle inactivity is associated with a loss in total mass termed disuse atrophy. Collectively the outcome of disuse is the same but may arise due to various processes such as muscle denervation due to spinal chord injury, limb casts as a result of fractures, chronic sedentarism and hospitalisation induced bed rest. A loss in muscle mass may have profound effects, such as the loss of strength and muscle function due to the loss of contractile elements and alterations in glucose metabolism. These changes increase the likelihood of individual developing

insulin resistance. As previously discussed, exercise result in an increases MPS, however during disuse, increased degradation does not seem to be the primary cause of atrophy. Instead it is proposed the lack of stimuli results in the reduction in basal MPS rates (Gibson et al. 1987; Phillips et al. 2009). It has also been demonstrated that within immobilised individuals, anabolic stimulation through the ingestion of AAs has a diminished effect (Glover et al. 2008). As protein turnover is a continual cycle of changes in the equilibrium of protein turnover, the loss of AA stimulus will result in net synthesis being less than basal and fasting induced degradation.

1.3.6.3 Sarcopenia

Beyond 50 years of age, muscle mass decreases approximately 1-2% per year, resulting in a loss of function as well as increased susceptibility to metabolic disorders. This phenomenon is termed sarcopenia. The prevalence of sarcopenia in individuals' aged 65-70 is approximately 13% and 24% for men and women respectively. One proposed manner of this decline may be due to a decrease in satellite cell populations within the elderly compared to healthy adults (Collins et al. 2007). Ultimately this may lead to an increased inability to respond to muscle damage through satellite cell regeneration. This decrease in satellite cell population has however been seen to be reduced or halted in aged rats who underwent exercise (Shefer et al. 2010).

Within aging, muscle mass predominantly declines through the reduction in fibre size and loss of type II (fast twitch) fibres rather than type I (slow twitch) (Deschenes 2004). Unlike other disease states, sarcopenia has not been associated with large changes in either basal MPS or MPB

(Cuthbertson et al. 2005). Instead it has been suggested to occur through a blunted responses to exercise as well as nutrition (Dorrens & Rennie 2003; Wilkes et al. 2009; Sakuma & Yamaguchi 2012; Kumar et al. 2009a). This has been characterised since individuals who undertake moderate exercise have been shown have a loss of muscle mass similar to those who are passive (Rutherford & Jones 1992).

Anabolic signalling mechanisms have been observed to differ between healthy young and old individuals who undergo resistance exercise (Kumar et al. 2009a). Protein synthesis was shown to increase in both age groups in response to exercise compared to basal values. However synthesis rates were markedly lower in older individuals compared to younger individuals 1-2 hours post exercise. The phosphorylation of P70S6K and 4EBP1, essential regulators of protein synthesis were also shown to be lower within the older group. Diminished anti-proteolytic effects of insulin have also been demonstrated within older individuals (Wilkes et al. 2009). Stimulation of MPS has also been shown to be reduced in response to small doses of EAAs within elderly subjects (Katsanos et al. 2005). These dampened responses to proteostatic mechanisms ultimately result in a net loss of muscle mass over time, as net synthesis rates do not exceed degradation. Although changes in protein metabolism are not predominantly altered in sarcopenia, a diminished response to both protein synthesis and degradation pathways will greatly impact overall protein turnover.

1.4 Vitamin D and the vitamin D receptor

1.4.1 Potential importance in muscle

Vitamin D was originally identified to be essential for the prevention of rickets (Arthur W. Ham 1934), with considerable investigations occurring into its mechanism and role in bone. VitD acts through the vitamin D receptor (VDR), expressed in multiple tissues (Norman 2008). Generation of a VDR knockout mice allowed the examination of its role within VitD signalling in multiple tissues. The VDR has been demonstrated to modulate cell proliferation, immune response and glucose homeostasis (Bouillon et al. 2008) Furthermore, demonstrations of VitD/VDR mediated functions in skeletal muscle have gathered considerable interest (Bouillon et al. 2014; Pojednic & Ceglia 2014).

1.4.2 Background

Vitamin D (VitD), a lipid soluble secosteroid, classically acts in the regulation of calcium (Ca^{2+}) and phosphate (P_i) homeostasis to maintain bone health (e.g. osteomalacia (Bhan et al. 2010) and osteoporosis (Rizzoli et al. 2008)), within target tissues, i.e. bone, intestines and kidney. VitD mediates and acts through the ubiquitously expressed vitamin D receptor (VDR) (Norman 2008). VitD deficiency is highly prevalent (<40% of adults) (Forrest & Stuhldreher 2011), effecting many tissues other than bone, with influences upon skeletal muscle function (Dhanwal et al. 2013), development of type 2 diabetes (T2D) (Pittas et al. 2007) and immune response (Panel & Nda 2010). The regulatory role VitD and the VDR may have within these tissues is currently unclear.

1.4.3 Vitamin D synthesis and metabolism

In order for VitD to exert a physiological response, it undergoes a series of conversion and hydroxylation steps (Figure 1.7). VitD can be acquired through the diet in the form of vitamin D_2 (ergocalciferol), or exposure of the skin to UV light at a wavelength of 290-315nm (Holick 1995). This converts 7-dehydrocholesterol to pre-vitamin D_3, whereupon thermal isomerization in the skin further converts pre-vitamin D_3 to Vitamin D_3 (cholecalciferol). The rate and efficiency of converting 7-dehydrocholesterol to vitamin D_3 is subject to multiple factors regulating UV exposure (Holick 1987). These include: sunscreen, skin pigmentation, season and latitude. The latter two may be the most influential, as in winter months (i.e. November to February) locations higher than 44^{O}N latitude, UV radiation is not of a sufficient strength to induce conversion (Kimlin et al. 2007; Spiro & Buttriss 2014). Vitamin D_2 and D_3 only differ in the structure of the side chain, but do not effect subsequent metabolism or physiological functions (Jones et al. 1998).

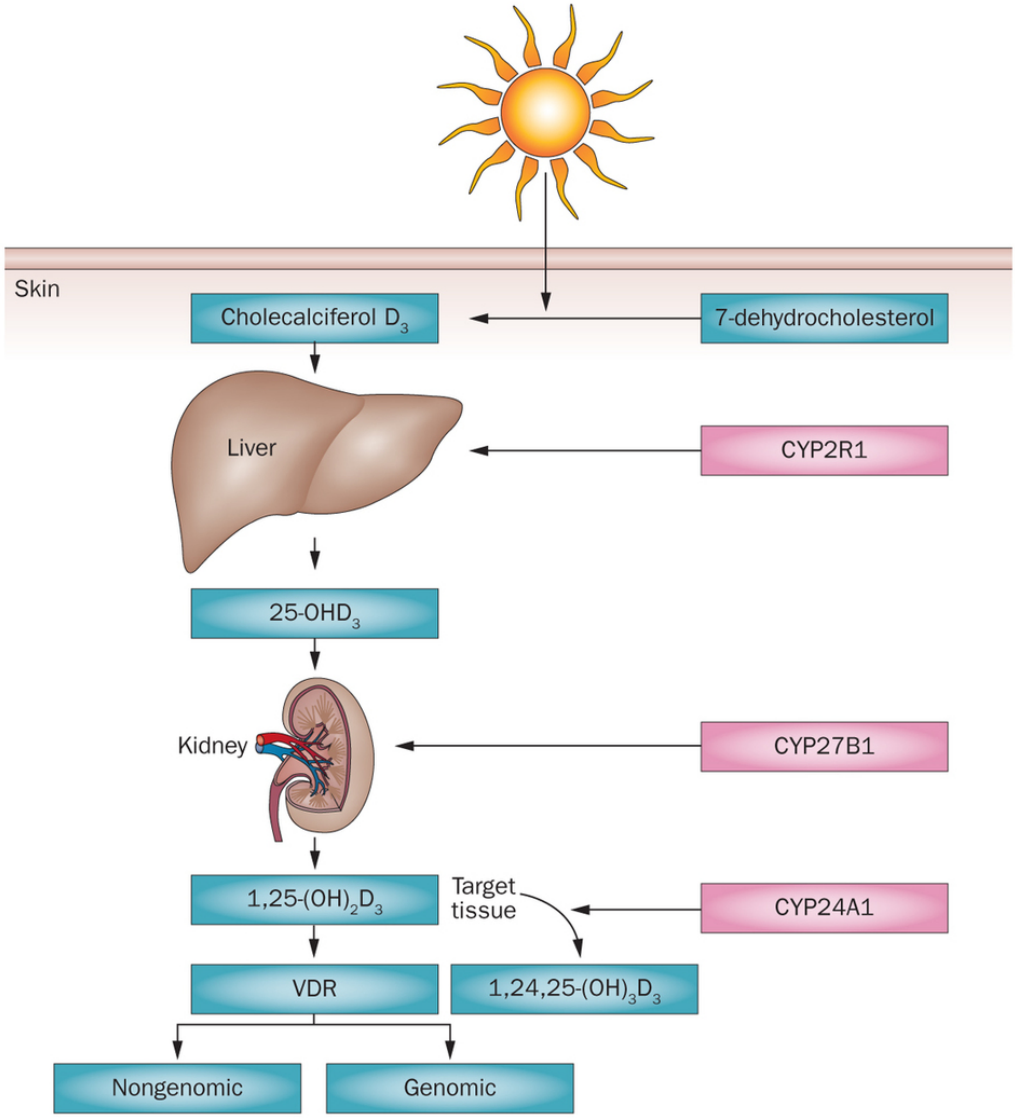


Figure 1.7 Vitamin D metabolism

Schematic diagram of VitD metabolism from initial 7-dehydrocholesterol conversion to vitamin D_3. Subsequent hydroxylation steps in the liver and kidneys produces active 1α,25[OH]$_2D_3$ by CYP27B1, whereby it acts through the VDR before inactivation by CYP24A1 to form 1,24,25[OH]D. Adapted from: (Blomberg Jensen 2014)

Once initially converted, vitamin D_3 is transported from dermal layers to the liver through the circulation, bound to the vitamin D binding protein (DBP) (Imawari et al. 1976). Despite initial conversion, vitamin D_3 and dietary D_2 are biologically inactive, requiring two independent enzymatic hydroxylation reactions to induce biological effects. The first reaction attaches a hydroxyl group to carbon-25, producing 25-hydroxyvitamin D

(25[OH]D) by a cytochrome P450 25-hydroxylase identified as the CYP2R1 protein (Cheng et al. 2004). Investigations be DeLuca identified the liver as the principal physiologic site of the initial hydroxylation, as isolation of the liver in rats eliminated 25[OH]D metabolism. Subsequently, 25[OH]D will undergo a second hydroxylation step by 1α-hydroxylase CYP27B1 producing the biologically active 1α,25-dihydroxyvitamin D (1α,25$[OH]_2$D). Finally, inactive 1,24,25[OH]D is produced through further hydroxylation by 25-hydroxyvitamin D_3-24-hydroxylase (CYP24A1) (Pike & Meyer 2012).

The cell-surface receptor megalin allows internalization of the 25[OH]D/DBP complex, with expression in skeletal muscle recently confirmed (Abboud et al. 2013). The kidneys are thought to be the main tissue responsible for systemic circulating 1α,25$[OH]_2$D levels, as people with renal failure are commonly VitD deficient (Del Valle et al. 2007; González et al. 2004). Additionally CYP27B1 mRNA levels can be 40 fold higher than other tissues (Omdahl et al. 2002). Despite this, CYP27B1 mRNA is expressed in multiple other tissues thought to be VitD sensitive such as skin (Bikle et al. 1986), intestinal (Anderson et al. 2008), bone (Anderson et al. 2010), macrophages (Adams & Gacad 1985) and skeletal muscle (Girgis, Mokbel, et al. 2014; Srikuea et al. 2012). The expression of extra-renal CYP27B1 is thought to be the basis that vitamin D has additional local functions, producing an auto/paracrine response within these tissues, separate from Ca^{2+}/ Pi homeostatic roles.

Expression of renal CYP27B1 is highly regulated by multiple factors to maintain Ca^{2+} and Pi homeostasis and other interrelated systems. Hypocalcaemia stimulates the release of parathyroid hormone (PTH) that in turn increases the expression of renal CYP27B1 (Brenza & DeLuca 2000).

The resulting 1α,25$[OH]_2$D binds to the VDR, increasing its expression and stimulating amplified transcription of Ca^{2+} transport proteins enabling Ca^{2+} reabsorption (Hoenderop et al. 2002). Similarly elevated Ca^{2+} levels suppress PTH secretion. Secretion of fibroblast growth factor 23 (FGF 23) in response to increased serum phosphate and 1α,25$[OH]_2$D levels down-regulates CP27B1 expression (Fukumoto 2014). Further to this high levels of 1α,25$[OH]_2$D, inhibit PTH and enhance FGF 23 secretion, producing a negative feedback mechanism.

1.4.4 The Vitamin D Receptor (VDR)

VitD mediates and acts through the ubiquitously expressed vitamin D receptor (VDR) (Norman 2008). The VDR is a nuclear receptor responsible for regulating gene transcription of multiple genes (Norman 2008). The receptor gene spans 75kb of genomic DNA, located on chromosome 12, and comprises of 11 exons and 11 introns (Zmuda et al. 2000). There are four commonly studied polymorphisms within the VDR transcript, *BsmI* (rs1544410), *TaqI* (rs731236), *FokI* (rs2228570), and *ApaI* (rs7975232). Gene transcript and mRNA stability is influenced by *BsmI, TaqI,* and *ApaI* polymorphisms (Whitfield et al. 2001), while the *FokI* polymorphism cause VDR proteins to be less responsive to VitD due to a single frame shift (Miyamoto et al. 1997). The VDR protein is comprised of 427 AA residues, with two functional domains; the N-terminal zinc-finger DNA binding domain and C-terminal ligand-binding domain (LBD), containing a hydrophobic region with a high affinity for 1α,25$[OH]_2$D (Rochel et al. 2000).

VitD/VDR mediates the gene expression of multiple proteins typically involved in Ca^{2+} regulation, along with those which are not such as insulin

like growth factor binding protein 3 (IGFBP-3) (Peng et al. 2004). Gene expression by the VDR is modulated by formation of a heterodimer with 9-cis-retinoic acid receptor (RXR) when bound to 1α,25$[OH]_2$D (MacDonald et al. 1993). Cheskis and Freedman (1994) demonstrated 1α,25$[OH]_2$D initially binds to a VDR monomer, forming an unstable quaternary complex that subsequently binds to DNA. RXR then binds to the VDR monomer, forming a heterodimer complex (VDR-RXR) (Cheskis & Freedman 1994). The resulting heterodimer is capable of accessing the deep groove of DNA, targeting specific VitD response elements (VDREs) to initiate gene transcription. When ligand bound, a structural change is induced in the VDR-RXR heterodimer, exposing a binding surface for a vitamin D receptor interacting protein (DRIP) co-activator complex to bind (Freedman et al. 1999), before interacting with Pol II complexes (Chiba et al. 2000). Recruitment of additional co-activators such as transcription factor 2B (TF2B) and steroid receptor coactivator-1 (SRC-1) are also required for VDR-RXR mediated gene transcription (Campbell et al. 2010; Torchia et al. 1998). As previously discussed the VDR down regulates CYP24B1 expression in response to 1α,25$[OH]_2$D. This is considered to occur through VDR-RXR binding to alternate negative VDREs, and subsequent binding of VDR-interacting repressors (VDIR) and histone deacetylator (HDAC) co-repressor complexes (Pike & Meyer 2012; Demay et al. 1992). Thus, gene expression or repression may be achieved by 1α,25$[OH]_2$D/VDR interactions.

Within the cell, VDR is primarily localized within the nucleus, when un-bound from 1α,25$[OH]_2$D in multiple tissues including skeletal muscle (Clemens et al. 1988; Berger et al. 1988; Buitrago & Boland 2010). Variations into the distribution between nuclear and cytosolic fractions

have been observed within some tissues, including kidney (28-39% cytosolic) and pancreas (23%), higher than normally observed (e.g. bone 16% cytosolic) (Walters et al. 1980). Immunocytochemical techniques have demonstrated 1α,25$[OH]_2$D bound VDR remains largely localized to the nucleus; however additional VDR translocation to the sarcoplasm and plasma membrane occurs (Buitrago & Boland 2010). In cardiac muscle, VDR additionally localizes with caveolae and t-tubules, becoming disassociated in the presence of 1α,25$[OH]_2$D (Zhao & Simpson 2010; Tishkoff et al. 2008). Furthermore in skeletal muscle the disruption of caveolae suppressed 1α,25$[OH]_2$D mediated effects (Buitrago & Boland 2010). Thus while the VDR may primarily reside within the nuclei, additional roles within the cytosol and plasma membrane have been demonstrated.

Expression of the VDR has been demonstrated within VitD target tissues such as bone (Wang et al. 2014), intestines (Khan et al. 2010) and liver (Barchetta et al. 2012). The presence of the VDR within skeletal muscle was originally contentious (Sandgren et al. 1991) with studies as recent as 2011 observing no expression (Wang & DeLuca 2011). However, systematic analysis of all commercially available VDR antibodies determined many were non-specific during immunocytochemical staining and immuno-blotting (Wang et al. 2010). At the time of publication, the Santa-Cruz D-6 antibody was the most reliable. VDR expression within skeletal muscle was robustly confirmed by Srikea *et al* (2012) using a robust combination of RT-PCR, DNA sequencing, immuno-blotting and immunocytochemistry. Furthermore, VDR expression was demonstrated to be expressed in human skeletal muscle, with high expression within cultured primary human myotubes and C_2C_{12} myoblasts (Girgis, Mokbel, et

al. 2014). Further analysis showed VDR expression was high in mice neonates, progressively decreasing though age. Additionally, proteomic analysis by large-scale tandem mass spectrometry confirmed VDR expression in myoblasts (Kislinger 2005). VDR positive nuclei have been confirmed in human skeletal muscle, with expression shown decrease throughout ageing (e.g. 450+ nuclei at 20y, compared to ~300 at 90y) (Bischoff-Ferrari, Borchers, et al. 2004). Thus, VDR is expressed within skeletal muscle, albeit at lower levels than classic VitD sensitive tissues such as intestines (Girgis, Mokbel, et al. 2014).

Despite the well-characterized role of the VDR within gene expression, non-transcriptional roles of the receptor have also been described (Norman 2006). 1α,25$[OH]_2$D administration has been demonstrated to induce rapid hormonal modulation of calcium transport within intestines (Nemere et al. 1984; Nemere & Norman 1990). Confirmation of a rapid non-transcriptional role has been shown through 1α,25$[OH]_2$D mediated Ca^{2+} stimulation occurring in the presence of cycloheximide, a potent protein synthesis inhibitor (de Boland & Boland 1987). Furthermore, investigations within chick myoblasts established 1α,25$[OH]_2$D induced rapid phosphorylation of protein kinase C (Nemere et al. 1998). Crucially, the presence of functional VDR was demonstrated to be required for 1α,25$[OH]_2$D mediated ion channel responses in osteoblasts (Zanello & Norman 2004) along with calcium transport in fibroblasts (Nguyen et al. 2004) and skeletal muscle (Zanello & Norman 2004).

Additional non-transcriptional roles have been purported within skeletal muscle (Buitrago et al. 2013). Formation of 1α,25$[OH]_2$D/VDR complexes localize to caveolae initiating the phosphorylation and activation of c-Src, a

tyrosine-specific protein kinase (Buitrago, Vazquez, et al. 2001; Buitrago et al. 2013). Subsequently, c-Src activates mitogen-activated protein kinases (MAPKs), extracellular signal-regulated kinase 1/2 (ERK1/2) and p38 (Buitrago, Boland, et al. 2001; Buitrago et al. 2006). Furthermore, 1α,25$[OH]_2$D stimulation of the VDR may activate AKT in a PI3K dependent manner regulating proliferation (Zhang & Zanello 2008). Taken together, these studies suggest 1α,25$[OH]_2$D bound VDR may have a duel function within transcriptional and non-transcriptional pathways; however potential roles of unbound VDR are unclear.

1.4.5 Vitamin D status

Assessment of overall VitD status is one that requires careful consideration of which of the several metabolic intermediates to use as the reference. This decision becomes further complicated with the identification of over 10 additional VitD excreted metabolites (DeLuca & Schnoes 1983). One aspect to consider is the metabolic half-life. Some VitD metabolites are shown to have a relatively short half life; interestingly 1α,25$[OH]_2$D has a half life of approximately 15 hours, not permitting accurate systemic measures chronically (Jones 2008). Additional considerations for the most representative metabolite are circulating concentrations and the mechanism of regulation. Circulatory levels of 25[OH]D are much greater ($nmol.L^{-1}$) than those of the biologically active 1α,25$[OH]_2$D ($pmol.L^{-1}$) (Aksoy et al. 2000). As 1α,25$[OH]_2$D metabolism is highly regulated by circulating PTH, Ca^{2+}, Pi and FGF 23 levels, conditions influencing kidney function will invariably alter circulating 1α,25$[OH]_2$D levels, meaning it is a poor choice for assessment (Nigwekar et al. 2014). Comparatively, 25[OH]D has a half life of approximately 15-30 days, reducing fluctuations in response to UV exposure or diet (Vieth 1999; Jones 2008). Overall,

measurement of 25[OH]D is considered the most representative of overall VitD status, due to the longer half-life and acquisition through both UV exposure and dietary means.

Assessment of total 25[OH]D is typically achieved through the combination of both dietary 25[OH]D_2, which contributes 10-20%, and UV dependent 25[OH]D_3 which provides 80-90% (Owens et al. 2014). Liquid chromatography tandem mass spectrometry (LC-MS/MS) is considered the 'gold standard' for assessing serum VitD as it allows the simultaneous measurement of both 25[OH]D_2 and 25[OH]D_3 within the same sample (Wallace et al. 2010; Shah et al. 2011; Singh 2010). Furthermore, LC-MS/MS provides a large detectable linear range, for example 0.5-84.4ng/ml (1.2-205 $nmol.L^{-1}$).

Categorization of VitD status has been greatly debated between governing bodies, depending on their respective populations. The current NHS guidelines of VitD status in the UK are generally aligned to WHO classifications (Table 1.2) (Scientific Advisory Committee on Nutrition (SACN) 2016; Lamberg-Allardt et al. 2013; Spiro & Buttriss 2014).

Table 1.2 Vitamin D status classification

Serum 25[OH]D	Status
<25 $nmol.L^{-1}$	Deficient
25-50 $nmol.L^{-1}$	Insufficient
50-75 $nmol.L^{-1}$	Adequate
>75 $nmol.L^{-1}$	Optimal

Insufficient levels between 25-50 nmol.L^{-1} are considered a grey area, whereby those towards the lower range are recommended to take supplementation. Furthermore, a review on health outcomes related to VitD status noted calcium homeostasis disturbances at serum concentration <75 nmol.L^{-1} (Heaney 2013; Holick 2006), with suggestions made to reclassify >100 nmol.L^{-1} as optimal (Zittermann 2003).

The prevalence of VitD deficiency within a population is highly reliant upon sunlight exposure and latitude as previously discussed. Within the UK, official statistics suggest that 61% of adults have insufficient levels, while 22% may be categorized as deficient (Public Health England & Food Standards Agency 2014). Similar estimations have been shown in US populations, with 42% of adults studied classed as insufficient (Forrest & Stuhldreher 2011). Indeed studies of populations in European nations (Cashman et al. 2016) and northern latitudes (>44^{O} North) have demonstrated high instances of insufficiency, including Finland (65%) (Cashman et al. 2015), Ireland (46%) (Cashman et al. 2013), Iceland (47%) (Harris et al. 2007), The Netherlands (34%) (van 't Riet et al. 2010) and Germany (61%) (Scheidt-Nave et al. 2012). However, a high prevalence of VitD deficiency has been reported in many countries where it may be assumed adequate sunlight exposure and strength occurs, such as Mexico, Brazil and Australia (Palacios & Gonzalez 2014). Such findings highlight the major public health problem vitamin D deficiency presents on a global scale (Figure 1.8).

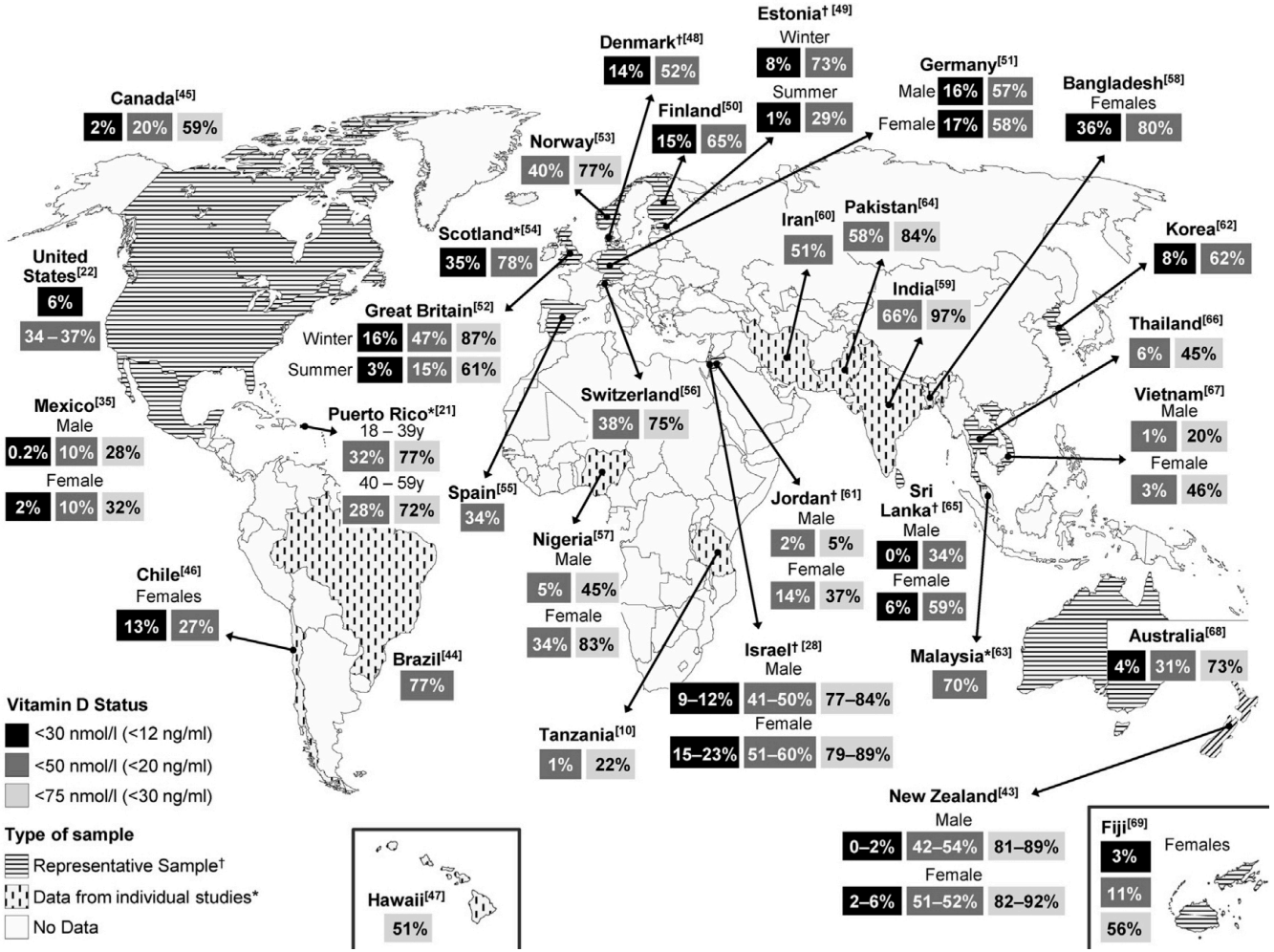


Figure 1.8 Worldwide prevalence of vitamin D deficiency in adults

Adapted from: (Palacios & Gonzalez 2014)

1.4.6 Skeletal Muscle and vitamin D: Observational Studies

The impact of VitD deficiency upon skeletal muscle, separate from Ca^{2+} homeostasis has been alluded to through VitD/VDR mediated signalling in skeletal muscle. Importantly, VitD deficiency has been associated with adverse effects upon muscle morphology, including type II muscle fibre atrophy, lipid infiltration and the presence of necrotic fibres (Yoshikawa et al. 1979). Furthermore, multiple observational and epidemiological studies have associated VitD deficiency with declines in skeletal muscle function (summarised in Table 1.3). One longitudinal study (n=979) in an elderly population (3-year follow up) demonstrated serum concentrations <50 $nmol.L^{-1}$ were associated with poorer physical performance with a greater long-term decline (Wicherts et al. 2007). Similarly, within community-dwelling older adults (n=686), serum levels <50 $nmol.L^{-1}$ were accompanied by decreased measures of physical activity, leg strength (assessed by dynamometer) and appendicular lean mass percentage (Scott et al. 2010). Another study of men and women (n=976) with serum concentration <50 $nmol.L^{-1}$ had a significantly lower hand grip strength than those >50 $nmol.L^{-1}$ (Houston et al. 2007), matching observation seen in hip fracture patients (Dhanwal et al. 2013).

These studies allude to an association between VitD status and skeletal muscle function. However, such studies are limited by their observational design, unable to determine the causal nature of the findings. In addition, secondary issues relating to Ca^{2+} and Pi homeostasis may induce the associated dysregulation of muscle function, separate from potential VitD effects. Furthermore, the majority of these studies are within elderly populations, likely to have pre-existing health concerns and frailty issues.

Table 1.3 Observational studies between vitamin D status and skeletal muscle function

Reference	Population	Timespan	Measures	Baseline 25[OH]D ($nmol.L^{-1}$ ±SD)	Outcome
(Dhanwal et al. 2013)	Hip fracture patients (n=95) Mean age: 61	2 years	Hand grip strength - dynamometer	25 ± 16	Significant positive correlation between 25[OH]D and hand grip strength.
(Buchebner et al. 2014)	Elderly women (n=715) Baseline age: 75	10 year follow-up	Incidence of fracture	62 ± 19	Greater incidence of hip fractures in low 25[OH]D groups after 5 and 10 years
(Wicherts et al. 2007)	Elderly men and women (n=979) Mean age: 75	3 year follow-up	Physical performance test	53 ± 25	25[OH]D <50 $nmol.L^{-1}$ was associated with poor physical performance and a greater decline
(Bolland et al. 2010)	Community dwelling postmenopausal women (n=1471) Mean age: 74	5 year follow-up	Hand grip strength – dynamometer	51 ± 18	No association between 25[OH]D and hand grip strength, with no greater instances of adverse conditions
(Menant et al. 2012)	Community dwelling elderly men and women (n=463) Mean age: 78	1 year follow-up	Neuromuscular function, balance and physical function	62 ± 25	25[OH]D <50 $nmol.L^{-1}$ was associated with poorer balance, reaction times, gait times and muscle strength. Greater instances of falls in men

(Scott et al. 2010)	Community dwelling elderly men and women (n=686) Mean age: 62	2-3 year follow-up	Physical activity (pedometer), leg strength (dynamometer), appendicular lean mass	55 ± 19	25[OH]D <50 nmol.L^{-1} was associated with decreased physical activity, leg strength and appendicular lean mass %.
(Michael et al. 2011)	Postmenopausal healthy women (n=534) Mean age: 70	6 year follow-up	Combined physical performance test (timed walk, chair-stand, and grip strength)	48 ± 21	25[OH]D >75 nmol.L^{-1} was associated with greater physical performance. Higher 25[OH]D did not reduce the rate of physical performance decline
(Houston et al. 2012)	Community dwelling elderly men and women (n=2641) Mean age: 75	4 year follow-up	Short physical performance battery test, leg strength, hand grip strength	~1/3 <50 nmol.L^{-1} (Mean measures unreported)	Reduced physical performance and slower gait speed was associated with 25[OH]D <50 nmol.L^{-1} initially and after 2y and 4y. Lower initial leg strength measures were associated with 25[OH]D <50 nmol.L^{-1}.
(Houston et al. 2007)	Community dwelling elderly men and women (n=2641) Mean age: 75	2 year	Short physical performance battery test, hand grip strength	58 ± 35	25[OH]D <25 nmol.L^{-1} was associated with reduced physical performance and hand grip strength.
(Bischoff-Ferrari, Dietrich, et al. 2004)	Community dwelling elderly men and women (n=4100) Mean age: 71	-	Physical performance (walking speed, sit-to-stand)	63 ± 25	25[OH]D >40 nmol.L^{-1} was associated with greater physical performance.

1.4.7 Skeletal Muscle and vitamin D: Supplementation Studies

Due to the limiting factors, inherent in the design of observational studies, randomized control trials (RCTs) are required; however few have been undertaken investigating the role of VitD in skeletal muscle function (Table 1.4). Studies that have been conducted have primarily investigated elderly populations (70-90 y), living within community based housing (Muir & Montero-Odasso 2011). These studies suggest long-term daily VitD supplementation (1α,25$[OH]_2D_3$) combined with calcium, reduce the risk of falls compared to calcium alone (Pfeifer et al. 2000; Bischoff et al. 2003; Prince et al. 2008). Year-long daily VitD supplementation has been shown to increase lower limb strength in elderly women (Zhu et al. 2010). Furthermore, a study by Ceglia *et al* (2013) demonstrated daily VitD supplementation alone increased muscle fibre CSA measures in mobility-limited women. Similarly, Sato *et al* (2005) showed prolonged supplementation alone increased skeletal muscle strength and type II fibre CSA measures. Thus, reductions in fall risk may be partially due to VitD mediated effects upon muscle function; however further demonstrations are required in other populations.

There are limited supplemental RCTs within young individuals investigating impacts upon skeletal muscle function, those that have been performed are often inconsistent. One study supplementing 4000IU 1α,25$[OH]_2D_3$ daily, showed improved early strength adaptations to resistance exercise-training (RET) (Carrillo et al. 2013). Nevertheless after the full 12 RET program, there was no significant difference in 1-RM measures. Within another study daily supplementation of 5000IU 1α,25$[OH]_2D_3$ in football players improved muscle function, shown by increased vertical jump height and decreased 10M sprint times (Close, Russell, et al. 2013). However, a similar study by

the same group whereby weekly VitD supplementation (20,000IU and 40,000IU) was given, no alteration within physical performance was observed (Close, Leckey, et al. 2013). Final 25[OH]D measures were elevated from baseline in the treatment groups of each study.

The disparities within these studies may reside with the small sample populations used (e.g. n=10 and n=30), and whether VitD supplementation may induce a measurable difference in relatively short timespan (2 or 3 months). Another possibility is the variance within baseline 25[OH]D measures. Indeed some studies identified high instances of VitD deficiency (e.g. 57% (Close, Leckey, et al. 2013)), however even those with maximal 25[OH]D exclusion criteria studied individuals who were classified as insufficient. Furthermore, within one study increased handgrip strength was demonstrated in response to supplementation despite no apparent increase in 25[OH]D (Cavalcante et al. 2015). Determination of the efficacy of VitD supplementation will require specific populations whereby baseline 25[OH]D measures are more homogeneous, and demonstrate increased VitD status in response to supplementation.

Table 1.4 Influence of vitamin D supplementation on skeletal muscle – Randomized control trials

Reference	Population	Supplementation	Timespan	Measures	Baseline 25[OH]D vs. final (nmol.L^{-1} ±SD)	Outcome
(Pfeifer et al. 2000)	Healthy women, 25[OH]D <50 nmol.L^{-1} (n=148) Mean age: 74	Ctrl 1200mg Ca vs. 1200mg Ca + 800IU 25D3 Daily Double blinded	8 weeks	Body sway, serum 25[OH]D, PTH	BL 25 ± 12 Ctrl 43± 21 25D3 66 ± 27	Decreased body sway, increased serum 25[OH]D and decreased PTH
(Bischoff et al. 2003)	Elderly women (n=122) Mean age: 83	Ctrl 1200mg Ca vs. 1200mg Ca + 800IU 25D3 Daily Double blinded	12 weeks	Incidence of falls, serum 25[OH]D	BL 30 Ctrl 28 25D3 65	Reduced incidence of falls and increased serum 25[OH]D
(Bischoff-Ferrari et al. 2006)	Community dwelling elderly men and women (n=445) Mean age: 71	Placebo vs. 500mg Ca + 700IU 25D3 Daily Double blinded	3 years	Incidence of falls, serum 25[OH]D	BL 75 ± 35 Placebo 71 ± 30 25D3 107 ± 38	Women had a reduced incidence of falls. Men, no difference.
(Prince et al. 2008)	Community dwelling elderly women (n=302) Mean age: 77	Ctrl 500mg Ca vs. 500mg Ca + 1000IU 25D3 Daily Double blinded	1 year	Incidence of falls	BL 45 ± 13 Ctrl 60 25D3 50	Reduced incidence of falls.
(Ceglia et al. 2013)	Mobility limited women (n=21) Mean age: 77	Placebo vs. 4000IU 25D3 Daily Double blinded	4 months	Muscle fibre CSA, VDR expression	BL 46 ± 11 Placebo 48 ± 12 25D3 82 ± 14	Greater muscle fibre CSA and intramyonuclear VDR expression.
(Close, Leckey, et al. 2013)	Club level male athletes (n=30) Mean age: 21	Placebo vs. 20,000IU 25D3 vs. 40,000IU 25D3 weekly Double blinded	3 months	1-RM bench press, leg press, vertical jump height	BL 51 ± 24 20,000IU ~84 40,000iu ~90 (Values not stated)	No measureable change in physical performance. 25[OH]D increased >50 nmol.L^{-1}

(Close, Russell, et al. 2013)	Male academy level football players (n=10) Mean age: 18	Placebo vs. 5000IU 25D3 daily Double blinded	2 months	1-RM bench press, back squat, sprint test, vertical jump height	BL ~38 Placebo ~70 25D3 ~100	Decreased 10M sprint times and increased vertical jump height.
(Zhu et al. 2010)	Community dwelling elderly women, 25[OH]D <60 nmol.L^{-1} (n=302) Mean age: 77	Placebo 1g Ca vs. 1g Ca + 1000IU 25D3 daily Double blinded	1 year	Lower limb strength – strain gauge, sit-to-stand	BL 44 ± 11 Placebo 45 ± 14 25D3 60 ± 14	Increased hip extensor and adductor strength. Reduction in sit-to-stand time
(Cavalcante et al. 2015)	Postmenopausal T2D women, 25[OH]D <75 nmol.L^{-1} (n=38) Mean age: 62	Olive oil vs. 6600IU 25D3 in olive oil weekly Double blinded	3 months	Hand grip strength, fasting glucose, HbA1c	BL 57 ± 10 Ctrl 57 ± 10 25D3 57 ± 11	Increased hand grip strength, no effect upon glycaemic control
(Carrillo et al. 2013)	Overweight men and women (n=23) Mean age: 26	Placebo vs. 4000IU 25D3 Daily Double blinded	3 months	Resistance exercise training, 1-RM leg extension, leg flexion, leg press, hip adduction, hip abduction, chest press, seated row, and lateral pull down	BL 48 ± 19 Placebo 59 ± 15 25D3 83 ± 18	Improved early (4 weeks) strength adaptation to resistance training No difference after 3 months
(Sato et al. 2005)	Elderly post-stroke women (n=96) Mean age:74	Placebo vs. 1000IU 25D3 Daily Double blinded	2 years	isometric hip strength, incidence of falls, muscle fibre CSA	BL 24 Placebo 13 25D3 83	Reduced incidence of falls, increased muscle strength and type II fibre CSA

1.4.8 Skeletal Muscle and the vitamin D Receptor: Human Studies

Within the previously discussed RCTs, very few assessed the expression of the VDR within skeletal muscle in response to VitD supplementation. However, a recent study by Agergaard *et al* (2015) in young and elderly individuals, demonstrated in response to a 12 week RET program, a moderate but non-significant increase in VDR mRNA expression in the young group was observed. Moreover, the elderly group showed no change in mRNA VDR expression (Agergaard et al. 2015). Additionally, young and old sub-groups were supplemented with VitD (1920IU 1α,25$[OH]_2D_3$ + 800mg calcium daily vs. 800mg calcium), but showed no difference in skeletal muscle function or VDR mRNA expression between supplemented and placebo groups. These findings are supported by a previous investigation demonstrating skeletal muscle VDR expression decreases with age (Bischoff-Ferrari, Borchers, et al. 2004). Thus, the expression of VDR may be important in the regulation of skeletal muscle.

This notion is further supported by studies identifying an association between VDR polymorphisms and skeletal muscle function. In one study, the expression of multiple VDR polymorphisms (*FokI*, *BsmI* and *TaqI* as previously discussed in 1.4.4) were measured in 253 men and 240 women, with quadriceps isometric and concentric strength assessed (Windelinckx et al. 2007). Interestingly, different VDR gene polymorphisms were associated with quadriceps strength in men and women. Men homozygous with *BsmI/BsmI* were correlated with greater strength compared to other haplotypes, whilst women *FokI/FokI* homozygous demonstrated greater strength. 25[OH]D status was unmeasured, thus the influence of reduced VitD responsiveness by the *FokI* polymorphism is unknown. Furthermore, whilst the stability of the VDR protein is altered by *BsmI* and *TaqI*

polymorphisms, the influence it has upon VitD/VDR mediated signalling is unspecified. Collectively these studies tentatively suggest a role of VDR expression and functionality with skeletal muscle, however its expression will have to be measured in future investigations.

1.4.9 Skeletal Muscle and vitamin D: Animal Models

Animal models are of great importance to investigate potential mechanisms VitD/VDR has upon skeletal muscle function and metabolism. Initial investigations by Birge and Haddad (1975) compellingly demonstrated VitD stimulation directly upregulated regulated protein metabolism. Within this study, [^{3}H] leucine incorporation into diaphragm muscle was increased in rats who received 1α,25[OH]$_2$D$_3$ orally (Birge & Haddad 1975). Furthermore, to separate systemic effects, foreleg muscles from VitD deplete rats were cultured. Administration of 1α,25[OH]$_2$D$_3$ enhanced muscular ATP content and leucine incorporation into new protein. Interestingly, sucrose density gradients demonstrated cytosolic protein fractions specifically bound to 25[OH]D$_3$. Although not specifically mentioned, it is likely the presence of translocated VDR instigated 25[OH]D$_3$ binding. Likewise, another study has demonstrated 25[OH]D$_3$ supplementation promoted muscle regeneration after crush injury (Stratos et al. 2013). Significant increases in prolyl-4-hydroxylase-β (P4Hβ) were observed, indicative of enhanced extra-cellular matrix (ECM) proteins, however there were no changes in satellite cell content. Moreover, supplemented animals significantly improved muscle force recovery after 48 days, in comparison to control animals.

Further investigations into potential functional benefits of VitD administration within rats however have produced conflicting results. For example, skeletal muscle hypertrophy in rats may be achieved through severing of the gastrocnemius tendon. One study showed administration of $1\alpha,25[OH]_2D_3$ two weeks or one day prior to surgery did not enhance the rate of muscle hypertrophy (Bikle et al. 1979). Thus, the mechanism by which VitD regulates skeletal muscle metabolism and growth may not be involved with mechanical stimulation.

Intriguingly, VitD deficiency may additionally influence muscle metabolism. Rats fed a prolonged diet deficient in VitD, but fortified with Ca^{2+} and Pi demonstrated muscle atrophy assessed by muscle fibre CSA (Bhat, Kalam, Qadri, et al. 2013). Furthermore, protein synthesis measured by C^{14}-tyrosine incorporation was reduced, whilst 3-methylhistidine (3-MH) release was increased (proxy of MPB). Subsequent analysis determined atrophy occurred through increased ubiquitin proteasomal mediated degradation, however anabolic signalling was unmeasured. Combined these studies further suggest a role of VitD within skeletal muscle maintenance.

1.4.10 Skeletal Muscle and the vitamin D Receptor: Animal Models

To further investigate the systemic role the VDR may have, VDR knockout (VDR-KO) VDR -/- mice were generated as a model (Li et al. 1997). These mice were phenotypically normal at birth, whereby they quickly became hypocalcaemic with increased PTH levels. Further investigations using VDR-KO mice by Endo et al (2003) specifically investigated skeletal muscle developmental regulation. Analysis of fibre morphology by histochemical staining determined VDR-KO muscle fibres were smaller with a greater

degree of variability compared to wild-type mice (Endo et al. 2003). Moreover, dysregulation in the expression of multiple MRFs were noted, whereby early neonatal myosin isoforms and *MYF5* mRNA expression was continually expressed. Additional VDR-KO studies have further demonstrated a potential role of the VDR within skeletal muscle function. Investigations by Girgis *et al* (2015) demonstrated VDR-KO mice had a reduction in grip strength at two and three months of age. VDR-KO fibres had a significantly reduced fibre diameter, with a greater accumulation of myonuclei per fibre (Girgis et al. 2015). Furthermore, VDR-KO mice displayed increased *MYF5*, *MyoD* and myostatin *mRNA* expression, indicative of myogenic dysregulation. Collectively these studies suggest a role of the VRD within skeletal muscle development and growth.

However, as alluded to previously, VDR-KO models are hypocalcaemic with increased PTH levels owing to impaired mineral ion homeostasis. Furthermore, increased bone volume and osteoblast numbers have been reported (Amling et al. 1999). As such, restoration of normal serum mineral ion and PTH levels is achieved through the use of 'rescue diets' containing twice the amount of calcium and phosphorus as in standard chow diets (Amling et al. 1999). Despite the utilisation of rescue diets, calcium homeostasis, particularly in skeletal muscle may still be deregulated. This is supported by the observation of a reduction in sarco-endoplasmic reticulum calcium transport ATPase (Serca) mRNA expression (Amling et al. 1999).

Further investigations support the notion that expression of the VDR has a functional role within skeletal muscle. A study by Srikuea *et al* (2012) modestly demonstrated that regenerating muscles displayed enhanced VDR

expression. Furthermore, within skeletal muscle, electrically stimulated resistance exercise has been shown to acutely increase VDR protein expression (0-3h) before returning to basal levels after 24h (Makanae et al. 2015). CYP27B1 expression was similarly increased, however only after 1h; suggesting local VitD metabolism may be regulated through enhanced VDR expression.

Collectively these studies suggest a role of the VDR within skeletal muscle growth and regeneration. However developmental dysregulation and the requirement of 'rescue diets' in VDR-KO animals to normalise secondary hypocalcaemia precludes the identification a mechanistic role.

1.4.11 Skeletal Muscle and the vitamin D Receptor: Cell Culture Models

In order to study the potential mechanisms of VitD and the VDR in skeletal muscle myogenesis, there have been a number of *in vitro* cell culture studies. In C_2C_{12} myoblasts, incubation with $1,25(OH)_2D_3$ has been shown to inhibit proliferation (Liu et al. 1996; Garcia et al. 2011) via altering G0/G1 to S-phase cell cycle progression (Artaza et al. 2010; Okuno et al. 2012; Girgis, Clifton-Bligh, et al. 2014). Myoblasts treated with exogenous $1,25(OH)_2D_3$ exhibited decreased *Myf5* expression (Girgis, Clifton-Bligh, et al. 2014), and an up-regulation of MyoD and myogenin; the later being known to initiate cell cycle withdrawal (Andrés & Walsh 1996). Furthermore, investigations on isolated human myoblasts treated with $1,25(OH)_2D_3$ demonstrated reduced proliferation, through influence of G1/S phase cell cycle regulators consistent with previous findings (Olsson et al. 2015). However contrasting studies have demonstrated exogenous $1,25(OH)_2D_3$ stimulated myogenesis in chick myoblasts, increased DNA synthesis and early proliferation (Capiati et al. 1999). Moreover, within

proliferating myoblasts, $1,25(OH)_2D_3$ increased [^{3}H]thymidine into DNA (Drittanti et al. 1989a). Likewise, exogenous $1,25(OH)_2D_3$ has been shown to promote proliferation through AKT phosphorylation in a PI3K dependant manner (Buitrago et al. 2012). Thus the effects of $1,25(OH)_2D_3$ upon myoblast proliferation remains unclear. These inconsistencies may possibly be due to differing experimental designs, such as chick vs. C_2C_{12} vs. human primary myoblasts and the concentration/duration of $1,25(OH)_2D_3$ administration.

Interestingly, VitD appears to augment myoblast differentiation. *In vitro*, exogenous $1,25(OH)_2D_3$ induces the gene expression of pro-myogenic insulin-like growth factor II (IGF-II), myosin heavy chain II (MHC II) and myostatin, along with other MRF's in C_2C_{12} cells (i.e. MyoD, myogenin, desmin) (Garcia et al. 2011; Tanaka et al. 2014). Furthermore both active $1,25(OH)_2D_3$ and inactive $25[OH]D_3$ have been demonstrated to enhance the expression of multiple myosin isoforms *in vitro* (van der Meijden et al. 2016). The observation of local VitD metabolism is supported by studies demonstrating CYP27B1 expression in myotubes (Srikuea et al. 2012). Furthermore, investigations by Salles *et al* (2013), demonstrated exogenous $1\alpha,25[OH]_2D_3$ enhanced insulin/leucine stimulated AKT/mTOR anabolic signalling, increasing protein synthesis in cultured myotubes (Salles et al. 2013). Collectively these studies demonstrate a potential pro-myogenic role of VitD within cultured models.

Available data tend to support the notion that exogenous VitD exerts its actions through the VDR in muscle. For instance, observed anti-proliferative effects of $1,25(OH)_2D_3$ were ameliorated by VDR knockdown (VDR-KD), while cyclin D3 and myogenin upregulation were also blocked

by VDR-KD (Irazoqui et al. 2014). In other studies, 1,25$(OH)_2D_3$-dependent Akt phosphorylation in regards to proliferation was attenuated by VDR-KD (Buitrago et al. 2013), as was 1,25$(OH)_2D_3$–dependent induction of multiple myosin isoforms (Tanaka et al. 2014). Furthermore, VDR-KD (by siRNA) myotubes demonstrated a lack of myosin induction, coupled with decreased myogenin and Mrf4 expression (Tanaka et al. 2014), although changes within anabolic signalling were not investigated. However, the influence of VDR-KD upon proliferation could not be investigated due to the high myoblast seeding densities needed for siRNA knockdown and differentiation to occur. Despite MRF dysregulation within VDR-KD cells, the role of the VDR within proliferation has yet to be investigated.

1.5 Summary

Vitamin D deficiency is highly prevalent within multiple populations. VitD deficiency has been associated with impaired skeletal muscle mass/function and metabolic dysfunction through unknown mechanisms. Skeletal muscle is an essential regulator of whole-body protein homeostasis and key tissue for glucose metabolism. Regulation of muscle metabolism is highly complex, requiring sensitivity to many internal/ external stimuli and the modulation of anabolic and catabolic responses. VitD exerts its actions through the ubiquitously expressed vitamin D receptor; moreover, through unknown mechanisms, an autonomous role of the receptor has been suggested in skeletal muscle. *In vitro* studies have demonstrated VitD/VDR modulates myoblast proliferation. Furthermore, *in vivo* animal models have revealed VDR-KO impairs muscle mass and function, however these findings are confounded by developmental dysregulation. Finally, VDR expression is modulated by resistance exercise, suggesting a role within muscle hypertrophy.

Thus, the aims of this thesis are:

1. Characterise how VDR-KD impacts myoblast proliferation and differentiation.
2. Explore how bi-directional modulation of VDR expression within developed skeletal muscle will impact protein and glucose metabolism.
3. Examine whether VitD status and VDR mRNA expression impact the response to hypertrophy inducing resistance exercise in humans.

Chapter 2 – General Methods

2.1 Immunoblotting

Samples were collected as stated in the chapter specific methods. Samples were centrifuged at 11,000 g for 10 min at 4^{O}C, the supernatant removed and quantified by Nanodrop. All samples were diluted in extraction buffer and 1x Laemmli loading buffer to the same concentration before loading onto a Criterion XT Bis-Tris 12% SDS-PAGE gel (Bio-Rad, Hemel Hempstead, UK) for electrophoresis for 1h at 200 V. Separated proteins were transferred onto a PVDF membrane for 45 min at 100 V, then blocked in 5% low-fat milk in Tris-buffered saline and 0.1% Tween-20 (TBST) for 1h at room temperature. Membranes were then incubated at 4^{O}C over night in 5% milk diluted in TBST primary antibody solutions. Afterwards membranes were washed 3 x 5 min with TBST and incubated for 1h at room temperature in their respective HRP conjugated secondary antibody. Membranes were washed 3 x 5 min in TBST and incubated for 5 min in enhanced chemiluminescence reagent (Millipore, Watford, UK) and visualized using a Chemidoc XRS.

2.2 Total Protein, RNA and DNA

Total cellular alkaline soluble protein (ASP), DNA and RNA were analysed by spectrophotometric measurement as described (Crossland et al. 2013). For whole muscle, 20mg of liquid nitrogen frozen muscle was freeze dried to remove the water content. Using clean sharp scissors, freeze dried muscle was homogenised in 0.3M NaOH. For cell culture, myotubes were scraped directly into 0.3M NaOH. Samples were subsequently incubated at 37^{O}C for 30 min before an aliquot was taken for measurement of total protein using a Nanodrop (Thermo Scientific). Thereafter, 1M perchloric acid (PCA) was added to the remaining sample and incubated at 4^{O}C for 10 min, before centrifugation at 3,000g for 10 min, washing in 0.2M PCA, and

the supernatant collected for RNA measurement. The resulting pellet was incubated at 70^{O}C for 1h in 2M PCA before centrifugation at 5,000g washing in 2M PCA, and collection of the supernatant for DNA measurement. RNA was quantified by the absorbance at 260 and 275nm and DNA at 268 and 284nm.

2.3 Muscle protein synthesis

Isolation of muscles into the specific cellular subfractions was undertaken as follows. Approximately 20mg of liquid nitrogen frozen muscle was added to 200µl ice-cold extraction buffer (pH 7.5, 50mM Tris-HCl, 1mM EDTA, 1mM EGTA, 10mM β-glycerophosphate, 50mM NaF and protease inhibitor tablet (Roche, West Sussex, UK)), before homogenisation with clean sharp scissors. Samples were then placed on a Vibrax shaker at 1000rpm for 10 mins at room temperature, before centrifugation at 11,000g for 15 min at 4^{O}C to pellet the myofibrillar, collagen and mitochondrial fractions. The sarcoplasmic protein containing supernatant was removed and ice cold 1M PCA added for protein precipitation. This was followed by centrifugation at 11,000g for 10 min at 4^{O}C, before washing the resultant sarcoplasmic pellet in 1M PCA. The myofibrillar, collagen and mitochondrial pellet was further washed in extraction buffer, before resuspension in mitochondrial extraction buffer (MEB) (pH 7.5 20mM MOPS, 110mM KCl, 1mM EGTA) and transferred to glass homogenizer. The pellet was manually homogenized 12 times and transferred to a new Eppendorf and centrifuged at 1000rpm for 10 min at 4^{O}C. The mitochondria containing supernatant was removed, and placed into a new Eppendorf before centrifugation at 11,000rpm for 15 min at 4^{O}C and the resultant pellet washed in MEB. The myofibrillar and collagen fractions were separated through the addition of 0.3N NaOH, vortex mixing and incubation at 37 ^{O}C for 30 min. The samples were then

centrifuged at 1000rpm for 10 min at 4^{O}C, before the solubilized myofibrillar supernatant transferred to a new Eppendorf. Myofibrillar proteins were precipitated through the addition of 1M PCA and centrifuged at 11,000rpm for 5 min at 4^{O}C. Mixed lysate samples were prepared by homogenizing frozen muscle as previously described, followed protein precipitation through the addition of 1M PCA and centrifugation at 11,000rpm for 15 min at 4^{O}C. All resulting pellets were finally twice washed in 70% ethanol, centrifuged at 3000g for 5 min at 4^{O}C. Protein-bound AAs were hydrolysed through resuspension of protein pellets in 0.1M HCl and added to Dowex H^+ resin slurry before incubation at 110 ^{O}C for 16h. AAs were then eluted from the resin with 2M NH_4OH and evaporated to dryness.

The AAs were then derivatized as their n-methoxycarbonyl methyl esters. Initially dried AAs were resuspended in ddH_2O and methanol before addition of pyridine. Methylchloroformate (MCF) was then pipetted directly in the aqueous mix and vortex mixed. After transfer to an Eppendorf, chloroform and 0.001M $NaHCO_3$ were added and vortex mixed. The aqueous phase was discarded and a molecular sieve added before transfer to an autosampler vial and capped. Incorporation of deuterium into protein bound alanine was determined by gas chromatograph-mass spectrophotometry (GC-MS/MS), alongside a standard curve of known L-alanine-2,3,3,3-d_4 enrichment.

D_2O enrichment of cell culture medium or blood plasma was measured using a modified acetone exchange method (Yang et al. 1998). 10N NaOH and acetone was added to the sample and vortex mixed for 15s. Following 24h incubation at room temperature, to allow the exchange of hydrogen

atoms for deuterium, acetone was extracted into n-heptane and transferred to an autosampler vial and capped. Deuterium exchanged acetone was determined by GC-MS/MS, alongside a standard curve of known D_2O enrichments.

The fractional synthesis rate (FSR) of each cellular fraction was determined from the incorporation of deuterium-labelled alanine into protein, using the culture media or blood plasma enrichment for precursor labelling. Enrichment was corrected for the mean number of deuterium moieties incorporated per alanine, 3.7 (Wilkinson et al. 2015). FSR was calculated using the following equation:

$$FSR\ (\%/day) = [(MPE_{Ala})]/[3.7x\ (MPE_{MW})\ x\ t]\ x\ 100$$

whereby MPE_{Ala} represents protein bound alanine enrichment, MPE_{MW} represents media or plasma water enrichment, and *t* signifies time in hours (Gasier et al. 2010).

2.4 Statistical analysis

Statistical analysis was performed using Graph Pad Prism (Version 7). All data are reported as means ±SEM, with significance set at $p<0.05$. All analysis was performed by either an unpaired (or paired where appropriate) t-test for two-group comparison, or a one-way ANOVA with Bonferroni post-hoc analysis between multiple groups. Correlations are presented as linear regression and analysed by Pearson‘s correlation.

Chapter 3 – The Role of the Vitamin D Receptor During Myogenesis

3.1 Introduction

The steroid hormone vitamin D (VitD) is involved in the regulation of calcium (Ca^{2+}) and phosphate (P_i) homeostasis to maintain bone health, e.g. prevent rickets (Arthur W. Ham 1934), osteomalacia (Bhan et al. 2010) and osteoporosis (Rizzoli et al. 2008). The mechanistic of action of VitD is through binding to its cognate vitamin D receptor (VDR), the expression of which has been ubiquitously demonstrated (i.e. in bone, kidney, intestinal cells) (Norman 2008). VDR is a nuclear receptor, binding DNA at VitD responsive elements to regulate transcription of a multitude of genes (Toell et al. 2000). Recent studies have confirmed expression of the VDR in skeletal muscle (Pike 2014; Srikuea et al. 2012). Furthermore, VitD has been demonstrated to enhance anabolic signalling *in vitro* (Salles et al. 2013), suggesting muscle to be a potential target of VitD actions (Srikuea et al. 2012; Ceglia et al. 2013). However, the mechanisms and actions VitD/VDR have upon skeletal muscle are unclear.

In vitro, exogenous VitD has been shown to decrease proliferation by promoting cell cycle withdrawal (Garcia et al. 2012; Artaza et al. 2010), reduce expression of myogenic regulatory factors (MRFs) (Okuno et al. 2012; Girgis et al. 2012) and augment differentiation, inducing IGF-II and myosin isoform expression (Garcia et al. 2011; Tanaka et al. 2014). Exogenous VitD up-regulates VDR transcription and VitD metabolism in skeletal muscle (van der Meijden et al. 2016). Furthermore, the VDR is required for VitD induced anti-proliferative effects (Irazoqui et al. 2014), while VDR-KD silencing (siRNA) lead to impaired myogenic differentiation (Tanaka et al. 2014). Nonetheless, this acute siRNA approach did not permit scrutiny of the role of the VDR in proliferation and terminal

myogenesis. Despite MRF dysregulation within VDR-KD cells, the role of the VDR within proliferation has yet to be investigated.

Overall, such observations demonstrate a role of VitD within myoblast proliferation and differentiation, however the role and mechanism the VDR has upon these remains unclear. Thus, the main objective of the current study was to investigate the role the VDR has upon myogenesis, namely proliferation and differentiation.

3.2 Aims and Hypothesis

The primary aim of this investigation was to characterise the impact reduction of VDR expression has upon myogenesis, regulation of protein metabolism and phenotype. Specifically, the objectives of this study were to:

- Measure the effect VDR-KD has upon myoblast proliferation and cell cycle control.
- Characterise essential aspects of VDR-KD cells as they differentiated into myotubes (i.e. protein, DNA and RNA content)
- Assess changes in VDR-KD myotube morphology compared to shRNA controls
- Measure changes in anabolic signalling and protein synthesis in VDR-KD myotubes.

It was hypothesised loss of the VDR would dysregulated myogenic proliferation through alteration of cell cycle progression. Moreover, VDR-KD cells would have blunted differentiation, characterised by impaired protein synthesis

3.3 Methodology

3.3.1 Cell culture

C_2C_{12} murine myoblasts (passage 6-10, ECACC, Salisbury, UK) were grown in Dulbecco's modified eagle's medium (DMEM, Invitrogen, Paisley, UK) supplemented with 10% (vol/vol) heat-inactivated foetal bovine serum (FBS, Sigma Aldrich, Poole, UK), penicillin (100U/ml), streptomycin (100µg/ml), amphoteracin B (250ng/ml), L-glutamine (2mM; all Sigma-Aldrich, Poole, UK) at 37^{O}C in a 5% CO_2 atmosphere (growth media).

Myoblasts were seeded in 6-well plates (Nunclon Delta; Thermo Scientific) and grown for 48h, before differentiation was induced by switching to media containing 2% FBS (vol/vol). Media was changed every 48h; in experiments where signalling was measured, media was changed 24h in advance to avoid associated acute perturbations.

3.3.2 shRNA interference

The lentiviral plasmid used (based on pLKO.1) was targeted towards the (3' UTR) mouse sequence 5'- TTA AAT GTG ATT GAT CTC AGG-3' of the mouse VDR gene; a non-targeting scrambled (SCR) shRNA sequence was used as a negative control, with a hairpin sequence: CCT AAG GTT AAG TCG CCC TCG CTC TAG CGA GGG CGA CTT AAC CTT AGG (Addgene, Cambridge, MA, USA). Oligonucleotides were obtained from ITDDNA USA and suspended, annealed and cloned into the pLKO.1 at the EcoRI, AgeI sites as per the pLKO.1 protocol from Addgene. Resultant plasmids were transformed in DH5α cells for amplification and isolated. HEK293FT cells (Invitrogen, Carlsbad, CA, USA) were grown in DMEM; 80–85% confluent plates were rinsed once with Opti-MEM (Invitrogen, Carlsbad, CA, USA) and then incubated with Opti-MEM for 4 h before transfections. psPAX2 and pMD2.G along with either scramble or pLKO.1 clones targeting mouse VDR (three clones) were added after mixing with Lipofectamine 2000 as per manufacturer's instructions (Invitrogen, Carlsbad, CA, USA). Opti-MEM was changed after overnight incubation with DMEM containing 10% FBS without antibiotics to allow cells to take up the plasmids and recover. Culture media was collected at 36 and 72 h post-transfection for viral particles. Viral particles present in the supernatant were harvested after a 15-min centrifugation at 1,500 *g* to remove cellular debris. The supernatant was further filtered using a 0.45-μm syringe filter. Supernatant-containing virus

was either stored at −80°C for long-term storage or at 4°C for immediate use. C_2C_{12} cells at 60% confluence were infected twice overnight with 3 ml of viral supernatant containing 8 $\mu g.ml^{-1}$ polybrene in serum-free–antibiotic-free DMEM. Fresh DMEM media containing 10% FBS, antibiotics and 2 $\mu g.ml^{-1}$ puromycin (Sigma, St. Louis, MO, USA) were added the next day. Cells that survived under puromycin selection were either harvested (as stable cells) and stored or used as myotubes following differentiation.

3.3.3 Myoblast population counts and BrdU assay

Myoblasts were seeded in 6-well plates at 54,000 cells per well. Counts were undertaken by trypsinisation of adherent cells into 1 ml DMEM. Measurements were taken every 24h after seeding and each well counted in quadruplicate using a haemocytometer. DNA synthesis of myoblasts was measured via the incorporation of BrdU in place of thymidine, and detected via colorimetric ELISA assay (#6813, Cell Signalling Technology) following the manufacturers recommendations. Cells were seeded within a 96-well plate (Nunclon Delta; Thermo Scientific) with the addition of BrdU at a final 1x concentration 24h before measurement.

3.3.4 Cell cycle analysis

Myoblasts were seeded in 6-well plates and allowed to proliferate for 24h before being synchronized to G1/ early S phase by incubation of 2 mmol/l hydroxyurea (Sigma-Aldrich) for 15h. Cell cycle lock was then released by changing the medium. After 12h cells were collected via trypsinisation, centrifugation before being re-suspended in PBS/ 1% (FBS) and fixed in ice cold 80% ethanol for at least 1h. Cells were pelleted by centrifugation at 300g and the ethanol decanted pellet washed in PBS. Cells were incubated in propidium iodide staining solution (0.1% Triton X-100, 10µg/ml PI

(Sigma-Aldrich), 100µg/ml RNase in PBS) for 30 min in the dark before flow cytometry analysis on a Coulter FC 500 (Beckman Coulter).

3.3.5 Myotube morphology

Media was aspirated from differentiated cells (Day 6) and washed twice in 2ml PBS before fixation in 2 ml PBS and methanol/ acetone (2:1:1) for 5 min at room temperature. Following aspiration 2 ml methanol/ acetone (1:1) was added for 5 mins at room temperature before aspiration. Flouroshield mounting medium with DAPI (Sigma Aldrich) was applied to allow visualization of myonuclei. Normal light and fluorescent images were taken and merged together; myotube diameters were measured using ImageJ software (National Institutes of Health, Frederick, MD). Myotubes were defined as containing 3+ myonuclei and measured at 3 equidistant sections along the entire length of the cell (i.e left end, middle, right end). Myotubes were only measured if the entire cell was visible in the FOV. Five random fields of view were chosen per well from 4 wells, with 5 myotubes per view measured in blinded images. Myotubes were stained with Phalloidin (Life Technologies, Manchester, UK) after fixing in a 1:5 dilution of 2% horse serum/ PBS before visualization.

3.3.6 Muscle protein synthesis (MPS) measures

Measurements of MPS were acquired in differentiated cells measuring the incorporation of the stable isotope tracer D_2O into newly synthesised proteins as discussed previously (2.3). Medium was changed 24h before the addition of D_2O to an enrichment of 5%. Cells were incubated for 2h under normal conditions, once complete 1 ml of medium was collected and cells scraped into cold extraction buffer (pH 7.5, 50mM Tris-HCl, 1mM EDTA, 1mM EGTA, 10mM β-glycerophosphate, 50mM NaF and protease

inhibitor tablet (Roche, West Sussex, UK)), before hydrolysis, derivatisation and analysis by GC-MS. Medium D_2O enrichment was referenced to a standard curve of known D_2O enrichments. The fractional synthetic rate (FSR) was calculated as previously described (2.3).

3.3.7 Quantitative RT-PCR

Myotubes were scraped into TRizol® reagent (Invitrogen) and RNA extracted according to the manufactures protocol. Firstly chloroform was added to the lysed tissue and centrifuged at 12,000g for 15min at 4 ^{O}C. The upper aqueous phase was removed and RNA precipitated with isopropanol and the resulting pellet washed in 80% ethanol. RNA was subsequently dissolved in 20µl RNAse-free water. RNA was quantified using a Nanodrop measuring the 260nm/280nm ratio. 1000ng of RNA was reversed-transcribed with a High-Capacity cDNA Reverse Transcription kit (Life Technologies) according to the manufactures protocol. Resulting cDNA was diluted 1:5 and 1µl added per well of 384-optical well plates (Life Technologies). Primers were designed using Primer Express® software (Table 3.1). Primers were mixed with SYBR Select Master Mix (Life Technologies) and aliquots of 10µl of final mastermix added to each well. Each biological replicate was carried out in duplicate. Thermal cycling was carried out on a ViiA®7 Real-Time PCR system (Life Technologies) for 2 min at 50^{O}C, followed by 2 min 95 ^{O}C and 40 cycles of 15s at 95 ^{O}C and 60s at 60^{O}C. GAPDH was used a housekeeping gene. Target mRNA expression was quantified using the ΔΔCt method and normalized to the scramble control.

Table 3.1 Primer sequences for cell culture qRT-PCR

Gene	Accession number	Forward primer	Reverse primer
GAPDH	NM_008084.3	GGGAGCCAAAAGGGTCATCA	TGATGGCATGGACTGTGGTC
VDR	NM_009504.4	GCTATTCTCCAAGGCCCACA	CCGGTTCCATCATGTCCAGT
Myh1	NM_030679.1	GCATCCCTAAAGGCAGGCTC	CAAACACCGATGACTTGGCG
Myf5	NM_008656.5	TCAGGAATGCCATCCGCTAC	CCCGGCAGGCTGTAATAGTT
Myogenin	NM_031189	AGGAGATCATTTGCTCGCGG	ATCCTCCACCGTGATGCTGT
Myomaker	NM_025376.3	CGCCGTGACATTCTGGAGTA	TGAAGGTCGATCTCTGGGGT
Mstn	NM_010834	AGTACGACGTCCAGAGGGAT	TTGCCATCCGCTTGCATTAG

3.3.8 Immunoblotting

Cells were scraped into cold extraction buffer before homogenization via repeated pipetting using a gel-loading tip. Differentiating cells were collected 0, 2, 4 and 6 days post differentiation media change, fully differentiated cells were collected 6 days post differentiation. Samples were centrifuged at 11,000 *g* for 10 min at 4^{O}C, the supernatant removed and quantified by Nanodrop. Samples were prepared and immunoblotting undertaken as described in 0. The primary antibodies for VDR (Ab109243) and myosin (MY-32) antibodies were diluted 1:1000 and obtained from Abcam (Cambridge, UK). P-AKT Ser473 (no. 4685), P-mTOR Ser2448 (no. 2976), P-eEF2 Thr56 (no. 2331), and P-S6RP Ser235/236 (no. 2211) were diluted 1:2000 (Cell Signalling Technology, Beverly, MA). Secondary antibodies for anti-rabbit (Cell Signalling Technologies) and anti-mouse (DAKO, Ely, UK) were diluted 1:2000 in 5% low-fat milk TBST. Chemiluminescence was visualized using a Chemidoc XRS. Bands were quantified in the linear range of density by quantification of volume

intensity and normalised to total protein loaded assessed by Coomassie brilliant blue staining of the membrane.

3.4 Results

3.4.1 Efficiency of lentiviral-mediated VDR knockdown

Initially it was important to confirm stable knockdown. VDR-KD C_2C_{12} myotubes demonstrated sustained knockdown by lentiviral-mediated shRNA in both mRNA (VDR-KD: 0.0004±0.00001 ΔΔCt vs. SCR: 0.008±0.0007, $p<0.0001$) and protein expression (VDR-KD: 0.99±0.01 vs. SCR: 0.59±0.06, $p<0.0001$) (Figure 3.1).

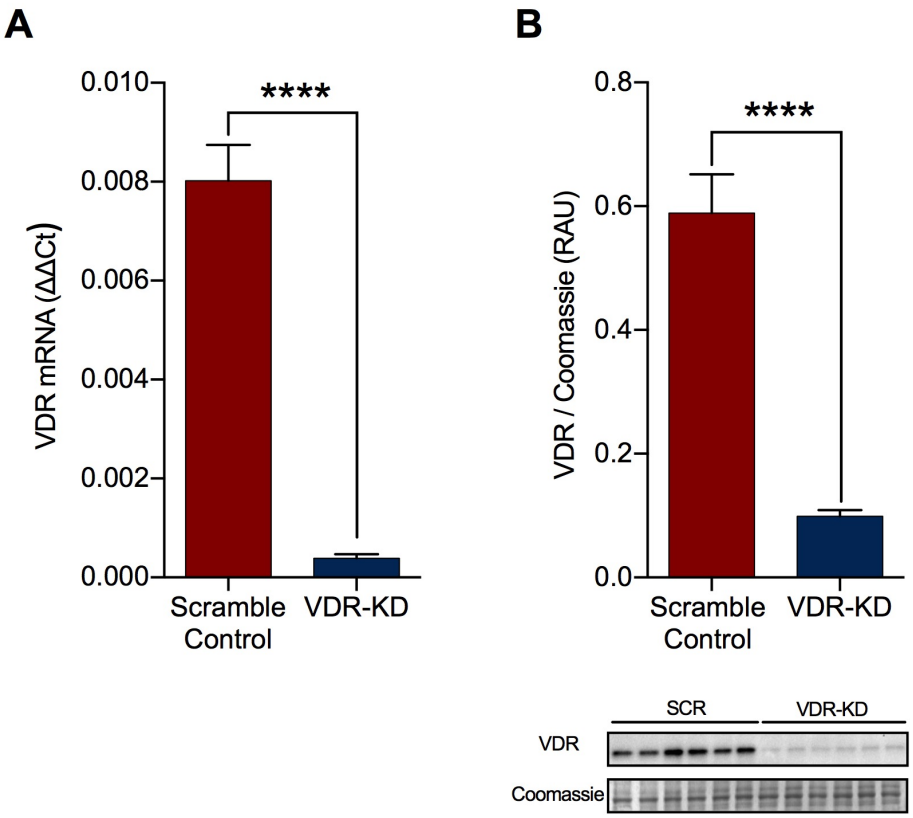


Figure 3.1 Efficacy of VDR-KD *in vitro*

(**A**) VDR mRNA expression measured by qRT-PCR presented as ΔΔCt. (**B**) VDR protein expression measured by immunoblotting presented as RAU. Values are means ±SEM, n=6. Statistical analysis via unpaired t-test, **** $p<0.0001$ vs. scramble controls.

3.4.2 Influence of VDR-KD upon myoblast proliferation

3.4.2.1 Myoblast population measures

Both VDR-KD and scramble controls demonstrated measureable rates of proliferation 48h after plating ($p<0.001$ and $p<0.01$ respectively). VDR-KD myoblasts proliferated at a reduced rate compared to scramble controls, with significantly fewer cells at 48h (VDR-KD -30±3%, $p<0.01$), 72h (VDR-KD -19%±3%,$p<0.001$) and 96h (VDR-KD -17%±0.1, $p<0.001$) after plating. (Figure 3.2)

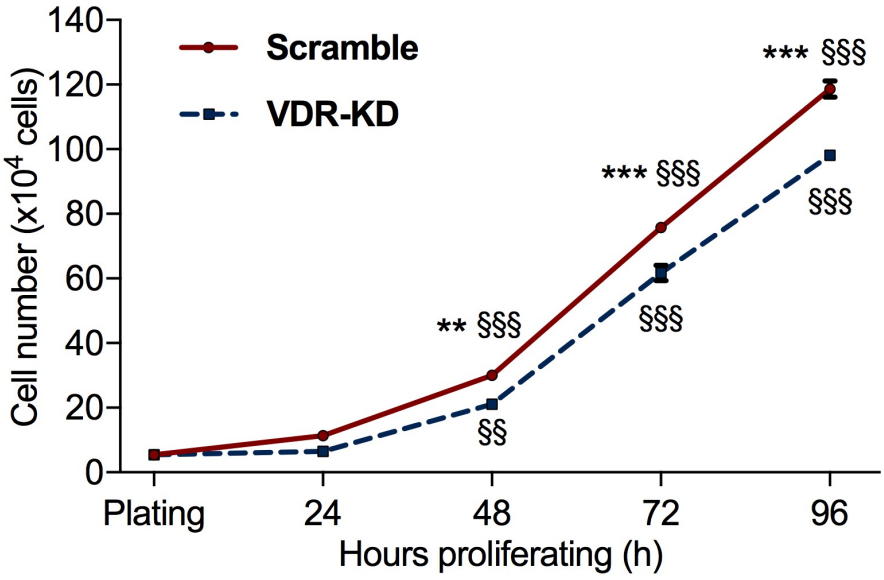


Figure 3.2 Proliferating myoblast populations

Cell population measures presented as total cell numbers per well. Both Scramble control and VDR-KD cells were plated at $5.4x10^4$ cells per well. Values are mean ±SEM, n=4 replicates. Statistical analysis via ANOVA with Tukey's post analysis, ** $p<0.01$, *** $p<0.001$ between groups at that time point, §§ $p<0.01$, §§§ $p<0.001$ vs. plating in that group.

3.4.2.2 Proliferating myoblast DNA synthesis

Myoblasts were seeded into wells and BrdU added to the culture media at 0, 24h and 48h post seeding for 24h. Both Scramble and VDR-KD myoblasts demonstrated increased DNA synthesis from plating; however increases were seen in scramble cells after 48h (24h: 1.53±0.14 vs. 48h: 2.66±0.15, $p<0.001$) and 72h in VDR-KD cells (24h: 1.54±0.11 vs. 72h: 2.76±0.18, $p<0.001$). Significant differences between scramble and VDR-KD cells were only observed 48h after seeding (VDR-KD: 1.95±0.07 vs. SCR: 2.66±0.15, $p<0.05$) (Figure 3.3).

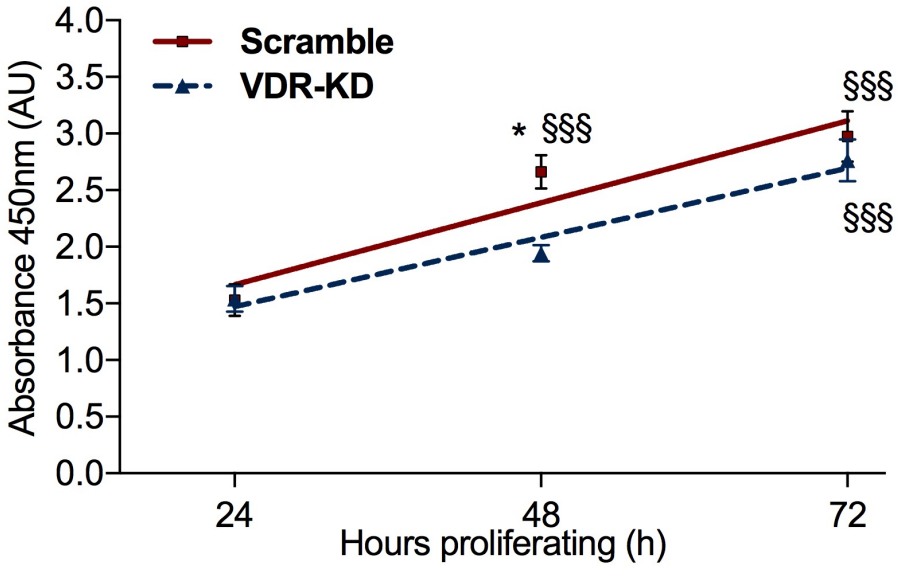


Figure 3.3 BrdU incorpetation

BrdU incorporation into proliferating scramble and VDR-KD myoblasts presented as RAU absorbance at 450nm. Values are mean ±SEM, n=10. Statistical analysis via ANOVA with Tukey's post analysis, * $p<0.05$ between groups at that time point, §§§ $p<0.001$ vs. 24h in that group.

3.4.2.3 Cell cycle analysis of proliferating myoblasts

Proliferating VDR-KD myoblast populations had a greater proportion of cells within G0/G1 phase of the cell cycle compared to scramble controls (VDR-KD: 52.1±3.5% vs. SCR: 47.4±4.3, $p<0.05$). No significant differences were observed between VDR-KD and scramble myoblast populations in either S phase or G2-M (Figure 3.4).

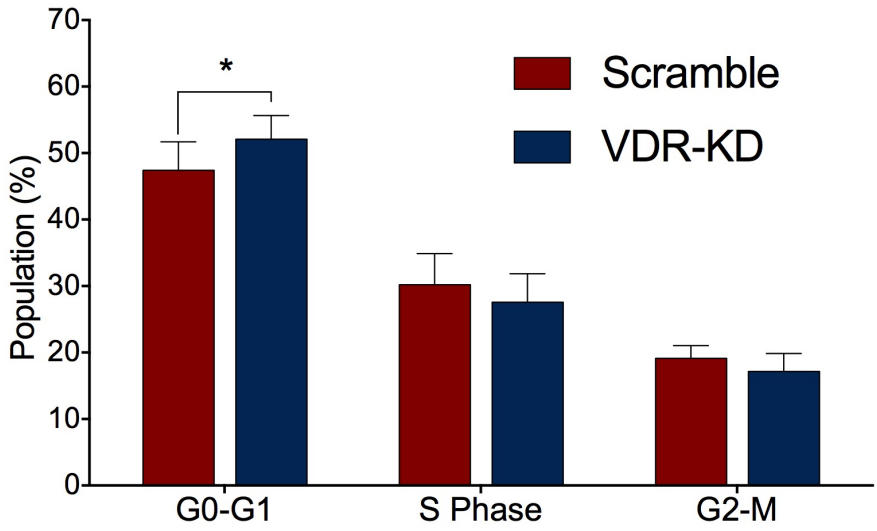


Figure 3.4 Cell cycle analysis

Analysis of myoblast cell cycle populations was assessed by flow cytometry, presented as percentage of total myoblast population. Values are means ±SEM, n=7. Statistical analysis via unpaired t-test, * $p<0.05$ vs. scramble controls.

3.4.3 Morphology of VDR-KD myotubes

Five days post differentiation induction; fewer differentiated VDR-KD myotubes were present as compared to scramble controls (VDR-KD: 18±1 myotubes/mm^2 vs. SCR 25±1, $p<0.0001$). VDR-KD myotubes that did form were significantly larger (VDR-KD: 23±0.5µm vs. SCR: 21±0.4, $p<0.01$) as a result of greater well surface are available (Figure 3.5).

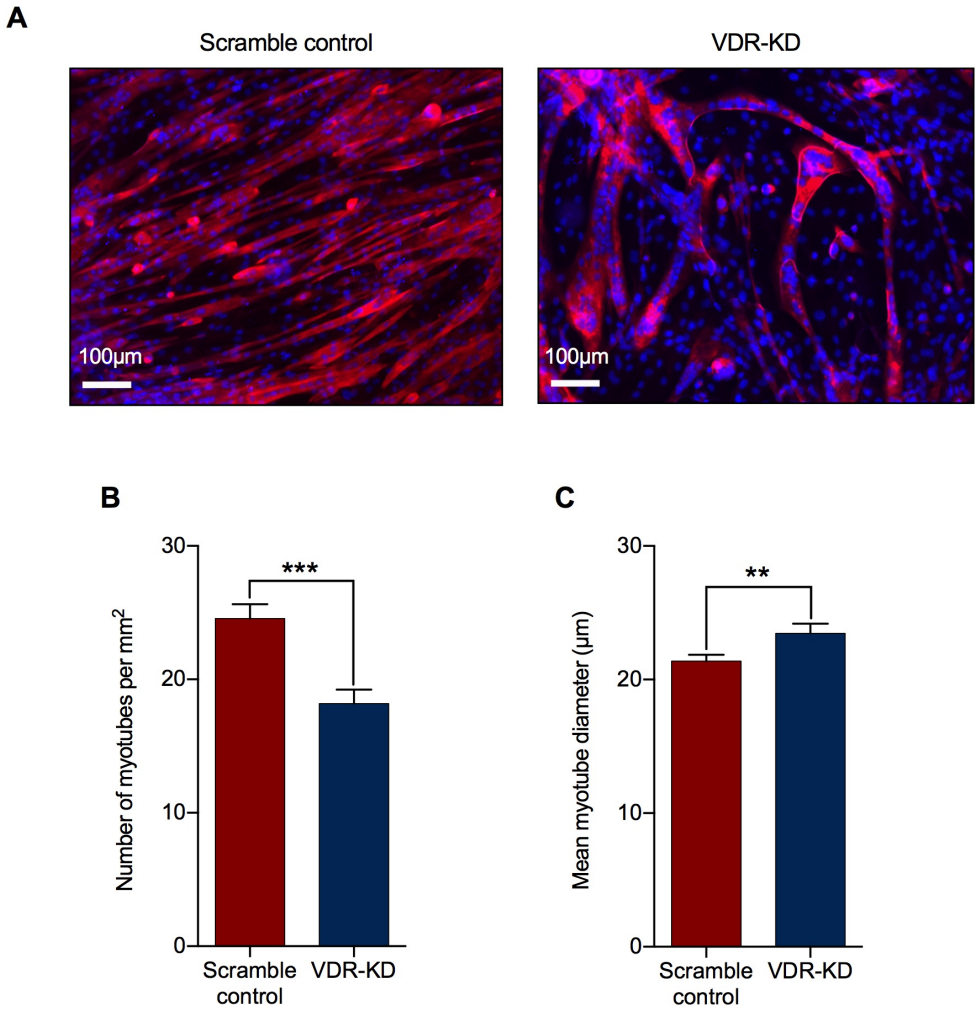


Figure 3.5 Myotube morphology characteristics

(**A**) Representative images of myotubes five days post differentiation. Cells were fixed and stained with phalloidin (actin) and DAPI (nuclei). Scale bars represent 100µm. (**B**) Number of myotubes present per mm^2. Only complete myotubes in the FOV were counted. (**C**) Myotube diameter measured in 3 equidistant locations per myotube, presented as mm^2. Values are means ±SEM, n=4 wells with 5 FOV analysed per well. Statistical analysis via unpaired t-test, ** $p<0.01$, *** $p<0.001$ vs. scramble controls.

VDR-KD cells were shown to have a higher proportion of myonuclei per myotube compared to scramble controls (VDR-KD: 24.6±1.1 vs. SCR: 9.6±0.3, $p<0.001$) (Figure 3.6) Some VDR-KD myotubes were observed to contain greater than 50 myonuclei, typically grouped within close proximity (Figure 3.5a).

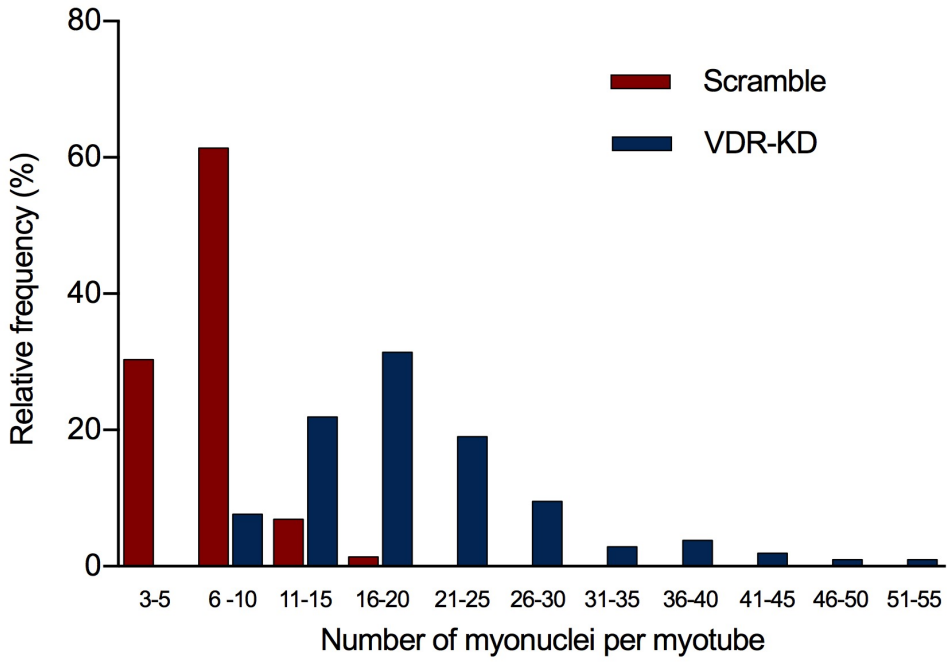


Figure 3.6 Distribution of myonuclei per myotube

Grouped distribution values of myonuclei per myotube in VDR-KD and scramble cells. Values are presented as a histogram of proportional frequency of myotubes. Only complete myotubes in the FOV were counted. n=4 wells with 5 FOV analysed per well. Mean values of each group analysed via unpaired t-test.

3.4.4 Differentiation characteristics

3.4.4.1 Myosin expression

No detectable myosin expression was observed in either group on 0 or 2 days post differentiation as to be expected. Myosin was first measured within both groups 4 days post differentiation, however it was markedly reduced between the groups at days 4 (VDR-KD: 0.12±0.02 vs. SCR: 1.0±0.2, NS) and 6 (VDR-KD: 0.5±0.1 vs. SCR: 3.9±0.6, $p<0.0001$). There was no significant increase in myosin expression in VDR-KD cells between days 4 and 6 post differentiation (Figure 3.7).

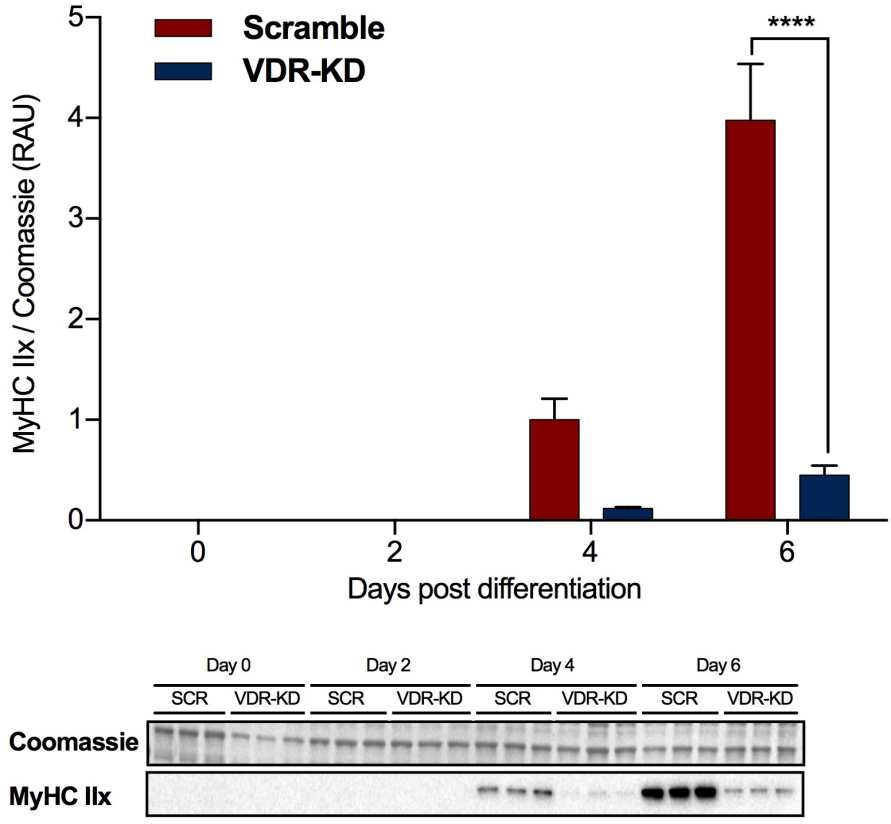


Figure 3.7 Myosin IIx protein expression throughout differentiation

MyHC IIx expression measured by immunoblotting presented as RAU. Values are mean ±SEM, n=6. Statistical analysis via ANOVA with Tukey's post analysis, **** $p<0.0001$ between groups at that time point.

3.4.4.2 Total protein, DNA and RNA

Total well alkaline soluble protein content increased throughout differentiation in both groups, but was significantly reduced at all time points in VDR-KD cells compared to scramble controls (VDR-KD: -20±3%, $p<0.001$). Both groups significantly increased total protein content compared to their respective day 0 values ($p<0.0001$) (Figure 3.8A). Overall DNA content unsurprisingly did not significantly change in differentiating scramble control cells, but continually increased in VDR-KD cells from day 0, with significant increases seen after 4 and 6 days post differentiation (D0: 4.9±0.5mg vs. D4: 16.7±1.4 vs. D6: 20.9±1.3, $p<0.0001$). Initial day 0 DNA content in VDR-KD cells was less than scramble controls (VDR-KD: 4.9±0.5mg vs. SCR: 12.2±0.9, $p<0.001$), but became higher 4 days (VDR-KD: 16.6±1.6mg vs. SCR: 13.5±1, N.S) and 6 days (VDR-KD: 20.9±1.3mg vs. SCR: 15.4±0.7, $p<0.01$) post differentiation (Figure 3.8B). Total RNA content increased throughout differentiation within scramble control cells, showing significant increases from day 0 at days 4 and 6 (D0: 52.2±7.0mg vs. D4: 98.0±4.5 vs. D6: 112.7±4.1, $p<0.0001$). VDR-KD cells showed no initial increase in RNA content until 4 days post differentiation (D0: 42.2±1.2 vs. D4: 71.7±4.7, $p<0.001$), and was significantly less than scramble controls on days 2 (VDR-KD: 40.0±0.9 vs. SCR: 73.4±6.5, $p<0.001$) and 4 (VDR-KD: 71.7±04.7 vs. SCR: 98.0±4.5, $p<0.01$) (Figure 3.8C).

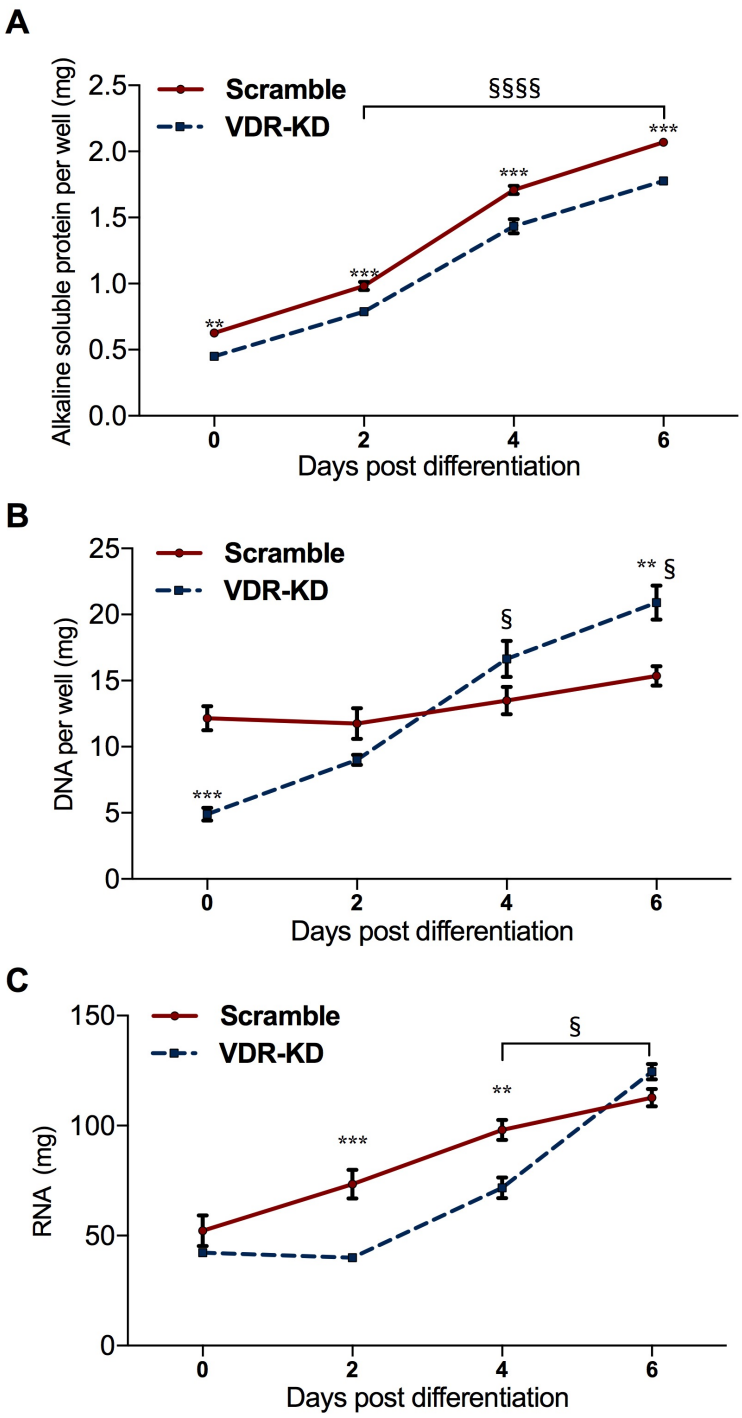


Figure 3.8 Total protein, DNA and RNA measures throughout differentiation

(**A**) Total well ASP, (**B**) DNA, (**C**) RNA. All total measurements are from the same wells at each time point, presented as mg. Values are mean ±SEM, n=6. Statistical analysis via ANOVA with Tukey's post analysis, ** $p<0.01$, *** $p<0.001$ between groups at that time point, § $p<0.05$, §§§§ $p<0.0001$ vs. Day0 in that group.

3.4.5 Differentiated myotubes

3.4.5.1 Myogenic regulatory factors and markers of differentiation

VDR-KD myotubes 6-days post differentiation demonstrated reduced mRNA expression of multiple myogenic regulatory factors, and markers of differentiation compared to scramble controls. These included Myosin heavy chain 1 (Myh1) (VDR-KD: 0.35±0.08 vs. SCR 1.00±0.11, p<0.001), Myomaker (VDR-KD: 0.16±0.02 vs. SCR 1.00±0.33, p<0.05), Myogenin (VDR-KD: 0.53±0.08 vs. SCR 1.00±0.22, NS), Myf5 (VDR-KD: 0.35±0.09 vs. SCR 1.00±0.14, p<0.01). Mstn expression was unchanged by VDR-KD.

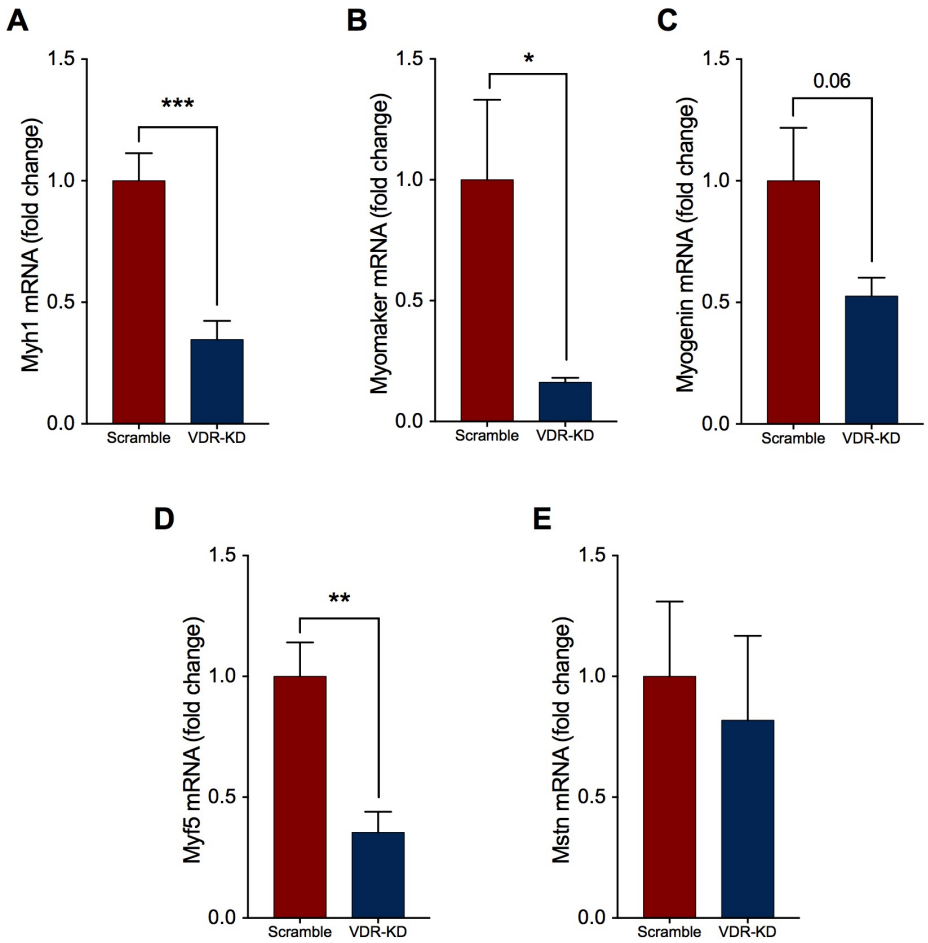


Figure 3.9 mRNA expression of myogenic regulatory factors

mRNA expression of (A) Myh1, (B) Myomaker, (C) Myogenin, (D) Myf5 and (E) Mstn in myotubes 6-days post differentiation, presented as fold change from scramble control. Values are means ±SEM, n=6. Statistical analysis via unpaired t-test, * $p<0.05$, ** $p<0.01$ *** $p<0.001$ vs. scramble controls.

3.4.5.2 *Myofibrillar fractional synthetic rates (FSR)*

Myofibrillar fractional synthetic rates were severely reduced in VDR-KD myotubes compared to scramble controls (VDR-KD: 0.87±0.06%/h vs. SCR: 1.46±0.04, $p<0.001$) (Figure 3.10).

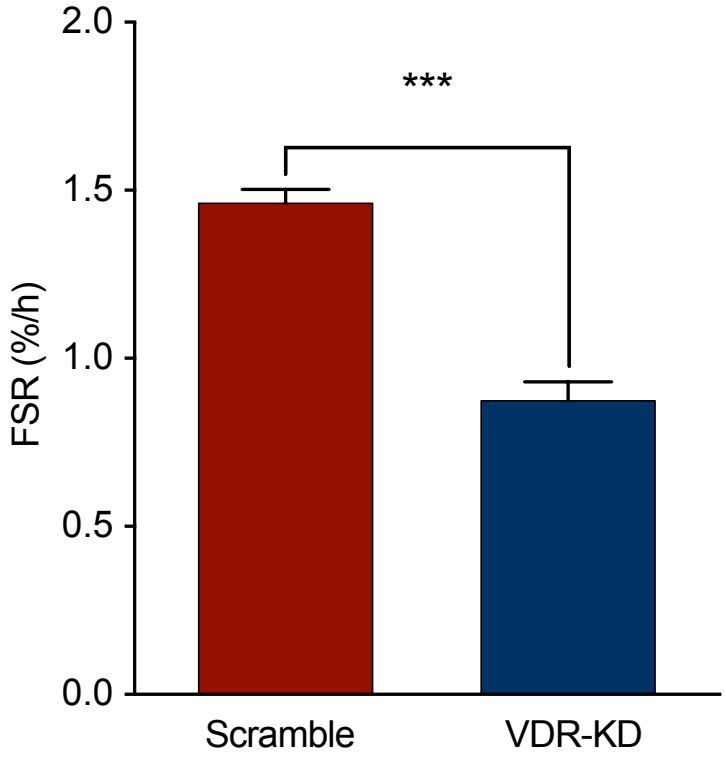


Figure 3.10 Myofibrillar fractional synthetic rates

Myofibrillar fraction synthetic rates in VDR-KD and scramble control cells, presented as %/h. Values are means ±SEM, n=6. Statistical analysis via unpaired t-test, *** $p<0.001$ vs. scramble controls.

3.4.5.3 *Anabolic signalling*

There was no influence of VDR-KD upon the expression of the anabolic intermediates mTOR, eEF2, RPS6 or 4E-BP1. However, AKT signalling demonstrated a small non significant decrease compared to scramble controls (VDR-KD: 0.69±0.07 vs. SCR: 1.00±0.13, NS) (Figure 3.11)

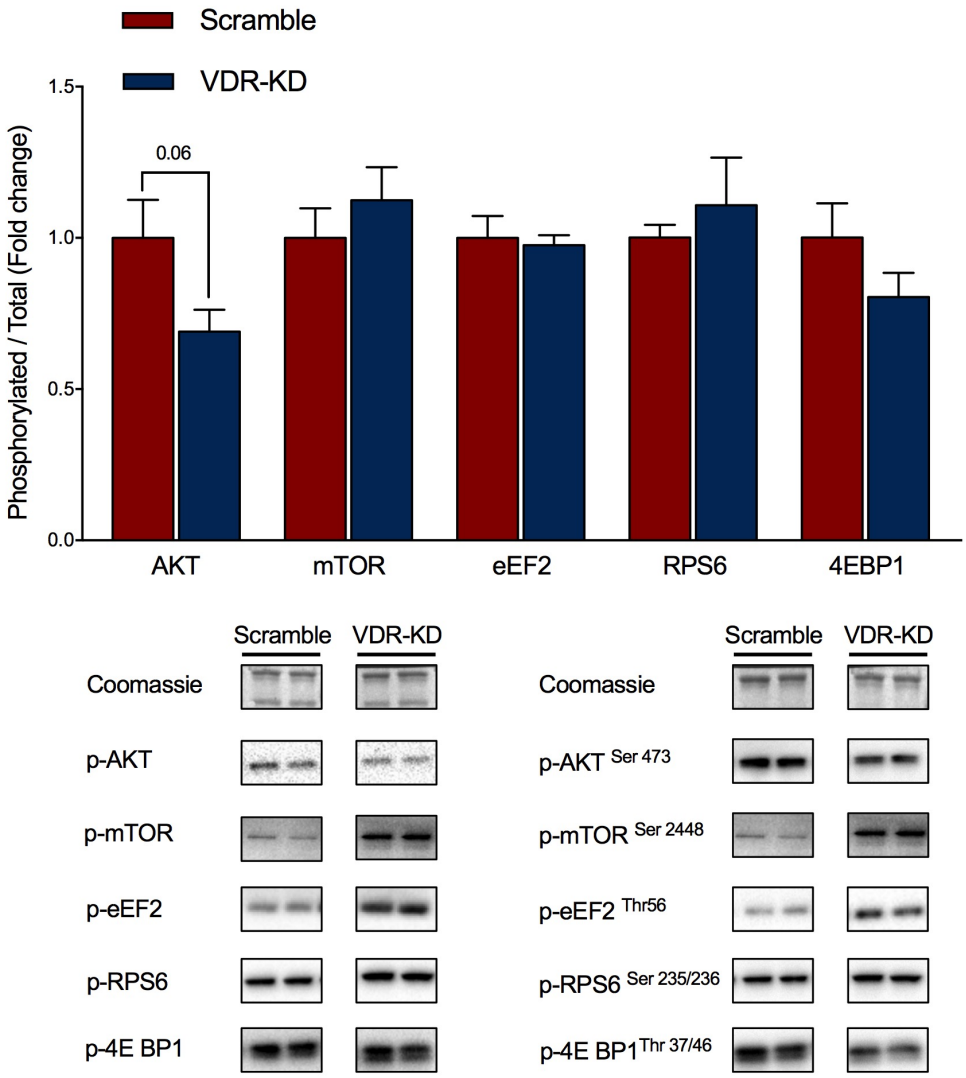


Figure 3.11 Anabolic signalling

Anabolic signalling expressed as phosphorylated levels by total expression for AKT, mTOR, eEF2, RPS6 and 4E-BP1 in VDR-KD and scramble myotubes. Measured by immunoblotting and presented as fold change from scramble controls. Values are means ±SEM, n=6. Statistical analysis via unpaired t-test.

3.5 Discussion

The aim of the current study was to investigate the impact loss of the VDR would have upon myogenesis. It was hypothesized loss of the VDR would impair myogenic development. Within this study it was demonstrated loss of the VDR impaired myogenesis, namely through reduced myoblast proliferation rates, combined with compromised myotube differentiation.

Initially we wanted to investigate the unknown role of the VDR upon myoblast proliferation. Despite the same seeding densities, proliferating VDR-KD myoblasts had reduced populations throughout each time point. Supporting this observation, measures of DNA synthesised (assessed by BrdU incorporation) showed moderate reductions in VDR-KD cells. Although these findings seem to oppose previous observations, the influence VitD has upon myoblast proliferation is currently ambiguous. Outcomes seem to be partially dependent on the duration of VitD administration and culture conditions. Enhanced myoblast proliferation has been demonstrated to occur during short incubation periods (4-24h) (Buitrago et al. 2012; Bellido et al. 1987), whereas longer (24h+) incubations inhibit proliferative rates, potentially through a reduction of MRFs (i.e. myogenin and Myf5) (Girgis, Clifton-Bligh, et al. 2014; Srikuea et al. 2012). Furthermore, typical myoblast growth media is supplemented with 10% serum, with exogenous $1,25(OH)_2D_3$ inducing anti-proliferative effects at this concentration (van der Meijden et al. 2016); whereas higher concentrations (15%) have displayed enhanced proliferative rates and DNA synthesis (Drittanti et al. 1989b). However, these studies did not investigate the autonomous role the VDR has upon proliferation.

Myoblast progression through the cell cycle was also investigated within these cells, to discern whether alterations within this process contributed to the impaired proliferation. Here we demonstrate that VDR-KD was associated with reduced myoblast proliferation and a greater proportion of myoblasts accumulated within the G0/G1 cell cycle phase. The data conflicts with work showing VDR-KD by similar lentiviral means did not influence the cell cycle (Irazoqui et al. 2014). It is important to note that within this study, myoblasts populations were not synchronised to one phase of the cell cycle. Conversely, within this study, myoblasts were synchronised into G1 phase through hydroxyurea incubation (Traganos et al. 1982), before subsequent released from the cell cycle lock and collected after 12h. It may be that synchronizing of VDR-KD myoblasts, emphasized cell cycle dysregulation, whereas these observations were obscured in the previous investigation. Moreover, cells in G1 phase will not have undergone DNA synthesis (S phase), consistent with our observations of diminished BrdU incorporation.

Based on previous results and literature, we hypothesized that VDR-KD would result in impaired myogenic development. In our investigation, once fully differentiated, the total number of VDR-KD myotubes was reduced compared to scramble controls. Within our study a continued cell culture model was utilised, in which following proliferation, differentiation was induced through serum starvation. As previously discussed, VDR-KD produced anti-proliferative effects, resulting in reductions in the total myoblast population compared to scramble controls. Thus, the population reduction may influence the total number of myotubes present. Myotubes that did develop had a greater diameter, appearing to contrary the phenotype seen in previous *in vitro* studies reporting thinner myotubes in

response to VDR-KD, although no measurements were reported (Tanaka et al. 2014). However, these studies achieved sustained knock-down using siRNA, requiring cells to be plated at a higher density, before immediate induction of differentiation, thus less space would have been available within the culture vessel. This further supports the notion that through the reduction of total myoblasts present, fewer but larger myotubes developed in the space available.

Further myotube morphological measures were undertaken, indicating an increased myonuclei content with VDR-KD myotubes that did develop. Within skeletal muscle it is generally believed each myonuclei is associated with a specific cytosolic volume, known as the myonuclear domain (van der Meer et al. 2011). The sheer number of myonuclei (+25) within some VDR-KD myotubes will undoubtedly result in larger myotubes, supporting earlier diameter measurements. Once switched to a reduced serum concentration, myoblasts undergo cell cycle withdrawal and terminally differentiate. Under these conditions, DNA content typically remains largely stable, as no proliferation is expected to be occurring (Smith et al. 1999). Consistent with this, DNA content of scramble control cells remained stable over the time course of differentiation, as little to no myoblast proliferation was occurring. Initial reductions observed in DNA content between scramble control and VDR-KD cells suggest a reduction in total myoblasts present, corresponding with earlier observations of impaired proliferation. However, throughout differentiation, VDR-KD cells continually increased DNA accumulation, representing active cell proliferation. This suggests that despite reductions in proliferative rates, VDR-KD myoblasts failed to undergo differentiation into post-mitotic myotubes, instead continuing to proliferate.

Expression of multiple MRFs and differentiation markers were also assessed within VDR-KD myotubes, demonstrating reduced mRNA expression. Myomaker, a differentiation marker recently described to be a key regulator of myoblast fusion (Millay et al. 2013) was considerably reduced within VDR-KD cells 6-days post differentiation. Furthermore expression of Myf5 and myogenin, known regulators of early and late stage differentiation respectively (Rudnicki et al. 1993; Andres & Walsh 1996), were significantly decreased in VDR-KD cells. Furthermore Myf5 mutant myoblasts have demonstrated reduced rates of proliferation, coupled with a delayed transition from proliferation to differentiation, resulting in fewer myotubes (Ustanina et al. 2007). The data complement the previous *in vitro* investigations by Tanaka *et al* (2014), showing reduced MRF expression in VDR-KD myotubes. Nonetheless, analysis of DNA content throughout differentiation adds a further facet to the observed reductions in MRF expression, supporting the concept of continual proliferation. Likewise, the opposite pro-differentiation increased myogenin expression by exogenous VitD upon cultured cells, coincides with this notion (Irazoqui et al. 2014; van der Meijden et al. 2016; Garcia et al. 2011). Thus the current data would imply the VDR modulates proliferative and differentiation aspects of myogenesis, with loss of the receptor resulting in a proliferative phenotype.

This lack of differentiation to post-mitotic cells in VDR-KD should be reflected by impairments in the synthesis of regulatory contractile proteins (e.g. myosin heavy chain) (Brown et al. 2012; Okuno et al. 2012; Guerin & Kramer 2009). In line with this, differentiating VDR-KD myoblasts showed

a substantial absence of myosin IIX protein accrual compared to shRNA controls, in addition to decreased myosin I mRNA expression. This matches previous observations of reduced RNA expression of multiple myosin isoforms by Tanaka *et al* (2014) in differentiated myotubes. In agreement with this, rates of myofibrillar muscle protein synthesis (MPS) were blunted in VDR-KD cells, matching reductions in total protein content seen throughout differentiation.

Capacity for protein synthesis may be estimated by the measurement of RNA content within various tissues since it reflects translational capacity as rRNA accounts for ~85% of cellular RNA (Sugden & Fuller 1991; Nader et al. 2002). Total RNA content within skeletal muscle has been shown to be reflective of synthetic capacity as increased protein synthesis in response to mechanical stimuli is associated with increased total RNA content (Goldspink et al. 1995). In this study differentiating VDR-KD myoblasts were shown to have reduced total RNA content compared to shRNA controls throughout differentiation until the final day 6 measurement. This suggests a decreased synthetic capacity as a result of VDR-KD, reflected in reductions myosin and myofibrillar MPS measures. Previous studies examining the role of the VDR within myogenesis have not directly investigated changes within rates of protein synthesis. Interestingly, exogenous $1,25(OH)_2D_3$ has been demonstrated to increase the expression of some ribosomal proteins (i.e. RPL21 and RPS4) (Freedman 1999), suggesting positive modulation of ribosomes and synthetic capacity.

Within skeletal muscle anabolic signalling regulators such as the AKT/mTOR-mediated pathway are frequently attributed to the modulation of protein synthesis within both *in vivo* and *in vitro* studies (Atherton et al.

2010a; Dickinson et al. 2011). Stimuli resulting in increased MPS, such as essential amino acid (EAA) administration or exercise are shown to be as a regulated by the phosphorylation of multiple signalling intermediates (i.e. AKT, S6RP, eEF2). Conversely, reduced signalling suggests a blunting of the MPS response, for examples through age-related anabolic resistance to EAAs (Cuthbertson et al. 2005). The modulation of anabolic stimuli by $1,25(OH)_2D_3$ has previously been investigated; for example stimulation of mTOR mediated signalling and protein synthesis was potentiated when $1,25(OH)_2D_3$ was administered with leucine and insulin compared to leucine and insulin alone (Salles et al. 2013). Such a modulation of anabolic signalling may clarify earlier studies showing increased myosin expression in response to $1,25(OH)_2D_3$ (Tanaka et al. 2014). Previous investigations demonstrated AKT mediated anabolic signalling was partially blunted in response to exogenous VitD in VDR-KD cells, suggesting the requirement of the VDR for VitD stimulated responses (Buitrago et al. 2013). It was speculated that in sequence with reductions in MPS rates, anabolic signalling would be reduced in VDR-KD cells. However, within this study, VDR-KD did not modify mTOR mediated anabolic signalling. This suggests the phenotype of impaired differentiation seen in VDR-KD cells, is likely not regulated though alterations in mTOR signalling. However, dissociations between protein phosphorylation status and MPS have been observed, whereby pathway flux may not necessarily be representative of MPS rates. (Atherton et al. 2010a; Greenhaff et al. 2008). Indeed in this study, decreased rate of MPS were not coupled with reduced pathway flux (phosphorylation as a proxy). Assessment of protein phosphorylation status over a time course in relation to MPS measures may have eluded to this apparent disconnect. Nonetheless, reduced MPS rates and myosin expression are likely resultant from the impairment of myoblast differentiation and subsequent lack of myotubes.

3.6 Conclusion

In summary, the data presented demonstrates loss of the VDR impairs myoblast proliferation and differentiation, resulting in a lack of induction into post-mitotic myotubes. These findings demonstrate an autonomous role of the VDR within myoblast proliferation. Additionally, the data clarify the mechanism of impaired differentiation through reductions in synthetic capacity and myofibrillar MPS rates, combined continual myoblast proliferation resulting in the absence of myotubes and MRF induction.

Chapter 4 – The Influence of Vitamin D Receptor Expression on Skeletal Muscle Metabolism *in vivo*

4.1 Introduction

As the previous *in vitro* study highlighted the role VDR has within skeletal muscle myogenesis, subsequent investigations into the impact it has upon established muscle were undertaken.

Epidemiological studies have linked VitD deficiency with a reduction in skeletal muscle mass and function (Dhanwal et al. 2013), increased risk of falls in elderly individuals (Bischoff-Ferrari, Dietrich, et al. 2004) and development of type 2 diabetes (T2D) (Pittas et al. 2007). Furthermore, chronic VitD deficiency is accompanied by severe skeletal muscle myopathies that can be rescued by VitD supplementation (Prabhala et al. 2000). In contrast, VitD supplementation has been shown to enhance muscle function and myofibre cross sectional area (CSA) in the elderly (Ceglia et al. 2013; Sato et al. 2005) and increase muscle function in athletes (Close, Russell, et al. 2013; Trial et al. 2015). While not entirely consistent (Halfon et al. 2015), the data suggest that VitD deficiency may have a deleterious impact on skeletal muscle.

Consistent with this, VitD has been shown to have cell autonomous effects in skeletal muscle. VitD acts through its ubiquitously expressed (Norman 2008) cognate vitamin D receptor (VDR). Recent studies have confirmed expression of the VDR (Pike 2014) and CYP27B1 (the gene responsible for conversion of inactive 25[OH]D_3 to active 1α,25[OH]$_2D_3$) in skeletal muscle (Srikuea et al. 2012), highlighting the skeletal muscle as VitD sensitive tissue.

As previously discussed, the VDR is proposed to have an autonomous role in myogenic development. Moreover, potential roles of the VDR have been reported *in vivo*, within established skeletal muscle. Studies have shown that VDR expression is positively linked to skeletal muscle regeneration following muscle damage (Srikuea et al. 2012), and that VDR is acutely upregulated in response to resistance-type exercise (Makanae et al. 2015). These investigations suggest the VDR has a role within mature skeletal muscle. Indeed, whole-body VDR knockout (VDR-KO) mice exhibit reductions in muscle fibre size and grip strength (Endo et al. 2003; Girgis et al. 2015) and dysregulation in the gene expression of myogenic regulatory factors (i.e. increased myf5 and myogenin) (Endo et al. 2003), matching previously discussed *in vitro* investigations. Nonetheless whole-body VDR-KO impacts Ca^{2+}/Pi homeostasis and bone metabolism, requiring rescue diets to normalize blood mineral ion levels (Amling et al. 1999). Thus, developmental dysregulation in VDR-KO models have precluded the identification of a post-natal role of the VDR in skeletal muscle. Overall, these findings provide tentative associations between VitD, the VDR and skeletal muscle mass; however, the mechanistic links the VDR may have within skeletal muscle has yet to be established.

4.2 Aims and hypothesis

As a subsequent study to the *in vitro* investigation, the present study aimed to characterise the role VDR expression has upon protein metabolism within developed skeletal muscle. Through modulation of VDR expression in established muscle, previously discussed developmental and mineral ion dysregulation would be avoided. The specific aims of this experimental chapter were:

- Confirm bi-directional modulation of VDR expression in rat skeletal muscle.
- Assess changes in fibre CSA and protein content.
- Measure essential aspects of protein metabolism, including anabolic/ catabolic signalling and protein synthesis.
- Characterise satellite cell content and proliferative markers.
- Determine changes in glucose metabolism in skeletal muscle.

It was hypothesised loss of the VDR would negatively impact muscle protein metabolism, whereas over-expression would positively enhance it. Specifically, it was hypothesised loss of the VDR would induce atrophy through dysregulated protein metabolism, whereas VDR over-expression would result in fibre hypertrophy.

4.3 Methodology

4.3.1 Animal handling and study design

All animal experimental procedures were undertaken and approved by the Royal Veterinary College's Ethics and Welfare committee, carried out under UK Home Office licence to comply with the Animals (Scientific Procedures)

Act 1986. Eight-week-old male Wistar rats were housed at 22 ± 0.5°C under a 12h day/ 12h night cycle and acclimatized to their new surroundings for one week. Animals this age were chosen due to time and location constraints. Animals were fed a standard chow diet (18% fat, 33% protein, and 48% carbohydrate as a percentage of total dietary energy) ad libitum. Four experimental groups were used, with two additional groups to assess basal and maximal D2O enrichment (Table 4.1), a total of 38 animals were used. *In vivo* electrotransfer (IVE) was performed as detailed below (4.3.2). Seven days' post IVE, groups 3 and 4 received D2O as detailed below (4.3.3). Ten days after IVE all rats were fasted overnight and either underwent an intraperitoneal glucose tolerance test (IPGTT) or euthanised by injection of pentobarbitone, undertaken as illustrated (Figure 4.1). Muscles were rapidly dissected after euthanasia; transverse sections were mounted on cork tiles in optimum cutting temperature (OCT) medium and snap-frozen in liquid nitrogen-cooled isopentane. The remaining muscle was freeze clamped and stored at -80^{O}C.

Table 4.1 Animal groups

Group	Designation	IPGTT	Body mass (g) ±SEM	N
Group 1	Basal D_2O enrichment	-	226±2	2
Group 2	Maximal D_2O enrichment	-	234±2	2
Group 3	VDR knockdown	-	256±6	7
Group 4	VDR over-expression	-	269±5	7
Group 5	VDR knockdown	Yes	251±5	10
Group 6	VDR over-expression	Yes	252±4	10

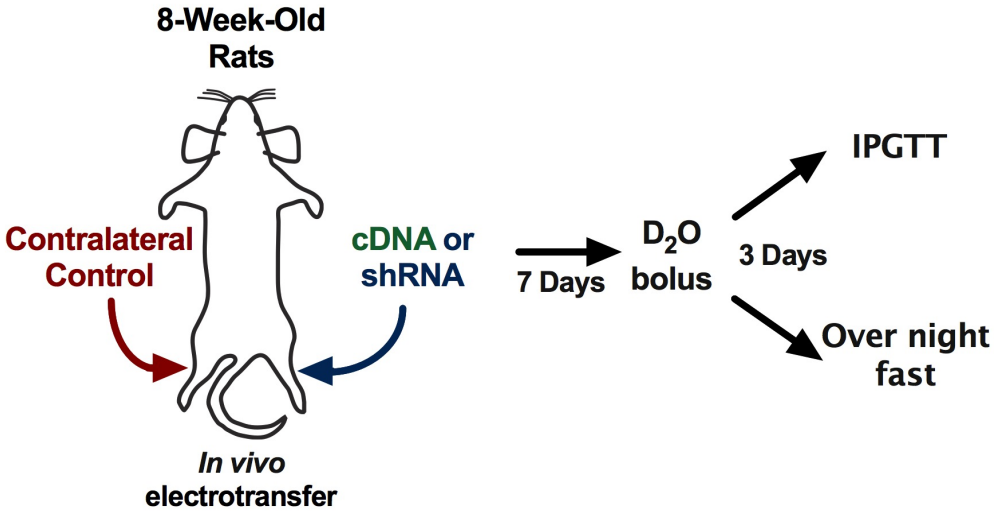


Figure 4.1 Schematic representation of study protocol

Schematic of *In vivo* protocol. Groups of animals received either cDNA or shRNA in the right *tibialis anterior* muscles, before IVE and left for 7 days. Animals were sacrificed three days after receiving a D_2O bolus.

4.3.2 *In vivo* electrotransfer

4.3.2.1 VDR-KD vector information

Vitamin D receptor knockdown (VDR-KD) was achieved in right hind leg *tibialis anterior* muscle through *in vivo* electrotransfer of four unique rat VDR pGFP-C-shLenti plasmid constructs driven by a U6 promoter (Table 4.2). These constructs spanned multiple regions of rat VDR mRNA (NM_017058.1) to ensure effective coverage and knockdown (Figure 4.2). Left leg *tibialis anterior* muscles received scramble cassette sequence controls (OriGene, Rockville, USA). Plasmid DNA amplification was undertaken within JM109 *Escherichia coli* cells under puromycin selection (0.5µg/ml) overnight. Plasmid DNA was purified using an endotoxin free plasmid Maxi Kit (Qiagen, Manchester, UK) as per the manufacturers instructions.

Table 4.2 VDR-KD shRNA sequences

	Sequences
shRNA 1	AATGGAGATTGCCGCATCACCAAGGACAA
shRNA 2	TCACCTCCGATGACCAGATTGTCCTGCTT
shRNA 3	GCTGGTGGAAGCCATTCAGGACCGCCTAT
shRNA 4	TTGTGCTGGAGGTGTTCGGCAATGAGATC



Figure 4.2 VDR-KD shRNA alignment

Demonstration of alignment for each shRNA with rat VDR mRNA.

4.3.2.2 VDR-OE vector information

Vitamin D receptor over-expression (VDR-OE) was achieved in right leg *tibialis anterior* muscle through *in vivo* electrotransfer of pCAGGS-mVDR vector constructs. The mouse cDNA sequence utilised was 92% homologous to rat VDR mRNA (Figure 4.3). To obtain pCAGGS-mVDR, myc-DDK-mVDR was subcloned in the pCAGGS vector. Left leg *tibialis anterior* muscles received empty pCAGGS vector controls. Plasmid DNA amplification was undertaken within JM109 *Escherichia coli* cells under puromycin selection (0.5µg/ml) overnight. Plasmid DNA was purified using an endotoxin free plasmid Maxi Kit (Qiagen, Manchester, UK) as per the manufacturers instructions.

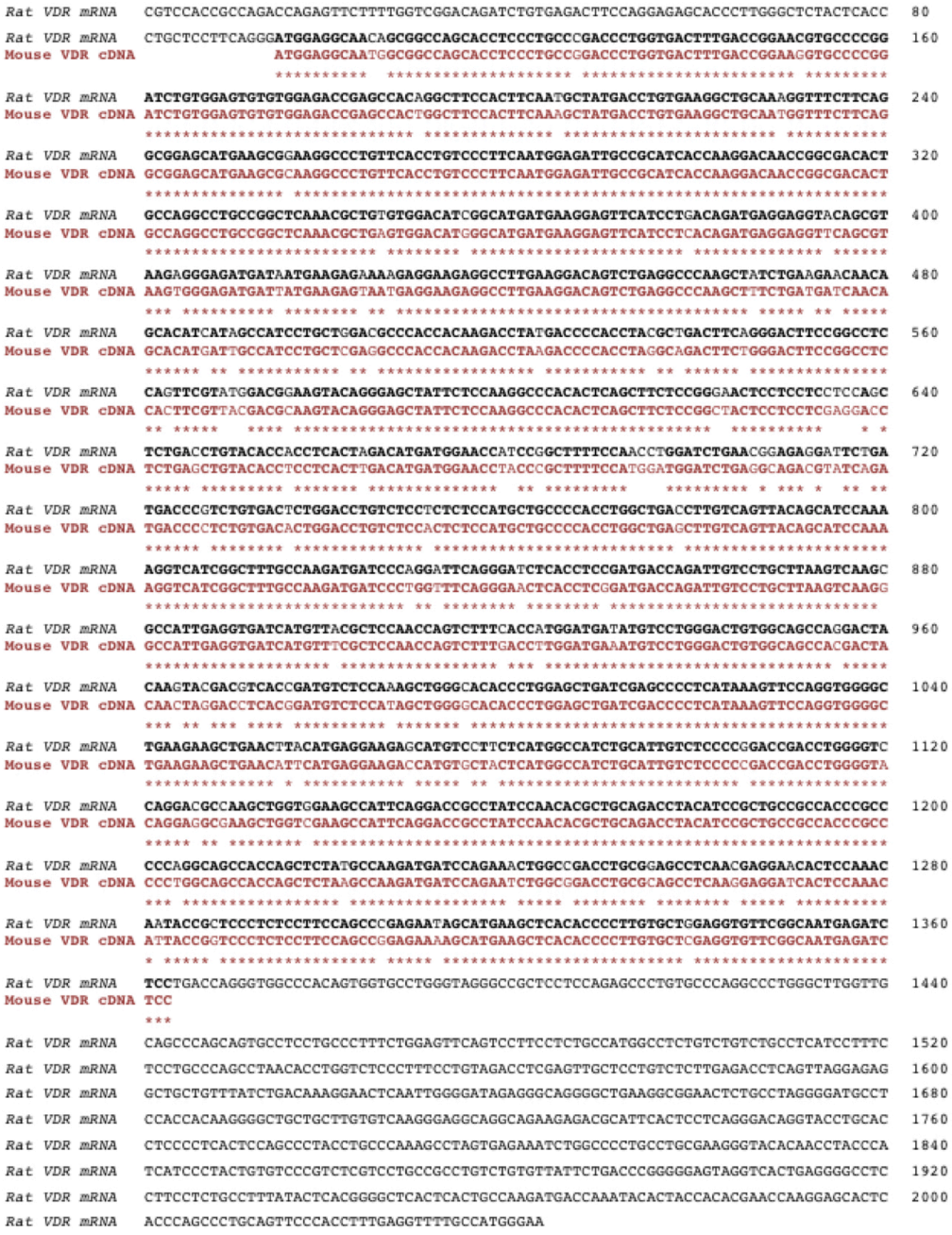


Figure 4.3 Mouse VDR cDNA homology

Demonstration of mouse cDNA homology to rat VDR mRNA.

4.3.2.3 *In vivo* electrotransfer (IVE)

Electrotransfer of DNA into live cells was first utilised by *Neumann* et al (1982), with the technique developing and improving over time (Miyazaki & Miyazaki 2009). DNA is injected intramuscularly in multiple locations. To allow for effective distribution throughout the muscle hyaluronidase is initially injected, to break down components of the extracellular matrix (ECM). This increases the space between fibres allowing greater delivery and decreasing muscle damage (McMahon et al. 2001). Electric-pulses applied by external electrodes stimulate electrotransfer; an initial short single high-voltage (HV) pulse permeabilises the fibre membrane, followed in quick succession by four low-voltage to electroporate the DNA (Figure 4.4). This combination of HV and LV pulses is the most efficient method of delivery, whilst minimising muscle damage (Hojman et al. 2007; Satkauskas et al. 2002). Animals are generally studied at least seven days after IVE to allow muscles to recover (Patel et al. 2012).

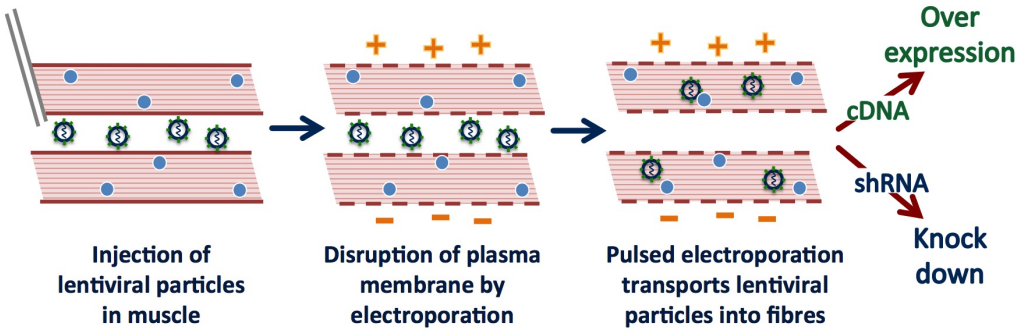


Figure 4.4 Principle of IVE

Illustration of IVE principle in developed skeletal muscle. Initially lentiviral particles are injects into the muscle before disruption of the plasma membrane by a high voltage pulse, followed by multiple low voltage pulses to drive the particles into the fibres.

In this study animals were anaesthetised under isofluorane (2.5%) and their hind limbs shaved and prepared with ethanol. *Tibialis anterior* muscles (TAM) were injected intramuscularly with six spaced 50 µl aliquots of DNA prepared in endotoxin-free sterile saline at 0.5mg/ml. VDR-KD

groups received VDR shRNA in right leg TAM and scramble shRNA in left leg TAM. VDR-OE groups received pCAGGS-mVDR in right leg TAM, and empty pCAGGS controls in left leg TAM. Immediately following, one HV (900 V/cm, 100 µ-sec pulse), and four LV (90 V/cm, 100 m-sec) pulses were administered across the distal limb via tweezer-electrodes attached to an ECM-830 electroporator (BTX, Holliston, MA). Animals subsequently received a subcutaneous injection of carprofen (50mg/kg), before recovery from anesthesia.

4.3.3 Muscle protein synthesis measures

Seven days post IVE, animals received a D_2O bolus through oral gavage (7.2mls/kg, 70 atom%). Group 1 animals received no D_2O for assessment of basal enrichment. For maximal D_2O body water enrichment, group 2 animals were euthanised 2h after oral gavage, and blood collected in pre-chilled tubes containing Lithium Heparin. These were subsequently cold centrifuged at 1750g, with plasma fractions separated into aliquots and frozen at -80^{O}C. Ten days after IVE (~72h of D_2O enrichment) groups 3 and 4 were overnight fasted and euthanised before bloods collected. Muscle samples were separated into their respective sub-cellular fractions, hydrolysed, derivatised and analysed by GC-MS as previously discussed (2.3). Body water enrichment of plasma from basal, maximal enrichment, and test samples were measured using the previously described acetone exchange method (2.3). Measurement of body water enrichment in groups two, three and four confirmed consistent enrichment between all groups and steady tracer decay (Figure 4.5).

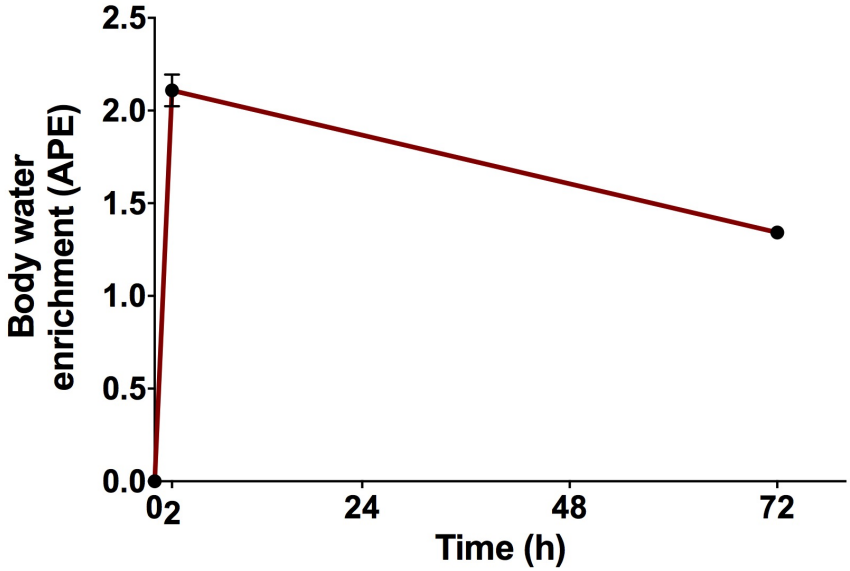


Figure 4.5 Body water enrichment

Acetone exchange measures of body water enrichment from blood plasma, in unenriched (n=2), maximal (n=2) and +72h enriched IVE groups (n=14). Values are means ±SEM.

4.3.4 Intraperitoneal glucose tolerance test (IPGTT)

Glucose uptake and muscle glycogen content were performed as described by (Roustit et al. 2014). Ten days post IVE, groups 5 and 6 were overnight fasted and glucose uptake into paired TA muscles was measured using an intraperitoneal glucose tolerance test (IPGTT), combined with administration of 2-[1,2- ^{3}H(N)]-Deoxy-D-glucose (^{3}H-2DG) Perkin-Elmer, Buckinghamshire, UK)) tracer. Approximately 5MBq ^{3}H-2DG glucose was administered per rat in 50% glucose/0.9% saline at 2g/kg body weight through intraperitoneal injection. Blood was collected in Lithium Heparin containing tubes by tail nick at 0, 15, 30, 60 and 90mins post injection for immediate blood glucose measurement by an Accu-Check Advantage meter (Roche Diagnostics, West Sussex, UK). Animals that demonstrated no increase in blood glucose were excluded from analysis. Plasma was separated and de-proteinised with zinc sulphate (2.75%) and saturated barium sulphate (0.3N), before centrifugation at 10,000g for 10mins.

Radioactivity for each timepoint was determined by liquid scintillation counting in Ultima Gold XR (Perkin-Elmer) on a beta counter (LS6500, Beckman Coulter, UK). Powdered muscles were homogenised in dH_2O by three equal polytron pulses (1sec each), before passage through columns containing AG 1-X8 resin (Bio-Rad, Hemel Hempstead, UK) to separate 3H-2DG-6-phosphate for liquid scintillation counting. Glucose uptake was estimated by dividing the ^{3}H-2DG-6-phosphate scintillation counts by the plasma glucose specific activity over 90 mins and was stated as per unit muscle mass.

For muscle glycogen analysis, powdered muscles were digested in KOH (1M), before glycogen was precipitated using Na_2SO_4 and ethanol. Following this, the glycogen pellet underwent further digestion overnight at 37^{O}C in acetate buffer (0.25M, pH 4.75) containing amyloglucosidase (0.3mg/ml). Samples were then incubated in phosphate buffer (0.12M pH 7.0) containing 4-aminoantipyrine (0.5mg/ml), peroxidase (1.6U/ml) and glucose oxidase (10U/ml) for 25mins at 37°C. Glycogen content was measured as the amount of glucose detected at 490nm, versus a standard curve and stated as per unit muscle mass.

4.3.5 Quantitative RT-PCR

For RNA extraction, ~10 mg of muscle was placed into Trizol ® reagent (Invitrogen) with two clean stainless steel bead and homogenised in a TissueLyser bead beater. RNA was extracted according to the manufactures protocol, firstly chloroform was added to the lysed tissue and centrifuged at 12,000g for 15min at 4 ^{O}C. The upper aqueous phase was removed and RNA precipitated with isopropanol and the resulting pellet washed in 80% ethanol. RNA was subsequently dissolved in 20µl RNAse-free water. RNA

was quantified using a Nanodrop measuring the 260nm/280nm ratio. 1000ng of RNA was reversed-transcribed with a High-Capacity cDNA Reverse Transcription kit (Life Technologies) according to the manufactures protocol. Resulting cDNA was diluted 1:5 and 1µl added per well of 384-optical well plates (Life Technologies). Primers were designed using Primer Express® software (Table 4.3). Primers were mixed with SYBR Select Master Mix (Life Technologies) and aliquots of 10µl of final mastermix added to each well. Each biological replicate was carried out in duplicate. Thermal cycling was carried out on a ViiA®7 Real-Time PCR system (Life Technologies) for 2 min at 50^{O}C, followed by 2 min 95 ^{O}C and 40 cycles of 15s at 95 ^{O}C and 60s at 60 ^{O}C. GAPDH was used a housekeeping gene. Target mRNA expression was quantified using the ΔΔCt method and normalized to the scramble control.

Table 4.3 Primer sequences for *in vivo* qRT-PCR

Gene	Accession number		Primer sequence
GAPDH	NM_017008.4	F	ATCCCGCTAACATCAAATGG
		R	GTGGTTCACACCCATCACAA
VDR	NM_017058.1	F	GGTTTCTTCAGGCGGAGCAT
		R	GGTGATGCGGCAATCTCCAT
4E-BP1	NM_053857.2	F	CCCGGGAGGAACCAGAATC
		R	TCATCGCTGGTAGGGCTAGT
EIF4E	NM_053974.2	F	AAACAAACGGGGAGGACGAT
		R	CACAGCAGTGTCTCTAGCCAA
P70S6K1	NM_031985.1	F	GCCTGTCAGCCCAGTCAAAT
		R	AGAGTTGGGCTGTCGGATTG
RPS6	NM_017160.1	F	GCGCCTGCTTTTGAGTAAGG
		R	TCCACAATGCATCCTCGGAC
RPL10	NM_031100.1	F	TATCCCCAATCGTGGTCCTC
		R	TTATTGAACCTCATTTGATAGCGCA
RPL21	NM_053330.1	F	TAGACATCAAGGGAATGGGCAC
		R	TTGTTCACAATGATGCCCACG
RPL23a	NM_001108283.1	F	AGCGAAGGCCTTGAAAGCTA
		R	AAAGTGGGTGACGTTCGGAT
RPL24	NM_022515.1	F	CGATGGGAAGGTTTTCCAGT
		R	ATATCAGCCAGAGAAGCGCC
RPL27	NM_022514.1	F	GCTGTCGAAATGGGCAAGTT
		R	GTCGGAGGTGCCATCATCAA
RPS3a	NM_017153.1	F	GTGGCAGACCATGATTGAAGC
		R	TTGTCTGCACTTCTCGGGTC

RPS9	NM_031108.4	F	GTCACGGGCCTGAGTTTGTA
		R	CCTCCACACCTCACGTTTGT
RPS11	NM_031110.1	F	TGTTTCAGGGACGTCCAGATT
		R	GAGCATTGGCTACAGTCCCC
RPS13	NM_130432.2	F	TCTCTCTTTGCTTCCAGACCT
		R	ATCACACCTATCTGGGAAGGAG
RPS28	NM_001105730.1	F	CCATCAAGCTGGCTAGGGTAA
		R	TCTCGAACAGGGCCTTTGAC
ATG5	NM_001014250.1	F	CAGAAGCTGTTCCGTCCTGT
		R	CCGTGAATCATCACCTGGCT
ATG7	NM_001012097.1	F	CAGCCTGTTCATCCAAAGTTCTTG
		R	CTGTGGTTGCTCAGACGGT
Ctsl	NM_013156.2	F	CTATCGCCACCAGAAGCACA
		R	ACCACACTGGCCCTGATTCT
Casp3	NM_012922.2	F	CGGACCTGTGGACCTGAAAA
		R	CGGCCTCCACTGGTATCTTC
m-calpain	NM_017116.2	F	TCGGCATCTATGAGGTCCCA
		R	ATTCTTGTGGGGCTCGAAGG
ATP2A3	NM_012914.1	F	TGCTGTTTTCTGGCACCAAT
		R	CAAATTCATCCAGCTTGCGCT
ATP5G3	NM_053756.1	F	TGCTGCGGCACGGATAAGA
		R	GCGGCGTGGATATAGGTGAC
ATP5J2	NM_001271117.1	F	CGAATTTCTGCGGACAACAGG
		R	CTGCAATACCACTGGGGGTG
Fstn	NM_012561.1	F	GTGTGCCATGAAGGAAGCTG
		R	TCCGAGATGGAGTTGCAAGA
Mrf4	NM_013172.2	F	TAAGGAAGGAGGAGCAAGCG
		R	GGGAGTTTGCGTTCCTCTGA
Myf5	NM_001106783.1	F	TCAAACGCATGTGCTTCAGAT
		R	GGTTGCAGGCTGTGAATTGG
MyoD	NM_176079.1	F	CTGCTCTGATGGCATGATGG
		R	CTCCACTATGCTGGACAGGC
MyoG	NM_017115.2	F	GTGAATGCAACTCCCACAGC
		R	CGAGCAAATGATCTCCTGGGT
Mstn	NM_019151.1	F	ACCATGCCTACCGAGTCTGA
		R	ATCCACAGCTGGGCCTTTAC
PAX7	NM_001191984.1	F	AGCCGAGTGCTCAGAATCAA
		R	TCCTCTCGAAAGCCTTCTCC
PCNA	NM_022381.3	F	GCAACTTGGAATCCCAGAACA
		R	AAGGTCCCGGCATATACGTG

4.3.6 Immunoblotting

For signalling targets, muscles were homogenised in ice-cold extraction buffer using clean sharp scissors. Samples were centrifuged at 11,000 g for 10 min at 4^{O}C, the supernatant was removed and quantified by Nanodrop. Extraction of VDR proteins required homogenisation and preparation in a hyperosmolar lysis buffer (HLB) (Urea 6.7M, Glycerol 10%, Tris-HCl 10mM, SDS 1%, DTT 1mM, PMSF 1mM and Protease Inhibitor Cocktail tablet

(Roche, West Sussex, UK)) as previously described (Girgis, Mokbel, et al. 2014). Samples were prepared and immunoblotting undertaken as described in 2.1. Primary and secondary antibodies were diluted as detailed in Table 4.4**.** Chemiluminescence was visualized using a Chemidoc XRS. Bands were quantified in the linear range of density by quantification of volume intensity. Values were normalised to total protein loaded assessed by Coomassie brilliant blue staining of the membrane.

Table 4.4 Primary and secondary antibody information

Primary antibody	Species	Supplier	Product ID	Dilution
VDR (D-6)	Mouse	Santa Cruz	SC-13133	1:2000
GAPDH	Rabbit	Cell signalling technology	5174	1:50,000
p-AKT ^{Ser473}	Rabbit	Cell signalling technology	4060	1:2000
Pan-AKT	Rabbit	Cell signalling technology	4685	1:2000
p-TSC2 ^{Thr1462}	Rabbit	Cell signalling technology	3611	1:2000
TSC2	Rabbit	Cell signalling technology	4308	1:2000
p-mTOR ^{Ser2448}	Rabbit	Cell signalling technology	2976	1:2000
mTOR	Rabbit	Cell signalling technology	2972	1:2000
p-P70S6K1 ^{Thr389}	Rabbit	Cell signalling technology	9234	1:2000
P70S6K1	Rabbit	Cell signalling technology	2708	1:2000
p-S6RP $^{Ser235/236}$	Rabbit	Cell signalling technology	2211	1:2000
S6RP	Rabbit	Cell signalling technology	2217	1:2000
p-4e-BP1 $^{Thr37/46}$	Rabbit	Cell signalling technology	2855	1:2000
4e-BP1	Rabbit	Cell signalling technology	9644	1:2000
p-eIF4E ^{Ser209}	Rabbit	Cell signalling technology	9741	1:2000
eIF4E	Rabbit	Cell signalling technology	9742	1:2000
Cathepsin L	Mouse	Abcam	Ab6314	1:2000
Beclin 1	Rabbit	Cell signalling technology	3495	1:2000
p-ULK ^{Ser555}	Rabbit	Cell signalling technology	5869	1:2000
p-AMPK ^{Thr172}	Rabbit	Cell signalling technology	2535	1:2000
p-Raptor ^{Ser792}	Rabbit	Cell signalling technology	2083	1:2000
LC3B	Rabbit	Cell signalling technology	2775	1:1000
Secondary antibody		**Supplier**	**Product ID**	**Dilution**
Anti-rabbit		Cell signalling technology	7074	1:2000
Anti-mouse		Cell signalling technology	7076	1:2000

4.3.7 Immunofluorescence, co-localization and satellite cell content

5µm thick muscle cross sections were cut at -22^{O}C using a Cryostat, mounted on glass slides before air-drying at room temperature. Sections were fixed in acetone/ ethanol (3:1) for 5 min, before washing three times in PBS.

For immunofluorescence, primary antibodies towards VDR (Rabbit, Ab109234, Abcam) and dystrophin (Mouse, MANDYS1 (3B7)), Developmental Studies Hybridoma Bank) were diluted in 5% goat serum in PBS 1:50 and 1:200 respectively. Antibodies were applied to each section and incubated for 2 hours in a humidity chamber at room temperature, before being washed in PBS three times. Secondary fluorescent anti-rabbit (Alexa Fluor® 594, A11012, Invitrogen) and anti-mouse (Alexa Fluor® 488, A21121, Invitrogen) antibodies were diluted in PBS 1:200 and sections incubated for 30 min in a humidity chamber at room temperature. Slides were subsequently washed three times in PBS, and a 1:1000 DAPI stain (Invitrogen) in PBS applied for 5 minutes before a three further PBS washes. Mounting media was applied to each section and dried in darkness overnight. Additional sections were probed using anti-MHC IIa (SC-71) or anti-MHC IIb (BF-F3) diluted 1:50 in PBS. Sections were subsequently imaged in a blinded fashion using a Nikon Eclipse E600 and analysed using Image Pro3D capture software. Three random fields of view were measured per section. Fibre CSA frequency distribution analysis was performed from: 920 control and 1578 VDR-KD IIa fibres, 1070 control and 1233 VDR-OE IIa fibres, 793 control and 800 VDR-KD IIb fibres, 1341 control and 1085 VDR-OE IIb fibres.

For mTOR and LAMP2 co-localization assessment, sectioning and fixing muscle was undertaken as previously described, before incubation with primary antibodies towards mTOR (#05-1592, Millipore) and LAMP2 (AP1824d, Abgent) in 5% goat serum in PBS at 1:200 and 1:100 respectively. Secondary fluorescent antibodies anti-mouse $IgG_{\gamma 1}$ (Alexa Fluor® 594, A11005) and anti-rabbit (Alexa Fluor® 488, A11034) were additional used as previously described. For analysis of $Pax7^{+}$ satellite cells (SCs) muscle cross sections were cut, mounted and air-dried as previously described. Sections were incubated with primary antibody towards Pax7 (DSHB) before incubation with a biotinylated anti-mouse secondary antibody (BA-9200, Vector Laboratories) as described in (Bankolé et al. 2013).

4.4 Results – Vitamin D receptor knockdown

4.4.1 Efficacy of VDR-KD

Ten days after IVE, right-leg VDR-KD TAM demonstrated sustained knockdown by IVE of lentiviral-mediated shRNA in both mRNA (VDR-KD: 40.9±9.2 % vs. SCR: 100.0±21.5, $p<0.01$) and protein expression (VDR-KD: 48.3±10.9 % vs. SCR: 100.0±15.1, $p<0.001$) (Figure 4.6).

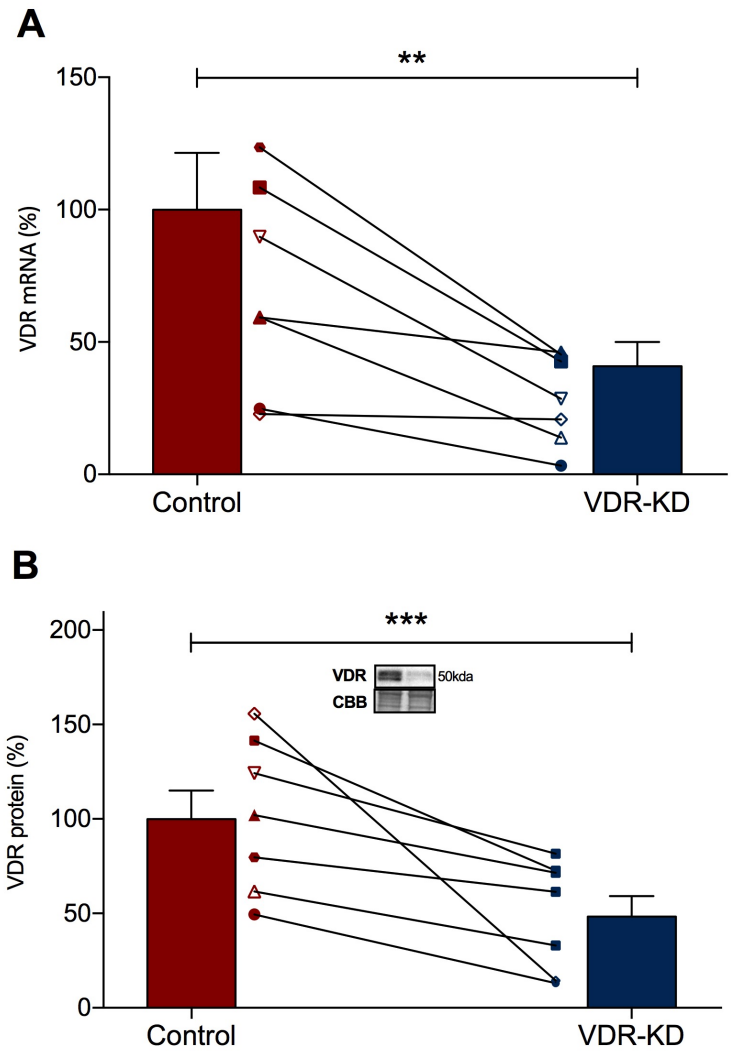


Figure 4.6 Efficacy of VDR-KD *in vivo*

(**A**) VDR mRNA expression measured by qRT-PCR presented as percentage change from control. (**B**) VDR protein expression measured by immunoblotting presented as percentage change from control. Values are means ±SEM, n=7. Statistical analysis via paired t-test, ** $p<0.01$, *** $p<0.001$ vs. scramble controls.

4.4.2 Muscle fibre cross sectional area

Mean VDR-KD muscle fibre CSA was reduced compared to scramble controls (VDR-KD: 1423±128 μm^2 vs. SCR: 1611±85, p<0.05) ten days post IVE. No difference was observed specifically within type IIa fibres, whereas VDR-KD type IIb fibres were reduced compared to scramble controls (VDR-KD: 2864±245 μm^2 vs. SCR: 2398±207, p<0.05) Figure 4.7.

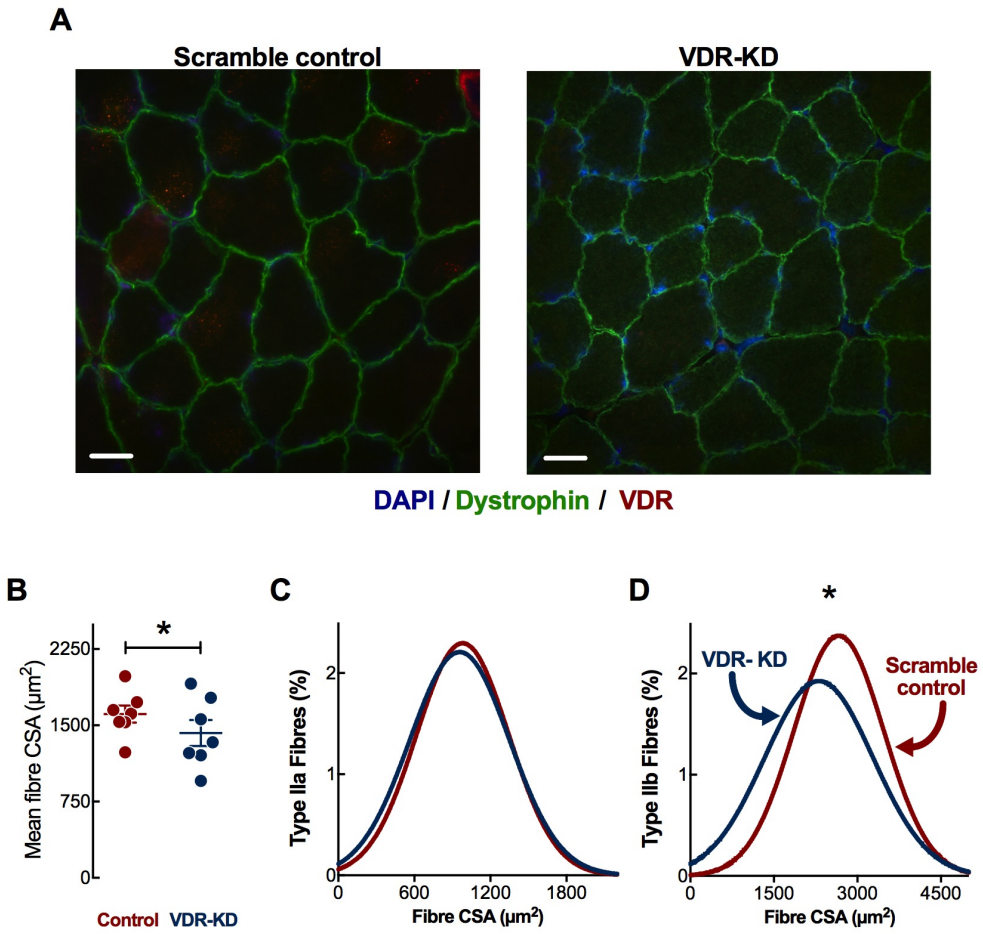


Figure 4.7 VDR-KD muscle fibre CSA measures

(**A**) Representative muscle fibre CSA images, Blue=DAPI, Green=Dystrophin, Red=VDR. Scale bars represent 200μm. (**B**) Overall fibre CSA mean, n=7 animals. (**C**) Distribution of type IIa fibre CSA mean, (Distribution represents 920 control and 1578 VDR-KD IIa fibres, n=7 animals) (**D**) Distribution of type IIb fibre CSA mean. (Distribution represents 793 control and 800 VDR-KD IIb fibres, n=7 animals). All fibre CSA measures are μm^2, analysed by Image Pro 3D software. Values are means ±SEM. Statistical analysis via paired t-test, * p<0.05 vs. scramble controls.

4.4.3 Total protein, DNA and RNA

To further confirm muscle atrophy total ASP, DNA and RNA were undertaken. Total ASP per mg of muscle in VDR-KD samples was reduced compared to scramble controls (VDR-KD: 0.4±0.1 mg/mg vs. SCR: 0.7±0.1, $p<0.05$). There was no observable difference in the RNA or DNA content between VDR-KD muscle and scramble controls (Figure 4.8).

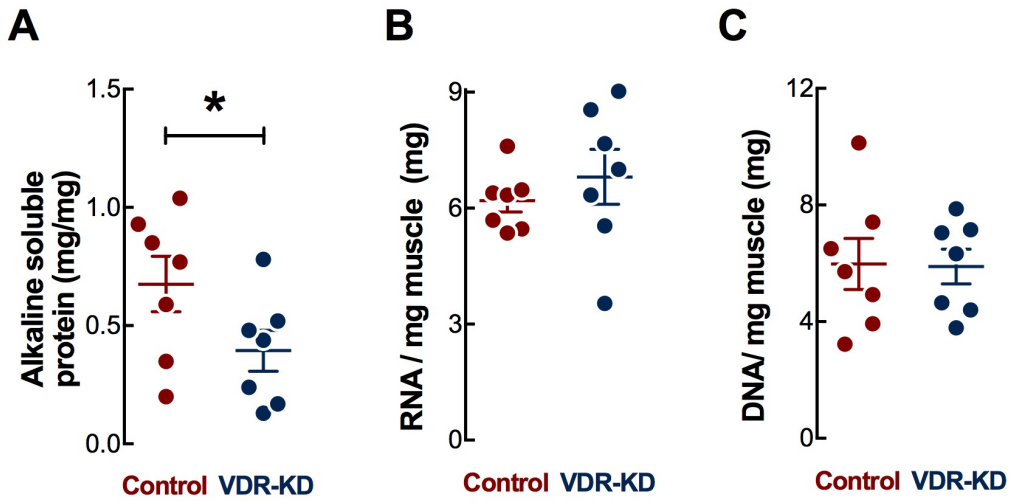


Figure 4.8 VDR-KD total protein, RNA and DNA

(**A**) Total ASP, (**B**) RNA, (**C**) DNA. All APS, RNA and DNA measures are from the same freeze-dried muscle samples, presented as per mg of muscle. Values are means ±SEM, n=7. Statistical analysis via paired t-test, * $p<0.05$ vs. scramble controls.

4.4.4 Protein fractional synthetic rates

There were no significant differences in the mixed lysate fractional synthetic rate between VDR-KD and scramble control muscles. Similarly, when individual subcellular fractions were measured no differences were observed (Figure 4.9).

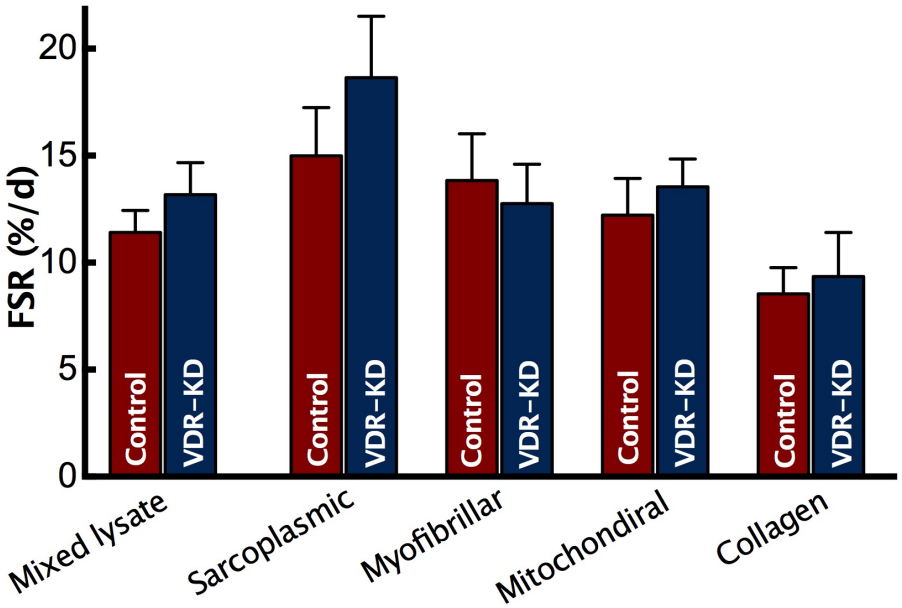


Figure 4.9 VDR-KD fractional synthetic rates

Protein synthetic rates for mixed lysate, sarcoplasmic, myofibrillar, mitochondrial and collagen subcellular fractions. Assessed by D_2O incorporation into leucine and measured by GC-MS/MS. Presented as FSR %/d. Values are means ±SEM, n=7. Statistical analysis via paired t-test. Statistical analysis via paired t-test.

4.4.5 Anabolic signalling

Anabolic signalling immunoblots were undertaken to confirm the unchanged FSR measures. There was no influence of VDR-KD upon either total or phosphorylated proximal mTOR signalling. Significant decreases in the total expression of P70S6K1 (VDR-KD: 66.4±10.1 % vs. SCR: 100.1±7.2, $p<0.05$), RPS6 (VDR-KD: 57.7±6.8 % vs. SCR: 100.3±4.9,

$p<0.05$) and 4E-BP1 (VDR-KD: 54.9±10.4 % vs. SCR: 100.0±10.4, $p<0.05$) were observed, whereas only phosphorylated 4E-BP1 was decreased (VDR-KD: 47.1±9.7 % vs. SCR: 100.0±12.7, $p<0.01$). There was no change in total mTOR expression or phosphorylation (Figure 4.10).

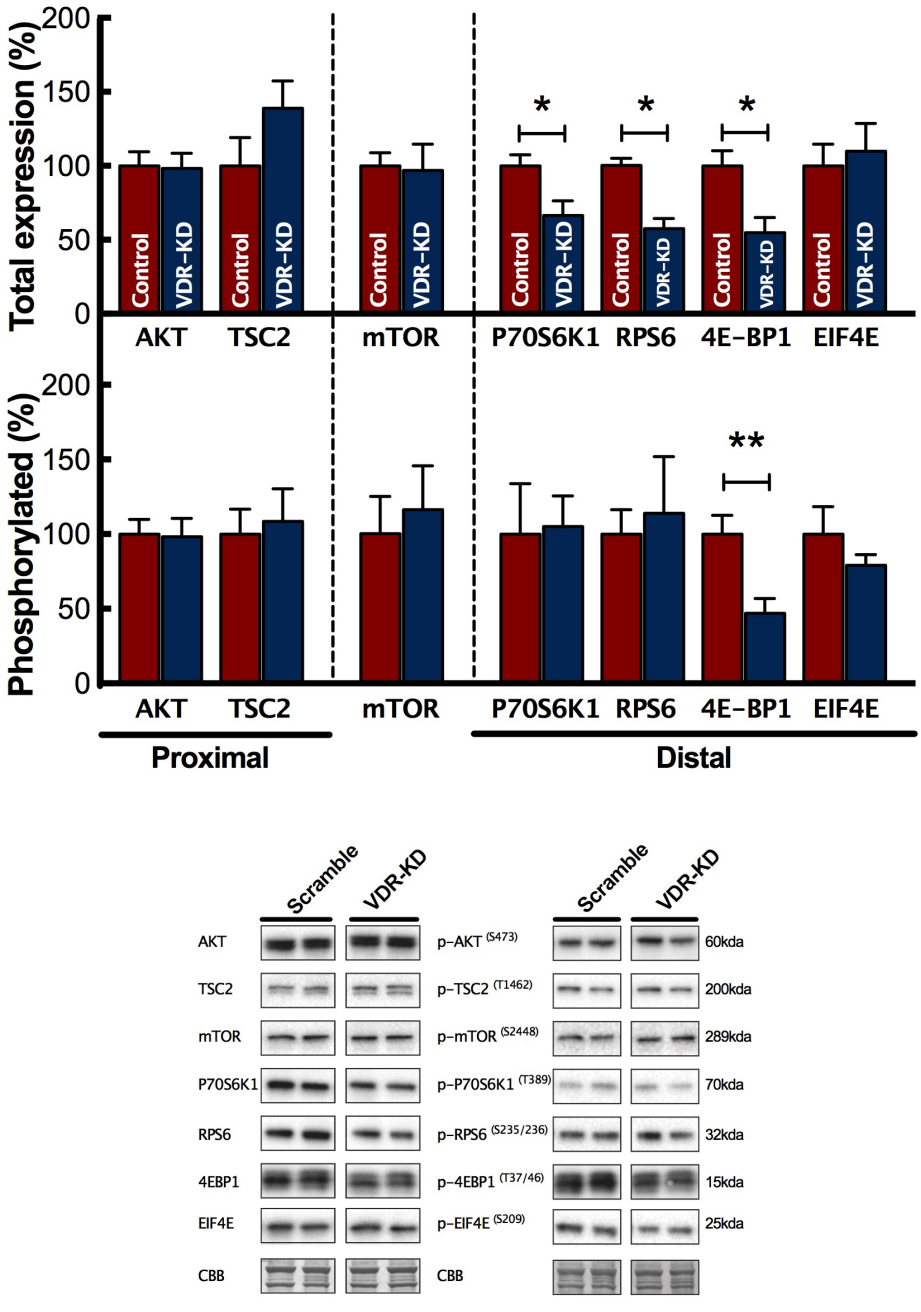


Figure 4.10 VDR-KD total and phosphorylated anabolic signalling

Expression of total and phosphorylated anabolic signalling in VDR-KD and scramble control muscles. Measured by immunoblotting, presented as percentage change from scramble controls. Values are means ±SEM, n=7. Statistical analysis via paired t-test, * $p<0.05$, ** $p<0.01$ vs. scramble controls.

There was no difference in the activation of anabolic signalling (i.e. levels of phosphorylation/ total expression) between VDR-KD and scramble control muscles (Figure 4.11).

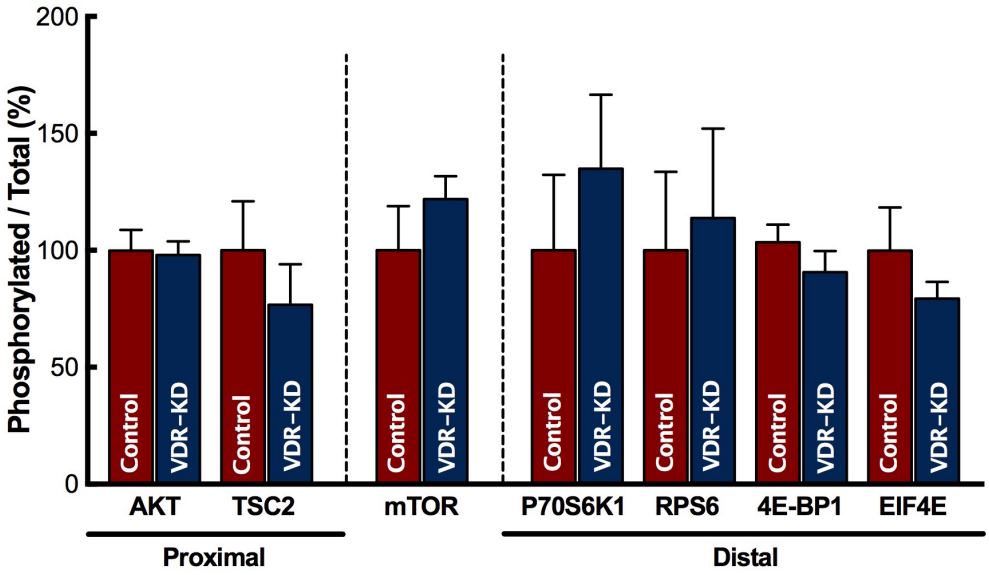


Figure 4.11 VDR-KD anabolic signalling activation

Activation of anabolic signalling in VDR-KD and scramble control muscles. Measured by immunoblotting, presented as phosphorylated/total expression percentage change from scramble controls. Values are means ±SEM, n=7. Statistical analysis via paired t-test.

4.4.6 Ribosomal mRNA expression

VDR-KD did not change ribosomal mRNA expression compared to scramble control muscles (Figure 4.12).

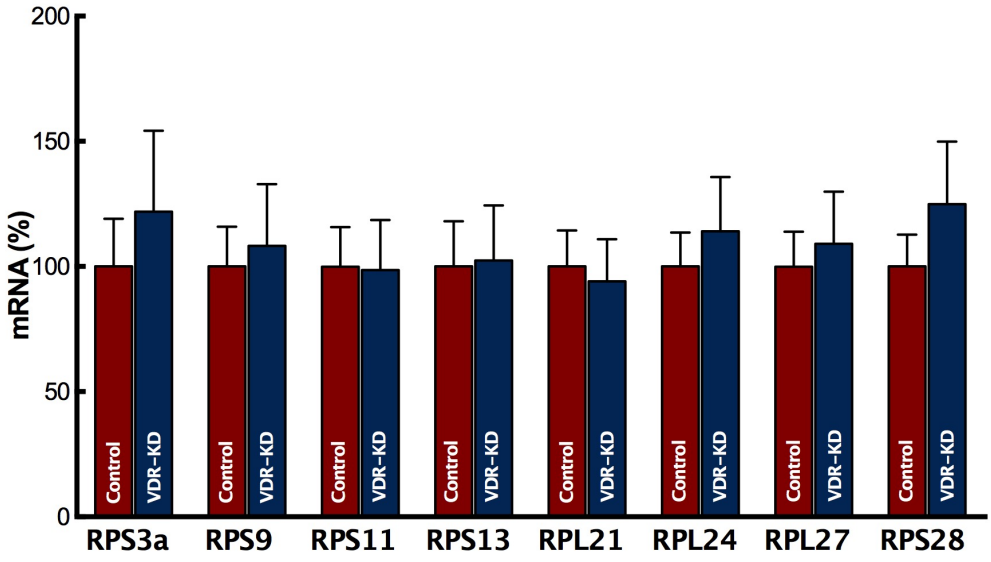


Figure 4.12 VDR-KD ribosomal RNA expression

Expression of ribosomal mRNA in VDR-KD and scramble control muscles. Measured by qRT-PCR, presented as percentage change from scramble controls. Values are means ±SEM, n=7. Statistical analysis via paired t-test.

4.4.7 Catabolic signalling

4.4.7.1 mRNA expression

To determine the basis of the decreased fibre CSA and ASP measures catabolic signalling markers were measured. VDR-KD muscles demonstrated greater mRNA expression of multiple catabolic related genes, depending on the proteolytic mechanism. These included autophagy markers *ATG7* (VDR-KD: 170±26 % vs. SCR: 100±15, $p<0.05$), *ATG5* (VDR-KD: 180±25 % vs. SCR: 100±20, $p<0.05$) and *Cathepsin L* (VDR-KD: 184±38 % vs. SCR: 100±20, $p<0.05$). Additionally, increases were

observed in *Caspase-3* (VDR-KD: 181±25 % vs. SCR: 100±17, $p<0.05$) and *m-calpain* (VDR-KD: 183±54 % vs. SCR: 100±15, NS) Decreased expression of *Atrogin-1* was also observed (VDR-KD: 62±14 % vs. SCR: 100±15, $p<0.05$) (Figure 4.13).

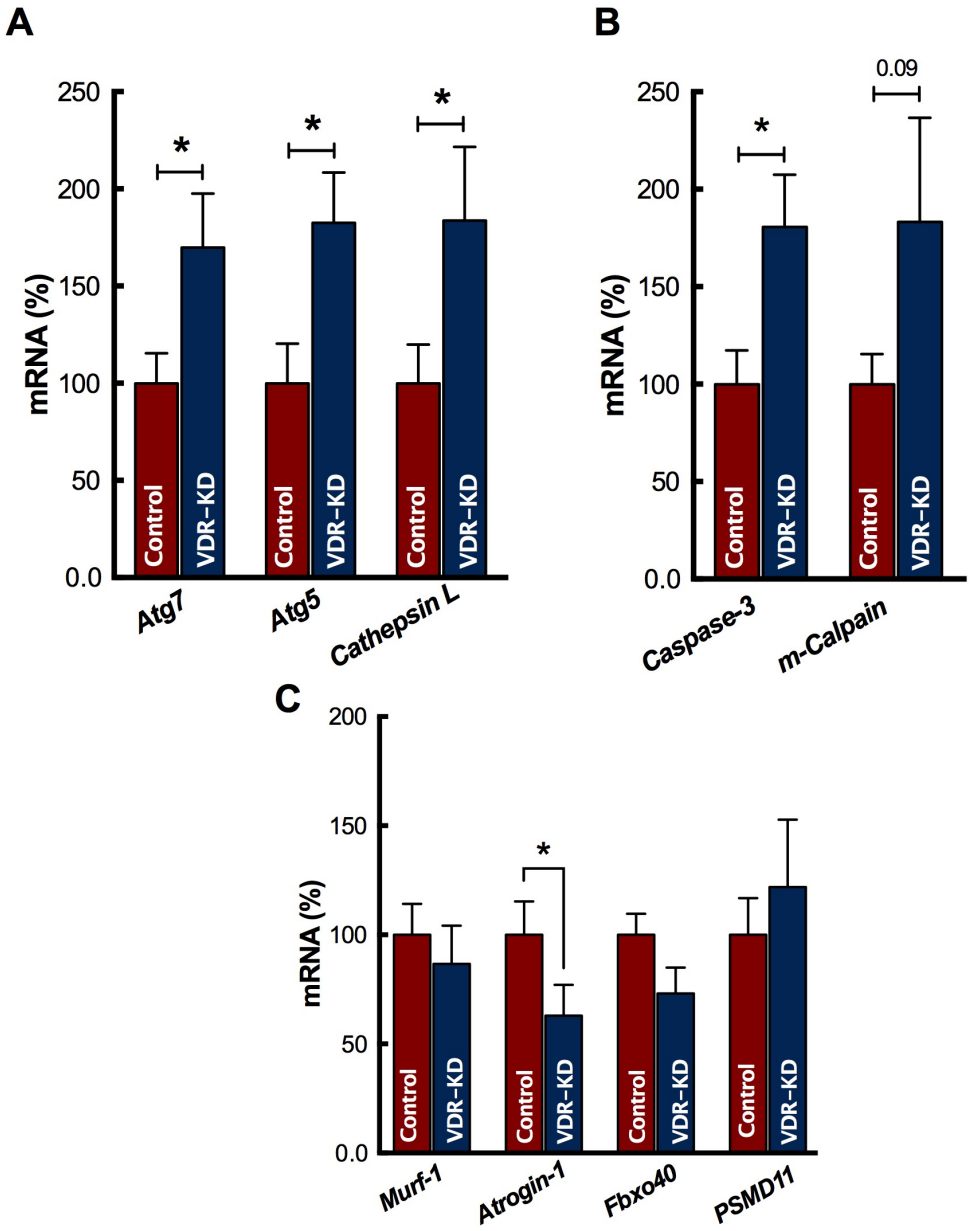


Figure 4.13 VDR-KD catabolic markers mRNA expression

mRNA expression of catabolic markers for (**A**) autophagy, (**B**) caspase/ calpain (**C**) and proteasomal mediated degradation in VDR-KD and scramble control muscles. Measured by qRT-PCR, presented as percentage change from scramble controls. Values are means ±SEM, n=7. Statistical analysis via paired t-test, * $p<0.05$ vs. scramble controls.

4.4.7.2 Protein expression

The protein expression of known autophagy markers were increased in VDR-KD muscles compared to scramble controls. Enhanced total expression of cathepsin L (VDR-KD: 172±29 % vs. SCR: 100±11, $p<0.05$), Beclin 1 (VDR-KD: 138±19 % vs. SCR: 100±22, $p<0.05$) and LC3B-II (VDR-KD: 184±43 % vs. SCR: 100±18, $p<0.05$). Increased phosphorylation of p-ULK (VDR-KD: 224±82 % vs. SCR: 100±49, $p<0.05$), p-AMPKα (VDR-KD: 135±22 % vs. SCR: 100±18, NS) and p-Raptor (VDR-KD: 162±28 % vs. SCR: 100±16, $p<0.05$) were also observed (Figure 4.14).

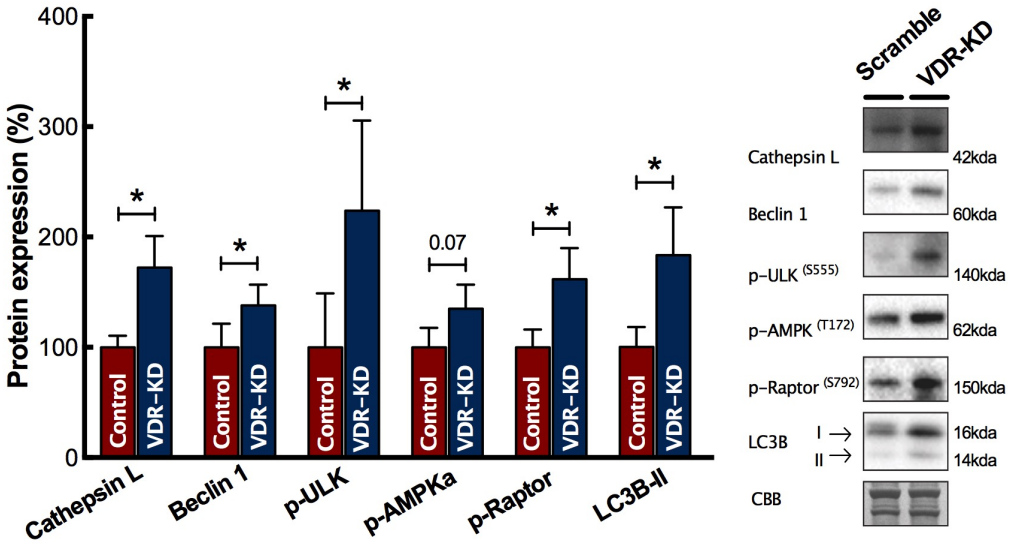


Figure 4.14 VDR-KD autophagy protein markers

Expression of total and phosphorylated autophagy markers in VDR-KD and scramble control muscles. Measured by immunoblotting, presented as percentage change from scramble controls. Values are means ±SEM, n=7. Statistical analysis via paired t-test, * $p<0.05$ vs. scramble controls.

4.4.8 Muscle glucose and glycogen

There was no measured difference in muscle glucose uptake or glycogen content between VDR-KD or scramble control muscles (Figure 4.15).

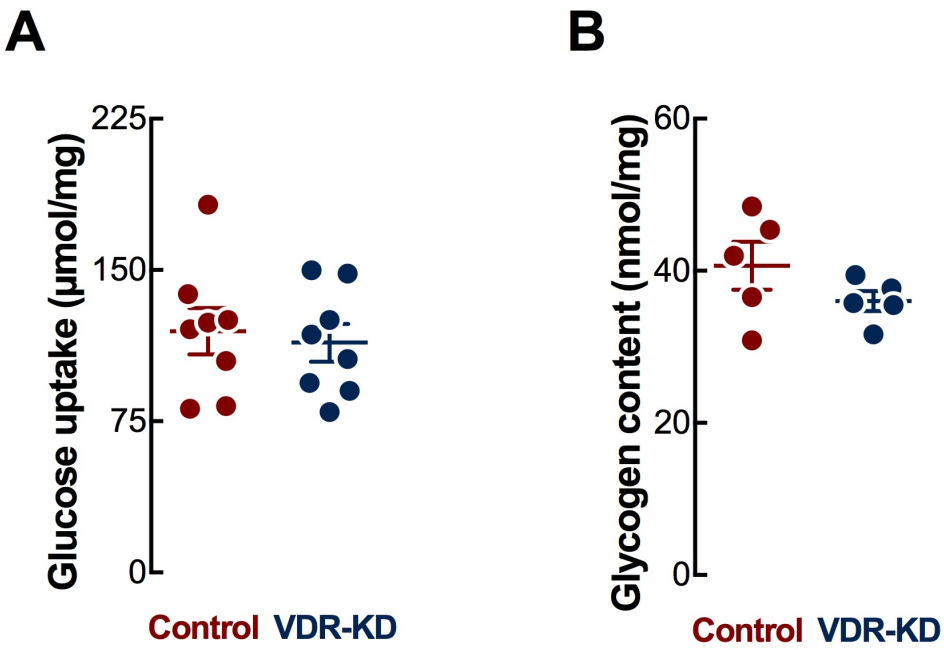


Figure 4.15 VDR-KD glucose metabolism

(**A**) Glucose uptake into VDR-KD and scramble control muscles measured by IPGTT and ^{3}H-glucose tracer uptake, n=8 (**B**) Glycogen content of VDR-KD and scramble muscles, n=5. Values are means ±SEM. Statistical analysis via paired t-test.

4.5 Results – Vitamin D receptor over-expression

4.5.1 Efficacy of VDR-OE

Ten days after IVE, right-leg VDR-OE TAM demonstrated sustained over-expression by IVE of pCAGGS-mVDR cDNA in both mRNA (VDR-OE: 2.8456±1.3391 ΔΔCt vs. Control: 0.0013±0.0004, $p<0.05$) and protein expression (VDR-OE: 1232±311 % vs. Control: 100.0±22, $p<0.001$) (Figure 4.16).

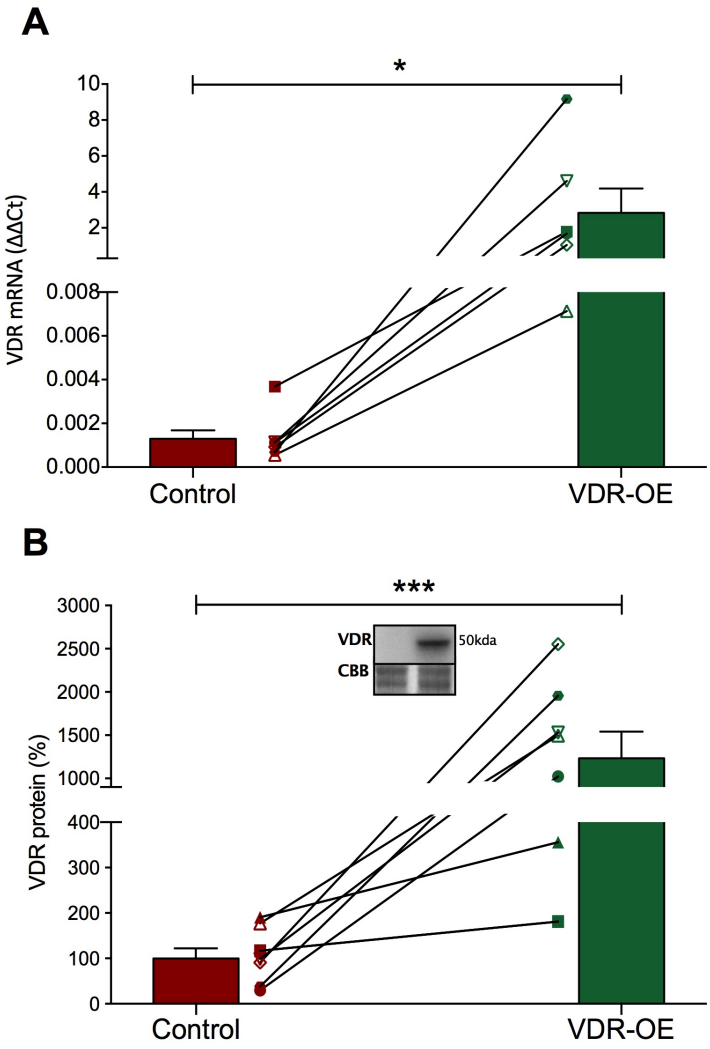


Figure 4.16 Efficacy of VDR-OE

(**A**) VDR mRNA expression measured by qRT-PCR presented as percentage change from control. (**B**) VDR protein expression measured by immunoblotting presented as percentage change from control. Values are means ±SEM, n=7. Statistical analysis via paired t-test, * $p<0.05$, *** $p<0.001$ vs. empty vector controls.

4.5.2 Muscle fibre cross sectional area

Mean VDR-OE muscle fibres were larger compared to empty vector controls (VDR-KD: 1904±116 μm^2 vs. Control: 1630±69, p<0.05) ten days post IVE. Type IIa fibres in VDR-OE muscles had a significantly larger CSA compared to empty vector controls (VDR-KD: 1408±76 μm^2 vs. Control: 1251±81, p<0.05), however type IIb fibres only displayed a moderate but non-significant increase (VDR-KD: 2422±266 μm^2 vs. Control: 2320±173, p<0.05) (Figure 4.17)

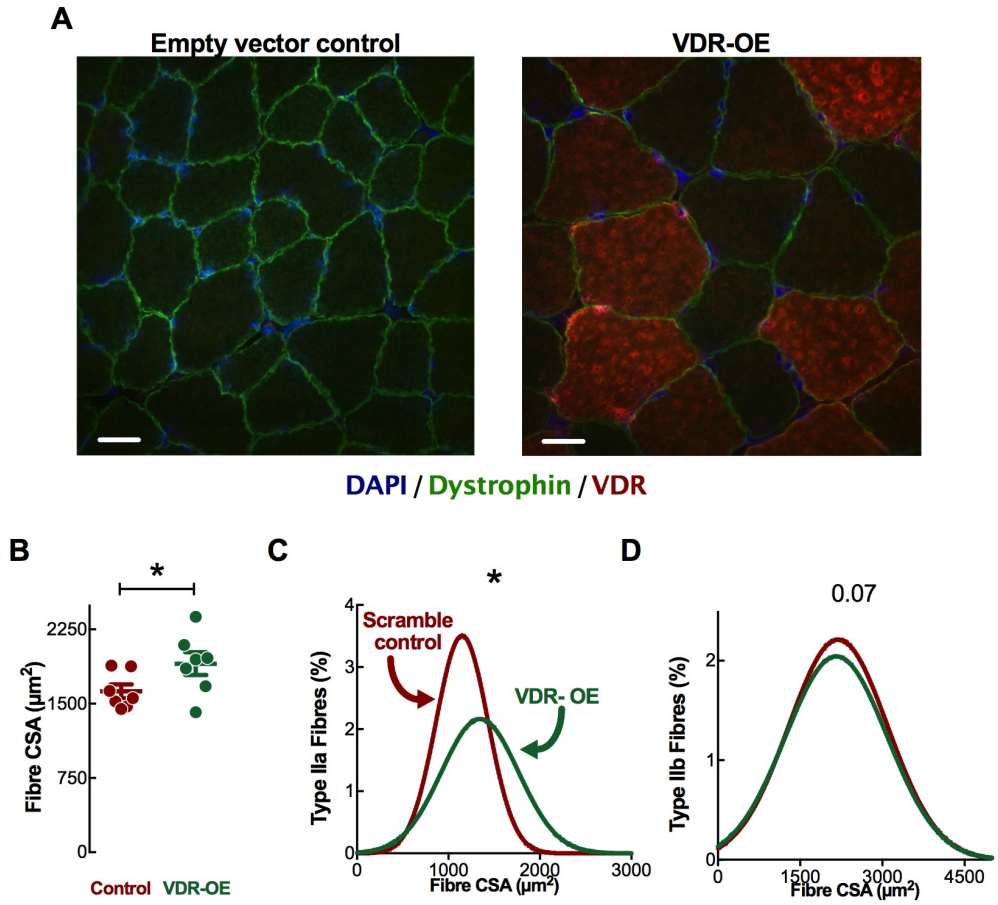


Figure 4.17 VDR-OE muscle fibre CSA measures

(**A**) Representative muscle fibre CSA images, Blue=DAPI, Green=Dystrophin, Red=VDR. Scale bars represent 200μm. (**B**) Overall fibre CSA mean, n=7 animals. (**C**) Distribution of type IIa fibre CSA mean. (Distribution represents 1070 control and 1233 VDR-OE IIa fibres, n=7 animals) (**D**) Distribution of type IIb fibre CSA mean. (Distribution represents 1341 control and 1085 VDR-OE IIb fibres, n=7 animals). All fibre CSA measures are μm^2, analysed by Image Pro 3D software. Values are means ±SEM. Statistical analysis via paired t-test, * p<0.05 vs. empty vector controls.

4.5.3 Total protein, DNA and RNA

Confirming fibre CSA measures, total ASP per mg of muscle in VDR-OE samples was increased compared to empty vector controls (VDR-OE: 0.9±0.1 mg/mg vs. Control: 0.6±0.1, $p<0.01$). The RNA content of VDR-OE muscles was also increased compared to empty vector controls (VDR-OE: 8.8±0.7 mg/mg vs. Control: 6.4±0.5, $p<0.01$). There was no measureable difference in the DNA content of either VDR-OE or empty vector control muscles (Figure 4.18).

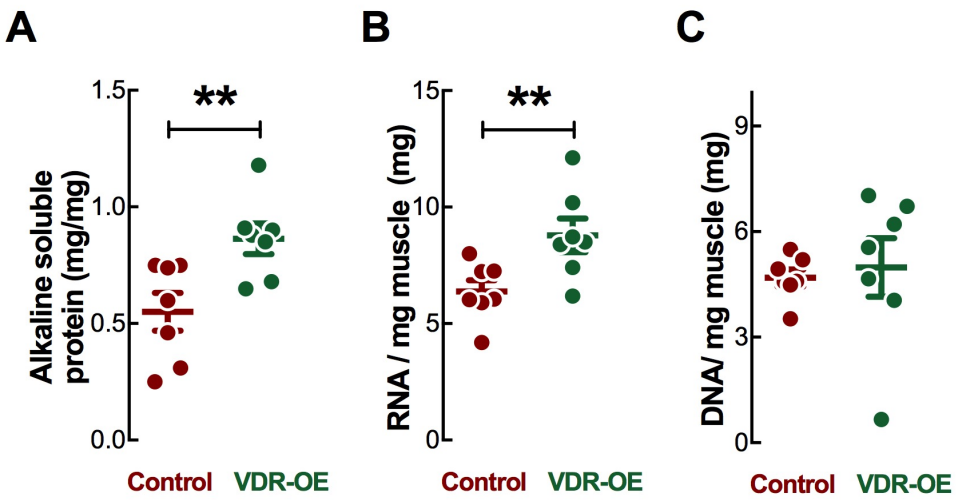


Figure 4.18 VDR-OE total protein, RNA and DNA

(**A**) Total ASP, (**B**) RNA, (**C**) DNA. All APS, RNA and DNA measures are from the same freeze-dried muscle samples, presented as per mg of muscle. Values are means ±SEM, n=7. Statistical analysis via paired t-test, ** $p<0.01$ vs. empty vector controls.

4.5.4 Protein fractional synthetic rates

Within VDR-OE muscles, mixed lysate fractional synthetic rates were greater than empty vector controls (VDR-OE: 17.3±2.2 %/d vs. Control: 10.2±0.7, $p<0.01$). Increases were additional observed in all measured protein subcellular fractions: sarcoplasmic (VDR-OE: 16.0±2. %/d vs. Control: 10.0±0.9, $p<0.01$), myofibrillar (VDR-OE: 15.9±2.6 %/d vs. Control: 11.0±0.7, $p<0.01$), mitochondrial (VDR-OE: 16.1±2.1 %/d vs. Control: 10.8±0.8, $p<0.05$) and collagen (VDR-OE: 13.6±1.7 %/d vs. Control: 9.2±0.6, $p<0.05$) (Figure 4.19).

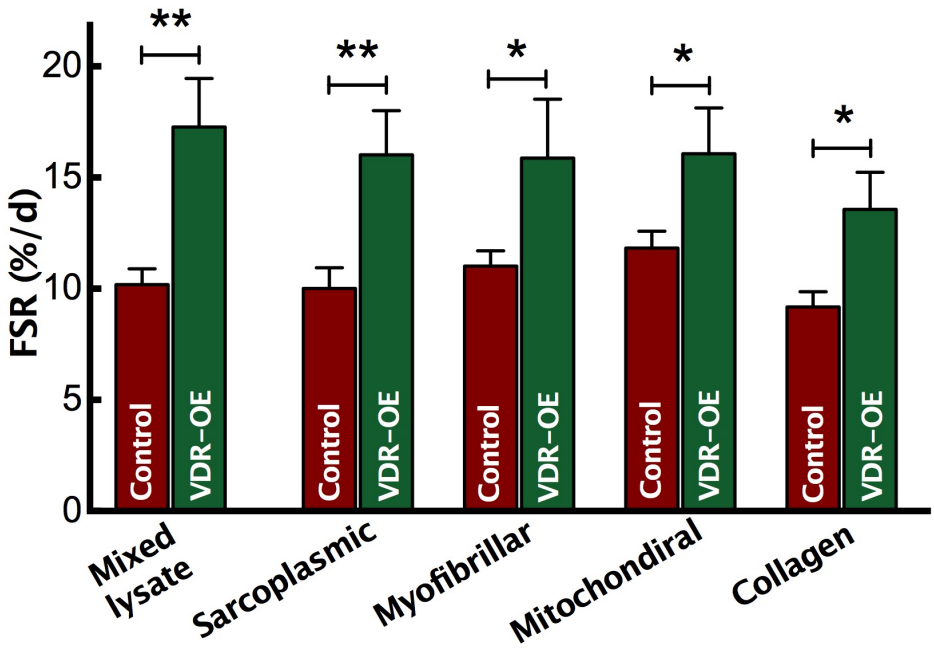


Figure 4.19 VDR-OE fractional synthetic rates

Protein synthetic rates for mixed lysate, sarcoplasmic, myofibrillar, mitochondrial and collagen subcellular fractions. Assessed by D_2O incorporation into leucine and measured by GC-MS/MS. Presented as FSR %/d. Values are means ±SEM, n=7. Statistical analysis via paired t-test. Statistical analysis via paired t-test, * $p<0.05$, ** $p<0.01$ vs. scramble controls.

4.5.5 Anabolic signalling

4.5.5.1 mRNA expression

To probe the origin of the increased FSR measures, anabolic signalling was assessed. VDR-OE muscles showed an increase in the mRNA expression of *eIF4E* (VDR-OE: 157±19 % vs. Control: 100±10, $p<0.05$), coupled with moderate but non-significant increases in *4E-BP1, RPS6KB1* and *RPS6* expression (Figure 4.20).

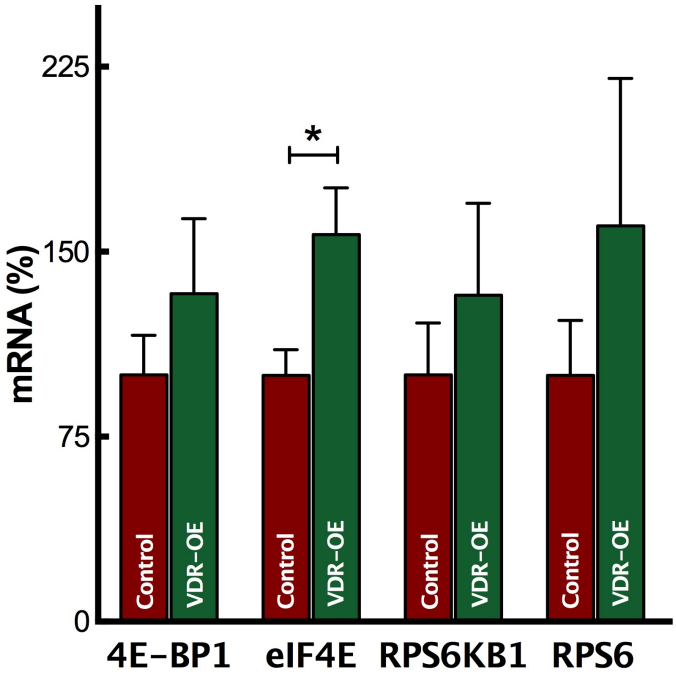


Figure 4.20 VDR-OE anabolic signalling mRNA expression

mRNA expression of anabolic regulatory genes in VDR-OE and empty vector control muscles. Measured by qRT-PCR, presented as percentage change from empty vector controls. Values are means ±SEM, n=7. Statistical analysis via paired t-test, * $p<0.05$ vs. empty vector controls.

4.5.5.2 Protein expression

VDR-OE muscles demonstrated increased total expression and phosphorylation of multiple mTOR signalling intermediates, primarily in distal signalling. Increased total expression of TSC2 (VDR-OE: 194.0±50.0 % vs. Control: 100.0±17.6, NS), mTOR (VDR-OE: 192.7±30.3 % vs. Control: 100.0±15.4, $p<0.05$), RPS6 (VDR-OE: 171.6±19.6 % vs. Control: 100.0±16.6, $p<0.05$), 4E-BP1 (VDR-OE: 157.1±21.1 % vs. Control: 100.0±16.5, $p<0.01$) and eIF4E (VDR-OE: 122.4±8.6 % vs. Control: 100.0±9.1, NS) were observed in VDR-OE muscles. VDR-OE muscles demonstrated increased phosphorylation of p-mTOR (VDR-OE: 249.9±45.9 % vs. Control: 100.0±15.4, $p<0.05$), p-P70S6K1 (VDR-OE: 392.3±109.6 % vs. Control: 100.0±32.3, $p<0.05$), p-RPS6 (VDR-OE: 233.4±38.8 % vs. Control: 100.0±15.1, $p<0.05$), p-4E-BP1 (VDR-OE: 215.3±32.1 % vs. Control: 100.0±9.5, $p<0.01$) and p-eIF4E (VDR-OE: 319.7±74.6 % vs. Control: 100.0±17.0, NS) (Figure 4.21).

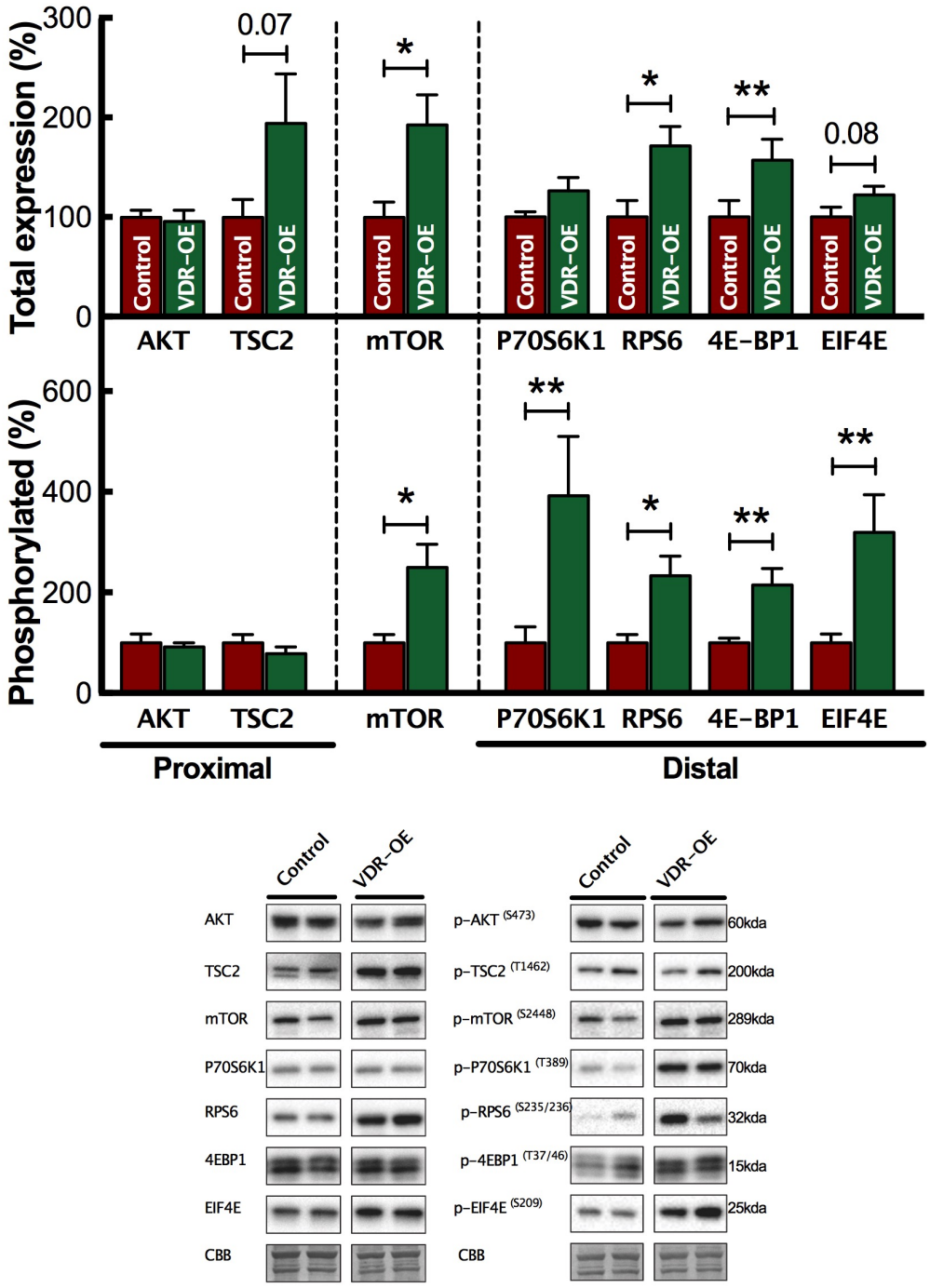


Figure 4.21 VDR-OE total and phosphorylated anabolic signalling

Expression of total and phosphorylated anabolic signalling in VDR-OE and scramble control muscles. Measured by immunoblotting, presented as percentage change from empty vector controls. Values are means ±SEM, n=7. Statistical analysis via paired t-test, * $p<0.05$, ** $p<0.01$ vs. empty vector controls.

Activation of anabolic signalling in VDR-OE muscles was significantly increased compared to empty vector controls. Namely P70S6K1 (VDR-OE: 278.3±70.1 % vs. Control: 100.0±8.0, $p<0.05$), RPS6 (VDR-OE: 155.9±25.9 % vs. Control: 100.0±15.1, $p<0.05$) and eIF4E (VDR-OE: 319.7±74.6 % vs. Control: 100.0±17.0, $p<0.05$) were significantly increased. Moderate but non-significant increases were also observed in mTOR (VDR-OE: 123.4±6.1 % vs. Control: 100.0±9.5, NS) and 4E-BP1 (VDR-OE: 128.9±12.1 % vs. Control: 100.0±9.6, NS) Figure 4.22.

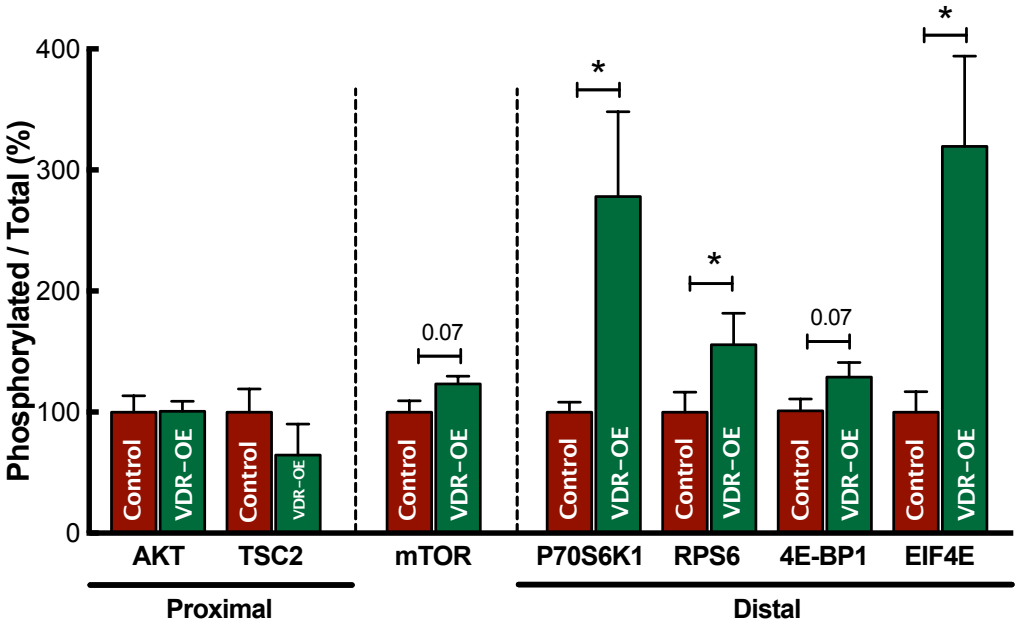


Figure 4.22 VDR-OE anabolic signalling activation

Activation of anabolic signalling in VDR-OE and empty vector control muscles. Measured by immunoblotting, presented as phosphorylated/total expression percentage change from scramble controls. Values are means ±SEM, n=7. Statistical analysis via paired t-test, * $p<0.05$ vs. empty vector controls.

4.5.6 mTOR co-localization

To further highlight and confirm increased mTOR activity, co-localization with LAMP2 was measured. VDR-OE muscles displayed a greater degree of mTOR co-localization with LAMP2 compared to empty vector controls (VDR-OE: 0.28±0.1 AU vs. Control: 0.24±0.2, $p<0.05$) and the membrane stain WGA (VDR-OE: 0.26±0.3 AU vs. Control: 0.16±0.2, $p<0.05$). There was no observed difference in LAMP2/WGA co-localization between VDR-OE muscles and empty vector controls (Figure 4.23).

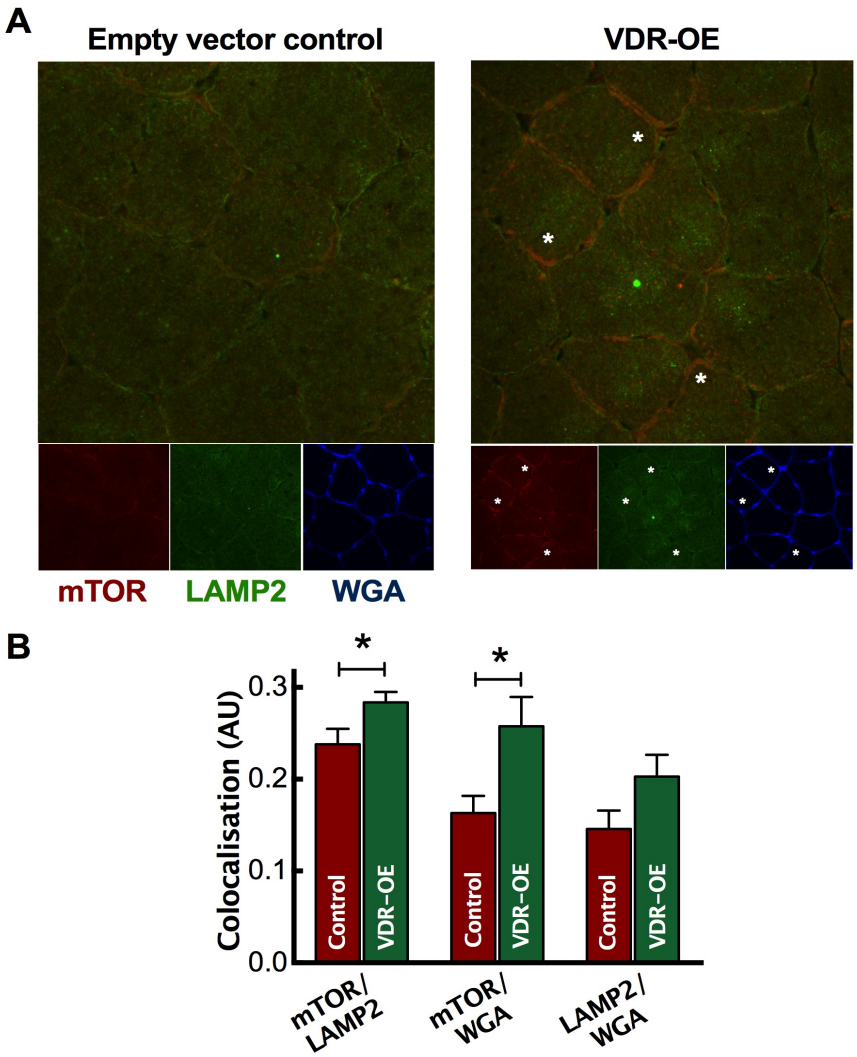


Figure 4.23 VDR-OE mTOR/LAMP2 co-localization

(**A**) Representative images of mTOR, LAMP2 and WGA immuno-histochemical stains in empty vector controls and VDR-OE muscles. (**B**) Quantification of co-localization between mTOR/LAMP2, mTOR/WGA and LAMP2/WGA. Values are means ±SEM, n=7, analysed by Image Pro 3D software. Statistical analysis via paired t-test, * $p<0.05$ vs. empty vector controls.

4.5.7 Ribosomal mRNA expression

As mTOR activity was enhanced, expression ribosomal proteins were assessed. Expression of multiple ribosomal mRNAs was increased in VDR-OE muscles compared to empty vector controls. These included *RPS9* (VDR-OE: 156.1±30.7 % vs. Control: 100.0±14.9, NS), *RPS11* (VDR-OE: 166.1±24.6 % vs. Control: 100.0±15.9, $p<0.05$), *RPS13* (VDR-OE: 155.9±18.6 % vs. Control: 100.0±14.3, $p<0.05$) *RPL21* (VDR-OE: 192.2±31.1 % vs. Control: 100.0±15.3, $p<0.05$) and *RPS28* (VDR-OE: 178.5±23.9 % vs. Control: 100.0±13.5, $p<0.05$) (Figure 4.24).

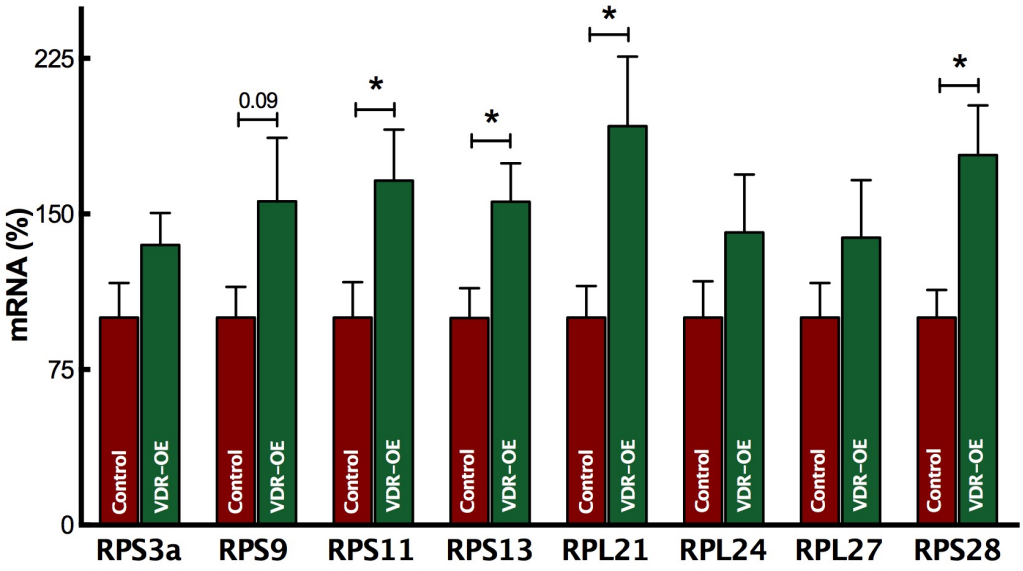


Figure 4.24 VDR-OE ribosomal mRNA expression

mRNA expression of ribosomal genes in VDR-OE and empty vector control muscles. Measured by qRT-PCR, presented as percentage change from empty vector controls. Values are means ±SEM, n=7. Statistical analysis via paired t-test, * $p<0.05$ vs. empty vector controls.

4.5.8 ATP synthase mRNA expression

Moderate increases in multiple ATP synthase subunits were observed in VDR-OE muscles, however it was only significant within *ATP2a3* expression (VDR-OE: 181.9±31.8 % vs. Control: 100.0±18.0, $p<0.05$) (Figure 4.25).

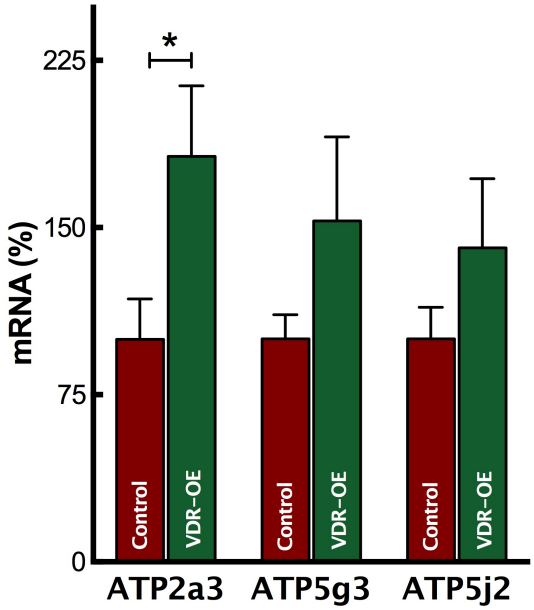


Figure 4.25 VDR-OE ATP synthase mRNA expression

mRNA expression of ATP synthase subunit genes in VDR-OE and empty vector control muscles. Measured by qRT-PCR, presented as percentage change from empty vector controls. Values are means ±SEM, n=7. Statistical analysis via paired t-test, * $p<0.05$ vs. empty vector controls.

4.5.9 Catabolic signalling

VDR-KD did not change autophagy related mRNA expression compared to scramble control muscles, although small non-significant increases were seen in *m-Calpain expression* (VDR-OE: 163±34 % vs. SCR: 100±13, $p<0.05$) Markers of proteasomal mediated degradation *Murf-1* (VDR-OE: 167.9±29.2 % vs. Control: 100.0±9.0, $p<0.05$) and *PSMD11* (VDR-OE: 191.4±29.6 % vs. Control: 100.0±19.6, $p<0.05$) were increased in VR-OE muscle (Figure 4.26).

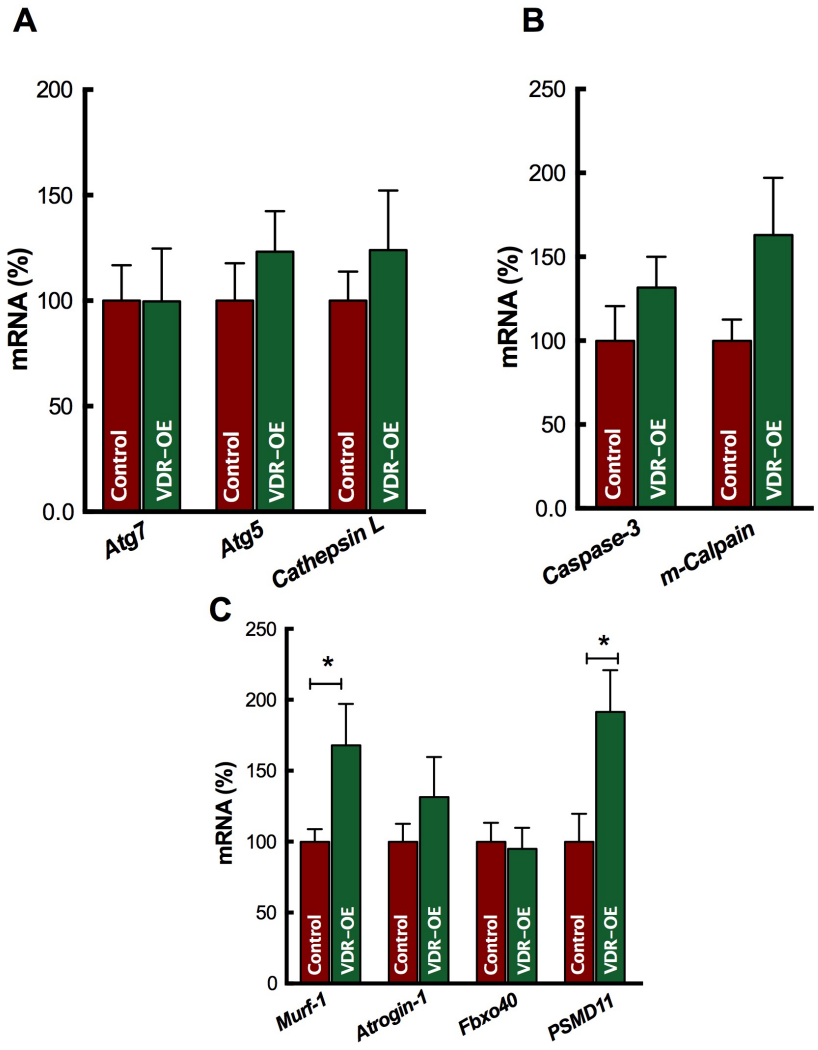


Figure 4.26 VDR-OE catabolic markers mRNA expression

mRNA expression of catabolic markers for (**A**) autophagy, (**B**) caspase/ calpain (**C**) and proteasomal mediated degradation in VDR-OE and empty vector control muscles. Measured by qRT-PCR, presented as percentage change from scramble controls. Values are means ±SEM, n=7. Statistical analysis via paired t-test, * $p<0.05$ vs. scramble controls.

4.5.10 Satellite cell content

There was no change in the distribution of specific fibre types between VDR-OE and empty vector control muscles. Staining for PAX7 positive nuclei demonstrated a small increase in satellite cells for all fibres in VDR-OE muscles compared to empty vector controls (VDR-OE: 0.020±0.004 vs. Control: 0.016±0.003, NS). Type IIx fibres displayed a greater satellite cell content per fibre in VDR-OE muscles controls (VDR-OE: 0.023±0.007 vs. Control: 0.013±0.003, $p<0.05$). There was no difference in satellite cell content in Type IIa, IIb or I fibres between VDR-OE and empty vector control muscles (Figure 4.27).

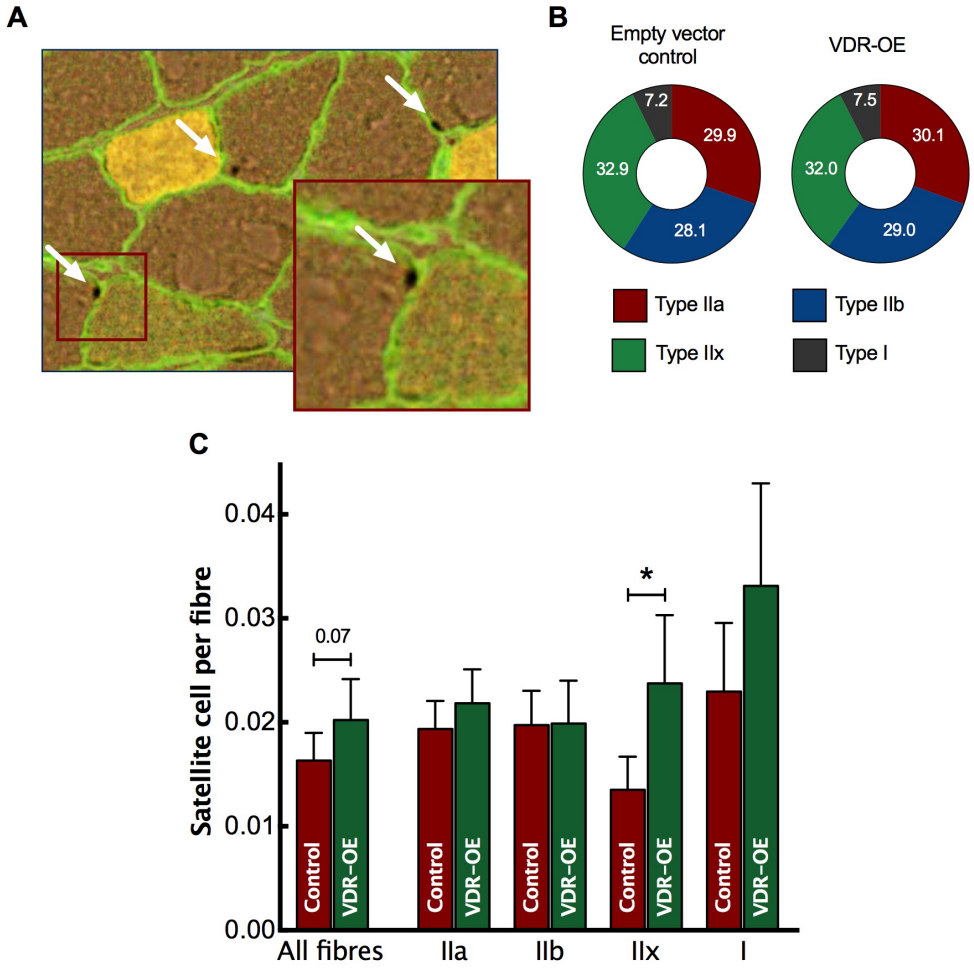


Figure 4.27 VDR-OE fibre type distribution and satellite cell content

(**A**) Representative images of fibre type analysis and Pax7 staining, arrows signify Pax7+ nuclei. (**B**) Fibre type distribution. (**C**) Quantification of satellite cells per fibre type. Values are means ±SEM, n=7. Statistical analysis via paired t-test, * $p<0.05$ vs. empty vector controls.

4.5.11 Proliferative and myogenic mRNA expression

There was a significant increase in mRNA expression of proliferative markers *Pax7* (VDR-OE: 135.3±7.4 % vs. Control: 100.0±12.7, $p<0.05$) and *PCNA* (VDR-OE: 205.6±38.7 % vs. Control: 100.0±22.3, $p<0.05$) in VDR-OE muscles (Figure 4.28).

VDR-OE muscles demonstrated decreased mRNA expression of *MSTN* (VDR-OE: 60.3±11.3 % vs. Control: 100.0±15.8, $p<0.05$) and a moderate increase in *FSTN* expression (VDR-OE: 154.9±33.6 % vs. Control: 100.0±16.1, NS) (Figure 4.28).

Expression of proliferative MRFs showed a small but non-significant increase in expression, namely *MyoD* (VDR-OE: 162.6±31.0 % vs. Control: 100.0±21.8, NS). There was no difference in *MyoG* or *Mrf4* expression (Figure 4.28).

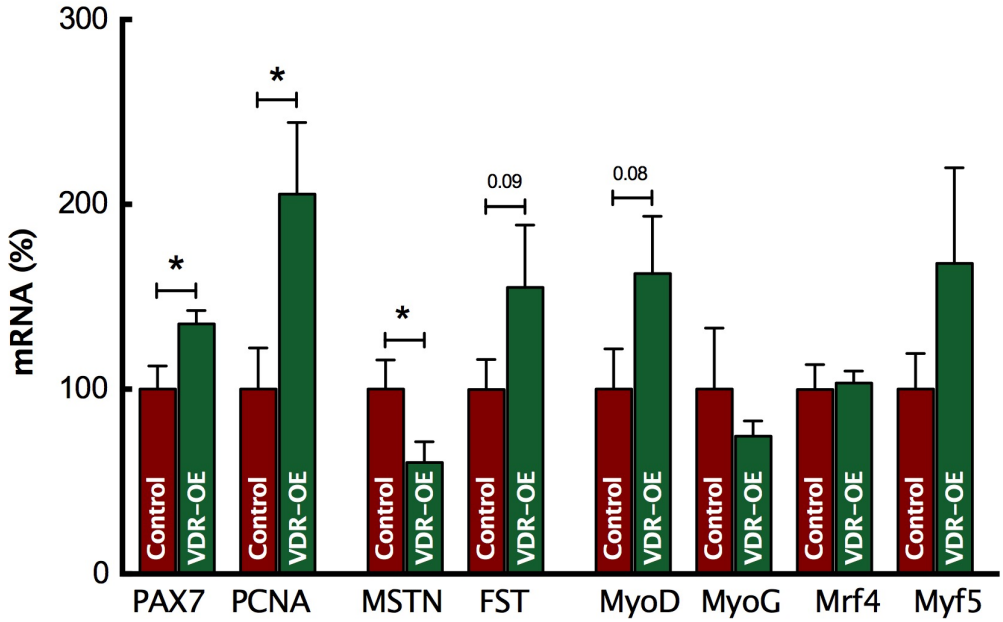


Figure 4.28 VDR-OE proliferative marker mRNA expression

mRNA expression of proliferative markers and MRF genes in VDR-OE and empty vector control muscles. Measured by qRT-PCR, presented as percentage change from empty vector controls. Values are means ±SEM, n=7. Statistical analysis via paired t-test, * $p<0.05$ vs. empty vector controls.

4.5.12 Muscle glucose and glycogen

There was no measured difference in muscle glucose uptake or glycogen content between VDR-OE or empty vector control muscles (Figure 4.29).

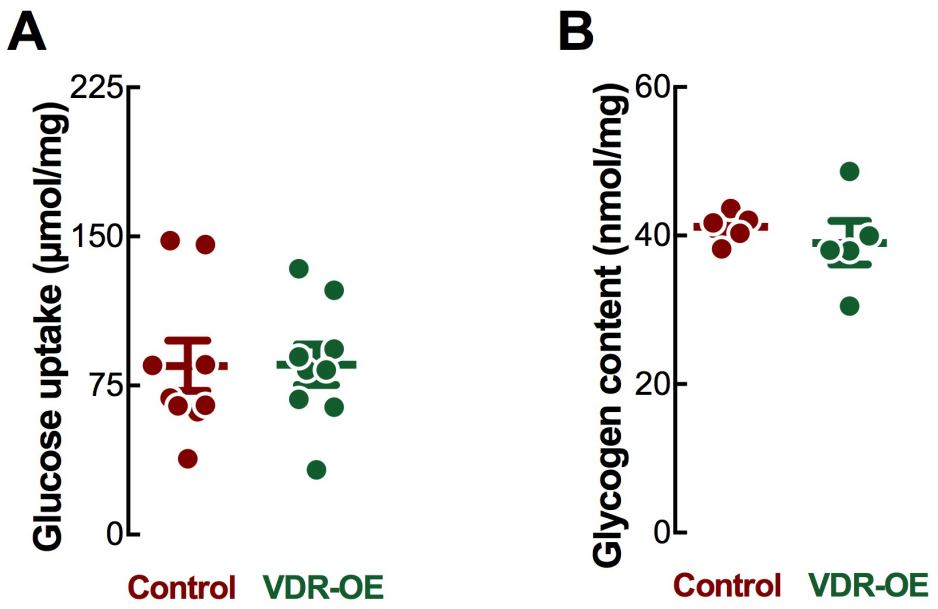


Figure 4.29 VDR-OE glucose metabolism

(**A**) Glucose uptake into VDR-OE and empty vector controls muscles measured by IPGTT and ^{3}H-glucose tracer uptake, n=8 (**B**) Glycogen content of VDR-OE and empty vector controls muscles, n=5. Statistical analysis via paired t-test.

4.6 Discussion

The aim of this current study was to investigate the influence modulation of VDR expression in established muscle would have upon metabolism. It was hypothesized loss of the VDR would negatively impact metabolic regulation, whereas over-expression would enhance it. VDR expression has been linked to improved muscle function and regeneration (Windelinckx et al. 2007; Srikuea et al. 2012), with great interest surrounding the benefits VitD supplementation may have. Yet, distinction between VitD stimulated actions and those autonomously regulated by VDR are unclear. Furthermore, the potential mechanism of action the VDR may have within regulating metabolic and molecular processes is poorly defined. Within this study it was demonstrated that VDR-KD elicited myofibre atrophy and promoted autophagy-mediated protein degradation, without impacting anabolic synthetic processes. In contrast, *in vivo* VDR-OE yielded myofibre hypertrophy through enhanced translational efficiency (mTOR-signaling), ribosomal biogenesis and satellite cell content, summarized in Figure 4.31.

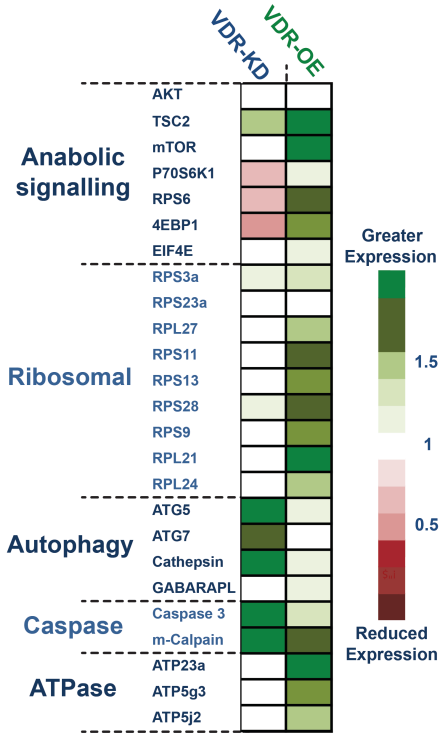


Figure 4.30 Summary of anabolic and catabolic markers

Initially, it was postulated VDR would have a role in terminally differentiated skeletal muscle, *in vivo*. The role of VDR-KD was investigated *in vivo* through lentiviral-mediated knockdown of the VDR to avoid confounding effects of developmental dysregulation and physiological changes (ionic disturbances) seen in knockout models (Endo et al. 2003). Employing *in vivo* electroporation (IVE) of vectors expressing VDR shRNA (or scrambled sequences in the contralateral limb), VDR-KD was confirmed in rat Tibialis' by qRT-PCT (-59.1±9.2%) and immuno-blotting (-51.7±10.9%).

VDR-KD muscles were observed to have markedly reduced myofibre CSA compared to controls. As *Tibialis'* muscle contains predominantly fast myosin isoforms, cryo-sections were immuno-stained for myosin IIa and IIb, which revealed stark reductions in type IIb fibre CSA in VDR-KD muscles. To verify myofibre atrophy, alkali-soluble protein (ASP) content was assessed and observed to decrease in ASP in VDR-KD muscles. Respective analysis of total RNA and DNA content demonstrated no changes within VDR-KD muscle. However, it must be noted the rats utilised in this study were still growing (8 weeks old initially); thus, whether the apparent fibre atrophy represented a blunting of growth or atrophy from original fibre CSA is unclear. Nonetheless, clear distinctions between scramble control muscles and VDR-KD demonstrates a role with muscle mass regulation. The data build upon previous observations; signifying whole body VDR knockout results in a decrease in fibre size (Girgis et al. 2015) through reduced protein content rather than fibre necrosis (Endo et al. 2003). Furthermore, this work suggests a post-natal role of the VDR within mature skeletal muscle, independent of myogenic effects.

Reduced protein content and myofibre atrophy arises where muscle protein degradation exceeds protein synthesis (Volpi et al. 2001), this could either occur through reduced protein synthesis and/or increased protein breakdown. Rates of MPS in mixed lysate, mitochondrial, myofibrillar, sarcoplasmic and collagen fractions all remained unchanged in VDR-KD muscles. There was a significant reduction in the total expression of distal mTOR anabolic signalling intermediates; however, when expressed as signalling activation (phosphorylation/ total expression), no reductions were observed. This indicate that the activation per unit remained the unchanged in VDR-KD muscle. Complementing the data, previous investigations have shown AKT phosphorylation *in vitro* was unchanged in response to VDR-KD (Buitrago et al. 2013), however, total AKT expression was unmeasured. Thus, it is likely the influences seen by VDR-KD do not acts through AKT mediated signalling. Combined, the data suggest loss of the VDR does not induce fibre atrophy through blunting of protein synthesis.

In this case, it was speculated that fibre CSA reductions and net loss of protein was regulated via proteolytic mechanisms. As hypothesized, it was found that mRNA of multiple autophagy and calpain related genes displayed amplified expression in VDR-KD muscles, however some proteasomal genes were reduced. To verify an increase in protein degradation, known markers of autophagy (Sandri 2013) were analyzed by western blotting techniques, indicating both an increase in total protein expression (i.e. Cathepsin L, LC3B-II) and levels of phosphorylation (i.e. p-ULKSer555, p-RaptorSer792). Measurement of autophagosomal LC3B-II by immuno-blotting is considered the 'gold-standard' for autophagy analysis, providing distinction between the differing molecular weights of LC3B-I and

LCB-II (Klionsky et al. 2012; Mizushima & Yoshimori 2007). Thus, increases in LC3B-II detection indicate a greater presence of autophagosomal vesicles, therefore relating to increased autophagy. The data indicate that loss of the VDR does not influence MPS rates or anabolic signalling within established muscle; rather, autophagy mediated protein degradation increases, resulting in fibre atrophy, clarifying previous observations of myofibre atrophy (Girgis et al. 2015). Interestingly, previous investigations have demonstrated muscle wasting occurring in VitD deficient rats through proteasomal mediated degradation, although VDR expression was unmeasured (Bhat, Kalam, Syh Qadri, et al. 2013). Protein degradation measures in VitD deficient animals receiving high-calcium rescue diets were partially rescued. Moreover, measures of autophagy were unchanged in response to VitD deficiency. The apparent disparity between the data sets may be explained by the notion that the autonomous role the VDR may have within skeletal muscle is separate from VitD stimulation. Indeed, within this study, each animal acted as its own unilateral control, thus plasma VitD would not have been an influencing factor. Secondary systemic changes in VitD deficiency such as hypocalcemia or PTH circulation may additionally be involved within the previous studies, separate from VDR mediated effects.

Indeed, loss of the VDR may not actively induce autophagy, rather its presence could be required to suppress degradation and signal a positive-growth environment. Taken together, these results provide the first mechanistic insight into the previously unexplained observations of muscle atrophy in VDR-KO models (Endo et al. 2003; Girgis et al. 2015).

Given that in vitro and in vivo VDR-KD evoked impaired myogenesis and muscle atrophy, it was hypothesized that over-expression would stimulate muscle hypertrophy. To assess this, IVE techniques were utilized, with one leg harbouring VDR cDNA over-expressing (VDR-OE) constructs and the contralateral, an empty vector. VDR-OE was confirmed by qRT-PCR (+190,000±9000%) and immuno-blotting (+1,232±311%). Additionally, VDR-OE was visible within fibres when immuno-stained using an anti-VDR antibody, and displayed myofibre hypertrophy. Despite no previous investigations into the impact VDR expression has upon muscle hypertrophy, the data are complemented by previous supplemental studies. Supplementation of VitD or an analog (1a-hydroxycholecalciferol), was observed to increase muscle fibre CSA measures (Sato et al. 2005; Sørensen et al. 1979). Characteristic of hypertrophy, VDR-OE muscles were additionally demonstrated to have increased total ASP and RNA content, signifying greater synthetic capacity. Collectively, these results suggest that the VDR rather than VitD is the basis for of VitD mediated fibre hypertrophy. VDR-OE mediated fibre hypertrophy contrasts the atrophic phenotype observed in previous VDR-KO/ VitD deficiency studies, and further clarified in this investigation. The data suggest an autonomous modulatory role of the receptor upon skeletal muscle mass.

Based upon the previous results, it was hypothesized that for hypertrophy to occur in VDR-OE muscles, rates of MPS would be enhanced, resulting in a net gain of protein content. A significant increase in global (i.e. mixed lysate) MPS rates within VDR-OE muscles was observed. Furthermore, MPS rates were increased within sarcoplasmic and mitochondrial protein fractions along with contractile myofibrillar and structural collagen fractions. Thus, VDR-OE results in the global enhancement of MPS. The

data build upon earlier analysis of VitD stimulated protein synthesis in rat diaphragm muscle, suggesting modulation by the VDR rather than VitD (Birge & Haddad 1975). Previous in vitro studies the addition of exogenous VitD to cultured myotubes demonstrated an increase in global MPS rates (Salles et al. 2013), however individual protein subfractions were not investigated, nor the autonomous role of VDR. These results are interesting as MPS rates are increased within multiple protein subfractions (i.e. both myofibrillar and mitochondrial), rather than any single one, suggesting an autonomous role of the VDR in global protein metabolism.

To investigate the molecular mechanisms behind the increased rates of MPS, the AKT/mTOR pathway, a key regulator of skeletal muscle hypertrophy (Bodine et al. 2001) was assessed. VDR-OE enhanced mTOR protein expression, along with multiple distal signalling intermediates (i.e. RPS6, 4E-BP1) supported by their increased mRNA expression. Increases within anabolic phosphorylation states and subsequent activation per unit (phosphorylation/ total) of the distal intermediates were also observed; demonstrating increased signalling capacity and activation by VDR-OE. Interestingly mTOR proximal proteins (i.e. AKT, TSC2) displayed no changes in activation; suggesting the mechanism of effect the VDR has is upon mTOR regulation. Interestingly, one study identified that the VDR is capable of binding to TSC2 (Henry et al. 1998), being speculated to have a TSC2 regulatory role. Indeed, modulation of TSC2 by the VDR could impact subsequent mTOR activity, however within this study no changes were seen in TSC2 phosphorylation. Further analysis of phosphorylation sites other than AKT mediated Thr1462 could allude to a potential function. Nonetheless, combined the data potentially clarify the mechanism through which VitD supplementation mediated fibre hypertrophy occurs.

The increased level of mTOR phosphorylation and subsequent signalling cascade suggest enhanced mTOR activation. To allow for assessment of this, immuno-histochemical staining for co-localization of mTOR and LAMP2 were undertaken. Within VDR-OE sections, mTOR localization with LAMP2 was significantly increased. Consistent with literature, activated mTOR localized to the lysosome, whereby the proxy measure of LAMP2 location may be used (Averous et al. 2014). Importantly, these results reflect enhancement of anabolic signalling and MPS seen by Salles et al, upon the addition of exogenous VitD to leucine/insulin treated myotubes. Furthermore, within that study, VDR expression was shown to increase in response to VitD treatment (Salles et al. 2013). Thus, the increased VDR observed may have resulted in enhanced mTOR activity and subsequent upregulation of MPS. These results demonstrate that modulation of anabolic signalling by VitD is likely mediated through the VDR, and regulated by the enhanced expression – a notion consistent with the previous in vitro data demonstrating the requirement VDR expression for VitD stimulation and response to an anabolic stimulus.

Since VDR-OE upregulated AKT/mTOR anabolic signalling, it was hypothesized that ribosomal biogenesis would respectively increase to advocate the greater rates of global MPS previously observed. Indeed previous measures of increased mRNA in VDR-OE muscle support this concept, as ~85% mRNA is ribosomal (Nader et al. 2002), reflecting a greater synthetic capacity. Moreover, mTOR signalling is a well-established regulator of ribosomal biogenesis, initiating translation of ribosomal proteins (RPs) (Chaillou et al. 2014). Within this study, multiple RPS and RPL mRNAs were upregulated by VDR-OE. Furthermore, both P70S6K1 and

RPS6, key regulators of Pol I aspects of ribosomal biogenesis (Roeder & Rutter 1970; Proud 2013), were identified to have increased phosphorylation. The synthesis of RPs is highly regulated, whereupon newly synthesized proteins are utilized for ribosomal assembly (Zhou et al. 2015). The data are in agreement with published ChIP-Seq datasets of VDR target genes within VitD treated monocytes; highlighting multiple genes involved within gene expression, protein synthesis and organization under VDR regulation (Satoh & Tabunoki 2013). Interestingly, increased expression of genes that had previously been identified to be VDR target genes (i.e. RPS11 and RPS13), along with those that were not (i.e. RPL21 and RPL24) were observed in this study. This may be due to the utilization of different tissues, combined with the exogenous VitD stimulation used to identify VDR target genes. Furthermore, ribosomal biogenesis and MPS are energetically demanding processes (Warner 1999), thus increased ATP synthase gene expression complement these observations. The data tentatively explain the positive regulation of muscle mass by VitD (Ceglia et al. 2013), suggesting the VDR may act as an anabolic capacitor within skeletal muscle; whereby in response to VDR-OE, AKT/mTOR mediated anabolic signalling is heightened, resulting in enhanced ribosomal biogenesis, culminating in greater rates of MPS. Modulation of these established mechanisms, clarify the previously reported positive role VitD/VDR has within skeletal muscle.

The observed fibre hypertrophy in VDR-OE muscle may be attributed to the increased anabolic signalling and rates of MPS. This notion is supported by the observation of steady expression of multiple markers of autophagy, caspase and calpain mediated protein degradation. Interestingly, proteasomal markers were increase in response to VDR-OE. While

apparently contradictory to earlier findings, enhanced rates of MPS will invariably result in increased quantities of abnormally folded proteins requiring degradation through proteasomal degradation (Lecker et al. 2006). Furthermore, increased mTOR signalling has been speculated to increase proteasomal mediated degradation as means of maintaining adequate amino acid pools required for greater MPS (Zhang et al. 2014). Additionally, cytosolic VDR, unbound from VitD ligands are susceptible to proteasomal mediated degradation (Peleg & Nguyen 2010). VDR is protected from degradation by nuclear localization and/or binding to VitD; within this study over-expressed VDR was localized within the cytosol, and so susceptible to degradation. Thus, protein anabolism occurred through increased net MPS, with MPB remaining largely unchanged.

Previous investigations have demonstrated increased VDR expression within damaged myofibrils of regenerating skeletal muscle (Srikuea et al. 2012), with additional localization to Pax7 positive nuclei (Srikuea & Hirunsai 2016). Within our study, VDR-OE alone in the absence of injury enhanced satellite cell recruitment and increased anabolic signalling. This matches earlier observations of decreased myoblast proliferation. Gene expression of Pax7 and PCNA, a marker of satellite cell entry into the cell cycle (Johnson & Allen 1993), showed increased expression within VDR-OE muscles. Furthermore, myostatin a known inhibitor of PAX7 and skeletal muscle hypertrophy (McFarlane et al. 2008), showed clear reductions in expression, complemented by a moderate increase in follistatin. Interestingly, reasonable (although non-significant) increases in primary proliferative MRF genes (i.e. MyoD and Myf5) were observed, whilst MRFs key to differentiation (i.e. Myogenin and Mrf4) remained unchanged (Sabourin & Rudnicki 2000). This may be a result of the relatively short

duration of VDR-OE (10 days). Additional measurements gathered at later timepoints might allude to whether satellite cells would undergo differentiation. This notion is supported by previous investigations demonstrating a pro-myogenic role of VitD supplementation inducing myoblast differentiation (van der Meijden et al. 2016). Combined the data suggest the VDR may act as an essential capacitor in response to a stimulus (e.g. injury), signalling a pro-growth environment, positively regulating satellite cell activity and muscle protein metabolism.

Finally, to investigate the potential role of the VDR within skeletal muscle glucose metabolism, an intra-peritoneal glucose tolerance tests (IPGTT) with a combined glucose tracer was performed (Roustit et al. 2014). Interestingly, neither VDR knockdown or over-expression resulted in changes in skeletal muscle glucose uptake or glycogen content. The data seemingly conflicts with previous investigations and meta-analysis, proposing a role of VitD within T2D and glucose metabolism, enhancing glucose transport (Mathieu et al. 2005; Pittas et al. 2007). One explanation could be that the VDR alone does not have an autonomous role within glucose metabolism, instead requiring binding of the VitD ligand. However, VDR-KD in the presence of VitD supplementation would be required to confirm this notion. Additionally, while VitD deficiency has been linked to development of T2D, it is speculated that it may be primarily involved with insulin secretion, rather than sensitivity (Park et al. 2015). Indeed, a previous study investigating pancreatic function using a whole-body VDR knockout mouse model, determined glucose stimulated insulin levels were considerably decreased (Zeitz et al. 2003). This augments our findings, suggesting that if VitD/VDR does indeed have a role within glucose

metabolism, it may reside within pancreatic insulin secretion rather than glucose uptake in skeletal muscle.

4.7 Conclusion

To summarize, the study presented is the first to identify a mechanistic role of the VDR within skeletal muscle. The data suggests expression of the VDR exerts a pro-growth stimulus, modulating satellite cell activity, enhancing anabolic signalling and synthetic capacity, resulting in enhanced rats of MPS. Furthermore, loss of the VDR results in fibre atrophy through MPB exceeding MPS evidenced by unchanged MPS/ anabolic signalling, and increased markers of autophagy (Figure 4.31). Indeed the data provide context to the mechanisms involved in observations of reduced muscle function and size in VDR-KO models (Endo et al. 2003; Girgis et al. 2015). However, the data are limited by the single timepoint available after IVE. Earlier additional measures of fibre CSA and satellite content would allow the temporal nature of the respective fibre atrophy and hypertrophy in VDR-KD and VDR-OE muscles.

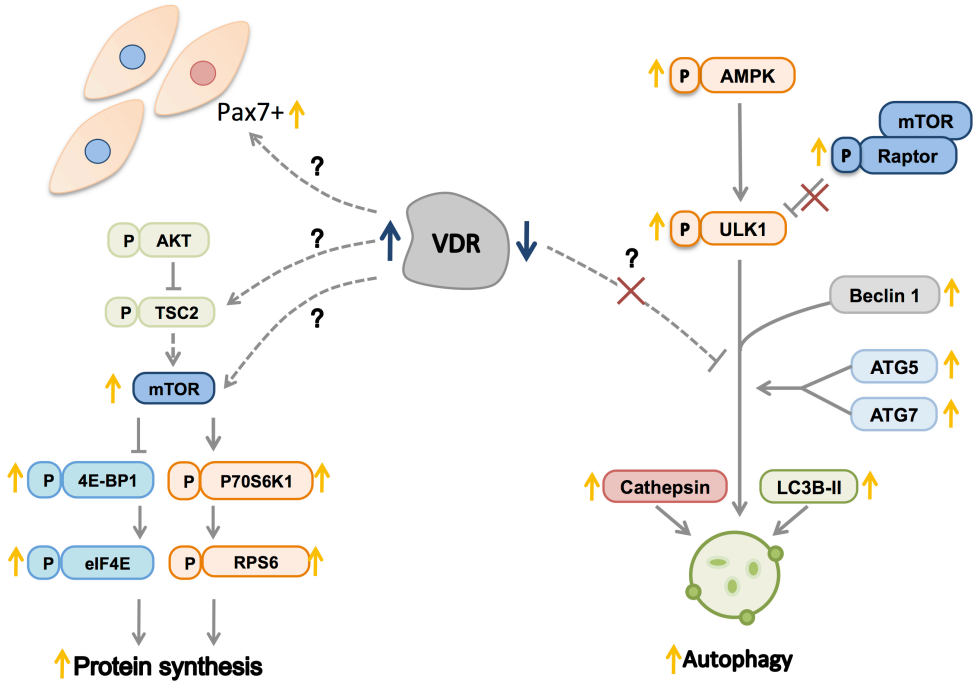


Figure 4.31 Potential mechanisms of VDR

Illustration of potential mechanisms the VDR may have upon protein synthesis, satellite cell proliferation and autophagy.

Chapter 5 – The Role of Vitamin D and the Vitamin D Receptor in Response to Resistance Exercise Training in Humans

5.1 Introduction

The findings of the previous study provide insight into the dual nature of VDR expression upon muscle metabolism; highlighting a gain and loss of function of VDR causes hypertrophy and atrophy respectively. However, the implications this has within human skeletal muscle metabolism are currently unclear.

As previously discussed, VitD deficiency has been observed to have adverse consequences upon musculoskeletal health, with reductions in skeletal muscle function (Dhanwal et al. 2013) and increased risk of falls observed (Bischoff-Ferrari, Dietrich, et al. 2004). Skeletal muscle is thought to be a VitD target tissue, as confirmation of VDR and CYP27B1 expression, combined with 25[OH]D_3 stimulatory effects suggest active VitD metabolism (Srikuea et al. 2012). VitD supplementation has been shown to improve muscle function and fibre cross sectional area, suggesting an active role within muscle metabolism (Ceglia et al. 2013; Sato et al. 2005). Moreover, RET, a potent initiator of muscle hypertrophy has been shown to acutely upregulate VDR expression (Makanae et al. 2015). These findings provide tentative epidemiological, pre-clinical and clinical links between VitD, the VDR and skeletal muscle mass. However, few studies have investigated VDR expression within supplemental studies, along with potential roles it may have within muscle metabolism.

5.2 Aims and hypothesis

Based on the previous findings that VDR expression exerts a pro-growth stimulus *in vivo*, the present study intended to demonstrate translational relevance of these observations in humans. Specifically, the aims of this investigation were to: characterise VDR expression and VitD status in response to a resistance exercise-training program.

- Characterise VitD status and VDR mRNA expression in skeletal muscle in resistance exercise-trained individuals.
- Determine whether either VitD status or VDR expression were correlated to the response to resistance exercise.
- Assess changes in expression of genes responsible for VitD metabolism.

It was hypothesized VitD status and VDR mRNA expression in skeletal muscle would be increased in response to a resistance exercise-training program.

5.3 Methodology

5.3.1 Study information and resistance exercise training

All samples were originally collected as part of the Derby resistance exercise training study, as previously reported (Phillips et al. 2013). The data presented in this thesis is of subsequent analysis of the data sets and additional testing of samples. Ethical approval for the original study and subsequent analysis was granted by The University of Nottingham Medical School Ethical Advisory Committee. Male and female healthy participants aged 18-75 were recruited, with the following exclusion criteria applied:

- Body mass index (BMI) <18 or 28>
- Blood pressure >160/100, and/or angina, heart failure or arrhythmia
- Presence of repertory diseases including COPD and asthma
- Presence of metabolic disorders including hypo and hyper parathyroidism and type I or II diabetes
- Active inflammatory bowel disease
- Clotting dysfunction
- Pregnancy
- Musculoskeletal or neurological disorders

Prior to study initiation, subjects underwent a screening session in which they provided written consent for study participation. They additionally underwent a medical examination including medical history, physical examination, an electrocardiogram (ECG) and blood tests (Glucose). Lean muscle mass was measured by dual energy X-ray absorptiometry (DEXA) (Lunar Prodigy II, GE Medical Systems). Subjects undertook a 20-week whole-body resistance exercise-training program, with biopsies taken pre and post training program (discussed bellow). After study completion, all screening measures including DEXA were reassessed. From the original cohort, 39 subjects were used for the subsequent analysis, as measured data sets and plasma samples were available.

The aim of the original study was to achieve skeletal muscle growth (muscular hypertrophy) through a resistance exercise-training regime. All subjects trained three times a week, with sessions lasting approximately 60 mins. Training intensity was 70% 1-RM, based on single sets of 12 repetitions with two-minute rests between sets. The number and order of sets completed varied between the three sessions with each session comprising of the same total number of repetitions (Table 5.1) Throughout

the RET program a trained instructor ensured proper form and technique with additional verbal encouragement.

Table 5.1 Resistance exercise training program

Exercise	Primary muscles trained	Session 1	Session 2	Session 3
Seated Chest Press	Pectorals, Deltoids, Triceps	2	4	1
Lat Pull Down	Latissimus Dorsi, Trapezius, Biceps	2	4	1
Seated Lever Row	Latissimus Dorsi, Biceps	2	-	4
Leg Extension	Quadriceps	2	4	1
Seated Leg Curl	Hamstrings	2	4	1
Seated Leg Press	Quadriceps, Hamstrings, Gluteals	2	-	4
Back Extension	Erector Spinae	2	-	2
Abdominal Curl	Abdominals	2	-	2
Number of sets		**16**	**16**	**16**

Biopsies of *Vastus Lateralis* muscle were taken pre-RET regime in fasted non-exercised conditions. Post RET biopsies were taken three-seven days after the final training session in a fasted non-exercised condition. All biopsies were taken under local anaesthesia (2% lidocaine) by conchotome biopsy forceps and subsequently frozen in liquid nitrogen. Blood was collected in pre-chilled tubes containing Lithium Heparin; plasma was separated by centrifugation and stored at -80^{O}C.

For some analysis, participants were divided into quartiles of lean mass changes in response to RET. The same quartiles as stated in the Derby resistance exercise training study were used for mRNA expression analysis

(n=44) (Phillips et al. 2013). This was undertaken to display responder status changes. For analysis of 25[OH]D, plasma samples were only available for n=37 of these participants (Table 5.2).

5.3.2 Microarray analysis

Microarray analysis was undertaken in the original study for each participant using muscle biopsies pre and post resistance exercise training (Phillips et al. 2013). RNA was extracted and purified as previously discussed and reverse transcribed using the Affymetrix 3' IVT express kit. RNA was hybridized to Affymetrix U133+2 arrays and scanned using an Affymetrix 3000 7G scanner. The resulting data set (GSE47881) was subsequently mined for *VDR*, *CYP27B1* and *CYP24A1* expression.

5.3.3 HOMA-IR

The Homeostatic model assessment of insulin resistance (HOMA-IR) was used to estimate insulin sensitivity. First defined by Matthews *et al* in 1985, HOMA-IR describes the relationship between glucose and insulin secretion in the fasted state. Values above 2.35 for men and 1.88 in women are considered to be suggestive of insulin resistance (Balkau & Charles 1999).

In this study, blood was collected in fasted subjects pre and post resistance exercise-training. HOMA-IR values were calculated using the original HOMA-IR model, using the following equation:

$$\text{HOMA-IR} = \frac{\text{Glucose (mmol.L}^{-1}) \times \text{Insulin } (\mu\text{U.mL}^{-1})}{22.5}$$

5.3.4 Plasma 25[OH]D analysis

Quantification of 25[OH]D_2 and 25[OH]D_3 was measured by liquid chromatography–mass spectrometry (LC-MS/MS). Deuterated $^2H_3$-

25[OH]D_2 and $^2H_3$-25[OH]D_3 (200ng/ml) internal standards in ethanol were added to each plasma sample before addition of ice cold methanol and incubated at 4^{O}C for 10mins. Heptane was subsequently added and vortex mixed for 30s. The heptane layer containing 25[OH]D_2, 25[OH]D_3 and internal standards was transferred to a boiling tube and evaporated to dryness. The dried samples were resuspended in acetonitrile (ACN):ddH_2O (65:35), vortex mixed and sonicated, before transfer to an Eppendorf and centrifuged to remove debris. Samples were then transferred to an autosampler vial and capped. Samples were assessed by LC-MS/MS, alongside a standard curve of known enrichments. Selected ion monitoring (SIM) for 25[OH]D_2/$^2H_3$-25[OH]D_2 and 25[OH]D_3/$^2H_3$-25[OH]D_3 was 394.93-395.73 / 397.95-398.75 and 382.93-383.73 / 385.95-386.75 respectively (Figure 5.1 and Figure 5.2). Validation for linearity and the range of detection was assessed as at least 3.375-100 ng/ml for both 25[OH]D_2 and 25[OH]D_3 (Figure 5.3 and Figure 5.4).

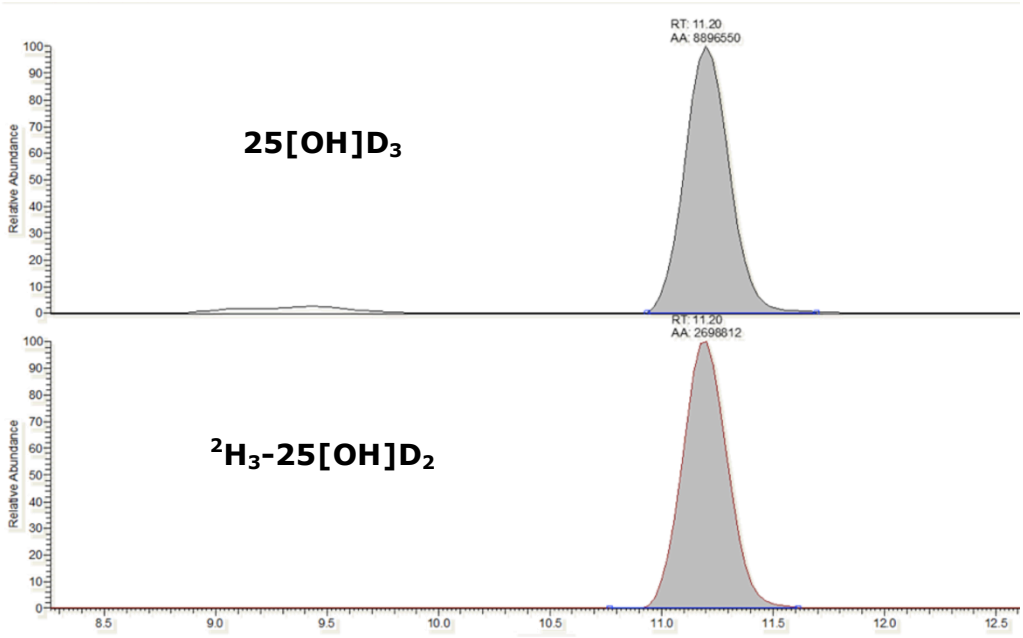


Figure 5.1 Chromatogram of 25[OH]D_2 and $^2H_3$-25[OH]D_2

Chromatogram of 25[OH]D_2 and spiked internal standard $^2H_3$-25[OH]D_2.

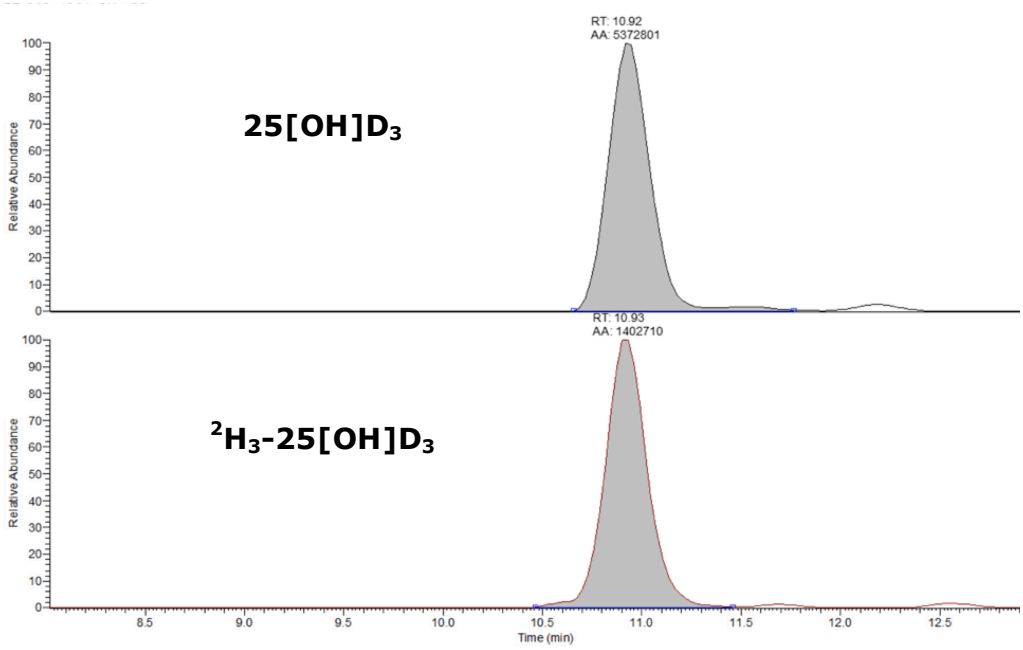


Figure 5.2 Chromatogram of 25[OH]D_3 and $^2H_3$-25[OH]D_3

Chromatogram of 25[OH]D_3 and spiked internal standard $^2H_3$-25[OH]D_3.

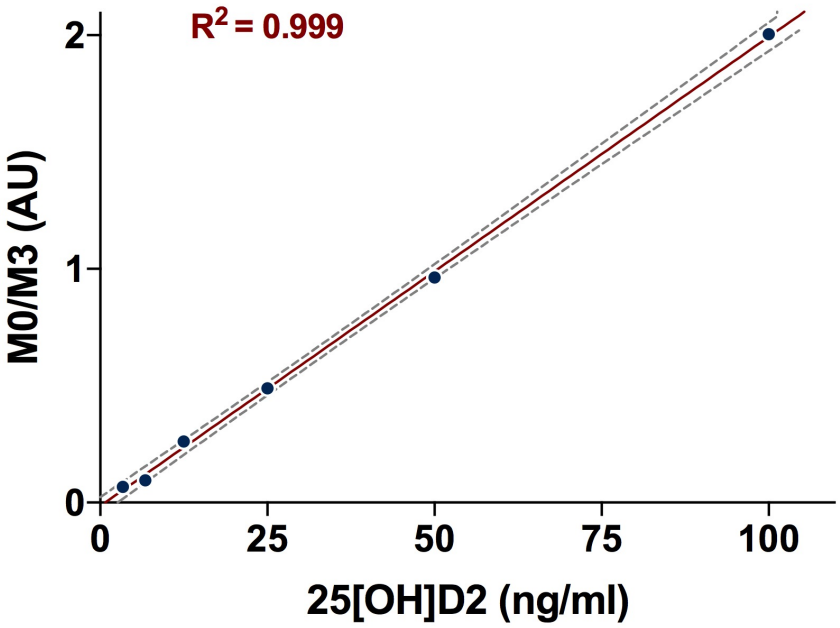


Figure 5.3 25[OH]D_2 range of detection

Standard curve of known concentrations of 25[OH]D_2. Dotted lines refer to the 95%CI.

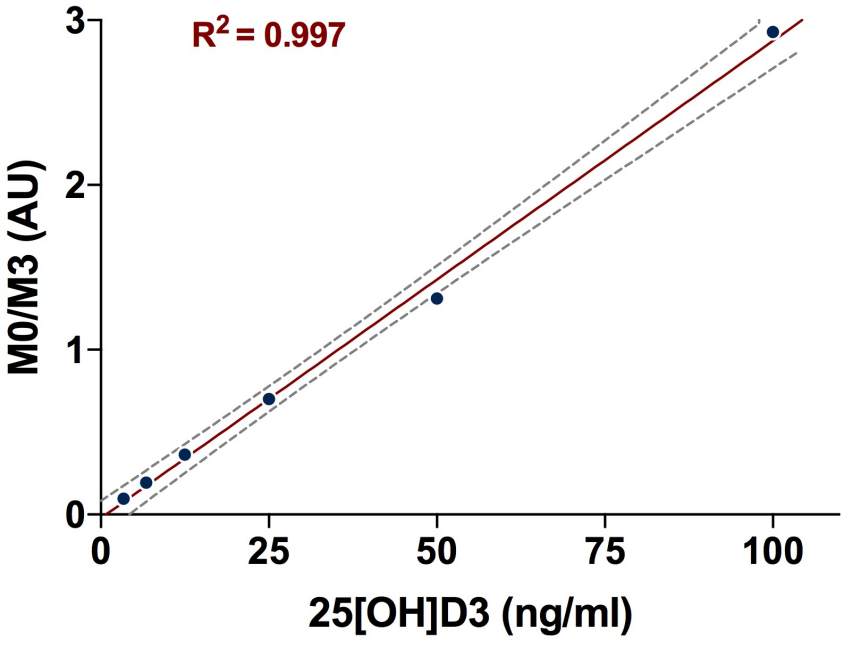


Figure 5.4 25[OH]D_3 range of detection

Standard curve of known concentrations of 25[OH]D_3. Dotted lines refer to the 95%CI.

5.4 Results

5.4.1 Participant quartile grouping

Participants were grouped into quartiles of lean mass changes in response to RET. Quartile 4 were significantly younger than quartile 1 (Q1 55.2 ± 3.7 vs. 37.2 ± 5.0, $p<0.05$).

Table 5.2 Participant quartile grouping characteristics

	Q1	Q2	Q3	Q4
n	11	11	11	11
Age	55.2 ± 3.7	56.2 ± 5.3	58.1 ± 3.2	36.4 ± 5.0*
Gender (%M)	67	56	45	56
Body weight (kg)	73.7 ± 8.1	74.3 ± 3.6	70.1 ± 3.8	73.0 ± 2.8
Lean mass (kg)	52.5 ± 4.1	47.8 ± 3.4	45.9 ± 3.1	49.2 ± 2.9
Lean mass change (%)	-2.3 ± 0.5	1.3 ± 0.1*	2.6 ± 0.2*	5.9 ± 1.0*
Fat mass (kg)	20.6 ± 2.1	22.1 ± 1.5	21.3 ± 1.9	20.3 ± 2.6
1 Leg 1RM (kg)	47.2 ± 6.4	40.3 ± 6.4	37.6 ± 4.9	51.7 ± 6.7
1 Leg 1 RM change (%)	21.2 ± 2.9	28.3 ± 8.5	22.1 ± 5.1	29.7 ± 10.3
Vitamin D status (nmol/l)	49.0 ± 6.3 (n=9)	43.3 ± 5.6 (n=9)	44.2 ± 6.1 (n=9)	38.3 ± 6.4 (n=10)

Quartiles of lean mass changes from all available participant data. Values are means ±SEM, n=44. Statistical analysis via t-test, * indicates significantly different from Q1. Vitamin D status is only reported in subjects where serum was available, n=37.

5.4.2 Whole-body lean mass changes

In response to 20-weeks whole-body resistance exercise training, participants were grouped into quartiles of mean gains in lean mass. Mean lean mass changes in quartile 1 were negative from baseline values, while quartiles 2, 3 and 4 incrementally increases lean mass (Figure 5.5).

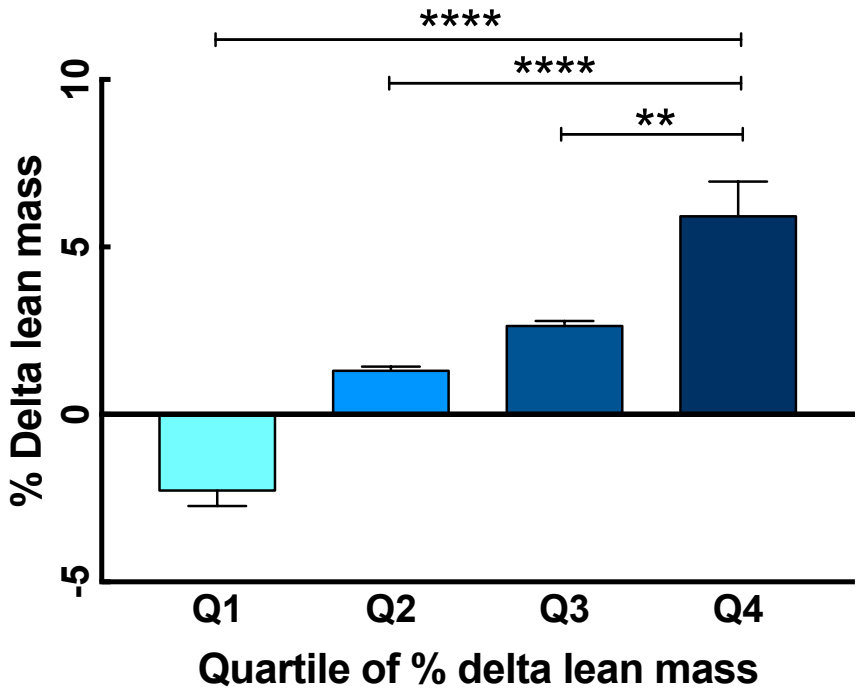


Figure 5.5 Quartiles of lean mass changes

Quartiles of lean mass changes to 20-weeks whole-body resistance exercise training in all participants. Measured by DEXA scans pre and post training regime and presented as % change from pre. Values are means ±SEM, n=44. Statistical analysis via t-test, * $p<0.05$, *** $p<0.001$, **** $p<0.0001$.

5.4.3 VDR mRNA expression

5.4.3.1 Pre and post training

VDR mRNA expression was unchanged between lean mass change quartiles pre-training. Post training, VDR expression was significantly greater in Q4 (117.6±7.8 AU) compared to Q1 (92.5±7.6 AU, $p<0.05$) Q4 VDR expression was moderately greater than Q2 (100.3±6.5 AU, $p<0.05$) and Q3 (104.4±3.0 AU, NS) (Figure 5.6).

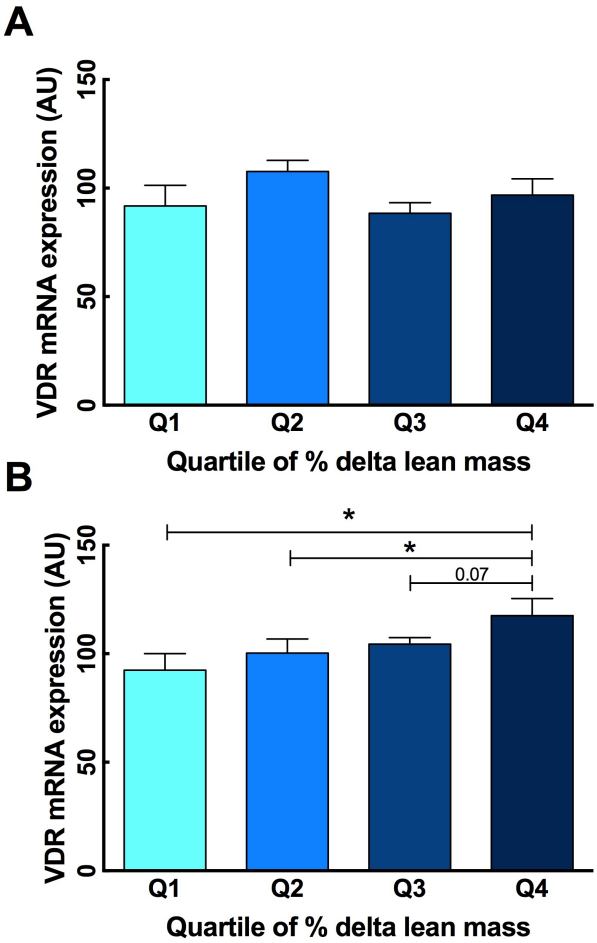


Figure 5.6 VDR expression pre and post training

VDR mRNA expression presented in lean mass change quartiles, (**A**) pre and (**B**) post-training regime in all participants. Values are means ±SEM, n=44. Statistical analysis via t-test, * $p<0.05$.

5.4.3.2 VDR mRNA Expression change

VDR mRNA expression significantly increased compared pre-training values in Q3 (+10.7±3.1%, $p<0.01$) and Q4 (+24.7±8.4%, $p<0.05$). Q4 increased significantly greater than Q1 (-2.1±8.1%, $p<0.05$) moderately over Q2 (+6.2±6.9%, NS) (Figure 5.7).

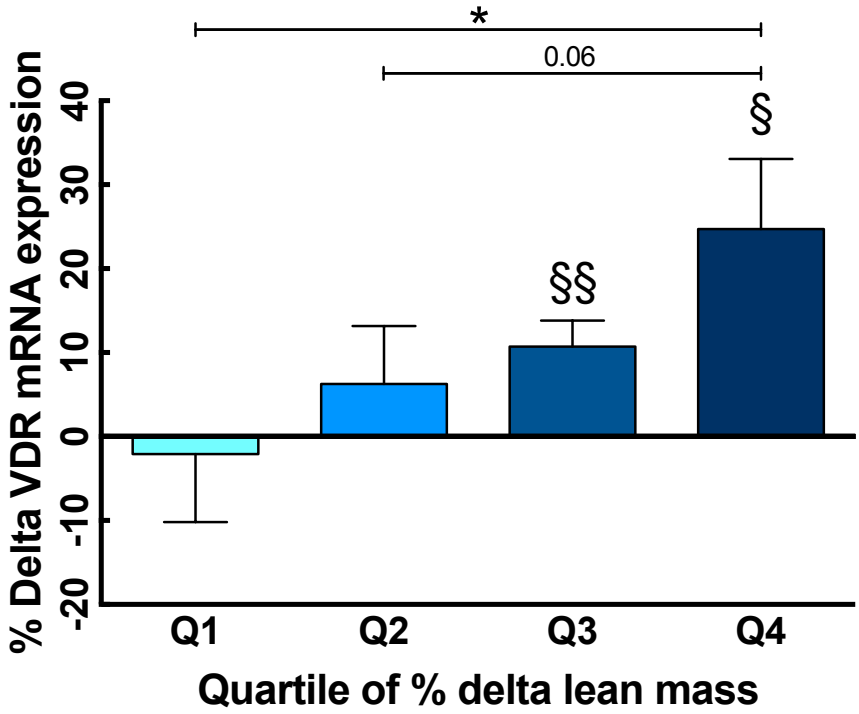


Figure 5.7 VDR expression change

VDR mRNA % Delta expression presented in lean mass change quartiles in all participants. Values are means ±SEM, n=44. Statistical analysis via t-test, * $p<0.05$ between quartile groups, § $p<0.05$, between pre and post training in that quartile.

5.4.3.3 VDR mRNA and lean mass changes

When examining the relationship between changes in VDR mRNA expression and lean mass, a positive correlation between the two was observed (Figure 5.8).

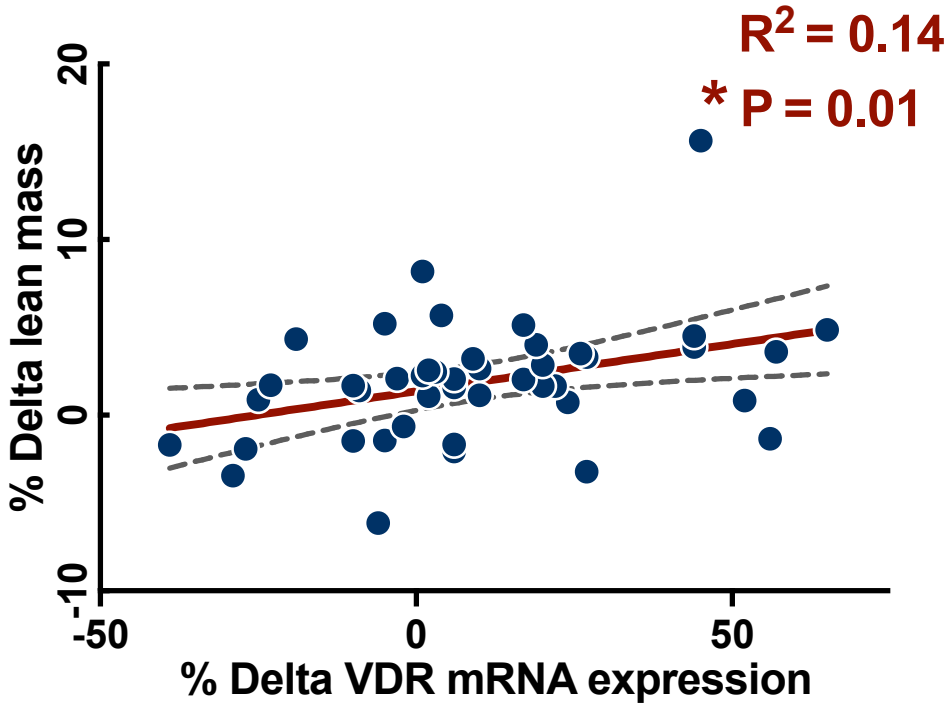


Figure 5.8 VDR mRNA and lean mass change correlations

Correlation between VDR mRNA expression and lean mass changes in response to 20-weeks whole-body resistance training in all particiapnts. Statistical analysis via Pearson's correlation, n=44. Dotted lines refer to the 95%CI.

5.4.4 Plasma Vitamin D status

5.4.4.1 Pre and post training

25[OH]D levels were unchanged between lean mass change quartiles pre-training. Post-training quartiles were increased in Q1 (+63.3±5 nmol/L, $p<0.05$) and Q2 (+58.4±9 nmol/L, $p<0.05$) compared to Q3 (+45.3±9 nmol/L) and Q4 (+43.1±6 nmol/L) (Figure 5.9).

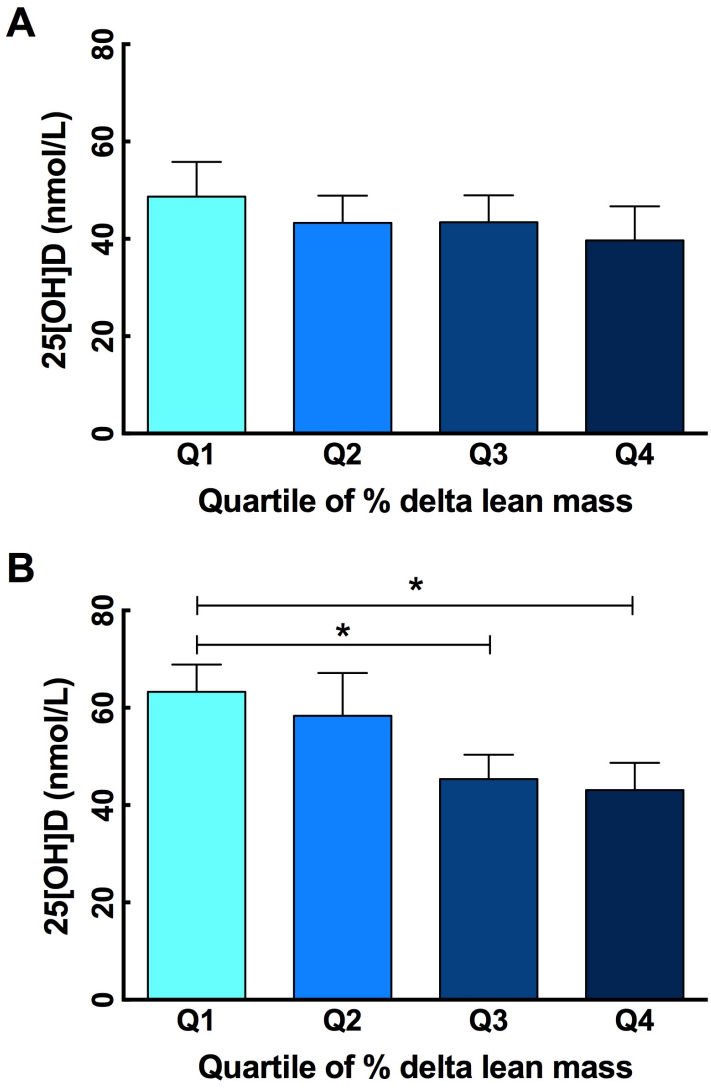


Figure 5.9 Vitamin D status pre and post training

Plasma 25[OH]D levels (**A**) pre and (**B**) post training, presented in lean mass quartiles, from participants with available serum. Measured by LC-MS/MS. Values are means ±SEM, n=37. Statistical analysis via t-test, * $p<0.05$.

5.4.4.2 Vitamin D status change

There was no significant change in 25[OH]D levels in any of the quartile groups from their pre-training levels. There was a moderate but non-significant difference in 25[OH]D level changes between Q1 (+18.1±9.3 nmol/L) and Q4 (+1.1±5.4 nmol/L,) (Figure 5.10).

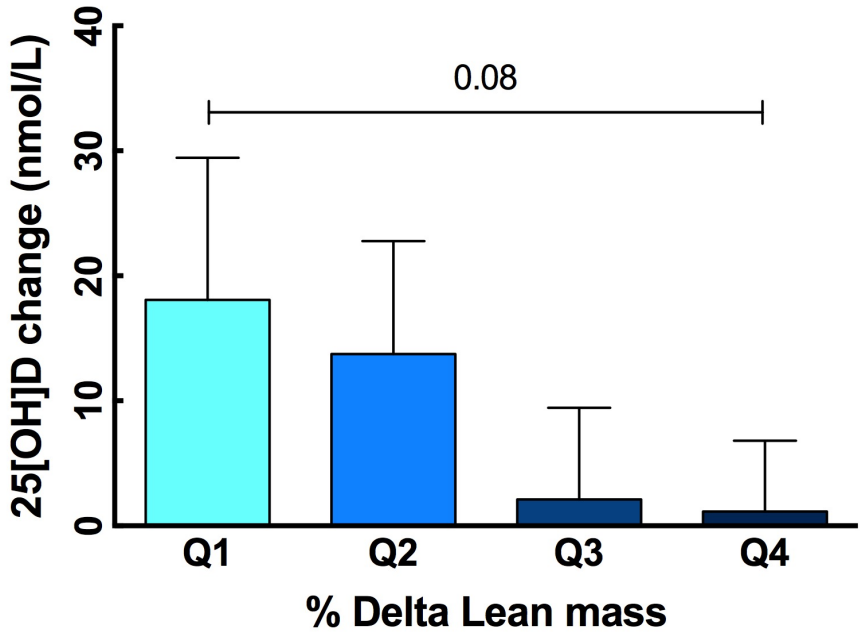


Figure 5.10 Vitamin D status change

Plasma 25[OH]D level changes between pre and post resistance exercise training regime presented in lean mass change quartiles, from participants with available serum. Measured by LC-MS/MS. Values are means ±SEM, n=37. Statistical analysis via t-test.

5.4.4.3 Vitamin D and lean mass changes

There was no correlation between changes in 25[OH]D levels and lean mass (Figure 5.11).

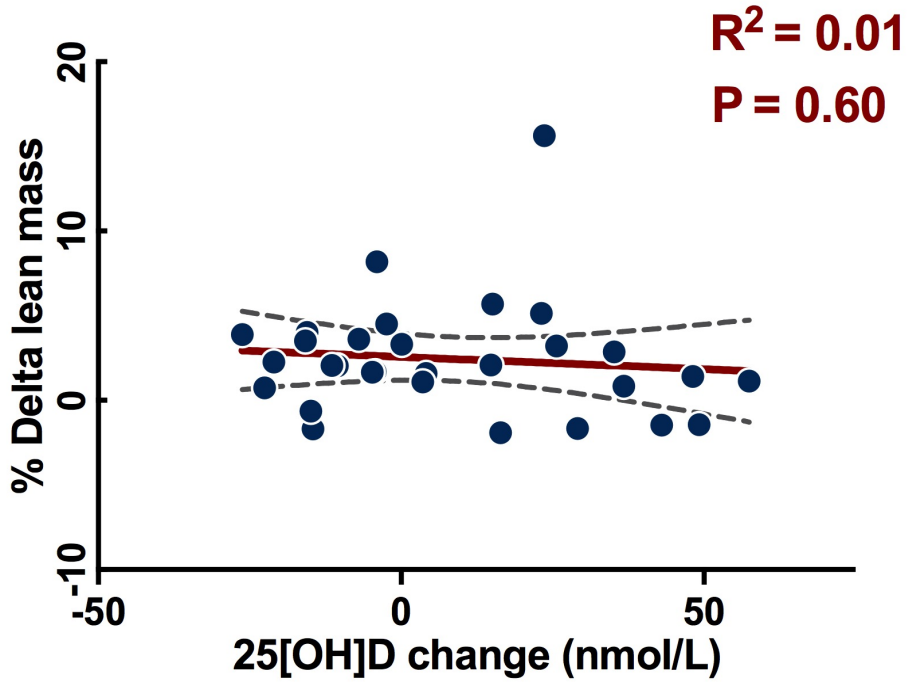


Figure 5.11 Vitamin D and lean mass change correlation

Correlation between 25[OH]D level and lean mass changes in response to 20-weeks whole-body resistance training, from participants with available serum. 25[OH]D measured by LC-MS/MS. Statistical analysis via Pearson's correlation, n=37. Dotted lines refer to the 95%CI.

5.4.4.4 Vitamin D and VDR mRNA pre and post training

There was no correlation between VDR mRNA expression and 25[OH]D levels at either pre or post resistance exercise training regime (Figure 5.12).

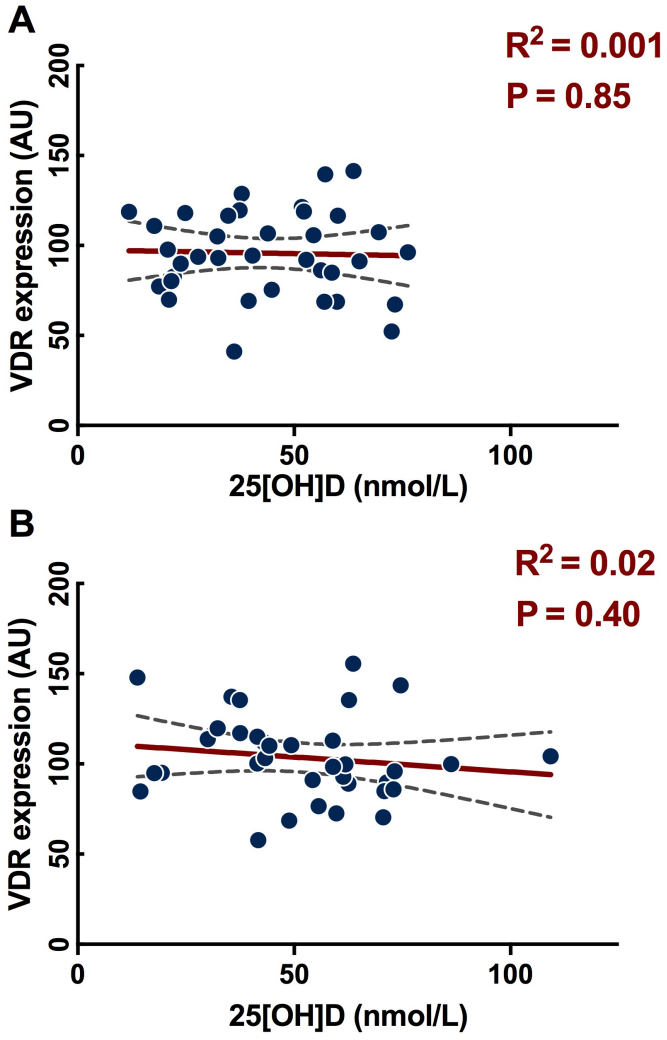


Figure 5.12 Vitamin D levels and VDR mRNA expression pre and post correlations

(**A**) Pre and (**B**) post resistance exercise training regime correlations between VDR mRNA expression and 25[OH]D levels, from participants with available serum. 25[OH]D measured by LC-MS/MS. Statistical analysis via Pearson's correlation, n=37. Dotted lines refer to the 95%CI.

5.4.4.5 Vitamin D and VDR mRNA changes

There was no correlation between the changes in 25[OH]D levels and VDR mRNA expression in response to training (Figure 5.13).

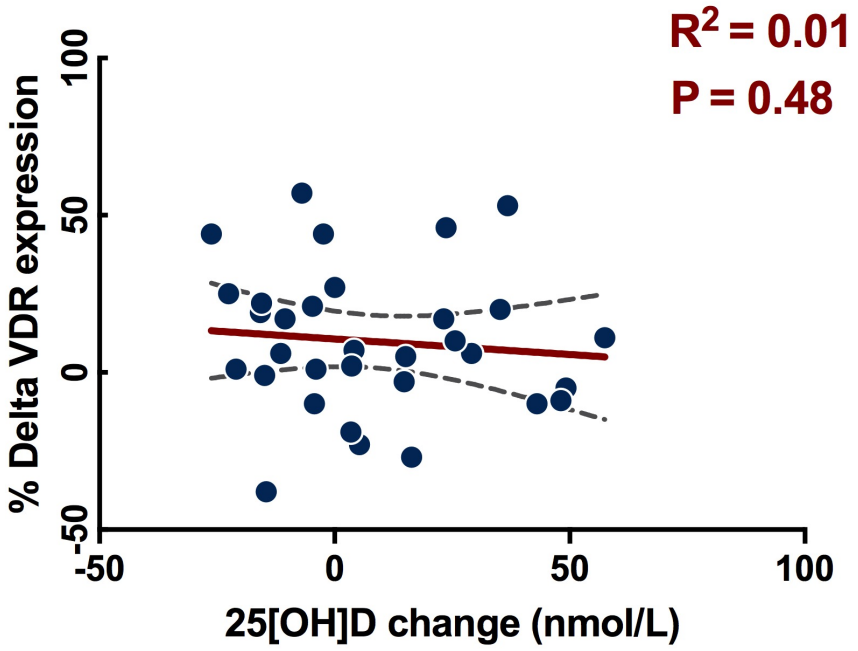


Figure 5.13 Vitamin D and VDR mRNA change correlation

Correlation between 25[OH]D level and VDR mRNA expression in response to 20-weeks whole-body resistance training, from participants with available serum. 25[OH]D measured by LC-MS/MS. Statistical analysis via Pearson's correlation, n=37. Dotted lines refer to the 95%CI.

5.4.5 CYP27B1 mRNA expression

5.4.5.1 Pre and post training

To assess local VitD metabolism CYP27B1 mRNA expression was measured. Grouped into lean mass change quartiles, pre-training expression was significantly lower in Q1 (16.0±3.9 AU) compared to Q2 (35.9±6.6 AU, $p<0.05$), Q3 (28.9±8.2 AU, NS) and Q4 (35.3±7.2 AU, $p<0.05$). Post training, there was no significant difference between any of the quartile groups (Figure 5.14).

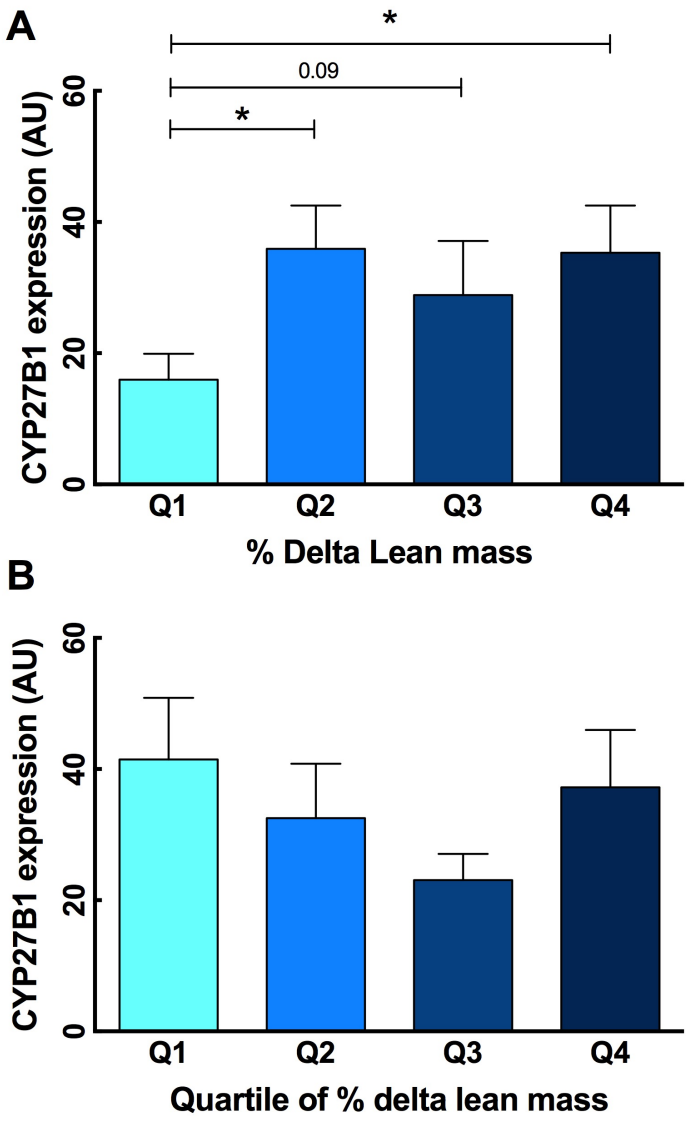


Figure 5.14 CYP27B1 mRNA expression pre and post training

CYP27B1 mRNA expression presented in lean mass change quartiles, (**A**) pre and (**B**) post-training. Values are means ±SEM, n=37. Statistical analysis via t-test, * $p<0.05$.

5.4.5.2 CYP27B1 mRNA expression change

CYP27B1 mRNA expression significantly increased compared pre-training values in Q1 (+237±85%, $p<0.05$). The degree of change was significantly greater than Q1 (+15±41%, $p<0.05$) and Q3 (+26±26%, $p<0.05$) (Figure 5.15).

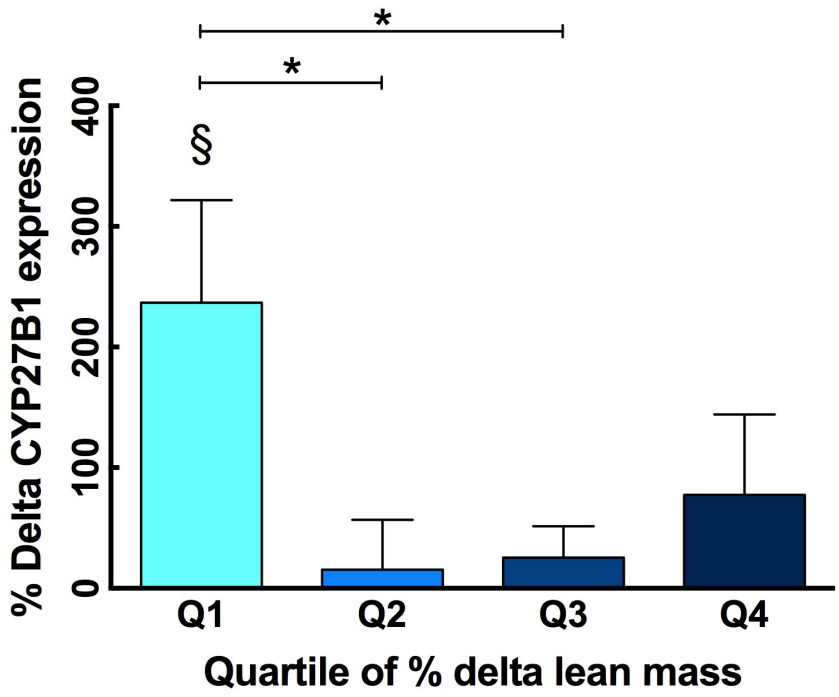


Figure 5.15 CYP27B1 mRNA expression change

CYP27B1 mRNA % Delta expression presented in lean mass change quartiles, Values are means ±SEM, n=37. Statistical analysis via t-test, * $p<0.05$ between quartile groups, § $p<0.05$ between pre and post training in that quartile.

5.4.5.3 CYP27B1, lean mass and VDR changes

There was no correlation between CYP27B1 mRNA expression and lean mass changes in response to training. CYP27B1 is under transcriptional regulation of VDR, with a positive correlation between the two observed (Figure 5.16).

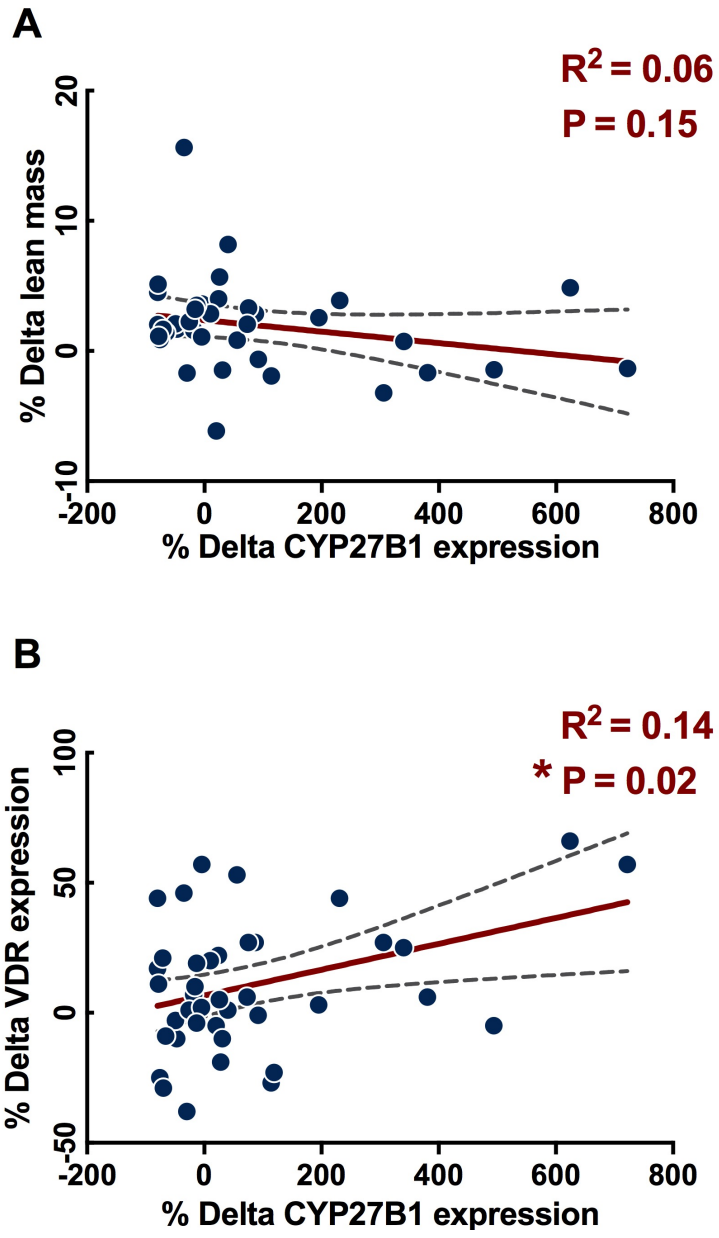


Figure 5.16 CYP27B1, lean mass and VDR correlations

(**A**) Correlation between CYP27B1 mRNA expression and lean mass changes, (**B**) CYP27B1 and VDR mRNA expression changes in response to 20-weeks whole-body resistance training. Statistical analysis via Pearson's correlation, n=37. Dotted lines refer to the 95%CI.

5.4.6 CYP24A1 mRNA expression

5.4.6.1 Pre and post training

Grouped into lean mass quartiles, there were no significant differences between groups pre-training. Post training Q3 was significantly greater than Q1 (Q3: 35.8±5.6 AU vs. Q1: 19.5±4.3, $p<0.05$) (Figure 5.17).

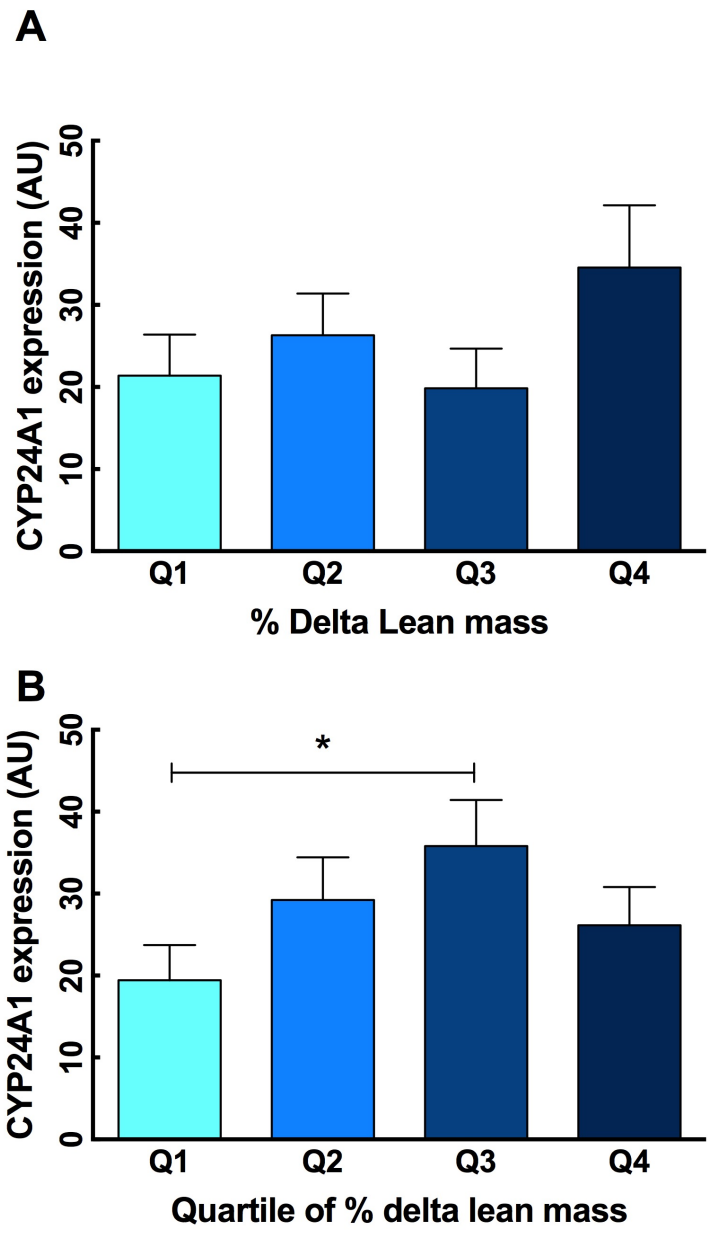


Figure 5.17 CYP24A1 expression pre and post training

CYP24A1 mRNA expression presented in lean mass change quartiles, (**A**) pre and (**B**) post-training. Values are means ±SEM, n=37. Statistical analysis via t-test, * $p<0.05$.

5.4.6.2 CYP24A1 mRNA expression change

CYP24A1 expression changes were not significantly different between quartiles, however Q3 expression showed significantly greater expression compared to pre-training levels (+284±128%, $p<0.05$) (Figure 5.18).

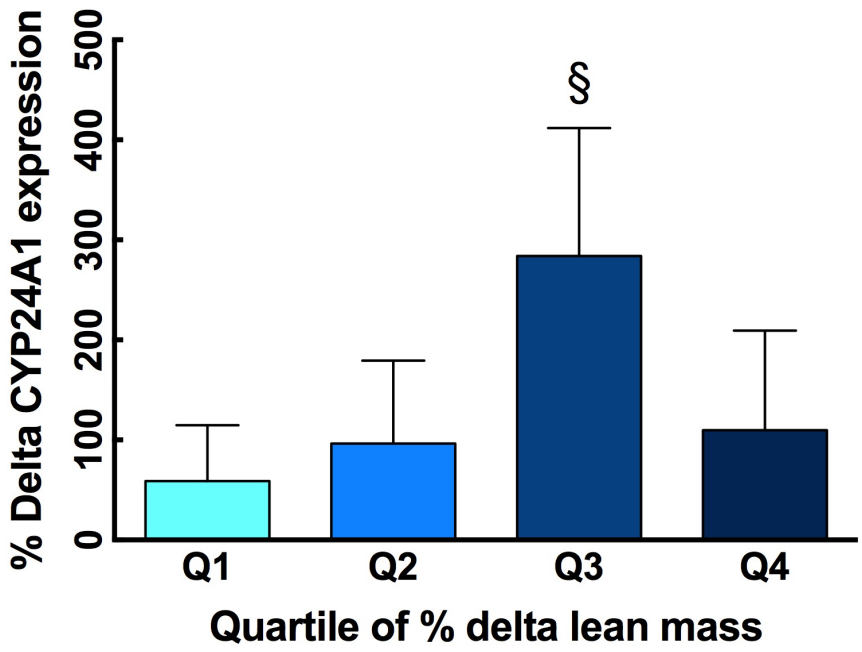


Figure 5.18 CYP24A1 expression change

CYP24A1 mRNA % Delta expression presented in lean mass change quartiles, Values are means ±SEM, n=37. Statistical analysis via t-test, § $p<0.05$ between pre and post training in that quartile.

5.4.6.3 CYP24A1, lean mass and VDR changes

There was no correlation between CYP24A1 mRNA expression and lean mass changes in response to training. Additionally, there was no association between CYP24A1 or VDR mRNA expression changes (Figure 5.19).

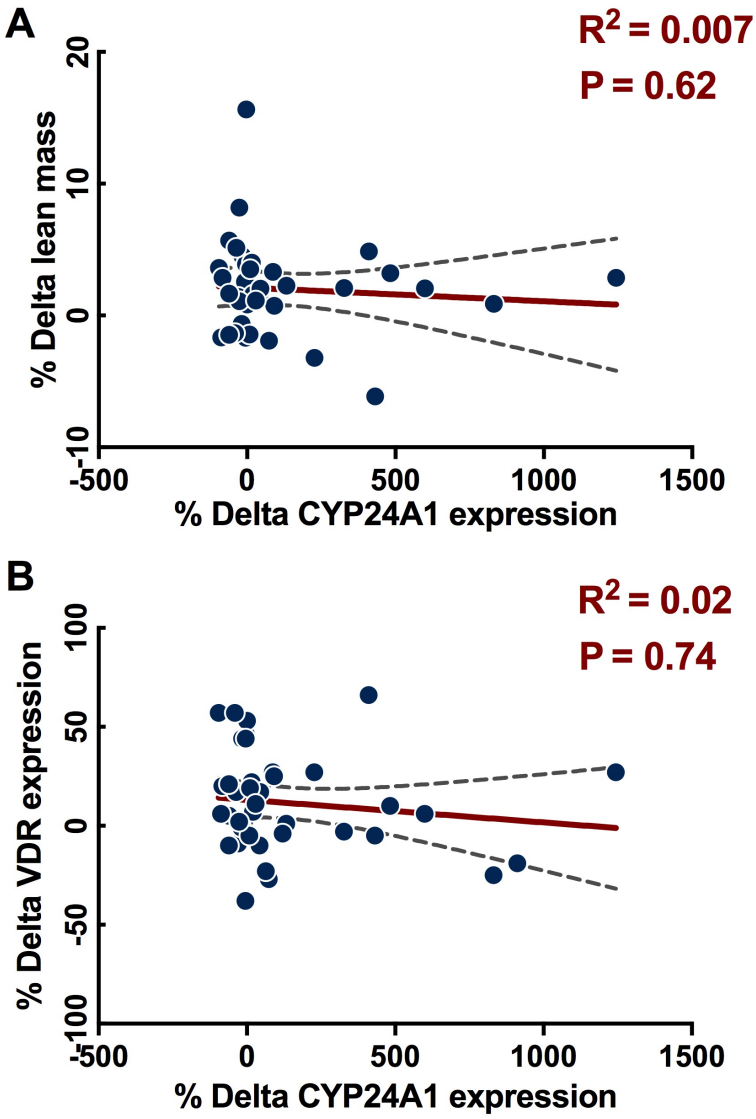


Figure 5.19 CYP24A1, lean mass and VDR correlations

(**A**) Correlation between CYP24A1 expression and lean mass changes, (**B**) CYP24A1 and VDR expression changes in response to 20-weeks whole-body resistance training. Statistical analysis via Pearson's correlation, n=37. Dotted lines refer to the 95%CI.

5.4.7 HOMA-IR analysis

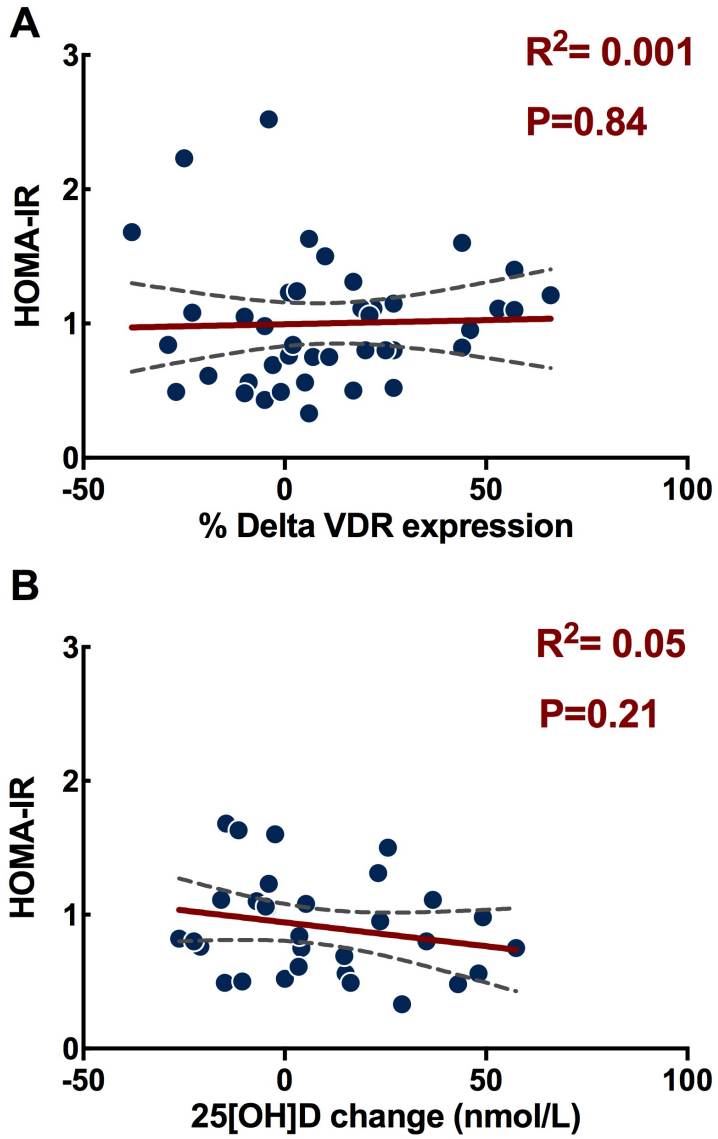


Figure 5.20 HOMA-IR, VDR expression and 25[OH]D correlations

(**A**) Correlation between HOMA-IR post training and VDR mRNA expression changes, (**B**) HOMA-IR and 25[OH]D level changes in response to 20-weeks whole-body resistance training. Statistical analysis via Pearson's correlation, n=37. Dotted lines refer to the 95%CI.

5.5 Discussion

The aim of the current study was to characterise VDR expression and VitD status in response to a program of resistance exercise training, giving clinical relevance to previously discussed findings. It was hypothesized VitD status and VDR expression in skeletal muscle would be modulated in response to exercise. VDR expression has been demonstrated in human skeletal muscle (Hamilton 2010), with expression shown to increase acutely in response to resistance exercise in rats (Makanae et al. 2015). Previous VitD supplemental RCTs have not investigated VDR expression when reporting skeletal muscle changes. Thus, whilst VDR expression may be an essential part in VitD mediated effects, and have additional autonomous functions, the expression and role of the VDR is currently unclear. This study demonstrates genuine implications for maintenance of muscle health, with VDR expression rather than VitD status positively associated in the response to resistance training in humans.

In order to determine the clinical relevance of the VDR upon skeletal muscle mass, VDR expression was measured in humans in response to muscle hypertrophy-inducing resistance exercise training (RET) (Phillips et al. 2013). Participants were 18-75 y and underwent 20 weeks of whole-body resistance exercise training, with body composition measures assessed by dual energy X-ray absorptiometry (DEXA) pre/ post RET. Additionally VDR gene expression was collected from microarray data of skeletal muscle biopsy samples pre/post RET. Subjects were grouped into quartiles based on their lean mass changes in response to RET.

Initially, VDR expression pre and post RET was investigated between quartile groups. Pre training expression remained unchanged between

groups, however post training demonstrated high responding Q3 and Q4 were significantly greater than low responder Q1. Indeed, to fully appreciate this relationship, quartiles of lean mass changes were plotted; demonstrating high responders to exercise showed the greatest increase in VDR expression. Interestingly low responders did not increase VDR expression post RET. Moreover, changes in VDR expression were positively correlated with lean mass changes. The data suggests that an individuals 'responder status' to resistance exercise may be partially modulated by VDR expression, supporting the notion of the VDR acting as an anabolic capacitor within skeletal muscle.

Previous investigations have demonstrated associations between VDR polymorphism genotypes and muscle strength in multiple populations (Bozsodi et al. 2016; Windelinckx et al. 2007; Bahat et al. 2010), supporting the concept of the VDR modulating muscle mass. However, these studies did not investigate the effect VDR expression or genotype had upon muscle mass/ strength changes in response to exercise. Interestingly one study uniquely demonstrated that skeletal muscle VDR protein expression immediately increased in response to acute resistance exercise in rats (Makanae et al. 2015). Furthermore, another study saw a moderate increase in VDR expression 48h after RET in young adults (Agergaard et al. 2015). However, this increase was not significant, potentially due to the relatively small sample size (n=10). The data support those previous findings, establishing that expression of the VDR may remain elevated past the initial exercise stimulus. Whether this higher expression continues past the training regime or the influence genotype upon responder status has yet to be determined.

The potential role(s) VitD status has upon skeletal muscle is currently still ambiguous, as some studies and meta-analysis have concluded VitD status positively correlates with muscle mass and strength (Kobza et al. 2013; Dhanwal et al. 2013; Beaudart et al. 2014; Tomlinson et al. 2015), whilst others have observed no effect (Rosendahl-Riise et al. 2016). These aspects were investigated within this study. VitD status was unchanged between groups pre-RET, but was increased in Q1 post RET. However, these changes in VitD status were not associated with lean mass response. Despite the regulation of VDR expression by VitD, no correlations were observed between plasma VitD levels and VDR expression either pre or post RET. As such, modulation of VDR expression was likely to not be in response to change in VitD status, rather the response to RET. VitD synthesis occurs primarily between March-October (Kimlin et al. 2007); however these studies were undertaken throughout the year, thus seasonal variance in VitD metabolism would not have influenced one particular group. The impact of VitD status upon muscle function is still ambiguous, with some studies reporting a positive association between VitD and physical performance (Wicherts et al. 2007; Barker et al. 2013), while others observe none (Ring et al. 2010). It is likely that VitD status alone may not regulate muscle function, rather requiring sufficient VDR expression, as previously observed. These results indicate basal plasma VitD status is disconnected from RET induced changes in muscle mass and VDR expression. This possibly explains the ambiguity seen within some VitD supplemental studies as often VDR expression is often unmeasured (Close, Russell, et al. 2013; Trial et al. 2015). However, these measures do not inform the influence VitD supplementation may have upon muscle mass or function and requires further investigation.

Previous investigations have established the expression of VitD metabolizing enzymes CYP27B1 and CYP24A1 within cultured myotubes and developed mouse muscle (Srikuea & Hirunsai 2016)(Srikuea et al. 2012). Indeed, administration of inactive 25[OH]D_3 to myoblasts, was shown to increase VDR expression to a similar degree as active 1α,25[OH]$_2D_3$. Additionally, siRNA-mediated knockdown of CYP27B1 removed the observed anti-proliferative influence of 25[OH]D_3 indicating muscle as active target of VitD metabolism (Srikuea et al. 2012). Despite no influence of plasma VitD status upon muscle mass, changes in the expression of CYP27B1 displayed a positive correlation with increased VDR expression. Interestingly, pre RET, CYP27B1 expression was reduced within Q1, increasing expression in response to RET to levels similar to other quartiles. This suggests that in response to RET, local VitD metabolism was enhanced in Q1. Furthermore, changes in the expression of VitD inactivating CYP24A1 was not associated with either lean mass or VDR expression changes. However, expression within Q3 increased post RET, the change in expression was not significantly different compared to that of the other quartiles. This is due to two participants with abnormally high post RET expression values. Thus, the data suggests local inactivation of VitD was not drastically altered in response to RET.

Combined these results suggest VDR expression rather than VitD status modulates response to RET. Moreover, in response to RET, VitD sensitivity in skeletal muscle is augmented; collectively enhancing local 1α,25[OH]$_2D_3$ metabolism through amplified CYP27B1 expression. Nonetheless, local metabolism of 1α,25[OH]$_2D_3$ by CYP27B1 have yet to be established.

Finally, previous studies and meta-analysis, have proposed VitD may have a role within T2D and glucose metabolism, enhancing glucose transport (Pittas et al. 2007). Investigations have observed inverse correlations between plasma 25[OH]D and HOMA-IR measures, within large (n=805) observational studies in non-diabetic elderly adults (Liu et al. 2009). Additional studies have displayed similar HOMA-IR correlations in adults at risk of developing T2D (n=712) (Kayaniyil et al. 2010). These correlative analysise in humans determined no relation between changes in VitD status and HOMA-IR. It is important to note that previous studies investigated the role of VitD status upon insulin resistance within specific populations and age groups, without undertaking RET. Within this study a range of healthy non-obese participants were utilised. Confounding variables that weren't required to be controlled in the original study, such as body adiposity and varying degrees of diet and recreational activity may have influenced HOMA-IR measures greater than VitD status.

Furthermore, in chapter 4 it was demonstrated neither the knockdown nor over-expression of the VDR influenced skeletal muscle glucose uptake or glycogen content. Indeed, a previous study investigating pancreatic function using whole-body VDR knockout, determined glucose stimulated insulin levels were considerably decreased by VDR knockout (Zeitz et al. 2003). This augments our findings, suggesting that if VitD/VDR does indeed have a role within glucose metabolism, it may reside within pancreatic insulin secretion rather than glucose uptake in skeletal muscle.

5.6 Conclusion

To summarize, the study presented demonstrates VDR expression correlates with exercise-induced hypertrophy in humans. Moreover, observations of VDR expression tracking with lean mass increases from RET, further support the notion that the VDR has an autonomous functional role within muscle metabolism. Interestingly similar to other investigations (Ring et al. 2010), no relationship between VitD status and response to RET was observed, suggesting VitD status alone may not regulate muscle function, further purporting the role of the VDR. Finally, matching earlier observations, neither VDR expression nor VitD status correlated with measures of insulin resistance. These results however do not rule out a role within glucose metabolism as VitD deficiency and/or supplementation may influence insulin section. In conclusion, these results demonstrate an essential aspect of the VDR expression within muscle protein metabolism, with genuine implications for maintenance of muscle health.

Chapter 6 – Discussion and Overview

This thesis aimed to define the mechanistic role the VDR has within skeletal muscle metabolism and health, presenting the implications VDR expression has upon muscle growth in humans.

VitD deficiency is highly prevalent in multiple populations throughout the world; including those in northern latitudes along with more equatorial ones. The influence of VitD deficiency upon bone metabolism and health is well documented to be involved in the development of osteomalacia and modulation of calcium homeostasis. Increasingly, VitD deficiency has been associated with the development and progression of sarcopenia in the elderly. Furthermore, sarcopenia and the associated loss of muscle function is a growing concern for the healthcare system as the number of individuals requiring care is increasing due the loss of mobility. VitD supplementation has been demonstrated to have beneficial effects upon muscle growth and function. However, there are conflicting reports of the benefit it may have. Indeed, it is likely that any potential benefits supplementation has will be upon those who are already deficient. Thus, a greater understanding into the role VitD may have within the regulation of skeletal muscle mass and function is of importance.

VitD acts through and mediates the VDR, regulates the transcription of multiple VitD responsive genes, but has additionally been implicated in rapid non-transcriptional signalling. Although originally contentious, expression of the VDR has been confirmed within skeletal muscle. Moreover, the VDR is proposed to have autonomous functions within skeletal muscle, however the role and mechanism of these are unclear.

The identification that *in vitro*, loss of the VDR impairs myoblast proliferation demonstrates an autonomous role of the VDR, separate from the influence of VitD stimulation. These findings heighten previous studies demonstrating a role of the VDR within cell cycle progression, specifically G0/G1 progression, clarifying differences seen in different culturing conditions. Furthermore, this study has illuminated the pro differentiation role the receptor has, as loss of the receptor impairs differentiation through reduced synthetic capacity, MPS and continual myoblast proliferation. Nevertheless, the disconnect between anabolic signalling and MPS measures requires further investigation into whether this may be due to changes in pathway flux. However, the role VDR may have within fully developed muscle cannot be determined through *in vitro* methods due to the nature of the model and VDR-KD induced myogenic dysregulation. As *in vitro* models are removed from normal physiological conditions (e.g. hormonal responses) investigations utilising in vivo models was certainly required.

Currently, little is understood about the mechanism of action the VDR may have within skeletal muscle. Previous investigations have attempted to investigate this role through the use of whole-body knockout models. However, such models are ensued by developmental dysregulation and require rescue diets to normalize blood mineral ion levels. Thus, these factors have precluded the identification of the role VDR may have within muscle. Demonstration that loss of the VDR within developed muscle induced fibre atrophy, confirms a role in skeletal muscle separate from calcium homeostasis and myogenesis. Furthermore, atrophy occurred not through a blunting of MPS, but rather through increased autophagy mediated MPB. It is important to note the apparent contrast between MPS

data within the *in vitro* and *in vivo* studies. This may be rationalized as VDR-KD eliciting an anti-differentiation phenotype in an *in vitro* model, whereas this influence is negated in developed muscle. The data provide context to previous to previous investigations demonstrating muscle atrophy in VDR-KO models (Endo et al. 2003; Girgis et al. 2015) and VitD deficient individuals (Scott et al. 2010). Thus, providing mechanistic insight into how this previously observed phenotype is achieved. Such observations have implications upon the regulation of skeletal muscle function in the elderly, as loss of the VDR has been associated with age (Bischoff-Ferrari, Borchers, et al. 2004). Thus, VDR expression may be involved in sarcopenic development and associated VitD deficiency. However, no further studies have investigated VDR expression within elderly populations.

Conversely, this study demonstrated increased VDR expression resulted in muscle fibre hypertrophy, increasing total protein content. Indeed, this data suggests VDR expression exerts a pro-growth stimulus, engaging a response similar to that during muscle regeneration. Incidentally, this occurred by increased rates of MPS through enhanced translational efficiency and ribosomal biogenesis. Furthermore, satellite cell activity was increased, providing additional myonuclei, available for hypertrophic growth. The data clarify potential anabolic effects of VitD seen within cell culture models (Salles et al. 2013), along with fibre hypertrophy observed from VitD supplementation (Ceglia et al. 2013), suggesting the VDR is an essential anabolic capacitor. Collectively, the data imply a truly mechanistic role of the VDR as an essential aspect of muscle protein metabolism.

The use of IVE techniques to bi-directionally modulate VDR expression within established muscle is of great novelty and removes the major limitations whole-body knockout models possess (i.e. developmental dysregulation and mineral ion dysregulation). Furthermore, as each animal acted as its own unilateral control direct comparisons could be made and the subsequent number of animals requires was reduced. Additionally, through both knocking down and over-expressing VDR producing reciprocal effects (i.e. fibre atrophy and hypertrophy), the validity of the findings is greater.

However, a significant caveat with the current *in vivo* studies is the limiting factor of a single time point available after IVE. An earlier measure would allow for temporal comparisons between fibre CSAs and satellite cell content to be made. This would elucidate whether VDR-KD induced atrophy was due to a halt in growth or reduction in fibre CSA. It would also be pertinent to investigate the impact VDR-OE a mediated increase in anabolic capacity has upon adaptations to resistance exercise or feeding. In doing so, this will give further insight into the mechanistic role VDR has within skeletal muscle. Another caveat within the *in vivo* investigations was the necessity for utilising younger animals instead of older adult ones. This would have informed upon the role the VDR has within muscles that are not actively growing.

Finally, while *in vitro* and *in vivo* investigations have discerned potential mechanistic roles of the VDR, the establishment of relevance within human population is required. This study observed VDR expression tracking with lean mass increases from RET, further supporting the notion that the VDR has an autonomous function within muscle metabolism. Importantly, this

provides genuine implications for VDR modulation in human skeletal muscle. Furthermore, loss of VDR expression in elderly muscle may be a contributing factor to sarcopenic development and VitD associated muscle weakness. Interestingly similar to other investigations (Ring et al. 2010), no relationship between VitD status and response to RET was observed, suggesting VitD status alone may not regulate muscle function, further purporting the role of the VDR. However, this study does not give insight into the potential benefits of VitD supplementation upon skeletal muscle function. Further investigations should be undertaken to determine whether loss of the receptor in age changes skeletal muscle VitD sensitivity and whether supplementation may rescue the loss of VDR.

Collectively, these findings demonstrate a clear role of the VDR within multiple aspects of regulating muscle mass, through modulation of myogenesis and protein metabolism. Previous investigations have demonstrated potential anabolic effects of VitD (Salles et al. 2013), however the mechanisms by which this occurs was unclear. These findings establish the necessity of the VDR for correct myogenic development and regulation of protein metabolism through modulation of anabolic/ catabolic mechanisms. Furthermore, these findings establish that expression of the VDR is modulated by exercise in a 'responder' status manner. Therefore, through exercise enhanced expression, the VDR increases anabolic capacity and subsequent protein metabolism. The implication of such modulation may explain age-related anabolic resistance exercise (Brook et al. 2016), as VDR expression in muscle has been shown to be reduced (Bischoff-Ferrari, Borchers, et al. 2004).

These findings provide context for further investigations to proceed. As it has been established VDR modulates anabolic/ catabolic signalling and resultant protein metabolism, it would be pertinent to investigate the role it may have within various disease states (e.g. cachexia) that impact muscle mass. Such investigations may provide insight into how these conditions may influence muscle protein metabolism and offer potential therapeutic targets. Additionally, as resistance exercise increases VDR expression, investigations into this mechanism may, as previously discussed clarify age-related anabolic blunting. Finally, the role VitD supplementation requires further infestation, specifically whether VDR expression is influenced by supplementation. Such inquiries would elucidate the role VDR/VitD has upon muscle, and crucially determine whether it is involved within disease states influencing muscle mass.

In conclusion, the findings of the present study provide insight into the dual nature of VDR expression upon muscle metabolism; highlighting a gain and loss of function of VDR causing hypertrophy and atrophy, respectively in rats. Furthermore, VDR expression correlates with exercise-induced hypertrophy in humans. The data imply a truly mechanistic role of the VDR as an essential aspect of muscle protein metabolism, with genuine implications for the maintenance of muscle health.

References

van ’t Riet, E. et al., 2010. Relationship between A1C and glucose levels in the general Dutch population: the new Hoorn study. *Diabetes care*, 33(1), pp.61–6.

Abboud, M. et al., 2013. Evidence for a specific uptake and retention mechanism for 25-hydroxyvitamin D (25OHD) in skeletal muscle cells. *Endocrinology*, 154(9), pp.3022–30.

Abou-Sleiman, P.M., Muqit, M.M.K. & Wood, N.W., 2006. Expanding insights of mitochondrial dysfunction in Parkinson’s disease. *Nature reviews. Neuroscience*, 7(3), pp.207–19.

Adams, J.S. & Gacad, M.A., 1985. Characterization of 1 alpha-hydroxylation of vitamin D3 sterols by cultured alveolar macrophages from patients with sarcoidosis. *The Journal of experimental medicine*, 161(4), pp.755–65.

Agergaard, J. et al., 2015. Does vitamin-D intake during resistance training improve the skeletal muscle hypertrophic and strength response in young and elderly men? – a randomized controlled trial. *Nutrition & Metabolism*, 12(1), p.32.

Aksoy, H. et al., 2000. Serum 1,25 dihydroxy vitamin D (1,25(OH)2D3), 25 hydroxy vitamin D (25(OH)D) and parathormone levels in diabetic retinopathy. *Clinical biochemistry*, 33(1), pp.47–51.

Amling, M. et al., 1999. Rescue of the skeletal phenotype of vitamin D receptor-ablated mice in the setting of normal mineral ion homeostasis: formal histomorphometric and biomechanical analyses. *Endocrinology*, 140(11), pp.4982–7.

Anderson, P.H. et al., 2010. Bone CYP27B1 gene expression is increased with high dietary calcium and in mineralising osteoblasts. *Journal of Steroid Biochemistry and Molecular Biology*, 121(1–2), pp.71–75.

Anderson, P.H. et al., 2008. Co-expression of CYP27B1 enzyme with the 1.5kb CYP27B1 promoter-luciferase transgene in the mouse. *Molecular and cellular endocrinology*, 285(1–2), pp.1–9.

Andres, V. & Walsh, K., 1996. Myogenin expression, cell cycle withdrawl, and phenotypic differentiation are temproarily seperable events that

precede cell fusion upon myogenesis. *Journal of Cell Biology*, 132(4), pp.657–666.

Andrés, V. & Walsh, K., 1996. Myogenin expression, cell cycle withdrawal, and phenotypic differentiation are temporally separable events that precede cell fusion upon myogenesis. *Journal of Cell Biology*, 132(4), pp.657–666.

Artaza, J.N. et al., 2010. 1,25(OH)2vitamin D3 inhibits cell proliferation by promoting cell cycle arrest without inducing apoptosis and modifies cell morphology of mesenchymal multipotent cells. *The Journal of steroid biochemistry and molecular biology*, 119(1–2), pp.73–83.

Arthur W. Ham, M.D.L., 1934. Hypervitaminosis D Rickets: The Action of Vitamin D. *British Journal of Experimental Pathology*, 15(4), p.228.

Ashrafi, G. & Schwarz, T.L., 2013. The pathways of mitophagy for quality control and clearance of mitochondria. *Cell death and differentiation*, 20(1), pp.31–42.

Atherton, P.J., Smith, K., et al., 2010. Distinct anabolic signalling responses to amino acids in C2C12 skeletal muscle cells. *Amino acids*, 38(5), pp.1533–9.

Atherton, P.J., Etheridge, T., et al., 2010. Muscle full effect after oral protein: time-dependent concordance and discordance between human muscle protein synthesis and mTORC1 signaling. *The American journal of clinical nutrition*, 92(5), pp.1080–8.

Averous, J. et al., 2014. Requirement for lysosomal localization of mTOR for its activation differs between leucine and other amino acids. *Cellular Signalling*, 26(9), pp.1918–1927.

Baar, K. & Esser, K., 1999. Phosphorylation of p70 S6k correlates with increased skeletal muscle mass following resistance exercise Phosphorylation of p70 S6k correlates with increased skeletal muscle mass following resistance exercise. *Am H Physiol Cell Physiol*, pp.120–127.

Bahat, G. et al., 2010. BsmI polymorphism in the vitamin D receptor gene is associated with leg extensor muscle strength in elderly men. *Aging clinical and experimental research*, 22(3), pp.198–205.

Balkau, B. & Charles, M.A., 1999. Comment on the provisional report from the WHO consultation. European Group for the Study of Insulin

Resistance (EGIR). *Diabetic medicine : a journal of the British Diabetic Association*, 16(5), pp.442–3.

Bankolé, L.-C. et al., 2013. Fibre type-specific satellite cell content in two models of muscle disease. *Histopathology*, 63(6), pp.826–32.

Baracos, V.E. et al., 1995. Activation of the ATP-ubiquitin-proteasome pathway in skeletal muscle of cachectic rats bearing a hepatoma. *The American journal of physiology*, 268(5 Pt 1), pp.E996-1006.

Barchetta, I. et al., 2012. Liver vitamin D receptor, CYP2R1, and CYP27A1 expression: relationship with liver histology and vitamin D3 levels in patients with nonalcoholic steatohepatitis or hepatitis C virus. *Hepatology (Baltimore, Md.)*, 56(6), pp.2180–7.

Barker, T. et al., 2013. Higher Serum 25-Hydroxyvitamin D Concentrations Associate with a Faster Recovery of Skeletal Muscle Strength after Muscular Injury. *Nutrients*, 5(4), pp.1253–1275.

Baumeister, W. et al., 1998. The proteasome: paradigm of a self-compartmentalizing protease. *Cell*, 92(3), pp.367–80.

Beaudart, C. et al., 2014. The effects of vitamin D on skeletal muscle strength, muscle mass and muscle power: a systematic review and meta-analysis of randomized controlled trials. *The Journal of clinical endocrinology and metabolism*, (July), p.jc20141742.

Belcastro, a N., Shewchuk, L.D. & Raj, D. a, 1998. Exercise-induced muscle injury: a calpain hypothesis. *Molecular and cellular biochemistry*, 179(1–2), pp.135–45.

Belizário, J.E., Lorite, M.J. & Tisdale, M.J., 2001. Cleavage of caspases-1, -3, -6, -8 and -9 substrates by proteases in skeletal muscles from mice undergoing cancer cachexia. *British journal of cancer*, 84(8), pp.1135–40.

Bellido, T. et al., 1987. The phospholipid and fatty acid composition of skeletal muscle cells during culture in the presence of vitamin D-3 metabolites. *Biochimica et biophysica acta*, 922(2), pp.162–9.

Berger, U. et al., 1988. Immunocytochemical detection of 1,25-dihydroxyvitamin D receptors in normal human tissues. *The Journal of clinical endocrinology and metabolism*, 67(3), pp.607–13.

Bhan, A., Rao, A.D. & Rao, D.S., 2010. Osteomalacia as a result of vitamin D deficiency. *Endocrinology and metabolism clinics of North America*,

39(2), p.321–31, table of contents.

Bhat, M., Kalam, R., Syh Qadri, S., et al., 2013. Vitamin D deficiency-induced muscle wasting occurs through the ubiquitin proteasome pathway and is partially corrected by calcium in male rats. *Endocrinology*, 154(11), pp.4018–4029.

Bhat, M., Kalam, R., Qadri, S.S., et al., 2013. Vitamin D Deficiency Induced Muscle Wasting Occurs through the Ubiquitin Proteasome Pathway and Is Partially Corrected by Calcium in Male Rats. *Endocrinology*, (C), pp.1–12.

Bikle, D.D. et al., 1986. 1,25-Dihydroxyvitamin D3 production by human keratinocytes. Kinetics and regulation. *The Journal of clinical investigation*, 78(2), pp.557–66.

Bikle, D.D. et al., 1979. Work-induced muscle hypertrophy in vitamin D-deficient rats. *The American journal of clinical nutrition*, 32(3), pp.515–6.

Birge, S.J. & Haddad, J.G., 1975. 25-hydroxycholecalciferol stimulation of muscle metabolism. *The Journal of clinical investigation*, 56(5), pp.1100–7.

Bischoff-Ferrari, H.A., Dietrich, T., et al., 2004. Higher 25-hydroxyvitamin D concentrations are associated with better lower-extremity function in both active and inactive persons aged > or =60 y. *The American journal of clinical nutrition*, 80(3), pp.752–8.

Bischoff-Ferrari, H.A., Borchers, M., et al., 2004. Vitamin D receptor expression in human muscle tissue decreases with age. *Journal of bone and mineral research : the official journal of the American Society for Bone and Mineral Research*, 19(2), pp.265–269.

Bischoff-Ferrari, H.A., Orav, E.J. & Dawson-Hughes, B., 2006. Effect of cholecalciferol plus calcium on falling in ambulatory older men and women: a 3-year randomized controlled trial. *Archives of internal medicine*, 166(4), pp.424–30.

Bischoff, H.A. et al., 2003. Effects of vitamin D and calcium supplementation on falls: a randomized controlled trial. *Journal of bone and mineral research : the official journal of the American Society for Bone and Mineral Research*, 18(2), pp.343–51.

Blomberg Jensen, M., 2014. Vitamin D and male reproduction. *Nature*

reviews. Endocrinology, 10(3), pp.175–86.

Bodine, S.C. et al., 2001. Akt/mTOR pathway is a crucial regulator of skeletal muscle hypertrophy and can prevent muscle atrophy in vivo. *Nature cell biology*, 3(11), pp.1014–9.

Bohé, J. et al., 2003. Human muscle protein synthesis is modulated by extracellular, not intramuscular amino acid availability: a dose-response study. *The Journal of physiology*, 552(Pt 1), pp.315–24.

Bohé, J. et al., 2001. Latency and duration of stimulation of human muscle protein synthesis during continuous infusion of amino acids. *The Journal of physiology*, 532(Pt 2), pp.575–9.

de Boland, A.R. & Boland, R.L., 1987. Rapid changes in skeletal muscle calcium uptake induced in vitro by 1,25-dihydroxyvitamin D3 are suppressed by calcium channel blockers. *Endocrinology*, 120(5), pp.1858–64.

Bolland, M.J. et al., 2010. Vitamin D insufficiency and health outcomes over 5 y in older women. *The American journal of clinical nutrition*, 91(1), pp.82–89.

Bouillon, R. et al., 2008. Vitamin D and human health: lessons from vitamin D receptor null mice. *Endocrine reviews*, 29(6), pp.726–76.

Bouillon, R., Gielen, E. & Vanderschueren, D., 2014. Vitamin D Receptor and Vitamin D Action in Muscle. , 155(April), pp.3210–3213.

Bowman, L.H., Rabin, B. & Schlessinger, D., 1981. Multiple ribosomal RNA cleavage pathways in mammalian cells. *Nucleic acids research*, 9(19), pp.4951–66.

Bozsodi, A. et al., 2016. Muscle strength is associated with vitamin D receptor gene variants. *Journal of orthopaedic research : official publication of the Orthopaedic Research Society*, p.n/a-n/a.

Brenza, H.L. & DeLuca, H.F., 2000. Regulation of 25-hydroxyvitamin D3 1alpha-hydroxylase gene expression by parathyroid hormone and 1,25-dihydroxyvitamin D3. *Arch Biochem Biophys*, 381(1), pp.143–152.

Brook, M.S. et al., 2015. Skeletal muscle hypertrophy adaptations predominate in the early stages of resistance exercise training, matching deuterium oxide-derived measures of muscle protein synthesis and mechanistic target of rapamycin complex 1 signaling.

FASEB journal : official publication of the Federation of American Societies for Experimental Biology, 29(11), pp.4485–96.

Brook, M.S. et al., 2016. Synchronous deficits in cumulative muscle protein synthesis and ribosomal biogenesis underlie age-related anabolic resistance to exercise in humans. *The Journal of Physiology*, 0, pp.1–19.

Brooke, M.H. & Kaiser, K.K., 1970. Muscle fiber types: how many and what kind? *Archives of neurology*, 23(4), pp.369–79.

Brown, D.M., Parr, T. & Brameld, J.M., 2012. Myosin heavy chain mRNA isoforms are expressed in two distinct cohorts during C2C12 myogenesis. *Journal of muscle research and cell motility*, 32(6), pp.383–90.

Bryant, N.J., Govers, R. & James, D.E., 2002. Regulated transport of the glucose transporter GLUT4. *Nature Reviews Molecular Cell Biology*, 3(4), pp.267–277.

Buchebner, D. et al., 2014. Vitamin D insufficiency over 5 years is associated with increased fracture risk-an observational cohort study of elderly women. *Osteoporosis international : a journal established as result of cooperation between the European Foundation for Osteoporosis and the National Osteoporosis Foundation of the USA*.

Buitrago, C., Vazquez, G., et al., 2001. The vitamin D receptor mediates rapid changes in muscle protein tyrosine phosphorylation induced by 1,25(OH)(2)D(3). *Biochemical and biophysical research communications*, 289(5), pp.1150–6.

Buitrago, C. & Boland, R., 2010. Caveolae and caveolin-1 are implicated in 1alpha,25(OH)2-vitamin D3-dependent modulation of Src, MAPK cascades and VDR localization in skeletal muscle cells. *The Journal of steroid biochemistry and molecular biology*, 121(1–2), pp.169–75.

Buitrago, C., Boland, R. & de Boland, A., 2001. The tyrosine kinase c-Src is required for 1,25(OH)2-vitamin D3 signalling to the nucleus in muscle cells. *Biochimica et Biophysica Acta (BBA) - Molecular Cell Research*, 1541(3), pp.179–187.

Buitrago, C., Pardo, V.G. & Boland, R., 2013. Role of VDR in 1α,25-dihydroxyvitamin D3-dependent non-genomic activation of MAPKs, Src and Akt in skeletal muscle cells. *The Journal of steroid biochemistry*

and molecular biology, 136, pp.125–30.

Buitrago, C.G. et al., 2006. MAP kinases p38 and JNK are activated by the steroid hormone 1alpha,25(OH)2-vitamin D3 in the C2C12 muscle cell line. *Journal of cellular biochemistry*, 97(4), pp.698–708.

Buitrago, C.G., Arango, N.S. & Boland, R.L., 2012. 1α,25(OH)2D3-dependent modulation of Akt in proliferating and differentiating C2C12 skeletal muscle cells. *Journal of cellular biochemistry*, 113(4), pp.1170–81.

Campbell, F.C. et al., 2010. The yin and yang of vitamin D receptor (VDR) signaling in neoplastic progression: operational networks and tissue-specific growth control. *Biochemical pharmacology*, 79(1), pp.1–9.

Capiati, D.A., Téllez-Iñón, M.T. & Boland, R.L., 1999. Participation of protein kinase C alpha in 1,25-dihydroxy-vitamin D3 regulation of chick myoblast proliferation and differentiation. *Molecular and cellular endocrinology*, 153(1–2), pp.39–45.

Carrillo, A.E. et al., 2013. Impact of vitamin D supplementation during a resistance training intervention on body composition , muscle function , and glucose tolerance in overweight and obese adults q. *Clinical Nutrition*, 32(3), pp.375–381.

Cashman, K.D. et al., 2013. Evaluation of Vitamin D Standardization Program protocols for standardizing serum 25-hydroxyvitamin D data: a case study of the program's potential for national nutrition and health surveys. *The American journal of clinical nutrition*, 97(6), pp.1235–42.

Cashman, K.D. et al., 2015. Standardizing serum 25-hydroxyvitamin D data from four Nordic population samples using the Vitamin D Standardization Program protocols: Shedding new light on vitamin D status in Nordic individuals. *Scandinavian journal of clinical and laboratory investigation*, 75(7), pp.549–61.

Cashman, K.D. et al., 2016. Vitamin D deficiency in Europe: pandemic? *The American journal of clinical nutrition*, 103(4), pp.1033–44.

Castellani, R. et al., 2002. Role of mitochondrial dysfunction in Alzheimer's disease. *Journal of neuroscience research*, 70(3), pp.357–60.

Cavalcante, R. et al., 2015. The effects of intermittent vitamin D3 supplementation on muscle strength and metabolic parameters in

postmenopausal women with type 2 diabetes : a randomized controlled study. , pp.149–154.

Ceglia, L. et al., 2013. A Randomized Study on the Effect of Vitamin D 3 Supplementation on Skeletal Muscle Morphology and Vitamin D Receptor Concentration in Older Women. *The Journal of Clinical Endocrinology & Metabolism*, 98(12), pp.E1927–E1935.

Chaillou, T., Kirby, T.J. & Mccarthy, J.J., 2014. Ribosome Biogenesis: Emerging Evidence for a Central Role in the Regulation of Skeletal Muscle Mass. *Journal of Cellular Physiology*, 229(11), pp.1584–1594.

Cheng, J.J.B.J. et al., 2004. Genetic evidence that the human CYP2R1 enzyme is a key vitamin D 25-hydroxylase. *Proceedings of the National Academy of Sciences of the United States of America*, 101(20), pp.7711–7715.

Cheskis, B. & Freedman, L.P., 1994. Ligand modulates the conversion of DNA-bound vitamin D3 receptor (VDR) homodimers into VDR-retinoid X receptor heterodimers. *Molecular and cellular biology*, 14(5), pp.3329–3338.

Chiba, N. et al., 2000. Binding of liganded vitamin D receptor to the vitamin D receptor interacting protein coactivator complex induces interaction with RNA polymerase II holoenzyme. *Journal of Biological Chemistry*, 275(15), pp.10719–10722.

Clemens, T.L. et al., 1988. Immunocytochemical localization of the 1,25-dihydroxyvitamin D3 receptor in target cells. *Endocrinology*, 122(4), pp.1224–30.

Close, G.L., Russell, J., et al., 2013. Assessment of vitamin D concentration in non-supplemented professional athletes and healthy adults during the winter months in the UK: implications for skeletal muscle function. *Journal of Sports Sciences*, 31(4), pp.344–353.

Close, G.L., Leckey, J., et al., 2013. The effects of vitamin D 3 supplementation on serum total 25[OH]D concentration and physical performance : a randomised dose – response study. , pp.692–696.

Cohn, S.H. et al., 1980. Compartmental body composition based on total-body nitrogen, potassium, and calcium. *The American journal of physiology*, 239(6), pp.E524-30.

Collins, C. a et al., 2007. A population of myogenic stem cells that survives

skeletal muscle aging. *Stem cells (Dayton, Ohio)*, 25(4), pp.885–94.

Crossland, H. et al., 2013. Focal adhesion kinase is required for IGF-I-mediated growth of skeletal muscle cells via a TSC2/mTOR/S6K1-associated pathway. *American journal of physiology. Endocrinology and metabolism*, 305(2), pp.E183-93.

Cuthbertson, D. et al., 2005. Anabolic signaling deficits underlie amino acid resistance of wasting, aging muscle. *The FASEB journal : official publication of the Federation of American Societies for Experimental Biology*, 19(3), pp.422–424.

Dahlmann, B., Rutschmann, M. & Reinauer, H., 1986. Effect of starvation or treatment with corticosterone on the amount of easily releasable myofilaments in rat skeletal muscles. *The Biochemical journal*, 234(3), pp.659–64.

Debigaré, R. & Price, S.R., 2003. Proteolysis, the ubiquitin-proteasome system, and renal diseases. *American journal of physiology. Renal physiology*, 285(1), pp.F1-8.

DeLuca, H.F. & Schnoes, H.K., 1983. Vitamin D: recent advances. *Annual review of biochemistry*, 52, pp.411–39.

Demay, M.B. et al., 1992. Sequences in the human parathyroid hormone gene that bind the 1,25-dihydroxyvitamin D3 receptor and mediate transcriptional repression in response to 1,25-dihydroxyvitamin D3. *Proceedings of the National Academy of Sciences of the United States of America*, 89(17), pp.8097–101.

Dennis, M.D., Jefferson, L.S. & Kimball, S.R., 2012. Role of p70S6K1-mediated phosphorylation of eIF4B and PDCD4 proteins in the regulation of protein synthesis. *The Journal of biological chemistry*, 287(51), pp.42890–9.

Deschenes, M.R., 2004. Effects of Aging on Muscle Fibre Type and Size. *Sports Medicine*, 34(12), pp.809–824.

Deval, C. et al., 2001. Identification of cathepsin L as a differentially expressed message associated with skeletal muscle wasting. *The Biochemical journal*, 360(Pt 1), pp.143–50.

Dhanwal, D.K. et al., 2013. Hand grip strength and its correlation with vitamin D in Indian patients with hip fracture. *Archives of osteoporosis*, 8(1–2), p.158.

Dickinson, J.M. et al., 2011. Mammalian target of rapamycin complex 1 activation is required for the stimulation of human skeletal muscle protein synthesis by essential amino acids. *The Journal of nutrition*, 141(5), pp.856–62.

Dorrens, J. & Rennie, M.J., 2003. Effects of ageing and human whole body and muscle protein turnover. *Scandinavian journal of medicine & science in sports*, 13(1), pp.26–33.

Dreyer, H.C. et al., 2006. Resistance exercise increases AMPK activity and reduces 4E-BP1 phosphorylation and protein synthesis in human skeletal muscle. *The Journal of physiology*, 576(Pt 2), pp.613–24.

Drittanti, L., de Boland, A.R. & Boland, R., 1989a. Modulation of DNA synthesis in cultured muscle cells by 1,25-dihydroxyvitamin D-3. *Biochimica et Biophysica Acta (BBA) - Molecular Cell Research*, 1014(2), pp.112–119.

Drittanti, L., de Boland, A.R. & Boland, R., 1989b. Modulation of DNA synthesis in cultured muscle cells by 1,25-dihydroxyvitamin D-3. *Biochimica et biophysica acta*, 1014(2), pp.112–9.

Du, J. et al., 2004. Activation of caspase-3 is an initial step triggering accelerated muscle proteolysis in catabolic conditions. *The Journal of clinical investigation*, 113(1), pp.115–23.

Endo, I. et al., 2003. Deletion of vitamin D receptor gene in mice results in abnormal skeletal muscle development with deregulated expression of myoregulatory transcription factors. *Endocrinology*, 144(12), pp.5138–44.

Forrest, K.Y.Z. & Stuhldreher, W.L., 2011. Prevalence and correlates of vitamin D deficiency in US adults. *Nutrition Research*, 31(1), pp.48–54.

Freedman, L.P. et al., 1999. Ligand-dependent transcription activation by nuclear receptors requiresthe DRIP complex. *Nature*, 398(6730), pp.824–828.

Freedman, L.P., 1999. Transcriptional targets of the vitamin D3 receptor-mediating cell cycle arrest and differentiation. *The Journal of nutrition*, 129(2S Suppl), p.581S–586S.

Fujita, S. et al., 2009. Essential amino acid and carbohydrate ingestion before resistance exercise does not enhance postexercise muscle

protein synthesis. *Journal of applied physiology (Bethesda, Md. : 1985)*, 106(5), pp.1730–9.

Fukumoto, S., 2014. Phosphate metabolism and vitamin D. *BoneKEy reports*, 3(February), p.497.

Furuno, K. & Goldberg, a L., 1986. The activation of protein degradation in muscle by Ca2+ or muscle injury does not involve a lysosomal mechanism. *The Biochemical journal*, 237(3), pp.859–64.

Furuno, K., Goodman, M.N. & Goldberg, A.L., 1990. Role of different proteolytic systems in the degradation of muscle proteins during denervation atrophy. *The Journal of biological chemistry*, 265(15), pp.8550–7.

Garcia, L. a et al., 2012. 1,25(OH)2vitamin D3 enhances myogenic differentiation by modulating the expression of key angiogenic growth factors and angiogenic inhibitors in C2C12 skeletal muscle cells. *Journal of Steroid Biochemistry and Molecular Biology*, 133(1), pp.1–11.

Garcia, L. a et al., 2011. 1,25(OH)2vitamin D3 stimulates myogenic differentiation by inhibiting cell proliferation and modulating the expression of promyogenic growth factors and myostatin in C2C12 skeletal muscle cells. *Endocrinology*, 152(8), pp.2976–86.

Gasier, H.G., Fluckey, J.D. & Previs, S.F., 2010. The application of 2H2O to measure skeletal muscle protein synthesis. *Nutrition & metabolism*, 7, p.31.

Gibson, J.N. et al., 1987. Decrease in human quadriceps muscle protein turnover consequent upon leg immobilization. *Clinical science (London, England : 1979)*, 72(4), pp.503–9.

Gingras, a C., Raught, B. & Sonenberg, N., 2001. Regulation of translation initiation by FRAP/mTOR. *Genes & development*, 15(7), pp.807–26.

Girgis, C.M. et al., 2012. The Roles of Vitamin D in Skeletal Muscle: Form, Function, and Metabolism. *Endocrine reviews*, 34(February), pp.1–51.

Girgis, C.M., Mokbel, N., et al., 2014. The vitamin D receptor (VDR) is expressed in skeletal muscle of male mice and modulates 25-hydroxyvitamin D (25OHD) uptake in myofibers. *Endocrinology*, 155(9), pp.3227–37.

Girgis, C.M. et al., 2015. Vitamin D Receptor Ablation and Vitamin D

Deficiency Result in Reduced Grip Strength, Altered Muscle Fibers, and Increased Myostatin in Mice. *Calcified tissue international*, 97(6), pp.602–10.

Girgis, C.M., Clifton-Bligh, R.J., et al., 2014. Vitamin D signaling regulates proliferation, differentiation, and myotube size in C2C12 skeletal muscle cells. *Endocrinology*, 155(2), pp.347–57.

Glickman, M.H. & Ciechanover, A., 2002. The ubiquitin-proteasome proteolytic pathway: destruction for the sake of construction. *Physiological reviews*, 82(2), pp.373–428.

Glover, E.I. et al., 2008. Immobilization induces anabolic resistance in human myofibrillar protein synthesis with low and high dose amino acid infusion. *The Journal of physiology*, 586(Pt 24), pp.6049–61.

Goldspink, D.F. et al., 1995. Muscle growth in response to mechanical stimuli. *The American journal of physiology*, 268(2 Pt 1), pp.E288–E297.

Goldstein, M.S. et al., 1953. Action of Muscular Work on Transfer of Sugars Across Cell Barriers: Comparison With Action of Insulin. *American Journal of Physiology -- Legacy Content*, 173(2).

Goll, D.E. et al., 2003. The calpain system. *Physiological reviews*, 83(3), pp.731–801.

González, E.A. et al., 2004. Vitamin D insufficiency and deficiency in chronic kidney disease. A single center observational study. *American journal of nephrology*, 24(5), pp.503–10.

Greenhaff, P.L. et al., 2008. Disassociation between the effects of amino acids and insulin on signaling, ubiquitin ligases, and protein turnover in human muscle. *AJP: Endocrinology and Metabolism*, 295(3), pp.E595–E604.

Guerin, C.M. & Kramer, S.G., 2009. Cytoskeletal remodeling during myotube assembly and guidance: Coordinating the actin and microtubule networks. *Communicative and Integrative Biology*, 2(5), pp.452–457.

Halfon, M., Phan, O. & Theta, D., 2015. Vitamin D: A review on its effects on muscle strength, the risk of fall, and frailty. *BioMed Research International*, 2015.

Hamilton, B., 2010. Vitamin D and human skeletal muscle. *Scandinavian*

journal of medicine & science in sports, 20(2), pp.182–90.

Hannan, K.M. et al., 2003. mTOR-dependent regulation of ribosomal gene transcription requires S6K1 and is mediated by phosphorylation of the carboxy-terminal activation domain of the nucleolar transcription factor UBF. *Molecular and cellular biology*, 23(23), pp.8862–77.

Hardy, D. et al., 2016. Comparative Study of Injury Models for Studying Muscle Regeneration in Mice. *Plos One*, 11(1), p.e0147198.

Harridge, S.D. et al., 1996. Whole-muscle and single-fibre contractile properties and myosin heavy chain isoforms in humans. *Pflügers Archiv : European journal of physiology*, 432(5), pp.913–20.

Harris, T.B. et al., 2007. Age, Gene/Environment Susceptibility-Reykjavik Study: multidisciplinary applied phenomics. *American journal of epidemiology*, 165(9), pp.1076–87.

Hawke, T.J. & Garry, D.J., 2001. Myogenic satellite cells: physiology to molecular biology. *Journal of applied physiology (Bethesda, Md. : 1985)*, 91(2), pp.534–51.

Heaney, R.P., 2013. Health is better at serum 25(OH)D above 30ng/mL. *The Journal of Steroid Biochemistry and Molecular Biology*, 136, pp.224–228.

Henry, K.W. et al., 1998. Tuberous sclerosis gene 2 product modulates transcription mediated by steroid hormone receptor family members. *Journal of Biological Chemistry*, 273(32), pp.20535–20539.

Hershey, J.W.B. & Merrick, W.C., 2000. Initiation of Protein Synthesis. In *Translational control of gene expression*. Cold Spring Harbor NY: Cold Spring Harbor Laboratory Press, pp. 33–88.

Hickner, R.C. et al., 1997. Muscle glycogen accumulation after endurance exercise in trained and untrained individuals. *Journal of applied physiology (Bethesda, Md. : 1985)*, 83(3), pp.897–903.

Hoenderop, J.G.J. et al., 2002. Modulation of renal Ca2+ transport protein genes by dietary Ca2+ and 1,25-dihydroxyvitamin D3 in 25-hydroxyvitamin D3-1alpha-hydroxylase knockout mice. *FASEB journal : official publication of the Federation of American Societies for Experimental Biology*, 16(11), pp.1398–406.

Hojman, P. et al., 2007. Gene expression profiles in skeletal muscle after gene electrotransfer. *BMC molecular biology*, 8, p.56.

Holick, M.F., 1995. Environmental factors that influence the cutaneous production of vitamin D. *The American journal of clinical nutrition*, 61(3 Suppl), p.638S–645S.

Holick, M.F., 2006. High prevalence of vitamin D inadequacy and implications for health. *Mayo Clinic proceedings*, 81(3), pp.353–73.

Holick, M.F., 1987. Photosynthesis of vitamin D in the skin: effect of environmental and life-style variables. *Federation proceedings*, 46(5), pp.1876–82.

Houston, D.K. et al., 2012. 25-hydroxyvitamin D status and change in physical performance and strength in older adults: the Health, Aging, and Body Composition Study. *American journal of epidemiology*, 176(11), pp.1025–34.

Houston, D.K. et al., 2007. Association between vitamin D status and physical performance: The InCHIANTI study. *Journals of Gerontology Series a-Biological Sciences and Medical Sciences*, 62(4), pp.440–446.

Hwang, P.M. & Sykes, B.D., 2015. Targeting the sarcomere to correct muscle function. *Nature Reviews Drug Discovery*, 14(5), pp.313–328.

Imawari, M., Kida, K. & Goodman, D.S., 1976. The transport of vitamin D and its 25-hydroxy metabolite in human plasma. Isolation and partial characterization of vitamin D and 25-hydroxyvitamin D binding protein. *The Journal of clinical investigation*, 58(2), pp.514–523.

Inoki, K. et al., 2002. TSC2 is phosphorylated and inhibited by Akt and suppresses mTOR signalling. *Nature cell biology*, 4(9), pp.648–57.

Irazoqui, A.P., Boland, R.L. & Buitrago, C.G., 2014. Actions of 1,25(OH)2-vitamin D3 on the cellular cycle depend on VDR and p38 MAPK in skeletal muscle cells. *Journal of molecular endocrinology*, 53(3), pp.331–43.

Jackman, R.W. & Kandarian, S.C., 2004. The molecular basis of skeletal muscle atrophy. *American journal of physiology. Cell physiology*, 287(4), pp.C834-43.

Jagoe, R.T. & Goldberg, a L., 2001. What do we really know about the ubiquitin-proteasome pathway in muscle atrophy? *Current opinion in clinical nutrition and metabolic care*, 4(3), pp.183–90.

Janssen, I. et al., 2000. Skeletal muscle mass and distribution in 468 men and women aged 18-88 yr. *Journal of applied physiology (Bethesda,*

Md. : 1985), 89(1), pp.81–8.

Johnson, S.E. & Allen, R.E., 1993. Proliferating cell nuclear antigen (PCNA) is expressed in activated rat skeletal muscle satellite cells. *Journal of cellular physiology*, 154(1), pp.39–43.

Jones, G., 2008. Pharmacokinetics of vitamin D toxicity. *American Journal of Clinical Nutrition*, 88(2), pp.582–586.

Jones, G., Strugnell, S. a & DeLuca, H.F., 1998. Current understanding of the molecular actions of vitamin D. *Physiological reviews*, 78(4), pp.1193–1231.

Kabeya, Y. et al., 2000. LC3, a mammalian homologue of yeast Apg8p, is localized in autophagosome membranes after processing. *The EMBO journal*, 19(21), pp.5720–8.

Katsanos, C.S. et al., 2005. Aging is associated with diminished accretion of muscle proteins after the ingestion of a small bolus of essential amino acids. *The American journal of clinical nutrition*, 82(5), pp.1065–73.

Kayaniyil, S. et al., 2010. Association of vitamin D with insulin resistance and beta-cell dysfunction in subjects at risk for type 2 diabetes. *Diabetes care*, 33(6), pp.1379–81.

Khan, A.A. et al., 2010. Regulation of VDR expression in rat and human intestine and liver – Consequences for CYP3A expression. *Toxicology in Vitro*, 24(3), pp.822–829.

Khorchid, A. & Ikura, M., 2002. How calpain is activated by calcium. *Nature structural biology*, 9(4), pp.239–41.

Kimball, S.R. et al., 1999. Leucine regulates translation of specific mRNAs in L6 myoblasts through mTOR-mediated changes in availability of eIF4E and phosphorylation of ribosomal protein S6. *The Journal of biological chemistry*, 274(17), pp.11647–52.

Kimlin, M.G., Olds, W.J. & Moore, M.R., 2007. Location and Vitamin D synthesis: Is the hypothesis validated by geophysical data? *Journal of Photochemistry and Photobiology B: Biology*, 86(3), pp.234–239.

Kislinger, T., 2005. Proteome Dynamics during C2C12 Myoblast Differentiation. *Molecular & Cellular Proteomics*, 4(7), pp.887–901.

Klionsky, D.J. et al., 2012. Guidelines for the use and interpretation of

assays for monitoring autophagy. *Autophagy*, 8(4), pp.445–544.

Kobza, V.M. et al., 2013. Vitamin D status and resistance exercise training independently affect glucose tolerance in older adults. *Nutrition Research*, 33(5), pp.349–357.

Kohn, T.A., Essen-Gustavsson, B. & Myburgh, K.H., 2007. Exercise pattern influences skeletal muscle hybrid fibers of runners and nonrunners. *Medicine and science in sports and exercise*, 39(11), pp.1977–84.

Kumar, V., Selby, A., et al., 2009. Age-related differences in the dose-response relationship of muscle protein synthesis to resistance exercise in young and old men. *The Journal of physiology*, 587(Pt 1), pp.211–7.

Kumar, V., Atherton, P., et al., 2009. Human muscle protein synthesis and breakdown during and after exercise. *Journal of applied physiology (Bethesda, Md. : 1985)*, 106(6), pp.2026–39.

Lamberg-Allardt, C. et al., 2013. Vitamin D - a systematic literature review for the 5th edition of the Nordic Nutrition Recommendations. *Food & nutrition research*, 57.

Laurent, G., Sparrow, M. & Millward, D., 1978. Turnover of muscle protein in the fowl. Changes in rates of protein synthesis and breakdown during hypertrophy of the anterior and posterior latissimus dorsi muscles. *Biochem. J*, 176, pp.407–417.

Lecker, S.H. et al., 2004. Multiple types of skeletal muscle atrophy involve a common program of changes in gene expression. *FASEB journal : official publication of the Federation of American Societies for Experimental Biology*, 18(1), pp.39–51.

Lecker, S.H. et al., 1999. Ubiquitin conjugation by the N-end rule pathway and mRNAs for its components increase in muscles of diabetic rats. *The Journal of clinical investigation*, 104(10), pp.1411–20.

Lecker, S.H., Goldberg, A.L. & Mitch, W.E., 2006. Protein degradation by the ubiquitin-proteasome pathway in normal and disease states. *Journal of the American Society of Nephrology : JASN*, 17(7), pp.1807–19.

Lepper, C., Partridge, T.A. & Fan, C.M., 2011. An absolute requirement for Pax7-positive satellite cells in acute injury-induced skeletal muscle regeneration. *Development*, 138(17), pp.3639–3646.

Li, Y.C. et al., 1997. Targeted ablation of the vitamin D receptor: an animal model of vitamin D-dependent rickets type II with alopecia. *Proceedings of the National Academy of Sciences of the United States of America*, 94(September), pp.9831–9835.

Lin, M.T. & Beal, M.F., 2006. Mitochondrial dysfunction and oxidative stress in neurodegenerative diseases. *Nature*, 443(7113), pp.787–95.

Liu, E. et al., 2009. Plasma 25-hydroxyvitamin d is associated with markers of the insulin resistant phenotype in nondiabetic adults. *The Journal of nutrition*, 139(2), pp.329–34.

Liu, M. et al., 1996. Transcriptional activation of the Cdk inhibitor p21 by vitamin D3 leads to the induced differentiation of the myelomonocytic cell line U937. *Genes and Development*, 10(2), pp.142–153.

Lowell, B.B. & Shulman, G.I., 2005. Mitochondrial dysfunction and type 2 diabetes. *Science (New York, N.Y.)*, 307(5708), pp.384–7.

MacDonald, P.N. et al., 1993. Retinoid X receptors stimulate and 9-cis retinoic acid inhibits 1,25-dihydroxyvitamin D3-activated expression of the rat osteocalcin gene. *Molecular and cellular biology*, 13(9), pp.5907–17.

Magnuson, B., Ekim, B. & Fingar, D.C., 2012. Regulation and function of ribosomal protein S6 kinase (S6K) within mTOR signalling networks. *The Biochemical journal*, 441(1), pp.1–21.

Makanae, Y. et al., 2015. Acute bout of resistance exercise increases vitamin D receptor protein expression in rat skeletal muscle. *Experimental physiology*, 100(10), pp.1168–76.

Mammucari, C. et al., 2007. FoxO3 controls autophagy in skeletal muscle in vivo. *Cell metabolism*, 6(6), pp.458–71.

Marimuthu, K., Murton, A.J. & Greenhaff, P.L., 2011. Mechanisms regulating muscle mass during disuse atrophy and rehabilitation in humans. *Journal of applied physiology (Bethesda, Md. : 1985)*, 110(2), pp.555–60.

Marzetti, E. et al., 2013. Mitochondrial dysfunction and sarcopenia of aging: from signaling pathways to clinical trials. *The international journal of biochemistry & cell biology*, pp.1–14.

Mathieu, C. et al., 2005. Vitamin D and diabetes. *Diabetologia*, 48(7), pp.1247–57.

Matthews, D.R. et al., 1985. Homeostasis model assessment: insulin resistance and beta-cell function from fasting plasma glucose and insulin concentrations in man. *Diabetologia*, 28(7), pp.412–9.

Mayer, C. et al., 2004. mTOR-dependent activation of the transcription factor TIF-IA links rRNA synthesis to nutrient availability. *Genes & development*, 18(4), pp.423–34.

McCarthy, J.J. et al., 2011. Effective fiber hypertrophy in satellite cell-depleted skeletal muscle. *Development (Cambridge, England)*, 138(17), pp.3657–3666.

McFarlane, C. et al., 2008. Myostatin signals through Pax7 to regulate satellite cell self-renewal. *Experimental Cell Research*, 314(2), pp.317–329.

McMahon, J.M. et al., 2001. Optimisation of electrotransfer of plasmid into skeletal muscle by pretreatment with hyaluronidase -- increased expression with reduced muscle damage. *Gene therapy*, 8(16), pp.1264–1270.

Medina, R., Wing, S.S. & Goldberg, a L., 1995. Increase in levels of polyubiquitin and proteasome mRNA in skeletal muscle during starvation and denervation atrophy. *The Biochemical journal*, 307 (Pt 3, pp.631–7.

van der Meer, S.F.T., Jaspers, R.T. & Degens, H., 2011. Is the myonuclear domain size fixed? *Journal of Musculoskeletal Neuronal Interactions*, 11(4), pp.286–297.

van der Meijden, K. et al., 2016. Effects of 1,25(OH)2D3 and 25(OH)D3 on C2C12 Myoblast Proliferation, Differentiation, and Myotube Hypertrophy. *Journal of Cellular Physiology*, 25(March).

Menant, J.C. et al., 2012. Relationships between serum vitamin D levels, neuromuscular and neuropsychological function and falls in older men and women. *Osteoporosis International*, 23(3), pp.981–989.

Michael, Y.L. et al., 2011. Serum 25-hydroxyvitamin D and physical performance in postmenopausal women. *Journal of women's health (2002)*, 20(11), pp.1603–8.

Millay, D.P. et al., 2013. Myomaker is a membrane activator of myoblast fusion and muscle formation. (Supp). *Nature*, 499(7458), pp.301–5.

Mitch, W.E. & Goldberg, A.L., 1996. Mechanisms of muscle wasting. The

role of the ubiquitin-proteasome pathway. *The New England journal of medicine*, 335(25), pp.1897–905.

Miyamoto, K. et al., 1997. Structural organization of the human vitamin D receptor chromosomal gene and its promoter. *Molecular endocrinology (Baltimore, Md.)*, 11(8), pp.1165–79.

Miyazaki, S. & Miyazaki, J., 2009. *Electroporation and Sonoporation in Developmental Biology* H. Nakamura, ed., Tokyo: Springer Japan.

Mizushima, N. & Yoshimori, T., 2007. How to Interpret LC3 Immunoblotting. *Autophagy*, 3(6), pp.542–545.

Muir, S.W. & Montero-Odasso, M., 2011. Effect of vitamin D supplementation on muscle strength, gait and balance in older adults: a systematic review and meta-analysis. *J Am Geriatr Soc*, 59, pp.2291–2300.

Nader, G. a, Hornberger, T. a & Esser, K. a, 2002. Translational control: implications for skeletal muscle hypertrophy. *Clinical orthopaedics and related research*, (403 Suppl), pp.S178–S187.

Nemere, I. et al., 1998. Identification of a membrane receptor for 1,25-dihydroxyvitamin D3 which mediates rapid activation of protein kinase C. *Journal of bone and mineral research : the official journal of the American Society for Bone and Mineral Research*, 13(9), pp.1353–9.

Nemere, I. & Norman, A.W., 1990. Transcaltachia, vesicular calcium transport, and microtubule-associated calbindin-D28K: emerging views of 1,25-dihydroxyvitamin D3-mediated intestinal calcium absorption. *Mineral and electrolyte metabolism*, 16(2–3), pp.109–14.

Nemere, I., Yoshimoto, Y. & Norman, A.W., 1984. Calcium transport in perfused duodena from normal chicks: enhancement within fourteen minutes of exposure to 1,25-dihydroxyvitamin D3. *Endocrinology*, 115(4), pp.1476–83.

Neumann, E. et al., 1982. Gene transfer into mouse lyoma cells by electroporation in high electric fields. *The EMBO journal*, 1(7), pp.841–5.

Nguyen, T.M. et al., 2004. The rapid effects of 1,25-dihydroxyvitamin D3 require the vitamin D receptor and influence 24-hydroxylase activity: Studies in human skin fibroblasts bearing vitamin D receptor mutations. *Journal of Biological Chemistry*, 279(9), pp.7591–7597.

Nigwekar, S.U., Tamez, H. & Thadhani, R.I., 2014. Vitamin D and chronic kidney disease-mineral bone disease (CKD-MBD). *BoneKEy reports*, 3, p.498.

Nobukuni, T. et al., 2005. Amino acids mediate mTOR/raptor signaling through activation of class 3 phosphatidylinositol 3OH-kinase. *Proceedings of the National Academy of Sciences of the United States of America*, 102(40), pp.14238–43.

Norman, A.W., 2008. From vitamin D to hormone D: fundamentals of the vitamin D endocrine system essential for good health. *The American journal of clinical nutrition*, 88(2), p.491S–499S.

Norman, A.W., 2006. Minireview: vitamin D receptor: new assignments for an already busy receptor. *Endocrinology*, 147(12), pp.5542–8.

O'Leary, M.F.N. et al., 2012. Denervation-induced mitochondrial dysfunction and autophagy in skeletal muscle of apoptosis-deficient animals. *American journal of physiology. Cell physiology*, 303(4), pp.C447-54.

Okuno, H. et al., 2012. 1α,25-dihydroxyvitamin D_3 enhances fast-myosin heavy chain expression in differentiated C2C12 myoblasts. *Cell biology international*, 36(5), pp.441–7.

Olsson, K. et al., 2015. Evidence for vitamin D receptor expression and direct effects of 1α,25(OH) $_2$ D $_3$ in human skeletal muscle precursor cells. *Endocrinology*, 25(October), p.en.2015-1685.

Omdahl, J.L., Morris, H.A. & May, B.K., 2002. Hydroxylase enzymes of the vitamin D pathway: expression, function, and regulation. *Annual review of nutrition*, 22(1), pp.139–166.

Owens, D.J., Fraser, W.D. & Close, G.L., 2014. Vitamin D and the athlete: Emerging insights. *European Journal of Sport Science*, 15(1), pp.73–84.

Palacios, C. & Gonzalez, L., 2014. Is vitamin D deficiency a major global public health problem? *Journal of Steroid Biochemistry and Molecular Biology*, 144(PART A), pp.138–145.

Panel, E. & Nda, A., 2010. Scientific Opinion on the substantiation of health claims related to vitamin D and normal function of the immune system and inflammatory response (ID 154 , 159), maintenance of normal muscle function (ID 155) and maintenance of normal cardiovascular

f. *EFSA Journal*, 8(1924), p.1468.

Park, S. et al., 2012. Calpain inhibition attenuated morphological and molecular changes in skeletal muscle of experimental allergic encephalomyelitis rats. *Journal of neuroscience research*, 90(11), pp.2134–45.

Park, S., Kim, D.S. & Kang, S., 2015. Vitamin D deficiency impairs glucose-stimulated insulin secretion and increases insulin resistance by reducing PPAR-γ expression in non-obese type 2 diabetic rats. *The Journal of Nutritional Biochemistry*, pp.1–9.

Patel, S. a et al., 2012. Overexpression of the adiponectin receptor AdipoR1 in rat skeletal muscle amplifies local insulin sensitivity. *Endocrinology*, 153(11), pp.5231–46.

Peleg, S. & Nguyen, C. V., 2010. The importance of nuclear import in protection of the vitamin D receptor from polyubiquitination and proteasome-mediated degradation. *Journal of Cellular Biochemistry*, 110(4), pp.926–934.

Peng, L., Malloy, P.J. & Feldman, D., 2004. Identification of a functional vitamin D response element in the human insulin-like growth factor binding protein-3 promoter. *Molecular endocrinology (Baltimore, Md.)*, 18(5), pp.1109–19.

Penna, F. et al., 2013. Autophagic degradation contributes to muscle wasting in cancer cachexia. *The American journal of pathology*, 182(4), pp.1367–78.

Peter, J.B. et al., 1972. Metabolic profiles of three fiber types of skeletal muscle in guinea pigs and rabbits. *Biochemistry*, 11(14), pp.2627–33.

Pfeifer, M. et al., 2000. Effects of a short-term vitamin D and calcium supplementation on body sway and secondary hyperparathyroidism in elderly women. *Journal of bone and mineral research : the official journal of the American Society for Bone and Mineral Research*, 15(6), pp.1113–8.

Phillips, B.E. et al., 2013. Molecular Networks of Human Muscle Adaptation to Exercise and Age G. Gibson, ed. *PLoS Genetics*, 9(3), p.e1003389.

Phillips, S.M. et al., 1997. Mixed muscle protein synthesis and breakdown after resistance exercise in humans. *The American journal of physiology*, 273(1 Pt 1), pp.E99-107.

Phillips, S.M., Glover, E.I. & Rennie, M.J., 2009. Alterations of protein turnover underlying disuse atrophy in human skeletal muscle. *Journal of applied physiology (Bethesda, Md. : 1985)*, 107(3), pp.645–54.

Pike, J.W., 2014. Expression of the vitamin d receptor in skeletal muscle: are we there yet? *Endocrinology*, 155(9), pp.3214–8.

Pike, J.W. & Meyer, M.B., 2012. Regulation of mouse Cyp24a1 expression via promoter-proximal and downstream-distal enhancers highlights new concepts of 1,25-dihydroxyvitamin D3 action. *Archives of Biochemistry and Biophysics*, 523(1), pp.2–8.

Pittas, A.G. et al., 2007. REVIEW : The Role of Vitamin D and Calcium in Type 2 Diabetes . A Systematic Review and Meta-Analysis. *The Journal of clinical endocrinology and metabolism*, 92(6), pp.2017–2029.

Pojednic, R.M. & Ceglia, L., 2014. The emerging biomolecular role of vitamin D in skeletal muscle. *Exercise and sport sciences reviews*, 42(2), pp.76–81.

Prabhala, a, Garg, R. & Dandona, P., 2000. Severe myopathy associated with vitamin D deficiency in western New York. *Archives of internal medicine*, 160(8), pp.1199–203.

Price, S.R. et al., 1996. Muscle wasting in insulinopenic rats results from activation of the ATP-dependent, ubiquitin-proteasome proteolytic pathway by a mechanism including gene transcription. *The Journal of clinical investigation*, 98(8), pp.1703–8.

Prince, R.L. et al., 2008. Effects of ergocalciferol added to calcium on the risk of falls in elderly high-risk women. *Archives of internal medicine*, 168(1), pp.103–8.

Program, R.M., 2008. The Molecular Regulation of Muscle Stem Cell Function. , LXXIII.

Proud, C.G., 2013. mTORC1 regulates the efficiency and cellular capacity for protein synthesis. *Biochemical Society transactions*, 41(4), pp.923–6.

Public Health England & Food Standards Agency, 2014. *NDNS results from years 1 to 4 combined of the rolling programme for 2008 and 2009 to 2011 and 2012*, London.

van Riggelen, J., Yetil, A. & Felsher, D.W., 2010. MYC as a regulator of ribosome biogenesis and protein synthesis. *Nature reviews. Cancer*,

10(4), pp.301–309.

Ring, S.M., Dannecker, E.A. & Peterson, C.A., 2010. Vitamin D status is not associated with outcomes of experimentally-induced muscle weakness and pain in young, healthy volunteers. *Journal of Nutrition and Metabolism*, 2010.

Rizzoli, R. et al., 2008. The role of calcium and vitamin D in the management of osteoporosis. *Bone*, 42(2), pp.246–9.

Rochel, N. et al., 2000. The crystal structure of the nuclear receptor for vitamin D bound to its natural ligand. *Molecular cell*, 5(1), pp.173–9.

Roeder, R.G. & Rutter, W.J., 1970. Specific nucleolar and nucleoplasmic RNA polymerases. *Proceedings of the National Academy of Sciences of the United States of America*, 65(3), pp.675–82.

Rong, L. et al., 2008. Control of eIF4E cellular localization by eIF4E-binding proteins, 4E-BPs. *RNA (New York, N.Y.)*, 14(7), pp.1318–27.

Rosendahl-Riise, H. et al., 2016. Vitamin D supplementation and its influence on muscle strength and mobility in community-dwelling older persons: a systematic review and meta-analysis. *Journal of human nutrition and dietetics : the official journal of the British Dietetic Association*, (1), pp.1–13.

Roustit, M.M. et al., 2014. Urocortin 3 activates AMPK and AKT pathways and enhances glucose disposal in rat skeletal muscle. *The Journal of endocrinology*, 223(2), pp.143–54.

Rudnicki, M.A. & Jaenisch, R., 1995. The MyoD family of transcription factors and skeletal myogenesis. *BioEssays : news and reviews in molecular, cellular and developmental biology*, 17(3), pp.203–9.

Rudnicki, M. a et al., 1993. MyoD or Myf-5 is required for the formation of skeletal muscle. *Cell*, 75(7), pp.1351–9.

Rutherford, O.M. & Jones, D. a, 1992. The relationship of muscle and bone loss and activity levels with age in women. *Age and ageing*, 21(4), pp.286–93.

Sabourin, L.A. & Rudnicki, M.A., 2000. The molecular regulation of myogenesis. *Clinical genetics*, 57(1), pp.16–25.

Sakuma, K. & Yamaguchi, A., 2012. Sarcopenia and age-related endocrine function. *International journal of endocrinology*, 2012(Il), p.127362.

Salles, J. et al., 2013. 1,25(OH)2 -vitamin D3 enhances the stimulating effect of leucine and insulin on protein synthesis rate through Akt/PKB and mTOR mediated pathways in murine C2C12 skeletal myotubes. *Molecular nutrition & food research*, 25, pp.1–10.

Sambasivan, R. et al., 2011. Pax7-expressing satellite cells are indispensable for adult skeletal muscle regeneration. *Development and Stem Cells*, 138(17), pp.3647–56.

Sancak, Y. et al., 2008. The Rag GTPases bind raptor and mediate amino acid signaling to mTORC1. *Science (New York, N.Y.)*, 320(5882), pp.1496–501.

Sancak, Y. & Sabatini, D.M., 2009. Rag proteins regulate amino-acid-induced mTORC1 signalling. *Biochemical Society transactions*, 37(Pt 1), pp.289–90.

Sandgren, M.E., Brönnegärd, M. & DeLuca, H.F., 1991. Tissue distribution of the 1,25-dihydroxyvitamin D3 receptor in the male rat. *Biochemical and biophysical research communications*, 181(2), pp.611–6.

Sandri, M., 2013. Protein breakdown in muscle wasting: role of autophagy-lysosome and ubiquitin-proteasome. *The international journal of biochemistry & cell biology*.

Sant'ana Pereira, J.A. et al., 1995. New method for the accurate characterization of single human skeletal muscle fibres demonstrates a relation between mATPase and MyHC expression in pure and hybrid fibre types. *Journal of muscle research and cell motility*, 16(1), pp.21–34.

Saric, T., Graef, C.I. & Goldberg, A.L., 2004. Pathway for degradation of peptides generated by proteasomes: a key role for thimet oligopeptidase and other metallopeptidases. *The Journal of biological chemistry*, 279(45), pp.46723–32.

Satkauskas, S. et al., 2002. Mechanisms of in vivo DNA electrotransfer: respective contributions of cell electropermeabilization and DNA electrophoresis. *Molecular therapy : the journal of the American Society of Gene Therapy*, 5(2), pp.133–40.

Sato, Y. et al., 2005. Low-dose vitamin D prevents muscular atrophy and reduces falls and hip fractures in women after stroke: a randomized controlled trial. *Cerebrovascular diseases (Basel, Switzerland)*, 20(3),

pp.187–92.

Satoh, J. & Tabunoki, H., 2013. Molecular network of chromatin immunoprecipitation followed by deep sequencing-based vitamin D receptor target genes. *Multiple sclerosis (Houndmills, Basingstoke, England)*, 19(8), pp.1035–45.

Scheidt-Nave, C. et al., 2012. German health interview and examination survey for adults (DEGS) - design, objectives and implementation of the first data collection wave. *BMC Public Health*, 12(1), p.730.

Schiaffino, S. & Reggiani, C., 2011. Fiber Types in Mammalian Skeletal Muscles. *Physiological Reviews*, 91(4), pp.1447–1531.

Scientific Advisory Committee on Nutrition (SACN), 2016. *Vitamin D and Health*, London.

Scott, D. et al., 2010. A prospective study of the associations between 25-hydroxy-vitamin D, sarcopenia progression and physical activity in older adults. *Clinical Endocrinology*, 73(5), pp.581–587.

Sener, A. & Malaisse, W.J., 1981. The stimulus-secretion coupling of amino acid-induced insulin release: insulinotropic action of branched-chain amino acids at physiological concentrations of glucose and glutamine. *European journal of clinical investigation*, 11(6), pp.455–60.

Shah, I. et al., 2011. Misleading measures in Vitamin D analysis: a novel LC-MS/MS assay to account for epimers and isobars. *Nutrition Journal*, 10(1), p.46.

Shefer, G. et al., 2010. Reduced satellite cell numbers and myogenic capacity in aging can be alleviated by endurance exercise. *PloS one*, 5(10), p.e13307.

Shor, B. et al., 2010. Requirement of the mTOR kinase for the regulation of Maf1 phosphorylation and control of RNA polymerase III-dependent transcription in cancer cells. *The Journal of biological chemistry*, 285(20), pp.15380–92.

Shulman, G.I. et al., 1990. Quantitative comparison of pathways of hepatic glycogen repletion in fed and fasted humans. *The American journal of physiology*, 259(3 Pt 1), pp.E335-41.

Singh, R.J., 2010. Quantitation of 25-OH-vitamin D (25OHD) using liquid tandem mass spectrometry (LC-MS-MS). *Methods in molecular biology (Clifton, N.J.)*, 603, pp.509–17.

Sjöblom, B., Salmazo, a & Djinović-Carugo, K., 2008. Alpha-actinin structure and regulation. *Cellular and molecular life sciences : CMLS*, 65(17), pp.2688–701.

Smerdu, V. et al., 1994. Type IIx myosin heavy chain transcripts are expressed in type IIb fibers of human skeletal muscle. *The American journal of physiology*, 267(6 Pt 1), pp.C1723–C1728.

Smith, C.W. et al., 1999. Effects of serum deprivation, insulin and dexamethasone on polysome percentages in C2C12 myoblasts and differentiating myoblasts. *Tissue & cell*, 31(4), pp.451–8.

Solomon, V. & Goldberg, a. L., 1996. Importance of the ATP-ubiquitin-proteasome pathway in the degradation of soluble and myofibrillar proteins in rabbit muscle extracts. *The Journal of biological chemistry*, 271(43), pp.26690–7.

Solomon, V., Lecker, S.H. & Goldberg, A.L., 1998. The N-end rule pathway catalyzes a major fraction of the protein degradation in skeletal muscle. *The Journal of biological chemistry*, 273(39), pp.25216–22.

Sørensen, O.H. et al., 1979. Myopathy in bone loss of ageing: improvement by treatment with 1 alpha-hydroxycholecalciferol and calcium. *Clinical science (London, England : 1979)*, 56(2), pp.157–61.

Spangenburg, E.E. & Booth, F.W., 2003. Molecular regulation of individual skeletal muscle fibre types. *Acta Physiologica Scandinavica*, 178(4), pp.413–424.

Spiro, A. & Buttriss, J.L., 2014. Vitamin D: An overview of vitamin D status and intake in Europe. *Nutrition Bulletin*, 39(4), pp.322–350.

Srikuea, R. et al., 2012. VDR and CYP27B1 are expressed in C2C12 cells and regenerating skeletal muscle: potential role in suppression of myoblast proliferation. *American journal of physiology. Cell physiology*, 303(4), pp.C396-405.

Srikuea, R. & Hirunsai, M., 2016. Effects of intramuscular administration of 1α,25(OH)2D3 during skeletal muscle regeneration on regenerative capacity, muscular fibrosis, and angiogenesis. *Journal of applied physiology (Bethesda, Md. : 1985)*, 120(12), pp.1381–93.

Stratos, I. et al., 2013. Vitamin D increases cellular turnover and functionally restores the skeletal muscle after crush injury in rats. *The American journal of pathology*, 182(3), pp.895–904.

Sugden, P.H. & Fuller, S.J., 1991. Regulation of protein turnover in skeletal and cardiac muscle. *The Biochemical journal*, 273(Pt 1), pp.21–37.

Suzuki, K. & Kono, T., 1980. Evidence that insulin causes translocation of glucose transport activity to the plasma membrane from an intracellular storage site. *Proceedings of the National Academy of Sciences of the United States of America*, 77(5), pp.2542–5.

Tanaka, M. et al., 2014. Vitamin D receptor gene silencing effects on differentiation of myogenic cell lines. *Muscle & nerve*, 49(5), pp.700–8.

Tasi, D. et al., 2011. Fiber Type Composition and Size of Fibers in the Rat Tibialis Anterior Muscle. , 28(3), pp.161–168.

Tedesco, F. & Dellavalle, A., 2010. Repairing skeletal muscle: regenerative potential of skeletal muscle stem cells. *The Journal of clinical …*, 120(1).

Tipton, K.D. & Ferrando, A. a, 2008. Improving muscle mass: response of muscle metabolism to exercise, nutrition and anabolic agents. *Essays in biochemistry*, 44, pp.85–98.

Tishkoff, D.X. et al., 2008. Functional vitamin D receptor (VDR) in the t-tubules of cardiac myocytes: VDR knockout cardiomyocyte contractility. *Endocrinology*, 149(2), pp.558–64.

Toell, A., Polly, P. & Carlberg, C., 2000. All natural DR3-type vitamin D response elements show a similar functionality in vitro. *The Biochemical journal*, 352 Pt 2, pp.301–9.

Tomlinson, P.B., Joseph, C. & Angioi, M., 2015. Effects of vitamin D supplementation on upper and lower body muscle strength levels in healthy individuals. A systematic review with meta-analysis. *Journal of science and medicine in sport / Sports Medicine Australia*, 18(5), pp.575–80.

Torchia, J., Glass, C. & Rosenfeld, M.G., 1998. Co-activators and co-repressors in the integration of transcriptional responses. *Current opinion in cell biology*, 10(3), pp.373–83.

Traganos, F., Darzynkiewicz, Z. & Melamed, M.R., 1982. The ratio of RNA to total nucleic acid content as a quantitative measure of unbalanced cell growth. *Cytometry*, 2(4), pp.212–8.

Tremblay, F. et al., 2007. Identification of IRS-1 Ser-1101 as a target of

S6K1 in nutrient- and obesity-induced insulin resistance. *Proceedings of the National Academy of Sciences of the United States of America*, 104(35), pp.14056–61.

Trial, D. et al., 2015. Acute Effects of Vitamin D 3 Supplementation on Muscle Strength in Judoka Athletes : A Randomized. , 0(0), pp.1–6.

Ustanina, S. et al., 2007. The myogenic factor Myf5 supports efficient skeletal muscle regeneration by enabling transient myoblast amplification. *Stem cells*, 25(8), pp.2006–2016.

Del Valle, E. et al., 2007. Prevalence of 25(OH) vitamin D insufficiency and deficiency in chronic kidney disease stage 5 patients on hemodialysis. *Hemodialysis international. International Symposium on Home Hemodialysis*, 11(3), pp.315–21.

Vieth, R., 1999. Vitamin D supplementation , 25-hydroxyvitamin D concentrations ,. , 25(1), pp.842–856.

Volpi, E. et al., 2001. Basal Muscle Amino Acid Kinetics and Protein Synthesis in Healthy Young and Older Men. *JAMA*, 286(10), p.1206.

Wahren, J. et al., 1971. Glucose metabolism during leg exercise in man. *The Journal of clinical investigation*, 50(12), pp.2715–25.

Wallace, A.M. et al., 2010. Measurement of 25-hydroxyvitamin D in the clinical laboratory: current procedures, performance characteristics and limitations. *Steroids*, 75(7), pp.477–88.

Walters, M.R., Hunziker, W. & Norman, A.W., 1980. Unoccupied 1,25-dihydroxyvitamin D3 receptors. Nuclear/cytosol ratio depends on ionic strength. *Journal of Biological Chemistry*, 255(14), pp.6799–6805.

Wang, Y., Becklund, B.R. & DeLuca, H.F., 2010. Identification of a highly specific and versatile vitamin D receptor antibody. *Archives of Biochemistry and Biophysics*, 494(2), pp.166–177.

Wang, Y. & DeLuca, H.F., 2011. Is the vitamin D receptor found in muscle? *Endocrinology*, 152(2), pp.354–363.

Wang, Y., Zhu, J. & Deluca, H.F., 2014. Identification of the vitamin D receptor in osteoblasts and chondrocytes but not osteoclasts in mouse bone. *Journal of Bone and Mineral Research*, 29(3), pp.685–692.

Wang, Y.X. & Rudnicki, M.A., 2011. Satellite cells, the engines of muscle repair. *Nature reviews. Molecular cell biology*, 13(2), pp.127–133.

Warner, J.R., 1999. The economics of ribosome biosynthesis in yeast. *Trends in Biochemical Sciences*, 24(11), pp.437–440.

Weigl, L.G., 2012. Lost in translation: regulation of skeletal muscle protein synthesis. *Current opinion in pharmacology*, 12(3), pp.377–82.

Weinmann, R. & Roeder, R.G., 1974. Role of DNA-dependent RNA polymerase 3 in the transcription of the tRNA and 5S RNA genes. *Proceedings of the National Academy of Sciences of the United States of America*, 71(5), pp.1790–4.

West, D.W.D. et al., 2015. Acute resistance exercise activates rapamycin-sensitive and insensitive mechanisms that control translational activity and capacity in skeletal muscle. *The Journal of Physiology*, 0, p.n/a-n/a.

Whitfield, G.K. et al., 2001. Functionally relevant polymorphisms in the human nuclear vitamin D receptor gene. *Molecular and cellular endocrinology*, 177(1–2), pp.145–59.

Wicherts, I.S. et al., 2007. Vitamin D status predicts physical performance and its decline in older persons. *The Journal of clinical endocrinology and metabolism*, 92(6), pp.2058–65.

Wilkes, E.A. et al., 2009. Blunting of insulin inhibition of proteolysis in legs of older subjects may contribute to age-related sarcopenia. *The American journal of clinical nutrition*, 90(5), pp.1343–50.

Wilkinson, D.J. et al., 2015. Internal comparison between deuterium oxide (D 2 O) and L - [ring - 13 C 6] phenylalanine for acute measurement of muscle protein synthesis in humans. *Physiological Reports*, 3(7), p.e12433.

Williams, a B. et al., 1999. Sepsis stimulates release of myofilaments in skeletal muscle by a calcium-dependent mechanism. *FASEB journal : official publication of the Federation of American Societies for Experimental Biology*, 13(11), pp.1435–43.

Windelinckx, A. et al., 2007. Polymorphisms in the vitamin D receptor gene are associated with muscle strength in men and women. *Osteoporosis international : a journal established as result of cooperation between the European Foundation for Osteoporosis and the National Osteoporosis Foundation of the USA*, 18(9), pp.1235–42.

Wolfe, R.R., 2006. The underappreciated role of muscle in health and

disease. *The American journal of clinical nutrition*, 84(3), pp.475–82.

Yang, D. et al., 1998. Assay of Low Deuterium Enrichment of Water by Isotopic Exchange with [U- 13 C 3] Acetone and Gas Chromatography ± Mass Spectrometry. , 321, pp.315–321.

Yoshikawa, S. et al., 1979. Osteomalacic myopathy. *Endocrinologia japonica*, 26(Suppl), pp.65–72.

Zanello, L.P. & Norman, A.W., 2004. Rapid modulation of osteoblast ion channel responses by 1alpha,25(OH)2-vitamin D3 requires the presence of a functional vitamin D nuclear receptor. *Proceedings of the National Academy of Sciences of the United States of America*, 101(6), pp.1589–94.

Zeitz, U. et al., 2003. Impaired insulin secretory capacity in mice lacking a functional vitamin D receptor. , 25(2).

Zhang, X. & Zanello, L.P., 2008. Vitamin D Receptor-Dependent 1α,25(OH)2 Vitamin D3-Induced Anti-Apoptotic PI3K/AKT Signaling in Osteoblasts. *Journal of Bone and Mineral Research*, 23(8), pp.1238–1248.

Zhang, Y. et al., 2014. Coordinated regulation of protein synthesis and degradation by mTORC1. *Nature*, 513(7518), pp.440–3.

Zhao, G. & Simpson, R.U., 2010. Interaction between vitamin D receptor with caveolin-3 and regulation by 1,25-dihydroxyvitamin D3 in adult rat cardiomyocytes. *Journal of Steroid Biochemistry and Molecular Biology*, 121(1–2), pp.159–163.

Zhou, X. et al., 2015. Ribosomal proteins: functions beyond the ribosome. *Journal of molecular cell biology*, 7(2), pp.92–104.

Zhu, K. et al., 2010. A Randomized Controlled Trial of the Effects of Vitamin D on Muscle Strength and Mobility in Older Women with Vitamin D Insufficiency. *J Am Geriatr Soc*, 58, pp.2063–2068.

Zittermann, A., 2003. Vitamin D in preventive medicine: are we ignoring the evidence? *British Journal of Nutrition*, 89(5), p.552.

Zmuda, J.M., Cauley, J. a & Ferrell, R.E., 2000. Molecular epidemiology of vitamin D receptor gene variants. *Epidemiol.Rev*, 22(2), pp.203–217.

Publications

Peer-reviewed publications

Bass, J, J. Wilkinson, D. Rankin, D. Phillips, B. Szewczyk, N. Smith, K. Atherton, P. 'An overview of technical considerations for Western blotting applications to physiological research', Scandinavian Journal of Medicine and Science in Sports, Published, Epub ahead of print.

Gaffney, C.J., **Bass, J.J**., Barratt, T.F. & Szewczyk, N.J. (2014) 'Methods to Assess Subcellular Compartments of Muscle in C. elegans'. *Journal of Visualized Experiments*, (93), p.e52043.

Lehmann, S., **Bass, J.J**. & Szewczyk, N.J. (2013) 'Knockdown of the C. elegans kinome identifies kinases required for normal protein homeostasis, mitochondrial network structure, and sarcomere structure in muscle'. *Cell communication and signalling : CCS*, 11 (1), p.71.

Conference proceedings

Bass JJ, Kazi AA, Deane CS, Nakhuda A, Wilkinson DJ, Phillips BE, Smith K, Craig D, Philp A, Tarum J, Kadi F, Szewczyk NJ, Cleasby M, Atherton PJ. Sarcopenia, Cachexia and Wasting Disorders, Berlin, 2016 – 'Regulation of skeletal muscle mass by the Vitamin D receptor'

Bass JJ, Szewczyk NJ, Wilkinson DJ, Smith K, Cleasby M, Atherton PJ. Biological Basis of Elite Performance, The Physiological Society, Nottingham, 2016 - Regulation of skeletal muscle mass and metabolism by the vitamin D receptor: evidence derived from pre-clinical *in vivo* studies'

Bass JJ, Deane CS, Kazi A, Quinlan J, Wilkinson D, Smith K, Szewczyk N, Atherton PJ. British Society for Research on Ageing, Liverpool, 2014 - 'Skeletal muscle cell autonomous role of the vitamin D receptor'

Bass JJ, Szewczyk NJ, Wilkinson DJ, Phillips BE, Smith K, Craig D, Philp A, Tarum J, Kadi F, Cleasby M, Atherton PJ. Physiology, Dublin, 2016 – 'The Vitamin D receptor regulates skeletal muscle mass *in vivo*'

Bass JJ, Szewczyk NJ, Wilkinson DJ, Smith K, Cleasby M, Atherton PJ. Biology of Ageing, Singapore, 2015 – 'The skeletal muscle autonomous role of the Vitamin D receptor in myogenesis and metabolism: evidence derived from both pre-clinical *in vitro* and *in vivo* studies'

Bass JJ, Deane C, Kazi A, Wilkinson D, Smith K, Szewczyk N, Atherton PJ. Physiology, Cardiff, 2015 - 'Defining the autonomous role of the vitamin D receptor in skeletal myogenesis'

Bass JJ, Deane C, Kazi A, Wilkinson D, Smith K, Szewczyk N, Atherton PJ. CMAR/ CIMA joint conference, Nottingham, 2015 – 'Skeletal muscle cell autonomous role of the vitamin D receptor in myogenesis'

Awards

2016 International Early-Career Physiologist Travel Award - The Physiological society.